Integrating neurotransmitter receptor architecture in whole-brain computational models of neurodegenerative disease progression

Ahmed Faraz Khan

Integrated Program in Neuroscience

McGill University, Montreal

July 2024

A thesis submitted to McGill University in partial fulfillment of the requirements of the degree of Doctor of Philosophy.

Abstract

Alzheimer's disease (AD) and Parkinson's disease (PD) are among the prevailing causes of dementia and movement disorder, respectively. These neurodegenerative diseases are physiologically complex and symptomatically heterogeneous. Neuropathologically, AD is characterized by the accumulation of amyloid plaques and tau tangles, along with characteristic patterns of gray matter atrophy. However, this multi-faceted disorder also involves other, often earlier physiological alterations such as inflammatory, vascular, metabolic, and neuronal activity dysregulation. While the main hallmarks of PD are the aggregation of α-synuclein and the selective death of the nigrostriatal dopaminergic neurons, many other nuclei in the central and peripheral nervous system are also affected. Most cases of AD and PD are sporadic, with uncertain etiology. We lack an integrative understanding of how multiple physiological systems contribute to disease progression, what molecular and cellular substrates underlie their interactions, and how these factors vary across individuals. As a result, no disease-modifying treatments exist despite decades of efforts.

Critically involved in inter-cellular communication, neurotransmission is a potential link between the varied pathophysiology of AD and PD. Multiple neurotransmitter systems are associated with both disorders and have been a focus of pharmacological treatment. The loss of the dopaminergic neurons of the substantia nigra defines the motor symptoms of PD, and the death of acetylcholine-producing neurons of the basal forebrain is implicated in AD and other dementias. Many other neurotransmitter systems are also linked to specific symptoms. Yet, a systematic understanding of neurotransmission dysfunction has been impeded by both technical and practical limitations of molecular imaging.

This thesis has attempted to address this gap using a whole brain computational model incorporating neurotransmitter receptor architecture as a mediator of macroscopic physiological interactions over the course of AD and PD progression. These receptor-enriched multifactorial causal models (re-MCM) combine longitudinal multi-modal neuroimaging data (including structural, functional, diffusion and perfusion MRI, and molecular imaging for amyloid, tau, dopamine transporter, and glucose metabolism) and templates of neurotransmitter receptor concentrations (measured by *post mortem* autoradiography). These subject-specific models are defined by interpretable parameters corresponding to i) regional effects due to receptor-mediated interactions between pathophysiological factors, and ii) propagation of abnormality along the structural connectome. By comparing model-inferred mechanisms with multi-domain symptoms across patients, latent "disease axes" can then be identified at the population level.

Our results support a multi-neurotransmitter view of AD and PD, and emphasize the need to consider individual patient-specific mechanisms driving disease progression. In AD, two prominent axes are found, corresponding to i) executive dysfunction and ii) memory, language, and visuospatial dysfunction. In PD, i) motor symptoms and psychomotor speed define the major axis, while ii) visuospatial, working memory and psychiatric symptoms characterize a secondary axis. Notably, the extent of model-inferred deviation from a normative distribution of neurotransmitter mechanisms is correlated with symptom severity.

This exploratory analysis of model-inferred latent mechanisms allows us to link neurochemistry with macroscopic neuroimaging alterations. In a wider context, the approach proposed in this thesis lays the groundwork for mechanistic insight into the biology of neurodegenerative diseases, as well as a systematic approach to personalized and precision medicine approaches to pharmacological target selection.

Résumé

La maladie d'Alzheimer (MA) et la maladie de Parkinson (MP) figurent, respectivement, parmi les principales causes de démence et de troubles du mouvement respectivement. Sur le plan neuropathologique, la MA se caractérise par l'accumulation de plaques amyloïdes et d'enchevêtrements de tau, ainsi que par des schémas caractéristiques d'atrophie de la matière grise. Cependant, ce trouble multifacette implique également d'autres altérations physiologiques telles que la dysrégulation inflammatoire, vasculaire, métabolique et neuronale. Alors que les principaux signes distinctifs de la MP sont l'agrégation de l'α-synucléine et la mort sélective des neurones dopaminergiques nigrostriés, de nombreux autres noyaux du système nerveux central et périphérique sont également affectés. La plupart des cas de MA et de MP sont sporadiques, avec une étiologie incertaine. Il manque une compréhension intégrative de la manière dont les multiples systèmes physiologiques contribuent à la progression de la maladie, quels substrats moléculaires et cellulaires sous-tendent leurs interactions, et comment ces facteurs varient d'un individu à l'autre. En conséquence, aucun traitement modificateur de la maladie n'existe malgré des décennies d'efforts.

Contrôleurs de communication intercellulaire, la neurotransmission est un lien potentiel entre la pathophysiologie variée de la MA et de la MP. De multiples systèmes neurotransmetteurs sont associés à ces deux troubles et ont été le point focal des traitements pharmacologiques, notamment les rôles bien connus de la dopamine dans le parkinsonisme et de l'acétylcholine dans la démence. De nombreux autres systèmes neurotransmetteurs sont également liés à des symptômes spécifiques. Cependant, une compréhension systématique de la dysfonction de la neurotransmission a été entravée à la fois par des limitations techniques et pratiques de l'imagerie moléculaire. Cette thèse a tenté de combler cette lacune en utilisant un modèle mathématique du

cerveau entier incorporant la concentration des neurorécepteurs comme médiateur des interactions physiologiques au cours de la progression de la MA et de la MP. Ces modèles combinent des données de neuroimagerie multimodale de patients avec des modèles post-mortem de concentrations de neurorécepteurs. Ces modèles spécifiques à chaque sujet sont définis par des paramètres interprétables correspondant à i) des effets régionaux dus aux interactions médiées par les récepteurs entre les facteurs pathophysiologiques, et ii) la propagation de l'anomalie le long du connectome structurel. En comparant les mécanismes inférés par le modèle avec les symptômes multi-domaines chez les patients, des "axes de maladie" latents peuvent alors être identifiés au niveau de la population.

Nos résultats soutiennent une vision multi-neurotransmetteur de la MA et de la MP, et soulignent la nécessité de considérer les mécanismes spécifiques à chaque patient conduisant à la progression de la maladie. Dans la MA, deux axes saillants sont trouvés, correspondant aux dysfonctions i) des fonctions exécutives et ii) de la mémoire, du langage et des habiletés visuospatiales. Dans la MP, i) les symptômes moteurs et la vitesse psychomotrice définissent l'axe principal, tandis que ii) les symptômes visuospatiaux, les troubles de la mémoire de travail et les symptômes psychiatriques caractérisent un axe secondaire. Notablement, l'étendue de l'écart inféré par le modèle par rapport à une distribution normative des mécanismes neurotransmetteurs est corrélée à la sévérité des symptômes.

Cette analyse exploratoire des mécanismes latents inférés par le modèle nous permet de relier la neurochimie aux altérations neuroimaging macroscopiques. Dans un contexte plus large, l'approche proposée dans cette thèse jette les bases d’une compréhension mécaniste de la biologie des maladies neurodégénératives, ainsi qu'une approche systématique de la médecine personnalisée et de la sélection de cibles pharmacologiques de précision.

Contents

Acknowledgements

Firstly, I would like to express my gratitude to Prof. Yasser Iturria-Medina. Everyone who has worked with Yasser can attest to his scientific insight, but his students have also been especially fortunate to have an excellent and supportive mentor who does not lose sight of the big picture.

The receptor data used in my thesis was collected by the late Prof. Dr. Karl Zilles and Prof. Dr. Nicola Palomero-Gallagher. Without their collaboration and input, this work would not have been possible. I would also like to thank Prof. Julien Doyon, Prof. Sylvain Baillet, Prof. Alexey Kostikov and Prof. Marco Leyton for their valuable contributions over the years as my doctoral advisory and candidacy exam committee. I am especially grateful to Prof. Roger Dixon, Prof. Sherif Karama and Prof. Mahsa Dadar for combing through this thesis and raising thoughtful and constructive points at the oral defence.

I am also grateful for the support and encouragement of Prof. Yashar Zeighami and Dr. P.-J. Toussaint, who have made me feel welcome since my first week at the MNI. Dr. Felix Carbonell, Dr. Gleb Bezgin, Dr. Robert Baumeister, and Dr. Sue-Jin Lin have provided valuable input to various stages of my work. My lab siblings have also created a wonderful environment. Thank you to Quadri Adewale, Lazaro Sanchez-Rodriguez, Mahdie Soltaninejad, Matthew Danyluik, Veronika Pak and Joon Hong, as well as lab alumni Dr. Amirhossein Shirazi and Atousa Assadi.

Finally, thank you to my family, friends and especially Nikita, for everything. This thesis is especially dedicated to my grandparents.

Contribution to Original Knowledge

Summary of novel contributions

The novel contributions of this PhD thesis include:

- an individualized, whole-brain mathematical model of multi-modal neuroimaging-measured physiological alterations, combining local receptor-mediated interactions and long-range pathophysiological propagation (Chapters 4, 5),
- validation that the receptor architecture of healthy aged brains is informative to the spatiotemporal evolution of pathophysiology in healthy ageing, AD and PD (Chapters 4, 5),
- model-inferred determinants of vulnerability to specific pathophysiology based on receptor expression (Chapter 5),
- the identification of 2 “disease axes” in AD, representing i) executive dysfunction, and ii) memory, language and visuospatial impairment (Chapter 4),
- the identification of 2 “disease axes” in PD, representing i) motor symptoms with a prominent GABAergic component, and ii) visuospatial, psychiatric (anxiety and depression) and memory dysfunction with strong cholinergic influence (Chapter 5),
- inference of patient-specific receptor alteration profiles, compared to normative models, that are correlated with symptom severity (Chapter 4), and
- quantification of regions of high receptor influence on physiological interactions (Chapter 5).

List of publications

The following are a list of first and co-author publications during this PhD.

First-author publications included in this thesis:

- **Ahmed Faraz Khan**, Yasser Iturria-Medina, "Beyond the usual suspects: multi-factorial computational models in the search for neurodegenerative disease mechanisms", Under review, 2024. (**Chapter 3**)
- **Ahmed Faraz Khan**, Quadri Adewale, Tobias R. Baumeister, Felix Carbonell, Karl Zilles, Nicola Palomero-Gallagher, Yasser Iturria Medina, Alzheimer's Disease Neuroimaging Initiative, "Personalized brain models identify neurotransmitter receptor changes in Alzheimer's disease", *Brain*, vol. 145, no. 5, pp. 1785-1804, 2022. https://doi.org/10.1093/brain/awab375 (**Chapter 4**)
- **Ahmed Faraz Khan**, Quadri Adewale, Sue-Jin Lin, Tobias R Baumeister, Yashar Zeighami, Felix Carbonell, Nicola Palomero-Gallagher, Yasser Iturria-Medina, "Patient-specific models link neurotransmitter receptor mechanisms with motor and visuospatial axes of Parkinson's disease", *Nature Communications*, vol. 14, no. 1, p. 6009, 2023. https://doi.org/10.1038/s41467-023-41677-w (**Chapter 5**)

Other publications:

- Quadri Adewale, **Ahmed Faraz Khan**, Sue-Jin Lin, Tobias R. Baumeister, Yashar Zeighami, Felix Carbonell, Daniel Ferreira, Yasser Iturria-Medina, "Patient-centered Transcriptomic and Multimodal Neuroimaging Determinants of Clinical Progression, Physical Activity and Treatment Needs in Parkinson's Disease", Submitted, 2024.

- Lazaro M. Sanchez-Rodriguez, **Ahmed Faraz Khan**, Quadri Adewale, Gleb Bezgin, Joseph Therriault, Jaime Fernandez-Arias, Stijn Servaes, Nesrine Rahmouni, Cecile Tissot, Jenna Stevenson, Hongxiu Jiang, Xiaoqian Chai, Felix Carbonell, Pedro Rosa-Neto, Yasser Iturria-Medina, "Transcriptomic signatures of Aβ- and tau-induced neuronal dysfunction reveal inflammatory processes at the core of Alzheimer's disease pathophysiology", Under review, 2023. https://doi.org/10.1101/2023.09.15.557737
- Quadri Adewale, **Ahmed Faraz Khan**, David A. Bennet, Yasser Iturria Medina, "Single-nucleus RNA velocity reveals synaptic and cell-cycle dysregulations missed by gene expression in neuropathologic Alzheimer's disease", *Scientific Reports*, vol. 14, 7269, 2024. https://doi.org/10.1038/s41598-024-57918-x
- Yasser Iturria-Medina, Quadri Adewale†, **Ahmed F. Khan**†, Simon Ducharme, Pedro Rosa-Neto, Kieran O'Donnell, Vladislav A. Petyuk, Serge Gauthier, Philip L De Jager, John Breitner, David A. Bennett, "Unified epigenomic, transcriptomic, proteomic, and metabolomic taxonomy of Alzheimer's disease progression and heterogeneity", *Science Advances*, vol. 8, no. 46, p. eabo6764, 2022. https://doi.org/10.1126/sciadv.abo6764 † These authors contributed equally to this work.
- Yasser Iturria-Medina, Félix M. Carbonell, Atousa Assadi, Quadri Adewale, **Ahmed Faraz Khan**, Robert Baumeister, Lazaro Sanchez-Rodriguez, "Integrating molecular, histopathological, neuroimaging and clinical neuroscience data with NeuroPM-box", *Communications Biology*, vol. 4, no. 1, pp. 614, 2021. https://doi.org/10.1038/s42003-021-02133-x

- Quadri Adewale, **Ahmed Faraz Khan**, Felix Carbonell, Yasser Iturria-Medina, Alzheimer's Disease Neuroimaging Initiative, "Integrated transcriptomic and neuroimaging brain model decodes biological mechanisms in aging and Alzheimer's disease", *eLife*, vol. 10, pp. e62589, 2021. https://doi.org/10.7554/eLife.62589
- Yasser Iturria-Medina, **Ahmed Faraz Khan**, Quadri Adewale, Amirhossein Shirazi, "Blood and brain gene expression trajectories mirror neuropathology and clinical deterioration in neurodegeneration", *Brain*, vol. 143, no. 2, pp. 661-73, 2020. https://doi.org/10.1093/brain/awz400

Contribution of Authors

I am the sole first author of 3 manuscripts (Chapters 3, 4 and 5) included in this thesis. Chapter 3 contains a review article submitted for publication in a journal, for which I conducted literature review and wrote the manuscript. Chapters 4 and 5 represent the original research contributions of this thesis. For these projects, I developed the majority of the methods, processed the data, conducted the analyses, interpreted results and wrote the manuscript.

The contributions of co-authors are summarized below.

Chapter 3:

- Yasser Iturria-Medina: conceptualized the structure of the review and revised the manuscript.

Chapter 4:

- Quadri Adewale: processed the data and provided methodological consultation, revised the manuscript,
- Tobias R. Baumeister: provided methodological consultation, revised the manuscript,
- Felix Carbonell: provided methodological consultation,
- Karl Zilles: acquired the receptor autoradiography data,
- Nicola Palomero-Gallagher: acquired the receptor autoradiography data, interpreted the results,
- Yasser Iturria-Medina: conceptualized and supervised the study, processed data, interpreted results, revised the manuscript.

Chapter 5:

- Quadri Adewale: processed the data and provided methodological consultation, revised the manuscript,
- Sue-Jin Lin: processed the data, interpreted the results, revised the manuscript,
- Tobias R. Baumeister: provided methodological consultation, revised the manuscript,
- Yashar Zeighami: processed the data, revised the manuscript,
- Felix Carbonell: provided methodological consultation,
- Nicola Palomero-Gallagher: acquired the receptor autoradiography data, interpreted the results,
- Yasser Iturria-Medina: conceptualized and supervised the study, processed data, interpreted results, revised the manuscript.

List of Figures

List of Tables

Table of Abbreviations

AD	Alzheimer's disease
ADAS	Alzheimer's Disease Assessment Scale
ADNI	Alzheimer's Disease Neuroimaging Initiative
AFT	Accelerated failure time
ALS	Amyotrophic lateral sclerosis
APOE	Apolipoprotein E
ASL	Arterial spin labeling
Aβ	Amyloid beta
BJLOT	Benton Judgement of Line Orientation Test
BOLD	Blood oxygenation level dependent
CBF	Cerebral blood flow
CSF	Cerebrospinal fluid
CTE	Chronic traumatic encephalopathy
CVD	Cerebrovascular disease
DIAD	Dominantly inherited Alzheimer's disease
DPM	Disease progression model
DPS	Disease progression score
EBM	Event-based model
EEG	Electroencephalogram
ESM	Epidemic spreading model
FA	Fractional anisotropy

fALFF	Fractional amplitude of low frequency fluctuations
FDG	2-[fluorine-18]fluoro-2- deoxy-d-glucose
FTD	Frontotemporal dementia
FTLD	Frontotemporal lobar degeneration
GABA	γ-aminobutyric acid
GDS	Geriatric Depression Scale
GPe	Globus pallidus externus
GPi	Globus pallidus internus
HVLT	Hopkins Verbal Learning Test
LNS	Letter Number Sequencing
MCI	Mild cognitive impairment
MCM	Multifactorial causal model
MCMC	Markov chain Monte Carlo
MD	Mean diffusivity
MDS-UPDRS	Movement Disorder Society - Unified Parkinson's Disease Rating Scale
MEG	Magnetoencephalography
MMSE	Mini-Mental State Examination
MoCA	Montreal Cognitive Assessment
NDM	Network diffusion model
PD	Parkinson’s disease
PHS	Polygenic hazard score

PLS	Partial least squares
PPMI	Parkinson's Progression Markers Initiative
re-MCM	Receptor-Enriched Multifactorial Causal Model
ROI	Region of interest
rs-fMRI	Resting state functional MRI
SDM	Symbol Digit Modalities
SF	Semantic fluency
SNpc	Substantia nigra pars compacta
SNpr	Substantia nigra pars reticula
STAIAD	State-Trait Anxiety Inventory for Adults
STN	Subthalamic nucleus
SuStaIn	Subtype and Stage Inference
SVD	Singular value decomposition
TDP-43	Transactive response DNA-binding protein 43
TVB	The Virtual Brain
VGAM	Vector generalized additive model
WMH	White matter hyperintensities

Chapter 1. Introduction

Background and rationale

Neurodegenerative disorders (NDD) involve progressive structural and functional alterations to specific neuronal populations, manifesting as clinical syndromes such as dementia and movement disorders [1]. While there are varied and complex genetic [2] and environmental [3] contributors, most cases of NDDs are "sporadic" and not attributed to Mendelian inheritance. The major risk factor for NDDs is ageing, with which they share molecular hallmarks such as genomic instability, epigenetic modifications, and mitochondrial dysfunction [4]. However, the causes of sporadic NDD onset, as a process distinct from normal ageing, remain unknown.

Alzheimer's disease (AD) and Parkinson's disease (PD) are the two most common NDDs, and the leading causes of dementia and movement disorder, respectively [5]. The prevalence of AD and PD is substantial in seniors and rises exponentially with age [6] [7]. In a globally ageing population, the number of individuals with dementia is expected to triple between 2019 and 2050 [8], and the worldwide burden of PD has already doubled in the past generation [9]. These trends represent enormous quality-of-life and economic costs, for the patient, their caregivers, the healthcare system, and wider society [10].

Yet, there are currently no treatments that can stop the progression of AD or PD, largely due to the incomplete understanding of disease biology, and the marked physiological and symptomatic variability between individuals [11]. The brain is a complex organ, with many physiological processes responsible for healthy function. Their disruption contributes to pathways shared across NDDs and with ageing, such as oxidative stress, apoptosis, genomic instability, impaired proteostasis, cellular senescence, and immune, metabolic and vascular

dysfunction [1] [4] [12]. Although NDDs are categorized by disease-specific symptoms and pathophysiology, there is notable inter-patient heterogeneity and inter-disease overlap [13] [14]. The underlying dysfunction often begins decades before symptom onset [15] [16] [17], with the etiology of sporadic disease onset being unknown.

AD is characterized by the neuropathological accumulation of amyloid plaques and tau tangles along with gray matter atrophy, but also involves many physiological alterations including vascular, inflammatory, metabolic and neuronal activity dysregulation [18] [19]. [20] [21] [22]. PD is primarily associated with the loss of nigrostriatal dopaminergic neurons, but has a complex pathophysiology encompassing many locations in the central and peripheral nervous systems [23] [24]. Particularly, both diseases exhibit selective vulnerability of neuronal populations from specific neurotransmitter systems, such as the basal forebrain cholinergic system in AD [25], and the adrenergic locus coeruleus and serotonergic raphe nuclei and their cortical projections in PD [24] [26].

In addition to the extensive evidence of disease-affected neurotransmission, these systems are targeted pharmacologically in the form of cholinesterase inhibitors for dementia and dopaminergic therapy for PD [25] [24]. However, this treatment is symptomatic and not disease-modifying. Despite recent progress in anti-amyloid monoclonal antibodies, they have also arguably failed to demonstrate clinically significant benefit [27] (although this may depend on the trial duration [28]). With an imperfect understanding of etiology and pathogenesis, we lack definitive biological markers of progression and targets for treatment. As a result, the diseases are currently incurable.

A major barrier to our scientific understanding of NDDs as well as their treatment is the missing link between cellular and molecular mechanistic dysfunction, their consequences on

regional, network and whole-brain integrity, and the appearance of clinical symptoms. In addition to case-control comparisons, there is a need for a systems-level understanding of NDDs as i) dysregulated physiological interactions [29], ii) the molecular and cellular features underlying vulnerability, and iii) how inter-individual variability in these interactions relates to symptomatic profiles.

A potential link between these disease factors is neurotransmission, which underlies communication and cell-cell interaction in the brain. Computational models of neurotransmission-mediated dysfunctional physiological interactions can address these current gaps in NDD research by a two-pronged approach: i) insight into disease biology and ii) improved characterization of individual patients and their therapeutic needs [30]. However, the lack of suitable radioligands and the expense of in vivo molecular imaging has been an impediment to identifying neurotransmission-based molecular mechanisms involved in the disease [31] [32].

To circumvent this limitation, this work introduces the receptor-enriched multi-factorial causal model (re-MCM), an extension of the original MCM framework [33] that incorporates neurochemical features in the form of a group-averaged neurotransmitter receptor autoradiography template for 15 receptor types. In these personalized, whole-brain models, patient-specific mechanistic effects are inferred by the role of receptor-mediated interactions between factors such as cerebral blood flow, glucose metabolism, neuronal activity, proteinopathy accumulation and atrophy. By introducing individual variability in neurotransmitter receptor influence on physiological interactions, these personalized models can infer the subject-specific patterns of receptor-mediated dysfunction and their relationship to

symptomatic deterioration in NDDs. This approach can thus offer interpretable yet data-driven insight into latent mechanisms of physiological dysfunction in AD and PD.

Objectives

To facilitate our evolving understanding of neurodegenerative disorders, our work presents the first integrative generative model linking multiple neurotransmitter receptors with macroscopic brain alterations and clinical symptoms. Importantly, estimating patient-specific, receptor involvement addresses an urgent clinical need by laying the foundation for model-based personalized treatment design. Furthermore, the novel methodology of using non-individualized receptor templates to infer patient-specific receptor involvement has broad applications in computational modeling when individualized imaging is infeasible.

The objectives of this thesis include:

1) Developing a dynamical system model of interacting pathophysiological variables (e.g., cerebral blood flow, functional activity, gray matter density, proteinopathy, etc.) in AD and PD with mediation by the regional concentrations of 15 neurotransmitter receptors,
2) Validation of these models (in their ability to fit the empirical data), and the contribution of receptor distribution maps,
3) Association of model-inferred mechanisms with multi-domain symptoms to identify interpretable latent biological mechanisms driving symptom severity,
4) Characterization of individual-specific neurotransmission dysfunction, and
5) Estimation of spatial contributions of these mechanisms.

Overview of thesis

To address these pressing issues in AD and PD, two of the most common neurodegenerative disorders, this thesis has introduced a dynamical system model of neurodegenerative disease progression incorporating interactions of imaging-derived physiological measures modulated by neurotransmitter receptor concentrations. Chapter 2 provides a brief overview of the range of pathological processes involved in AD and PD, as well as the strengths and limitations of (neuroimaging, etc.) techniques to quantify their spatiotemporal profiles. Chapter 3 is a literature review of computational modeling approaches applied to (mainly *in vivo* neuroimaging) data, from data-driven models of biomarker trajectories to mechanistically interpretable dynamical system and biophysical models, with a focus on their ability to evaluate disease hypotheses. Chapters 4 and 5 introduce the receptor-informed multifactorial causal model (re-MCM) and its applications to AD and PD, respectively. Finally, Chapter 6 discusses the results of this thesis, its limitations, and potential directions of future work.

Chapter 2. Imaging pathophysiology in neurodegenerative disorders

Preface

This chapter provides a brief overview of the pathophysiology of Alzheimer's disease (AD), Parkinson's disease (PD) and related disorders, as well as the landscape of neuroimaging modalities used in research and clinical contexts. Chapter 3 complements the literature review in this section, by discussing computational modeling approaches to integrating multi-modal biomarker data and evaluating mechanistic hypotheses.

Pathophysiology and disease mechanisms

This section discusses the physiological mechanisms believed to contribute to disease progression, potential interactions between these processes, and the role of neurotransmission in relation to different cell types and physiological systems.

Proteinopathy

The aggregation of specific misfolded proteins is a defining feature of the major neurodegenerative disorders. This subsection introduces the main proteinopathies implicated in AD, PD and related disorders.

Amyloid

From the first pathological studies by Alois Alzheimer in the early 20th century, extracellular plaques and intracellular neurofibrillary tangles have been the hallmark pathology

of AD [34]. Later molecular studies identified the peptide amyloid beta as the main component of the plaques, leading to the amyloid cascade hypothesis, summarized in Figure 2.1 [35]. This theory considers all other AD pathophysiology, such as tangles and neuronal death, to be downstream of the accumulation of amyloid beta peptides.

Amyloid pathology is produced by the improper cleavage of amyloid precursor protein (APP), a transmembrane protein whose function is not fully understood [36]. The non-amyloidogenic pathway cleaves APP within the β-amyloid (Aβ) fragment, while the amyloidogenic pathway produces β-amyloid monomers [37], which aggregate into fibrils and plaques [38]. These aggregations are believed to have neurotoxic effects via glutamatergic excitotoxicity, inhibitory GABAergic interneuron dysfunction, ion channel disruption and dendritic degeneration [39] [40] [41]. Prion-like seeding followed by cell-to-cell spreading of amyloid has been demonstrated in animal models [42] [43]. In the human brain, amyloid plaques are first observed in the neocortex, spreading to the allocortex, basal ganglia, midbrain and eventually the pons and cerebellum [44]. The balance between production and clearance is blamed for the aggregation of amyloid, with the latter mechanism primarily implicated in non-genetic cases [45] [46] [37]. An alternative viewpoint proposes that the true mechanism involves a loss of healthy protein function (proteinopenia), rather than a gain of toxic protein function (proteinopathy) [47]. However, the precise roles of amyloid and its homeostasis in health and disease remain open questions [48], and its localization may involve regional vulnerability due to a combination of molecular/cellular architecture, synaptic activity, metabolic demands, neurovascular impairment and other physiological factors.

While amyloid pathology may precede the appearance of cognitive symptoms by up to a decade, the correlation with cognitive deterioration is weaker than for other factors such as tau

tangles [40]. Although amyloid may influence age of onset (e.g., in genetic variants), the rate of progression appears to have an amyloid-independent component [41]. Furthermore, in vivo and post mortem evidence shows that brains of many non-demented individuals have amyloid pathology [40] [49], suggesting a more complex etiology involving other physiological factors. Finally, the current generation of anti-amyloid monoclonal antibody trials have had mixed results [50] [51]. It seems unlikely that amyloid clearance alone is a viable route to preventing or curing AD [52], and the failure of anti-amyloid therapy is partially blamed on the other main proteinopathy culprit: tau [41].

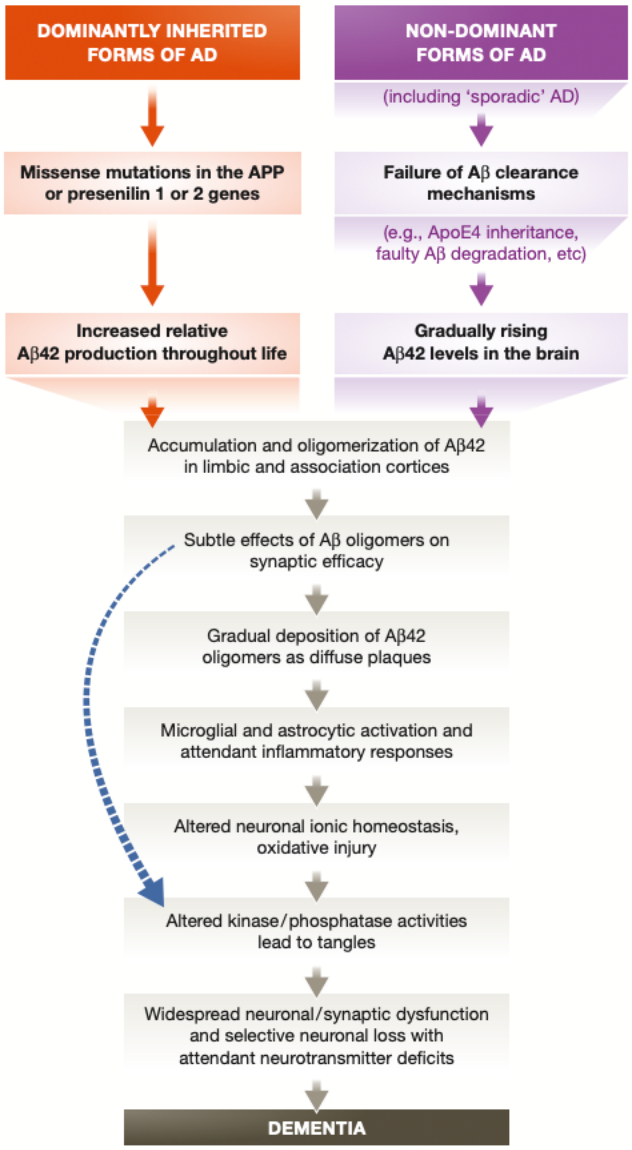

Figure 2.1. The amyloid cascade hypothesis of AD.

A sequence of pathogenic events is believed to occur due to either increased Aβ42 production (in dominantly inherited AD) or decreased Aβ42 clearance (sporadic AD). Figure adapted with permission from [40].

Tau

An alternate hypothesis of AD pathobiology gives primacy to tau, a protein involved in microtubule polymerization and stabilization [49]. In the healthy brain, tau is primarily found in axons, where it undergoes phosphorylation to detach itself from microtubules for transport. Tau

pathology involves the accumulation of the protein in a hyperphosphorylated state either as neurofibrillary tangles in neuronal cell bodies, or as threads in axons or dendrites [49]. Neurofibrillary tau tangles impede synaptic transmission by altering electrophysiological properties [53], resulting in increased input resistance, reduced action potential amplitude and delayed dynamics. Cognitive decline correlates better with the burden of tau rather than amyloid, and, as with amyloid, neurofibrillary tau tangles have been observed in clinical populations well before AD symptoms [21].

While amyloid is considered to be upstream of tau in the traditional, linear pathological cascade [54], there is evidence that the proteins interact in a more complex feedback loop [55]. Generally, amyloid is believed to "trigger" or facilitate tau pathology. In addition to amyloid directly inducing tau oligomerization and indirectly promoting tau release via hyperactivity, microglial activation, neuronal hyperexcitability, vascular alterations and lipid metabolism and other physiological processes may be intermediary modulators [41].

Tau pathology also propagates along connected cells spatially in a characteristic pattern described by Braak and Braak [56]: it is first evident in the transentorhinal region (stages I and II), spreading to limbic areas (stages III and IV) and the neocortex (stages III and IV). This progression pattern is correlated with cognitive and clinical manifestations [56]. Despite evidence for the interactions of these two proteins and amyloid-facilitated tau spreading, the spatiotemporal patterns of amyloid and tau are distinct (Figure 2.2), suggesting independent effects as well [57] [41].

Beyond AD, tauopathies encompass a wide range of neurological conditions with diverse symptoms, such as frontotemporal dementia (FTD), and progressive supranuclear palsy (PSP)

[58]. More broadly, tau pathology is present in 92-100% of neurodegenerative disease patients' brains [59].

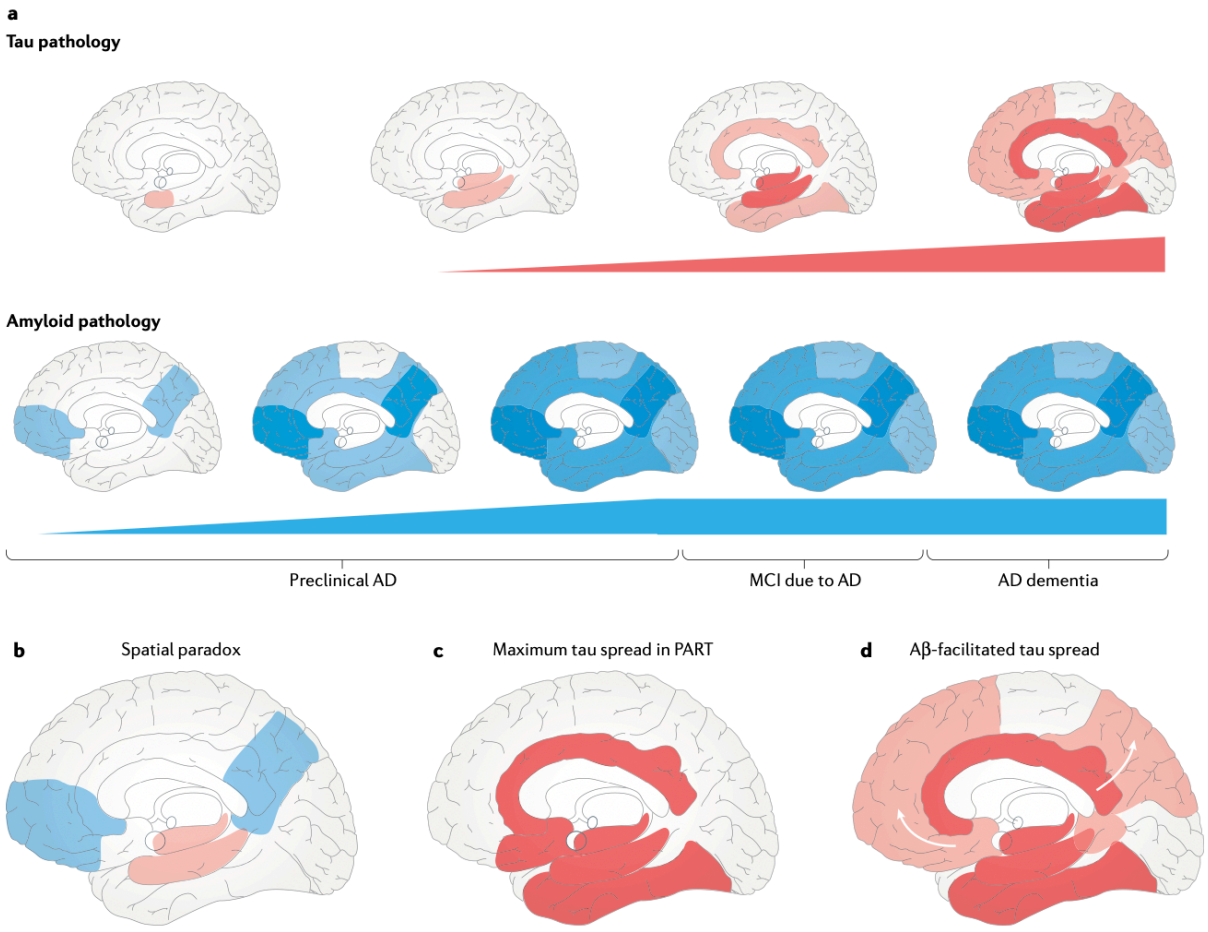

Figure 2.2. The spatial paradox of amyloid and tau propagation in AD.

a) Tau and amyloid follow characteristic spatial spreading patterns in the AD spectrum. b) Although the conventional belief has been that amyloid facilitates tau pathology, the two originate in distinct brain regions. c) In primary age-related tauopathy (PART), amyloid pathology is not present, and tau does not spread to neocortical regions. d) On the other hand, in the presence of amyloid pathology, tau does spread to the neocortex, and this pattern is associated with AD. Figure adapted with permission from [60].

α-synuclein

Synucleinopathies are another major neuropathologically-defined macrofamily of disorders, ranging from multiple system atrophy (MSA) to dementia with Lewy bodies (DLB) and PD [61]. Synucleinopathies vary in clinical presentation; some combination of motor

symptoms and autonomic dysfunction occurs in almost all cases, but cognitive, psychiatric and olfactory dysfunction can also occur in PD and DLB.

The shared neuropathological feature of synucleinopathies is Lewy bodies, the primary component of which is the cytoplasmic aggregations of α-synuclein. This misfolded protein is primarily found in presynaptic terminals, and is believed to be involved in synaptic maintenance, mitochondrial homeostasis, dopamine metabolism and chaperone activity [62]. Propagation of α-synuclein along connected cells is believed to facilitate the spreading of pathology [63].

In vivo α-synuclein imaging in humans is not currently possible, and candidate PET radioligands suffer from cross-binding to amyloid fibrils [64]. While not yet part of the routine clinical workflow, emerging methods for CSF α-synuclein quantification are a proposed component of biomarker-based staging systems of PD [65]. Previously, the main line of evidence has been pathological evaluations, which shows co-occuring α-synuclein in most AD patients [66].

TDP-43

Transactive response DNA-binding protein 43 (TDP-43) is normally localized in nuclei and associated with transcriptional regulation [67]. TDP-43 is linked to several neurodegenerative diseases, particularly the frontotemporal dementia (FTD) and amyotrophic lateral sclerosis (ALS) spectrum [68]. Lacking in vivo PET radioligands [69], much of our evidence of its role in AD and PD comes from neuropathological evaluations. Co-occurrence of cytoplasmic inclusions of hyperphosphorylated TDP-43 proteinopathy was found to occur in around 37% of autopsied brains with a neuropathological diagnosis of AD, and the combination of AD and TDP-43 pathology raised the odds of AD dementia [70]. TDP-43 co-pathology was found in 7.2% of neuropathologically confirmed PD cases and 19% of PD dementia cases [67].

Whether TDP-43 pathology in isolation is sufficient for disease onset is an open question, given the frequency of co-pathology [71]. Ultimately, neuropathological burden (including amyloid, tau and Lewy body pathology as well as micro- and macroscopic infarcts) explains less than one-third of the variance in rate and onset of cognitive decline [72], suggesting the need to consider other physiological processes as well.

Inflammation

Long established as a feature of neurological conditions such as chronic traumatic encephalopathy (CTE), ALS and multiple sclerosis (MS), sustained neuroinflammation is increasingly seen as a core pathophysiology of AD, PD (where it is associated with increased dementia risk [73]), other neurodegenerative diseases and ageing [21] [74] [75] [76]. Activation of the immune system is observed in nearly all pathological conditions [74], and progressive immunodeficiency is a characteristic of ageing [75]. While both adaptive and innate immune cells activation is involved, the latter differentiate disorders such as AD from primarily inflammatory disorders such as MS [74]. While inflammatory activity in the brain is not necessarily always harmful, similar pathways seem to have both protective and deleterious effects under different conditions [77] [76].

Initially believed to be a by-product of neuronal cell death, neuroinflammation may be an early mediator of disease onset and progression, acting as an intermediary in processes such as amyloid seeding of tau pathology and α-synuclein toxicity [21] [77]. In animal models, microglial activation even seems to initiate amyloid and tau pathology [74]. The peripheral immune system also appears to be involved, notably via the gut-brain axis in PD [78] and systemic inflammation in AD [74]. Furthermore, both AD and PD are linked to risk variants of genes associated with inflammation [74] [75].

As the primary immune cells of the central nervous system, microglia naturally play a key role in maintaining a healthy inflammatory response. Microglial activation and microglia-neuron interactions are regulated by multiple cellular signaling pathways, including cytokines and neurotransmitters [77] [21]. Astrocytes are also believed to be involved via their role in maintaining homeostasis and neuron-glia communication [79]. Extracellular release of GABA by astrocytes inhibits the inflammatory response of activated microglia, and the microglial $GABA_B$ receptors are particularly associated with this anti-inflammatory role [21]. Recent evidence from in vivo proteomic markers suggests that astrocyte reactivity is the key factor modulating amyloid-induced tau hyperphosphorylation [80]. Nicotinic cholinergic receptors on astrocytes and microglia are implicated in amyloid metabolism, as well as in amyloid-related oxidative stress and neurotoxicity [81]. Furthermore, glial nicotinic cholinergic receptors also modulated neurotransmission via indirect interactions with NMDA, AMPA and GABA receptors, as well as with the regulation of intracellular calcium [81]. The activation of GABA, cholinergic and adrenergic receptors also reduces microglial inflammatory response [82] [21]. On the other hand, glutamatergic neurotransmission and the immune system are involved in many bidirectional interactions involving glia, astrocytes, and oligodendrocytes. Particularly, impaired glial clearance of extrasynaptic glutamate may dysregulate synaptic glutamatergic neurotransmission [79]. The adrenergic system is believed perform an anti-inflammatory role via glial cell binding and free radical scavenging [83], reducing excitotoxic, oxidative and amyloid-dependent damage.

The complex regulation of inflammatory activity in the brain involves diverse cell types and signalling pathways, including neurotransmission. While the exact immunological mechanisms contributing to disease progression are unknown and likely complex [75] [74], they

are considered potential therapeutic targets. However, although epidemiological studies have associated anti-inflammatory treatments with a reduced risk of AD and PD [21] [75], clinical trials have failed to replicate these observations [84] [74]. Further work needs to be done to identify molecular markers associated with disease-linked neuroinflammation and potential treatment response [79]. In addition to fluid markers of neuroinflammation, recently developed translocator protein (TSPO) tracers for PET imaging may offer a window into the in vivo spatiotemporal progression [76], although they are impeded by cost, low signal-to-noise ratio, and *TSPO* gene polymorphisms affecting binding [75].

Cerebral blood flow

The brain receives up to one-fifth of cardiac blood output [85], and altered cerebral blood flow (CBF) is a clinically relevant facet of conditions from stroke to hypertension. Many lines of evidence support early and chronic brain hypoperfusion in AD, before other pathological changes or symptom onset [86] [87] [12]. Ageing is associated with a 15% drop in CBF between the ages of 20 and 65, independently of structural alterations [87]. Neuropathologically, small vessel disease (which may include thickened walls, inflammation and edema) is present in the majority of elderly brains, and often co-occurs with amyloid pathology [44]. Contributing to age-associated degeneration, there is also a close relationship between cerebrovascular ageing and immunosenescence [88]. If vascular risk factors (which almost universally reduce CBF) are also present, impaired neuron-astroglial metabolism may result in sufficient ischemia and hypoxia to cause cognitive impairment [87]. Epidemiologically, AD shares these risk factors, such as stroke, hypertension and carotid atherosclerosis, as well as pathology and symptoms with vascular dementia [12] [89].

In addition to the shared epidemiological and neuropathological features, there are AD-associated molecular and cellular correlates of vascular dysfunction. These include amyloid cytotoxicity, impaired amyloid clearance, blood-brain barrier breakdown, and immune and inflammatory dysregulation [90] [89]. Sustained ischemia and hypoxia are believed to induce amyloid pathology [87], which in turn may in turn impair neurovascular function [89]. Furthermore, apolipoprotein E (*APOE*), associated with amyloid clearance in AD, also has a vascular role in lipid metabolism and cholesterol transport [90].

Finally, the close coupling between neuronal activity, metabolism and perfusion requires intercellular signalling between neurons, glia, endothelial cells and blood vessels. The brain modulates cerebral perfusion by i) systemic regulation of blood flow, ii) cerebrovascular autoregulation of arterial wall stiffness in response to blood pressure, and iii) regional, activity-dependent distribution of blood (neurovascular coupling). Neurotransmitters are primarily involved in signalling for vascular regulation (primarily glutamate) [91] and neurovascular coupling (dopamine) [92]. The loss of the vasodilatory cholinergic system may also contribute to impaired blood flow, and this may be the basis of cholinergic symptomatic therapy [90]. Similarly, glutamatergic activity drives glucose metabolism [93], which is closely tied to its bloodborne delivery.

Given its early occurrence and severe consequences on metabolic, inflammatory and neuronal function, vascular dysfunction may have causative, additive, or synergistic contributions to other pathology (a topic further explored in the following chapter). The vascular hypothesis of AD considers hypoperfusion (and hypometabolism) to be the driving force, leading to subsequent neurodegenerative alterations [87] [12]. The synthesis of this evidence linking

vascular, metabolic and inflammatory dysregulation supports their inclusion in potential biomarker definitions of AD [18].

In contrast, cognitive impairment in PD appears to be independent of co-existing vascular pathology [94]. On the wider PD spectrum, vascular lesions are associated with Braak stage in Parkinson's disease dementia (PDD) but not PD [95]. However, vascular PD is a distinct clinical diagnosis used for patients with gait impairment and subcortical white matter lesions, or other pathology consistent with a vascular cause (e.g., stroke or ischemic injury) [96].

Metabolism

The brain is a mass-disproportionate consumer of energy, and vulnerable to damage from insufficient nutrients [19]. A regionally heterogeneous hypometabolism of glucose is also implicated in the cascade resulting in cognitive decline in AD [20]. Historically, the prevailing opinion has held that hypometabolism is a consequence of reduced neural function in AD. The loss of synapses and reduced neurotransmitter production are implicated in the inhibition of mitochondrial enzymes, increased oxidative stress and synaptic dysfunction [97]. These factors would reduce the metabolic demand for glucose due to a loss of function.

However, it has more recently been proposed that hypometabolism is an early event in AD. Notably, carriers of ε4 allele of *APOE* display pockets of cortical hypometabolism decades before AD symptoms appear. A systemic and relatively early deterioration in glucose metabolism, which is common in the elderly, may selectively strain brain regions with a high energetic demand [20]. Dysregulation of glucose metabolism and impaired glycolysis may initiate pathogenic pathways [19]. As a consequence, fuel-deprivation may induce pathologies [87] such as microvascular alterations, tau hyperphosphorylation, regional starvation, atrophy,

amyloid deposition, mitochondrial dysfunction, and oxidative damage via increased gluconeogenesis [20].

In addition to neurons and glial cells, endothelial cells of capillaries in the brain and the blood-brain barrier also undergo structural and oxidative damage in AD [98]. Smooth muscle cells in artery walls are also flattened [99]. Many of the strongest risk factors for AD are in fact vascular, such as a prior history of stroke which doubles the risk of dementia [89]. Vascular and metabolic dysfunctions can lead to cognitive decline, even when CBF is not reduced enough to cause ischemic injury [100]. Furthermore, mitochondrial dysfunction and oxidative damage are also observed in other disorders, such as PD [101]. Thus, vascular and metabolic systems are also potential targets for therapeutics, potentially via receptor pathways.

Neurotransmission

Most of the brain's intense demand for energy [102] is used for synaptic transmission [103]. This function is performed by neurotransmitters, the main signalling molecules of the brain. Neurotransmission is an ancient chemical system, with diverse secretory cell types already present before the evolution of nervous systems [104]. It underlies physiological processes from the cellular scale to cognition, mood, and behaviour. Maintaining optimal intra- and extra-cellular concentrations of neurotransmitters, vesicular transporters, and receptors is a dynamic and carefully regulated process [105], with deviations having severe functional consequences linked to diseases [106]. Notably, synapse loss has been known to be a much stronger correlate of neuropsychological symptoms than plaques and tangles [97]. Neurotransmission is involved in many disease-affected processes with functional consequences. These molecular and cellular processes are critical components of a mechanistic understanding of neurodegenerative disorders, and neurotransmitter receptors are important pharmacological targets [25].

Neurotransmitters can have wide variety of chemical structures, including amino acids (such as glutamate and GABA), monoamines (such as dopamine, serotonin, adrenaline/epinephrine, and histamine), peptides (such as oxytocin and opioid peptides), purines (such as adenosine) and others (such as acetylcholine) [107]. Their receptors are protein structures embedded in cell membranes to which synaptic neurotransmitters bind. Ionotropic receptors are large assemblies of several proteins forming an ion channel through the membrane, whereas G protein-coupled receptors (GPCRs) are usually a single protein [108]. When a neurotransmitter binds to its ionotropic receptor, conformational changes rapidly open the ion channel, while the neurotransmitter is attached or until desensitization. On the other hand, GPCRs respond significantly slower, by activating intermediary GTP-binding proteins, and have long-term effects on neuronal excitability [109]. The nicotinic acetylcholine receptor (nAChR) and the $GABA_A$ receptor are examples of fast ionotropic receptors, whereas the muscarinic acetylcholine receptors and $GABA_B$ receptors are GPCRs.

Neuronal cells can be partially defined by neurotransmitter expression, which offers insight into their functional specialization. Pyramidal neurons are associated with cortical regions, and long-range connections between distant brain regions. They mainly express glutamate, the primary excitatory neurotransmitter. Inhibitory interneurons modulate activity within their vicinity by releasing the neurotransmitter GABA. While it is best known peripherally for its role in neuromuscular junctions, acetylcholine is expressed by excitatory interneurons in the CNS. The monoamine family, comprised of serotonin, and the catecholamines dopamine, adrenaline and noradrenaline, has modulatory roles. Given the complexity of neurotransmission from the sub-cellular to circuit and network levels, there remain

many open questions about the roles of distinct neurotransmitter families, their co-expression and interactions, their sub-cellular pathways of action and their disruption in disease [109].

Neurotransmission is mainly associated with neuron-neuron signalling, with transmitters released from vesicles into the synapse and binding to receptors post-synaptic on the post-synaptic neuron. However, these molecules (neurotransmitters, transporters, and receptors) mediate signalling in a variety of other cell types and cellular structures. Sub-cellular organization is important for signal transmission; autoreceptors on pre-synaptic neurons can modulate neurotransmitter release [110]. The cholinergic system is involved in blood flow regulation via endothelial cells and anti-inflammatory pathways via microglia [111]. While glutamate is primarily associated with its key role as the main excitatory neurotransmitter, its receptors are expressed in many cell types in the brain and periphery [112]. Microglia also express many types, such as glutamatergic, GABAergic, adrenergic, dopaminergic, cholinergic, opioid and cannabinoid receptors [113]. Through volume transmission, they sense their environment and modulate the release of chemicals such as chemokines and cytokines, which in turn affect neuronal function [114]. The effects of these released molecules may be either protective or neurotoxic, and the interplay between these diverse systems is not fully understood [114]. Under normal physiological function, it is believed that active neurotransmission is required to suppress microglial activation [114] [113].

Synaptic energy consumption generally decreases with aging, and, since the number of receptors at a synapse is energetically constrained, receptor systems are also affected [103]. In addition to age-related degradation, in vivo PET imaging studies have provided evidence for receptor binding changes in AD and PD with specific symptomatic correlates.

The roles of specific forms of neurotransmission in NDDs is well established, namely dopaminergic deficit in PD and cholinergic loss in AD [25]. However, both disorders involve dysfunction in multiple additional neurotransmitter systems, often with robust symptomatic associations. While not considered primarily a neurotransmitter disease, AD is associated with long-term receptor-induced degeneration, such as excessive glutamatergic excitotoxicity leading to neuronal death [32] and the basal forebrain cholinergic system suffers early degeneration, the degree of which is correlated with clinical progression [48]. Beyond the cholinergic and glutamatergic system, serotonin- and norepinephrine-producing neurons are also damaged [115]. Neurons belonging to different neurotransmitter systems show differential sensitivity to amyloid toxicity, with cholinergic neurons being the most vulnerable, followed by serotonergic, dopaminergic, and least of all GABAergic neurons [116].

Recent studies have correlated spatial variability in neurotransmitter gene expression with neurovascular [117] and structural-functional decoupling [118] in PD. Furthermore, specific neurotransmitter-symptom associations have been identified, such as cholinergic freezing of gait and dementia [119], serotonergic depression and tremor [120], and adrenergic postural symptoms [121]. These pathways are depicted in Figure 2.3. The multi-neurotransmitter involvement in PD is acknowledged by the dual syndrome hypothesis [122], which posits that dopamine-mediated fronto-striatal executive impairment and cholinergic visuospatial dementia are co-occurring processes.

For decades, neurotransmission has been a key pharmacological target for AD and PD [123] [124]. Cholinesterase inhibitors (ChEIs) have been used to increase cholinergic neurotransmission as symptomatic therapy for dementias due to AD, PD, vascular dementia or Lewy body disease [125], and the NMDA antagonist memantine is used to reduce glutamatergic

excitotoxicity [25]. The standard for PD treatment has been dopaminergic therapy using precursors such as levodopa, although this can result in treatment non-response as well as severe side effects [123] [126].

In the following subsections, a brief overview of the role of major neurotransmitter families is provided, along with molecular and clinical evidence of dysfunction in AD and PD.

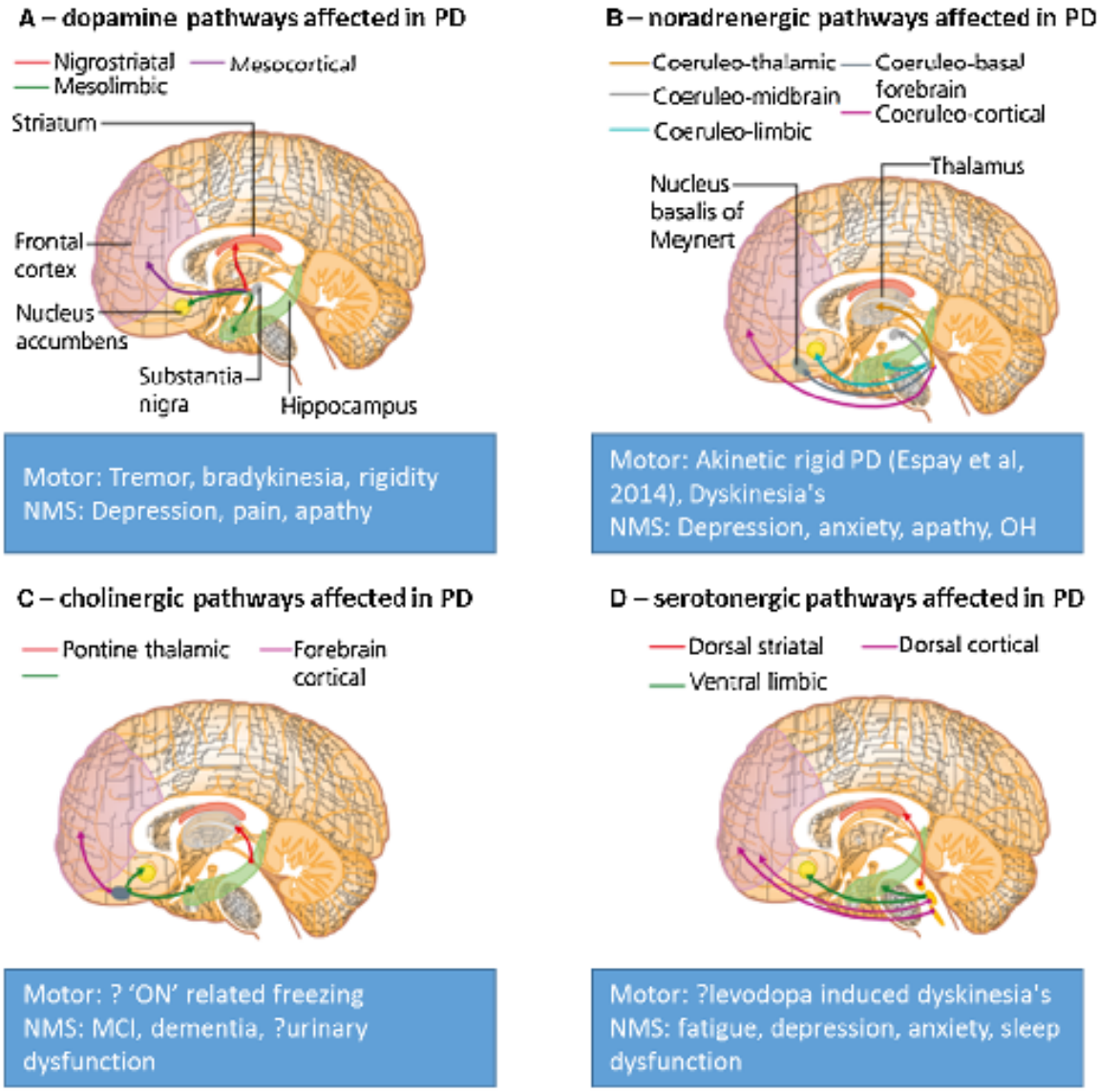

Figure 2.3. Multi-neurotransmitter dysfunction in PD.
Figure adapted with permission from [24].

Acetylcholine

Acetylcholine (ACh) is a prominent neurotransmitter in both the central and peripheral nervous systems. In the brain, cholinergic neurotransmission is associated with attention, learning, memory, stress, and sleep cycle regulation [127]. Cholinergic neurons in the brain may be projection neurons, involved in long-range connections, or interneurons participating in local circuits. Cholinergic receptors may be ionotropic nicotinic receptors or muscarinic GPCRs, with the latter influencing a diverse range of cation channels to enable either hyper- or de-polarization [127]. While muscarinic receptors are usually excitatory in cortical regions (although inhibition is also possible) [127], nicotinic receptors are believed to have a modulatory role [127].

The nucleus basalis of Meynert in the basal forebrain is the main source of cholinergic input to the hippocampus, amygdala and prefrontal cortex, involved in attention and memory [127]. In AD patients, these cholinergic projection neurons are lost [128]. Simultaneously, depolarization-induced acetylcholine release, uptake of the precursor choline and activity of the ACh-synthesizing enzyme choline acetyltransferase are also reduced [128]. This evidence of selective vulnerability and symptomatic association is the basis of the cholinergic hypothesis of AD [128]. Similar cholinergic loss is also observed in other neurodegenerative disorders such as PD, where the severity of neuronal loss is correlated with cognitive impairment [119], suggesting a shared mechanism contributing to dementia across disorders. Acknowledging this cholinergic component, the dual syndrome hypothesis of PD proposes that distinct processes underlie different aspects of neuropsychological presentation: dopaminergic denervation of fronto-striatal circuits leads to executive impairment, while the cholinergic system contributes to memory and visuospatial dysfunction that leads to dementia [122].

There is evidence for the interaction of the cholinergic system with other pathophysiological factors [129], such as amyloid- and tau-producing molecular pathways. Neurofibrillary tangles are higher in individuals taking muscarinic antagonist medication [130], and acetylcholine loss has also been implicated in a vascular pathway, via disruptions of neurovascular coupling in AD [131]. In relation to amyloid, the cholinergic system may have a neuroprotective role; stimulation of cholinergic receptors may increase non-amyloidogenic APP metabolism, and anti-muscarinic therapy increases amyloidogenic metabolism [128] [130]. For decades, one of the few clinically effective symptomatic treatments of AD (and more broadly other dementias) has been cholinesterase inhibitors, which increase the levels of acetylcholine available at synapses [129].

Glutamate

Glutamate is by far the most abundant neurotransmitter in the mammalian brain, with concentrations 3 orders of magnitude above those of dopamine, norepinephrine, and serotonin [132]. As the main excitatory neurotransmitter expressed widely throughout the brain, it is highly co-localized with functional activity [133]. Glutamatergic synaptic transmission is mediated by a variety of receptors serving specialized roles, from ionotropic N-methyl-d-aspartate (NMDA), α-amino-3-hydroxy-5-methyl-4-isoxazolepropionic acid (AMPA) and kainate receptors to the metabotropic receptor family [134]. They are involved in critical aspects of learning and memory; for example, long term potentiation/depression is a form of synaptic plasticity elicited by the coincident activity of pre- and post-synaptic neurons. The process is activated by the stimulation of NMDA receptors and involves the addition or removal of AMPA receptors at the synapse [135].

Maintaining appropriately low levels of extracellular excitatory neurotransmitter concentrations is important for a high signal-to-noise ratio, and to avoid neuronal hyperactivity, which can lead to cell death [132]. Astrocytes are heavily involved in maintaining this extracellular homeostasis and recycling neurotransmitters such as glutamate and γ-aminobutyric acid (GABA) [136]. There is a close relationship between glutamate recycling and glucose metabolism [137], with an increase in glucose uptake at glutamate release [138].

Glutamate-induced excitotoxicity is implicated in cell death across neurodegenerative disorders, including AD and PD [139]. Excitotoxicity may also be triggered by other pathophysiological conditions, such as ischemia [140]. Under disrupted oxygen or glucose access, AMPA and kainate receptors appear to mediate oligodendrocyte death and axonal loss via hypoxic-ischemic damage [141]. The effects of amyloid may be specific to sub-cellular structure, promoting extra-synaptic NMDA response in low concentrations (by limiting glutamate uptake and causing glutamate spillover) but inducing synaptic depression (by reducing NMDA receptor activity and inducing its endocytosis) at higher concentrations [142] [143]. Additionally, excessive tau leads to NMDA receptor hyperactivity via the kinase Fyn [142], flooding neurons with dangerous levels of calcium. Conversely, excessive extra-synaptic NMDA activity may also lead to tau overexpression [144]. Believed to inhibit these pathways of excitotoxicity, NMDA receptor antagonists such as memantine are used for symptomatic treatment in AD [142].

Dopamine

Dopaminergic neurons are primarily found in the midbrain, mainly projecting to various brain regions from the substantia nigra pars compacta (SNc) and ventral tegmental area (VTA) [116]. Via the meso-striatal pathway (linking the SNc to the caudate and putamen nuclei) and glutamatergic corticostriatal projections, the dopaminergic system is involved in controlling

voluntary movement. Dopamine is also involved in reward via the meso-cortico-limbic pathway, from the VTA to the hippocampus, cortex and nucleus accumbens [116].

In neurodegenerative diseases, dopamine is most associated with the dysfunction of the meso-striatal pathway, where the loss of striatal dopaminergic signalling results in increased GABAergic inhibition of thalamo-cortical connections and subsequently the motor symptoms of parkinsonism [101]. As shown in Figure 2.4, this occurs due to dopaminergic neuronal death and reduced dopamine synthesis in the substantia nigra pars compacta (SNpc). The dopamine precursor levodopa is the basis of pharmacological treatment of PD, and non-pharmacological treatments such as deep brain stimulation (DBS) are used to target this circuit when dopaminergic therapy fails [145].

However, other conditions also involve dopaminergic degeneration. Ageing is also associated with reduced dopaminergic neurotransmission, lower expression of some D_2 receptor subtypes, and decreased dopamine transporter (DAT) expression in several regions [116]. Apathy and executive dysfunction are also linked to the impairment of dopaminergic neurotransmission, and the subsequent effects in areas with dopaminergic projections such as the frontal and prefontal cortices [116]. In AD patients, dopamine modulates the excitability of cortical cholinergic neurons [146], the binding potential of hippocampal D_2 dopaminergic receptors correlates with memory performance [147], and the presence of dopamine-related symptoms is associated with worsened clinical progression [116].

The wider catecholaminergic system, which includes dopamine, noradrenaline and adrenaline, displays complicated receptor alterations in AD [25]. Receptor densities may be either reduced or increased, potentially due to compensatory mechanisms. Dopaminergic also has

wide-ranging influence on other disease-affected processes, such as its mediation of neurovascular coupling [92].

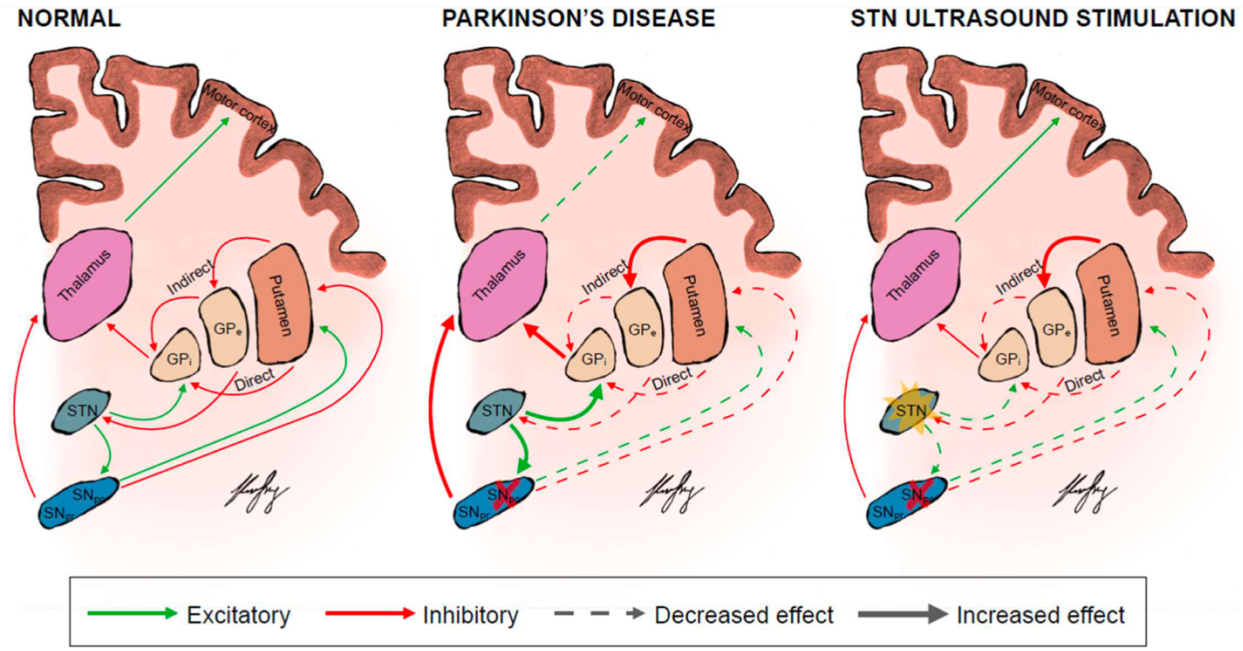

Figure 2.4. The basal ganglia circuit in PD.

Under normal conditions, the direct pathway enables movement, while the indirect pathway inhibits it. In PD, the loss of dopaminergic function in the substantia nigra pars compacta (SNpc) results in increased inhibitory signaling to the thalamus, resulting in motor symptoms. This circuit is targeted pharmacologically as well as surgically, with the subthalamic nucleus (STN) being an important stimulation target for focused ultrasound. Figure adapted with permission from [148].

GABA

The primary inhibitory neurotransmitter γ-aminobutyric acid (GABA) is synthesized from glutamate [149] [150]. It regulates neuronal excitability and maintains an appropriate excitatory/inhibitory (E/I) balance, which are critical factors for memory formation, learning and cognition among other functions [150]. Although GABAergic interneurons initially appeared to be spared in AD, there is evidence for a GABAergic role. While the disrupted E/I balance is partially explained by glutamate and acetylcholine, GABAergic compensatory mechanism

initiated by amyloid-induced, glutamate-triggered $GABA_A$ receptor response may also be involved [150].

GABA is a common pharmacological target for anaesthesia, with evidence linking general anaesthesia with tau pathology [151]. In cultured neurons, GABA receptor activation increased tau hyperphosphorylation [152]. Conversely, in transgenic mice, tau appears to hyperactivate GABAergic interneurons, hinting at a potential positive feedback loop in AD. [152]

Adrenaline

At the behavioural level, the adrenergic system is involved in functions such as attention, learning and memory [153]. The locus coeruleus (LC), a brainstem structure containing half the adrenergic system [153], is an early site of neurodegenerative pathology across disorders [154]. In AD, the LC loses approximately 70% of its neurons [153]. Tau deposition and neurodegeneration occurs early in the pre-symptomatic phase of AD, while α-synuclein deposition also occurs here in PD [154] [155] [156]. Degeneration of the LC is even better correlated with AD onset and duration than the cholinergic nucleus basalis of Meynert [157]. The locus coeruleus projects to the hippocampus, which is associated with memory deficiency in AD. The α_1 adrenergic receptor, which is involved in hippocampal memory and learning, undergoes alterations in AD, and has been proposed as a potential therapeutic target [158].

The adrenergic system is also involved in interactions with various pathophysiological factors. The noradrenergic system is implicated in the tau hyperphosphorylation cascade; amyloid oligomers bind to the α_2 receptor, which signals glycogen synthase kinase 3 (GSK-3β) activation and tau phosphorylation [159]. Rodent models of PD also suggest that the adrenergic system plays a protective role against neuroinflammation and neurodegeneration [160].

Additionally, the α_2 adrenergic in cerebral microvessels receptors increased by approximately 60%, while the α_1 receptor is reduced by approximately 25% in the cortices of AD patients, but not in normal ageing [161]. Furthermore, agonistic autoantibodies of the α_1 adrenergic receptor were found in 50% of AD patients [162], suggesting an involvement with immune response.

Serotonin

Serotonin, or 5-hydroxytryptamine (5-HT), has a variety of functions as a neurotransmitter and a hormone. As the latter, it is involved with glucose homeostasis and adiposity [163]. In the brain, it is associated with mood, anxiety and sleep, and is an important pharmacological target in psychiatric disorders. Notably, patients of neurodegenerative diseases experience psychiatric symptoms at heightened rates, with estimates ranging from half to over two-thirds of dementia patients suffering from depression [164] [165] . The use of the most common class of antidepressants, selective serotonin reuptake inhibitors (SSRIs), is linked to a statistically significant improvement in cognitive performance on the Mini-Mental State Examination (MMSE) [164]. [166]. It must be noted that many antipsychotics used in psychiatric contexts act on multiple neurotransmitter systems, such as Risperidone (a dual dopamine and serotonin receptor antagonist), sometimes with unclear mechanisms [25] [25].

Elements of the serotonergic system are selectively altered in AD, with more severe depletion of serotonin in early-onset AD brains. The concentrations of $5HT_2$ receptors are generally reduced while the loss of $5HT_2$ receptors has region-specific correlations with aggression (temporal cortex) and cognitive decline (hippocampus) [167] [168] [25]. Stimulation of $5HT_{4A}$ serotonergic receptors promotes a non-amyloidogenic cleavage of amyloid precursor protein (APP), and is considered neuroprotective [169]. In PD patients, cortical serotonin transporter density varied inversely with PET-derived amyloid load [170].

Serotonin and the catecholamines (adrenaline, epinephrine and dopamine) also have important roles in the gastrointestinal system, controlling blood flow, gut motility, nutrient absorption, innate immunity and the microbiome, with known alterations in PD [171]. Although serotonin cannot cross the blood-brain barrier, the peripheral serotonergic system also exerts effects on the brain via the vagus nerve [172] [163].

Imaging pathophysiology

Many of the dysfunctional systems in NDDs are imaged in clinical and research settings (Figure 2.5). This section provides a brief overview of the physical mechanisms behind common neuroimaging modalities, such as magnetic resonance imaging (MRI), positron emission tomography (PET), and single-photon emission computed tomography (SPECT), particularly to characterize the spatial distributions of pathology in living subjects. In addition, the biological relevance and utility in studying AD and PD is discussed.

Structural MRI

Structural MRI modalities are used to non-invasively evaluate macroscopic changes to gray and white matter. MRI is based on the principle of nuclear magnetic resonance (NMR); nuclei in a strong magnetic field produce an electromagnetic signal when perturbed by a secondary, weaker oscillating field. In a scanner, a strong external magnetic field aligns the magnetic moments of hydrogen nuclei (i.e., protons) in tissue, and a secondary radio frequency (RF) pulse is then applied perpendicularly to perturb the magnetization. This new net magnetization has two components: longitudinal and transverse, and the precession of the transverse component around a receiver coil induces a current, which in turn produces the MR signal and resulting image. By applying the external magnetic field as a gradient, the source of

the MR signal can be determined. When the secondary RF pulse is turned off, the magnetization of nuclei exponentially decays to equilibrium with the magnetic field. Tissue-specific properties influence the spin-lattice/longitudinal (T1) and spin-spin/transverse (T2) relaxation times, which forms the basis of contrast in structural images.

Parameters of the magnetic field gradient and RF sequences, such as the repetition time (TR) between applied pulse sequences and the time to echo (TE) between applied and received pulses, can be modulated to enhance contrast in the signal. This allows images to be sensitive to specific tissue properties, such as fat and water content. Common pulse sequence schemes include spin echo (produced by pairs of RF pulses and used for T1- and T2-weighted images), gradient echo (where a dephasing gradient field is followed by a rephasing gradient of the opposite polarity, used in functional MRI), and echo planar (where the gradient is rapidly and repeatedly reversed, used in diffusion-weighted MRI).

Some of the most common and well characterized types of MR images are T1- and T2-weighted scans. Produced using short TE and TR, anatomical structures and gray matter have a higher signal in T1-weighted images. Using longer TE and TR, T2-weighted images are instead determined by the spin-spin or transverse relaxation time (T2), which describes how quickly protons go out of phase after the RF pulse is applied. T2-weighted images are typically used to image white matter structures. The resulting images can be further processed to obtain surface- or volume-based estimates, such as cortical thickness, surface area and gray matter density.

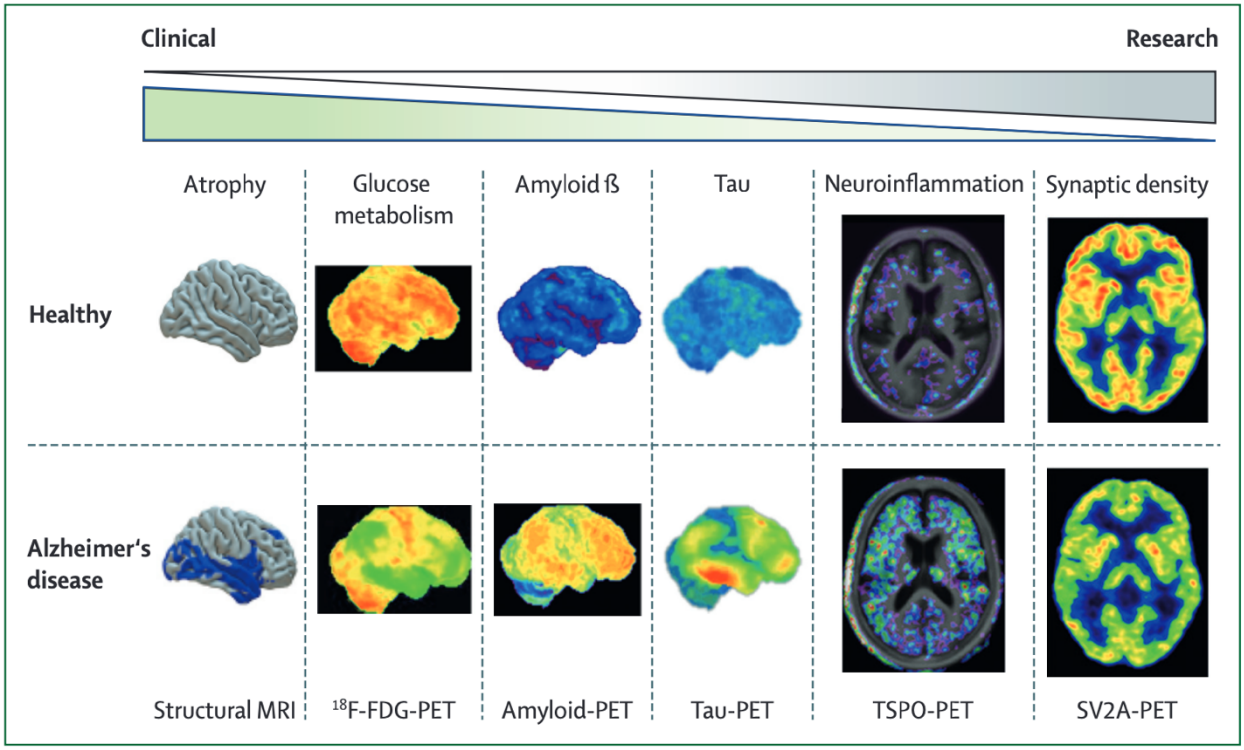

Figure 2.5. Common clinical and research applications of neuroimaging in AD. While some imaging modalities, such as T1 MRI and its resulting gray matter atrophy maps, are established tools in clinical practice, other modalities are emerging with newly validated molecular tracers (e.g., TSPO and SV2A). Figure adapted with permission from [173].

Gray matter density

By definition, neurodegeneration implies tissue loss. Topographical patterns and rates of atrophy are correlated with cognitive impairment [174], for the whole brain and specific regions. In AD, atrophy canonically begins in the medial temporal lobe (including the hippocampus), and extending along a temporal-parietal-frontal progression [175]. Subtype analysis suggests the presence of consistent spatial patterns of atrophy in AD: atypical, limbic-predominant, hippocampal-sparing and mild patterns [176] [177]. In PD, gray matter atrophy is also observed, associated with dementia, predictive of dopaminergic treatment response [178], and distinct between motor subtypes [179]. In non-demented PD patients, performance on multiple cognitive domains is correlated with regional gray matter volume [180].

T1/T2 ratio

The ratio of T1 to T2 signal, while originally presumed to reflect myelin content [181], has become a measure of microstructural integrity [182] [183]. A major practical advantage is the use of images from the two most ubiquitous scanning protocols. Furthermore, compared to diffusion MRI metrics, the T1/T2 ratio is not susceptible to the crossing fiber problem. While the precise interpretation of the T1/T2 signal is unresolved [184], it correlated strongly with dendrite density in MS patients [185]. The T1/T2 ratio thus provides a view of tissue microstructure that is complementary to measures such as myelin water fraction, fractional anisotropy and mean diffusivity, with which it shares low covariance [182].

Diffusion MRI

The motion of molecules such as water in biological tissue is constrained by microstructure, primarily axonal membranes, and modulated by properties such as myelination [186]. Diffusion-weighted MRI exploits this property to obtain a signal that is sensitive to the diffusive freedom of water molecules along different directions, which reflects microstructure. This is usually achieved via the phase dispersion in multiple (6+) non-collinear directions. Commonly used pulse sequences rely on the attenuation of spin rephasing due to the motion of molecules between pulses. Due to its sensitivity to cellular architecture, diffusion MRI is useful for quantifying various aspects of tissue microstructure [187] and connectivity through tractography [188] [189].

Fick's first law of diffusion describes the diffusive flux vector J of a particular molecule with a concentration $\boldsymbol{C}$ at position $\mathbf{r}$ and time t as

$$\boldsymbol{J}(\mathbf{r}, \boldsymbol{t}) = -\boldsymbol{D}\nabla\boldsymbol{C}(\mathbf{r}, \boldsymbol{t}),$$

where D is the diffusion tensor (in the general case of anisotropic diffusion)

$$\boldsymbol{D} = \begin{bmatrix} D_{xx} & D_{xy} & D_{xz} \\ D_{xy} & D_{yy} & D_{yz} \\ D_{xz} & D_{yz} & D_{zz} \end{bmatrix}.$$

In a small volume, the change in concentration can be described as function of the flux

$$\frac{\partial C}{\partial t} = -\nabla \cdot J(\mathbf{r}, \boldsymbol{t}),$$

which leads to Fick's second law

$$\frac{\partial C}{\partial t} = \boldsymbol{D}\nabla^2 \mathbf{C}(\mathbf{r}, \boldsymbol{t}).$$

The spatiotemporal probability of finding a particle is defined by

$$\mathbf{P}(\mathbf{r}, t) = \frac{\mathbf{C}(\mathbf{r}, \boldsymbol{t})}{\boldsymbol{N}}.$$

With anisotropic diffusion, the probability of a particle being displaced from $\boldsymbol{r_0}$ to $\boldsymbol{r}$ is given by [190]

$$\mathbf{P}(\mathbf{r}|\mathbf{r_0}, t) = \frac{\mathbf{1}}{\sqrt{|\mathbf{D}|(\mathbf{4}\pi t)^{\mathbf{3}}}} e^{-\frac{(\mathbf{r}-\mathbf{r_0})^T \boldsymbol{D}^{-1}(\mathbf{r}-\mathbf{r_0})}{\mathbf{4}t}}.$$

The Bloch-Torrey equation [191] modifies the Bloch equation (describing the temporal evolution of the magnetization vector $\boldsymbol{M}$) to account for diffusion:

$$\frac{d\boldsymbol{M}}{dt} = \underbrace{\gamma \boldsymbol{M} \times \boldsymbol{B}_0}_{\text{Magnetic torque}} + \underbrace{\begin{pmatrix} -\frac{M_x}{T_2} \\ -\frac{M_y}{T_2} \\ \frac{M_0 - M_z}{T_1} \end{pmatrix}}_{\text{Relaxation}} + \underbrace{D\nabla^2 C}_{\text{Diffusion}},$$

where T_1 and T_1 are the relaxation time constants, M_x and M_y are the transverse components, M_z is the longitudinal component, and B_0 is the magnetic field vector. In diffusion-weighted imaging (DWI), the baseline MR signal S_0 experiences exponential decay [192]

$$S = S_0 e^{-bD},$$

where D is the (scalar) diffusion coefficient and the b-value determines the diffusion weighting. In practice, pulse sequences may vary, but for a pure rectangular pulse, this is given by the Stejskal-Tanner formula

$$b = \gamma^2 \delta^2 G^2 (\Delta - \frac{\delta}{3}),$$

where γ is the gyromagnetic ratio, δ is the gradient duration, G is the gradient magnitude and Δ is the time interval between gradient onset and the refocusing pulse.

While in diffusion tensor imaging (DTI),

$S = S_0 e^{-BD}$,

The diffusion tensor can be estimated from a series of diffusion-weighted images with different gradient directions.

The primary uses of diffusion MRI as quantitative markers of disease progression arise from measures relating to microstructure, and connectomes reconstructed from fiber tractography [189].

Microstructural measures from diffusion imaging

Scalar quantities derived from the diffusion tensor are interpreted as measures of microstructural integrity [182]. From an eigendecomposition of the diffusion tensor, we can obtain several quantities such as axial diffusivity (AD), radial diffusivity (RD), fractional anisotropy (FA) and mean diffusivity (MD).

- AD is the eigenvalue of the diffusion tensor along the primary axis:
    - $\mathrm{AD} = \lambda_1,$
- RD is the average of the eigenvalues along the axes perpendicular to the main direction of diffusion:

$$\mathrm{RD} = \frac{\lambda_2+\lambda_3}{2}.$$

The quantities are usually interpreted to reflect tissue properties along these axes; AD is assumed to reflect axonal density, while RD is a measure of myelination.

- MD is the average of all the eigenvalues of the diffusion tensor:

$$\mathrm{MD} = \frac{\lambda_1+\lambda_2+\lambda_3}{3},$$

and thus represents an overall measure of the mobility of water molecules in all directions. Increased MD is associated with edema.

- FA is a measure of the directional freedom of diffusion:

$$\mathrm{FA} = \sqrt{\frac{1}{2}}\frac{\sqrt{(\lambda_1-\lambda_2)^2+(\lambda_1-\lambda_3)^2+(\lambda_2-\lambda_3)^2}}{\sqrt{\lambda_1^2+\lambda_2^2+\lambda_3^2}}$$

FA is high in directed tissue, such as most white matter regions, and low in more isotropic tissue such as gray matter [193]. Changes to FA are associated with axonal integrity.

It is usually assumed that AD corresponds to axonal density, RD reflects myelination, MD is a measure of edema, and FA quantifies axonal integrity. However, these quantities are indirect measures of diffusive freedom, and have ambiguous links to specific tissue alterations. For example, FA may decrease due to reduced myelination, axonal density, or axonal coherence [194]. Co-existing pathological mechanisms (e.g., inflammation, axonal injury and demyelination) can confound interpretation [195]. Ex vivo histopathological studies in animals also question any simple injective interpretations. While diffusion measures are sensitive to white matter pathology, the correspondence between AD and RD and histological markers of axonal density and myelination depends on the scale of analysis (e.g., pixel/voxel-scale vs. ROI-based) and type of pathology (e.g., mouse spinal cord contusion injury vs. multiple sclerosis-type lesions) [196]. FA matches immunofluorescence markers of myelin in two-photon laser

microscopy of mouse brains, particularly in white matter regions with consistent fiber orientations and low dispersion, while RD is inconsistently associated with myelin in white matter [197].

Furthermore, the mathematical assumptions behind these interpretations may not be valid in all cases due to complex fiber geometry within each voxel. Biophysical models are typically used to estimate tissue microstructure from the diffusion MRI signal; axons are typically modeled as straight cylinders, and potential undulating trajectories may lead to an overestimation of properties such as diameter [192]. Diffusion measures such as FA can also suffer from the "crossing fibers" problem; voxels containing orthogonal fibers will have a low FA suggesting the absence of directed structure [193]. A variety of biophysical models attempt to account for tissue complexity, from the simple ball-and-stick model to multi-compartment models considering extra-axonal space [192] [198].

Despite ambiguous interpretation, DTI-derived measures can be useful features for quantifying white matter integrity, showing alterations in ageing [194], AD [199] and PD [200]. Gray matter is assumed to contain more heterogeneous tissue with more problematic interpretation. However, diffusion measures can still be informative; PD patients exhibit higher subcortical gray matter MD compared to controls [201], and cortical MD is sensitive to longitudinal alterations in the AD continuum [202].

Estimating macroscopic brain connectivity from the diffusion weighted imaging

Neuronal communication necessitates connectivity at various spatial scales from local circuits to macroscopic brain networks. The physical substrate of this connectivity is the myelinated axon bundles that make up white matter. By stitching together information from the

diffusion MRI signal from neighbouring voxels at various orientations, these bundles can be reconstructed through the process of fiber tractography [203].

Typically, local (voxel) fiber orientations are used to define a three dimensional vector field, with long-range fiber connections as streamlines of this field. However, complex tissue architecture, with different orientations, can be present simultaneously in each voxel. The simplest methods assume a single deterministic fiber orientation per voxel from the diffusion tensor, whereas higher-order methods define a probabilistic fiber orientation distribution function (fODF) [204]. From reconstructed tracts and streamlines, a whole-brain connectome can be generated. Generally, the edges between the regions of interest are weighted by the number of reconstructed streamlines.

In contrast to experimental methods for microscopic connectivity mapping (such as light microscopy, tract tracing, electron microscopy, etc.), diffusion tractography is non-invasive but limited to macroscopic analysis (i.e., at the scale of brain regions). Diffusion tractography cannot resolve the direction of connectivity, and it can be difficult to determine the origin and end points of fiber tracts. As tractography does not directly image the connections, it must be kept in mind that generated tracts and connectomes are, to some extent, a virtual construct rather than a ground truth confirmation of connectivity between two regions [205].

Nevertheless, fiber tractography has been a useful tool in characterizing the structural connectivity of the brain. The resulting connectomes can themselves be studied using the framework of graph theory [188]; concepts such as centrality, modularity and global efficiency are frequently used to describe and interpret individual and group differences in connectomics [206]. Another downstream application of particular relevance to neurodegenerative disorders is

the structural connectome-based modeling of pathology spreading, covered in Chapter 3 [207] [208] [209] [210].

Functional MRI

In the 1980s, the activation-dependent increase in blood oxygenation was observed by PET studies [211]. The magnetic susceptibility of blood is oxygenation dependent; deoxyhemoglobin is paramagnetic, while oxygenated hemoglobin is not. Blood oxygenation can thus modulate the dephasing of NMR signal in blood and nearby tissue [212]. Consequently, this blood oxygenation dependent (BOLD) signal can be observed via the T2* parameter, which is the transverse relaxation rate in the presence of inhomogeneities due to intrinsic imperfections in the magnetic field or tissue-induced field distortions [213].

In functional MRI (fMRI), BOLD signal has been used as a proxy of neuronal activity without the need for an exogeneous contrast agent [214]. As a result of its non-invasive methodology, fairly high spatial and temporal resolution, and integration with other common MRI protocols, fMRI has overtaken PET as the technique of choice for functional imaging [215].

While fMRI is often used to investigate the neural correlates of task performance, resting state functional activity (rs-fMRI) has emerged as a potential marker of neurodegenerative disorders such as AD [216]. Metrics based on functional connectivity (FC) are popular, derived from the temporal correlations in the BOLD signal between brain regions. Age-related alterations in resting state activity have been observed, with purported mechanisms including white matter degeneration, neurotransmission dysfunction and proteinopathy deposition [217]. As an alternative to measures, such as FC and regional homogeneity, that integrate information across brain regions, localized measures such as the fractional amplitude of low frequency fluctuations (fALLF) are also altered in disease [218]. These low frequency fluctuations seem to be localized

in gray matter [216]. FC, FC dynamics and fALFF are similarly informative rs-fMRI measures for classifying AD, and the marginal information gain from combining the metrics is minimal [219]. In distinguishing PD patients from controls, fALFF has 92% sensitivity and 87% specificity [220].

Finally, the BOLD signal is not a perfect representation of neuronal activity. There is the risk of contamination from non-neuronal fluctuations (e.g., cardiac and respiratory cycles) and bulk head motion [216]. Technically, fMRI reflects the hemodynamic response to mass neuronal activity [215]. This hemodynamic origin must be kept in mind when interpreting fMRI data in the context of other related modalities (e.g., FDG-PET for glucose metabolism and ASL MRI for CBF). There are several biochemical steps separating synaptic transmission, calcium dynamics, metabolic demand, neurovascular coupling and the BOLD signal measured by fMRI. This leaves the precise timing, cellular source and neurotransmission systems responsible for activity unresolved [221]. The signal also reflects dynamically changing factors, such as hemodynamic response function, which can vary spatially between brain regions and temporally across contexts [215].

Arterial spin labeling

Given the physiological and clinical importance of CBF, many methods have emerged to image brain hemodynamics using PET, SPECT, MRI, computed tomography (CT), and ultrasound [222]. These modalities vary in their clinical practicality, sensitivity, spatial coverage, and resolution. Arterial spin labeling (ASL) is a technique to measure perfusion using MRI without the use of a contrast agent, by magnetically “tagging” endogenous water molecules upstream of the target tissue. This allows relatively fast and convenient perfusion imaging during routine MRI scanning. While methods for labelling vary, the core idea of ASL is to measure the

small downstream change in MR signal due to the flow of (e.g., inverted magnetization), typically by subtracting a control image from the tagged acquisition [223]. This flow-weighted map can then be converted into a perfusion map.

The flow signal is a small fraction (~1%) of the background signal [222]. A high signal-to-noise ratio is needed to observe changes; ASL cannot detect flow that is below a certain threshold (~10mL/100g per minute) [222]. Due to the subtraction of the two images, ASL is sensitive to motion. Furthermore, signal from large vessels is suppressed, and the flow in micro-vessels is emphasized. Generally, ASL predicts blood flow well in gray matter, with retest consistency in the same subjects [222]. Technical advances and clinical studies have validated the relevance of ASL-derived measures of CBF alterations in the AD continuum [224] [87].

Molecular imaging with PET and SPECT

Unlike structural and diffusion MRI, which primarily image anatomical structures, molecular imaging aims to measure the spatial distribution of specific molecules which are involved in critical biochemical processes. This is often achieved using an injected radiopharmaceutical contrast agent that crosses the blood-brain barrier, binds to the target molecule, and contains an isotope that produces ionizing radiation. The produced photons are measured by detectors and then a three-dimensional image is reconstructed tomographically. In positron emission tomography (PET), proton decay in the radioisotope emits a positron, and its annihilation with a nearby electron creates a pair of gamma energy photons. These photons travel in opposite directions, and PET scanners are designed for the coincident detection of such photon pairs. In single-photon emission tomography (SPECT), gamma radiation is directly emitted by the isotope, and a collimator is used to restrict the photon acceptance again for spatial precision.

PET radiolabels typically use the isotopes ^{18}F (with a half-life of 110 minutes) or ^{11}C (with a half-life of 20 minutes) [225], and ^{123}I is a common SPECT isotope [226].

While PET generally has superior resolution and sensitivity, practical considerations and availability may favour SPECT in some applications [225]. PET spatial resolution is constrained to the millimeter scale by fundamental physical effects, such as positron travel between production and annihilation and acollinearity of emitted photons [227]. Both PET and SPECT are also limited by (detector or collimator) geometric response, photon penetration and scattering [228]. However, some effects can be negated through technological modifications (e.g., simultaneous MRI-PET to reduce positron travel with an external magnetic field) or modeled and corrected during reconstruction (e.g., correction of attenuation due to tissue traversal, and improved source estimation using time-of-flight).

Lacking a collimator, PET is more sensitive to emission events, has higher spatial resolution and uses isotopes with significantly shorter half-lives compared to SPECT. Although this latter point allows higher doses to be used during the scan, it presents logistical difficulties and requiring cyclotrons onsite [228]. More importantly, the availability of radiotracers constrains PET and SPECT imaging to specific molecules [229]. This is particularly evident in neuroimaging applications, where radiopharmaceuticals are further limited by the extremely selective permeability of the blood-brain barrier [230].

When tracers are available for the molecule of interest, PET and SPECT offer an unmatched ability for in vivo imaging. Radiolabel development strives for high affinity, high specificity, ease of radiosynthesis, blood-brain barrier penetration, uptake into the structure of interest, in vivo stability and well characterized kinetics [225]. In recent years, amyloid and later tau PET tracers have been established in research and clinical practice for AD and related

disorders [231]. There are also ongoing efforts to develop tracers for other protein aggregates, such as α-synuclein and TDP-43, as well as other relevant markers such as glial activation and myelin [232] [233] [234]. These developments in molecular imaging can enable the in vivo quantitative assessment of increasing numbers of biochemical processes, and support a biological definition of neurodegenerative disorders [235] [236].

FDG PET

The radiotracer 2-[fluorine-18]fluoro-2- deoxy-d-glucose (FDG) is used to assess glucose metabolism. FDG is one of the most common PET tracers, and an established component of the clinical workflow in fields ranging from oncology and neurology. Hypometabolism due to reduced activity in glutamatergic synapses and astrocytes is an early marker of future progression to AD in individuals with mild cognitive impairment [173]. When patients have similar memory test performance, patterns of hypometabolism show differences between AD, DLB, FTLD and other neurological disorders [237].

Amyloid PET

One of the main insights from PET imaging is the spreading of proteinopathy, which could previously only be characterized semi-quantitatively during neuropathological examination [238]. PET tracers for amyloid, such as Pittsburgh compound B (PiB), florbetapir, florbetaben and flutemetamol, have also been established in research and clinical settings [231]. PiB binds to different variants of extracellular amyloid plaques as well as vascular deposits [231]. Amyloid PET shows more diffuse spreading, unlike characteristic regional vulnerability to tau pathology and neurodegeneration in AD [48]. Amyloid PET can be positive in cognitively normal individuals, particularly older APOE4 carriers, and in other neurodegenerative disorders at increasing rates with age [239].

Tau PET

Tau PET tracers such as flortaucepir have emerged in the past decade [231], allowing the characterization of spatiotemporal spreading patterns of tau and comparison with post-mortem Braak stages [56] [240]. Epidemic spreading models of tau PET data suggest that, while anatomical connectivity explains tau propagation patterns, the regional presence of amyloid may accelerate tau spreading [241]. Subtypes of tau deposition trajectories have been identified in AD [242], and distinct tau spatial patterns correspond to atrophy subtypes [177]. Based on modeling, tau pathology may influence memory performance differently during disease progression; via reduced functional connectivity in cognitively unimpaired individuals, but posterior hippocampal atrophy in mild cognitive impairment patients [243].

The primary clinical utility of tau PET imaging is differential diagnosis of AD from other neurodegenerative conditions. However, this is less effective in mild cognitive impairment and other tauopathies cannot be reliably identified, partially due to overlap in regions with off-target binding [244]. Nevertheless, among imaging biomarkers, tau PET corresponds to cognitive decline better than hippocampal volume, amyloid PET and CSF measures [245] [246], and has established itself in biomarker-based definitions of AD, such as the A/T/N framework [236].

Neurotransmitter receptors and transporters

Molecular imaging modalities such as PET and SPECT have also enabled the in vivo spatial characterization of neurotransmitter receptors and transporters. Common clinical applications range from the dopaminergic system in movement disorders [226] to the serotoninergic system in psychiatric disorders [225].

Although PET spatial resolution is superior, SPECT is cheaper and does not require on-site cyclotron facilities. For these reasons, it is widely used in the clinic, particularly for

dopaminergic imaging for the differential diagnosis and progression monitoring of PD patients as well as in psychiatric disorder [247]. Targets range from post-synaptic D_1 and D_2 receptors to pre-synaptic ^{18}F-FDOPA (the fluorinated form of L-DOPA, the dopamine precursor) and ^{123}I-Ioflupane, used to image the dopamine transporter (DAT) [226].

PET radiotracers also exist for serotonergic, norepinephrine, opioid, cholinergic, GABA, glutamate and cannabinoid targets [229], many of which are important targets in psychiatric disorders [247] as well as neurodegeneration [225]. In addition to numerous case-control studies showing molecular alterations in disease, receptor PET occupancy studies are useful tools in drug development [248] [249].

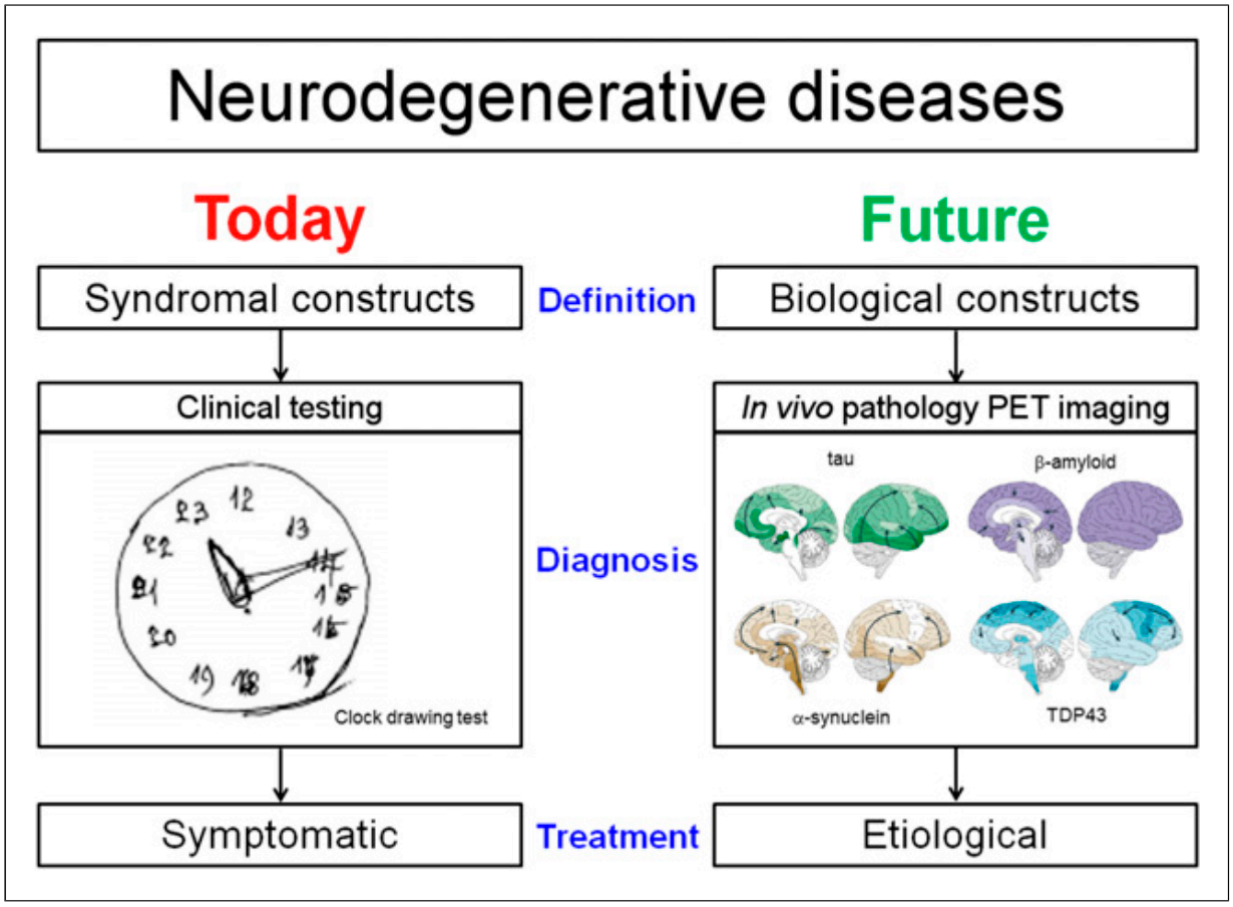

Figure 2.6. Biological definitions of neurodegenerative diseases.

While symptomatic presentation is currently a key criterion for diagnosis, robust biomarkers and potentially new, data-driven disease definitions would allow objective diagnosis using in vivo imaging (and other) markers. Figure adapted with permission from [235].

Magnetic resonance spectroscopy

Magnetic resonance spectroscopy (MRS) is the neuroimaging analogue of NMR spectroscopy, which is frequently used in chemistry. While MRI can image anatomical structure (sensitized to some tissue property), MRS instead quantifies the biochemical composition of a localized area [250] [251]. Local magnetic fields for NMR-active nuclei, such as hydrogen protons, vary based on the specific electron distributions of their bonded molecules, resulting in distinct spectral peaks in the NMR signal. Unlike single-target PET and SPECT, this allows the simultaneous quantification of multiple chemicals including neurotransmitters such as glutamate and GABA, without requiring radioligands [250] [251]. Furthermore, unlike the synaptic targets of PET and SPECT radioligands, intracellular chemicals also contribute to the MRS signal [251]. Functional MRS can also resolve metabolite levels during task and resting state conditions [251].

MRI signal originates from the abundant hydrogen protons in water and fat, but MRS targets much rarer metabolites and chemicals. With limited sensitivity, spatial resolution and coverage, MRS is restricted to specific, small regions of interest [250] [251], and not feasible for routine whole-brain imaging like PET and SPECT.

Histochemical autoradiography

In addition to in vivo molecular imaging methods, the spatial distributions of neurotransmitter receptors can be quantified post-mortem using immunohistochemistry in combination with in vitro autoradiography [252]. Typically, a donor brain is sliced, stained and then imaged for one or multiple targets [253].

Unlike PET and SPECT, post mortem autoradiography is not sensitive to motion during scanning. Theoretically, the maximum resolution from post-mortem autoradiography (effectively constrained by the slice width) can far exceed the millimeter-scale maximum resolution of PET imaging [227]. While appropriate radioligands that bind to molecular targets are required, restrictions of clinically approved in vivo radioligands are eased. However, access to post mortem brains, the expense of histological quantification and the technical difficulties of reconstructing three dimensional brain maps can limit practical utility.

Conclusion

The clinical syndromes of AD and PD are primarily characterized by dementia and movement disorder, respectively. While the underlying pathobiology has long been defined by proteinopathy (amyloid and tau in AD, and Lewy bodies in PD), both are now acknowledged to be multi-system disorders, involving vascular, metabolic and inflammatory alterations.

The molecular pathways mediating these pathophysiological processes are not fully understood. However, the selective vulnerability of neuronal populations based on neurotransmitter and receptor expression, molecular evidence of interactions between neurotransmission and pathophysiology, and symptomatic benefit from neurotransmitter-based therapy suggest the involvement of multiple neurotransmitter systems.

There are a number of open questions about the etiology and pathogenesis of AD and PD. Why do proteinopathies, such as amyloid plaques and tau tangles, originate in and propagate along specific brain regions? What neurochemical features support the regional vulnerability to long-term physiological changes such as atrophy and microstructural damage? How can we determine individualized therapeutic needs from clinical and neuroimaging data (e.g., cholinergic medication in PD [122])? Improved spatiotemporal characterization using multi-modal

neuroimaging and other in vivo biomarkers offers a pathway to answer these questions, for an unbiased biological definition of NDD onset and progression (Figure 2.6).

Chapter 3. Beyond the usual suspects: multi-factorial computational models in the search for neurodegenerative disease mechanisms

Ahmed Faraz Khan, Yasser Iturria-Medina

Preface

The causes of neurodegenerative disease onset are not well understood, and it is often unclear whether observed features such as proteinopathy accumulation are upstream causes or downstream effects. Enabled by the maturity of large observational neuroimaging studies, a number of studies have attempted to align (often multi-modal) data from diverse groups of patients to understand the spatiotemporal progression of features such as atrophy, or the temporal relationship between different biomarkers. In addition to these models of biomarker trajectories, causal models of interacting biological factors explicitly incorporate interactions between these processes. Increasingly, there are also attempts to link macroscopic but easily observable features with more detailed but difficult-to-acquire molecular and cellular atlases of gene and receptor expression. Finally, multi-scale biophysical models of neuronal activity attempt to incorporate modalities with diverse spatial and temporal resolutions.

This chapter provides a broad overview of this spectrum of computational models, their applications to understanding neurodegenerative disease progression, and how they can impact our understanding of disease biology and influence clinical practice.

The contents of this chapter are under review for an invited review article.

Abstract

From Alzheimer's disease to amyotrophic lateral sclerosis, the molecular cascades underlying neurodegenerative disorders remain poorly understood. The clinical view of neurodegeneration is confounded by symptomatic heterogeneity and mixed pathology in almost every patient. While the underlying physiological alterations originate, proliferate, and propagate potentially decades before symptomatic onset, the complexity and inaccessibility of the living brain limit direct observation over a patient's lifespan. Consequently, there is a critical need for robust computational methods to support the search for causal mechanisms of neurodegeneration by distinguishing pathogenic processes from consequential alterations, and inter-individual variability from intra-individual progression. Recently, promising advances have been made by data-driven spatiotemporal modeling of the brain, based on in vivo neuroimaging and biospecimen markers. These methods include disease progression models comparing the temporal evolution of various biomarkers, causal models linking interacting biological processes, network propagation models reproducing the spatial spreading of pathology, and biophysical models spanning cellular- to network-scale phenomena. In this review, we discuss various computational approaches for integrating cross-sectional, longitudinal and multi-modal data, primarily from large observational neuroimaging studies, to understand i) the temporal ordering of physiological alterations, ii) their spatial relationships to the brain's molecular and cellular architecture, iii) mechanistic interactions between biological processes, and iv) the macroscopic effects of microscopic factors. We consider the extents to which computational models can evaluate mechanistic hypotheses, explore applications such as improving treatment selection, and discuss how model-informed insights can lay the groundwork for a pathobiological redefinition of neurodegenerative disorders.

Introduction

Over a century after Charcot, Alzheimer and Lewy, we still do not fully understand the pathogenic causes of sporadic neurodegenerative disorders, such as Alzheimer's disease (AD), Parkinson's disease (PD), amyotrophic lateral sclerosis (ALS), and frontotemporal dementia (FTD) [254]. Consequently, despite recent advances in anti-amyloid therapy for early AD [255] [256], disease modifying treatments generally remain elusive [257]. With a projected three-fold increase in the incidence of dementia by 2050 [8], there is an urgent imperative to identify and therapeutically target the root molecular causes of neurodegeneration.

Historically, physiological changes to the living brain could not be observed. Characteristic post-mortem pathological features, such as amyloid plaques and neurofibrillary tangles in AD or spinal cord degeneration in ALS, were only identified after the advent of histology and the clinic-anatomical method [258] [259]. Lacking early biomarkers, the nosology of neurodegenerative diseases has been driven primarily by clinical symptoms. For example, the diagnosis of AD is an evolving concept, with distinct clinical and pathobiological definitions, intertwined with the historical concept of "senile dementia" [260]. However, there is significant symptomatic as well as pathological overlap between neurodegenerative diseases [261] and with normal brain aging [4]. As such, even expert clinicians can make erroneous diagnoses, with around one-fifth of patients being clinically misdiagnosed with AD or PD compared to post-mortem pathological examination [262] [263]. Formalized criteria attempt to codify supportive and exclusionary features to standardize diagnosis [264], but, without definitive biological definitions and markers, it can be difficult to distinguish risk factors from prodromal disease features to place patients along an expected progression timeline [265]. As a result, our current conceptions of the major neurogenerative "diseases" are arguably in fact syndromes, grouped

together by shared clinical manifestation but potentially obscuring diverse underlying physiological mechanisms [266] [267] [11].

On the other hand, neuropathological examination at autopsy shows that most patients have mixed pathology [268] [269] [270] [271] [272] [273] [274]. From autopsy analysis of 10 pathologies in individuals from 8 diagnostic classes, Robinson et al. found 161 different pathological combinations, with up to 7 present concurrently in a given individual [275]. In particular, tau pathology is nearly universal across the major neurodegenerative disorders [59]. In addition to the characteristic accumulation of amyloid and tau, co-pathological TDP-43 and α-synuclein are present in one-third and half of AD patients, respectively [59]. AD is also associated with neuroinflammation and metabolic dysregulation [22] [18] [19], and shares risk factors, pathology and symptoms with vascular dementia [12]. Patients of both sporadic and genetic variants of FTD have tau, TDP-43 and other proteinopathies [276], likely forming a continuum with ALS patients [277]. Furthermore, FTD itself encompasses several clinical syndromes with shared symptoms, including behavioural variant FTD, (semantic and non-fluent) primary progressive aphasias, progressive supranuclear palsy (PSP), and corticobasal syndrome (CBS) [278]. Synucleinopathies, such as PD, dementia with Lewy bodies (DLB) and REM sleep behaviour disorder, also exhibit overlapping clinical, neurochemical and morphological characteristics [279]. While PD is primarily associated with movement dysfunction due to nigrostriatal dopaminergic loss, patients also present various neurobiological alterations having strong associations with multiple neurotransmitter systems and peripheral organs [280]. The presence of co-pathologies could affect the observed efficacy of treatments and clinical trials [281], and require a more nuanced approach involving individualized and multi-factorial treatment [282].

While early pathological studies were limited to post-mortem autopsy, the advent of in vivo biomarkers in recent decades has allowed quantitative assessment throughout disease progression starting from preclinical or prodromal stages. Non-invasive neuroimaging techniques have enabled the characterization of structural, functional, proteinopathy, vascular and metabolic alterations, revealing long periods of preclinical pathogenesis [17]. Trading spatial specificity for improved temporal resolution, electrophysiological modalities such as EEG/MEG can evaluate regional and network activity dysfunction [283]. On the other end, bulk tissue and single cell/nucleus transcriptomics can achieve microscopic spatial resolution, although they are dependent on the acquisition of post-mortem brain tissue and thus more restricted in spatial coverage and sample size [284] [285]. In addition, many plasma, cerebrospinal fluid (CSF) and peripheral markers have shown promise for integration into clinical practice [286].

Following the emergence of potential in vivo biomarkers, there have been increasing efforts to define neurodegenerative diseases, and categorize and stage patients based on underlying biological alterations rather than by clinical symptoms [236] [287] [288] [289] [290] [291]. For an autosomal dominant disorder with a genetic continuum such as Huntington's disease (HD), the starting point can be defined by genotype, followed by pathological biomarkers, and finally the appearance of symptoms and functional changes [291]. Alternatively, the amyloid/tau/neurodegeneration (A/T/N) framework [289] does not consider temporal ordering, but instead categorizes patients along an "Alzheimer's continuum" based on a combination of binary features: namely, the presence of (e.g., CSF or PET) markers of amyloid and tau pathology as well as neurodegeneration or neuronal injury (e.g., hippocampal volume, cortical thickness, or CSF neurofilament light) [292]. With the development of CSF α-synuclein seed amplification assays [293], biomarker-based criteria are now emerging for PD. Two recently

proposed approaches, SynNeurGe and the Neuronal Synuclein Disease Integrated Staging System (NSD-ISS), classify PD- and DLB-related disorders based on genotype, the presence of (e.g., CSF) α-synuclein, and imaging markers of PD-associated neurodegeneration without necessitating clinical symptoms [294] [65]. Theoretically, biomarker-based categorization can also flexibly incorporate other forms of pathology (e.g., vascular or metabolic indices in AD [18]) and alternative markers of the same pathology, although alignment with symptoms and clinical diagnosis appears to be sensitive to the specific choice of biomarkers for the A/T/N framework [292]. Biomarker-driven categorization is expected to improve the biological homogeneity of preclinical and prodromal subjects enrolled in clinical trials [294] [65] [291], but it remains to be seen whether the correct physiological factors are being considered [295]. The implications of clinical and pathological intra-disease heterogeneity and inter-disease overlap require further clarification. Perhaps a more integrative taxonomy of neurodegenerative disorders is needed, considering the multi-dimensional variability of clinical, anatomical, molecular, and etiological factors. To this end, a branching hierarchy considering divergence in genetics, followed by molecular pathways, and finally modifiable risk factors has been proposed [296].

Regardless of disease definitions, there are critical open questions about the mechanisms of onset and progression. Are the varied manifestations of each disorder diverging responses to a common, latent cause, or a combination of distinct underlying processes resulting in similar clinical syndromes [287] [297]? Are the various culprit proteinopathies the true etiology of neurodegenerative disorders, or are they the consequences of compensatory mechanisms [298]? What factors underlie varying therapeutic needs and treatment responses of patients with the similar clinical diagnosis?

To address these questions, there is a need for a systems-level understanding of interactions across various physiological systems and levels of brain organization [29]. Multi-modal computational modeling can support these efforts by integrating data types across spatial and temporal scales in biologically interpretable formulations. In this review, we cover recent advances in the computational modeling of spatiotemporal brain alterations in various neurodegenerative disorders. We particularly emphasize how data-driven *in silico* models, which are fit to empirical observations without necessitating detailed *a priori* knowledge about underlying mechanisms, can evaluate disease hypotheses and impact clinical practice. We present these approaches in an increasing order of mechanistic detail. We begin by introducing continuous- and discrete-time disease progression models (DPMs) that stitch together data from cross-sectional observational studies to infer the order of physiological alterations and their variability in patients. Although these methods can flexibly incorporate multiple modalities with minimal *a priori* specification, they cannot resolve potential interactions between physiological variables. Addressing this consideration with causal structure, we discuss dynamical system models of interacting physiological factors and network propagation. These models have an element of mechanistic insight, and recent studies have extended them with the molecular and cellular architecture of the brain. Finally, we consider multi-scale biophysical models, where effects explicitly propagate from microscopic cellular mechanisms to mesoscopic circuits and macroscopic signals reproducing empirical neuroimaging and electrophysiological data. Together, this body of work follows the general theme of inferring latent disease mechanisms by fitting interpretable whole-brain computational models to observable biomarker data.

Biomarker trajectories in latent disease time

Neurodegenerative disorders can affect multiple symptomatic domains, including memory, language and executive dysfunction, and involve diverse physiological alterations, such as proteinopathy, cerebrovascular impairment, atrophy and hypometabolism. Often, the profile of physiological and symptomatic deterioration is characteristic to the stage of disease progression. For example, incontinence followed by sleep disorders are some of the earliest symptoms of PD (occurring 1-2 decades before motor symptoms) [299], and, during the long prodromal phase of AD, decline in semantic memory precedes more global cognitive deficit and eventually dementia [300].

The idea that the neurodegenerative disease progression follows stereotypical hierarchies quantifiable by biological (rather than clinical) variables can be traced to *post mortem* pathological staging [301]. In the early 1990s, Braak and Braak identified a characteristic sequence of neurofibrillary tangle progression in the brains of AD patients (Fig. 3.1a), from transentorhinal (Stages I-II) to limbic (Stages III-IV) and finally neocortical (Stages V-VI) regions [302]. Neuropathological staging has since been attempted for various proteinopathies, diseases and cohorts [303] [304]. These studies emphasize the importance of the disease-specific spatiotemporal progression of pathological factors; for example, while tau pathology is involved in both AD and chronic traumatic encephalopathy (CTE), it follows distinct spreading patterns in the two disorders [301].

The establishment of *in vivo* (PET, MRI and CSF) markers in clinical practice has offered a chance to extend staging systems to the preclinical phase, closer to pathogenesis. In an influential work, Jack et al. proposed a hypothetical cascade of multiple biomarkers in AD [54], conceptually similar to Fig. 3.1b. Echoing the traditional amyloid hypothesis [305], these

biomarker curves implied that abnormal levels of amyloid and tau accumulation are followed by structural alterations, which finally lead to clinical symptoms [54]. An important corollary of this would be that upstream physiological alterations can signal the onset of symptoms, allowing early diagnosis and treatment. Enabled by large, observational imaging initiatives in various neurodegenerative disorders [306, 307, 308], many studies have since attempted to test hypothetical cascades and uncover the true orderings of biomarker alterations using DPMs.

Constructing disease trajectories from cross-sectional data

These DPMs are generally data-driven, typically fitting monotonic functions to empirical biomarker data with minimal assumptions about the underlying mechanisms. A key problem in fitting such trajectories is the absence of observations covering the entire course of disease progression in any single subject. Longitudinal studies are typically much shorter than the decades-long periods of preclinical, prodromal, and finally symptomatic progression of most neurodegenerative disorders. As a result, inferring population biomarker trajectories over the entire course of a disease requires stitching together data from subjects at varying disease stages (Fig. 3.1b) [309]. This data, whether a single visit or a sequence of measurements, can have inter-individual variability in disease stage and severity, and subjects may not follow the same trajectory.

For simplicity, we first consider the case where there is a common population trajectory. Individuals' snapshots must be temporally aligned to correctly place each subject in the population trajectory. Continuous-time DPMs usually achieve this by arranging subjects according to a latent temporal variable, usually referred to as "disease age", "disease time", "disease progression score" (DPS) or pseudotime. This disease age is distinct from chronological age but better reflects onset and progression from patients' markers [310]. To fit long-term,

multivariate population biomarker trajectories from longitudinal snapshots over a shorter period, a popular approach for continuous-time DPMs has been to combine i) mixed-effects modeling to account for subject-specific random effects on a fixed population trajectory, and ii) self-modeling regression to adjust the population trajectory for individualized onset and rate of progression along a common latent disease time. In the remainder of this section, we will discuss some applications of this paradigm (as well as others) to various neurodegenerative disorders.

Familial age of onset as scaffolding for disease time

Due to a degree of predictability imposed by genetic risk, autosomal dominant disorders such as dominantly inherited AD (DIAD) and familial FTD are a suitable testbed for the DPM temporal alignment problem. In these disorders, individuals highly likely to progress to dementia can be identified in the preclinical phase. DIAD is relatively rare (around 1% of total AD cases) [15] and occurs significantly earlier (around 30-50 years of age) [311]. Unlike sporadic AD, which has no Mendelian inheritance pattern, DIAD is associated with pathogenic mutations of amyloid protein precursor (*APP*), presenilin-1 (*PSEN1*) and presenilin-2 (*PSEN2*) [15]. Although age of onset can vary, with over one-quarter of at-risk siblings developing familial AD more than 10 years apart in age [312], a systematic review and meta-analysis suggests that parental age of onset explains over 38% of the variance [313]. Likewise, autosomal dominant inheritance is observed in 10-15% of FTD patients due to mutations in genes such as progranulin (*GRN*), microtubule-associated protein tau (*MAPT*) and chromosome 9 open reading frame 72 (*C9orf72*), as well as others [314]. The influence of genetic risk on age of onset in familial FTD is genotype-dependent [315]. This heritability of disease onset age has informed early attempts at modeling biomarker progression in DIAD.

For example, Bateman et al. estimated expected years to/since disease onset in DIAD by subtracting parental age of onset from patients' chronological age [15]. This estimate was used to fit linear mixed effects models of multi-modal biomarkers. The resulting trajectories suggest that CSF amyloid is the earliest biomarker to become abnormal (declining up to 25 years before symptom onset), followed by amyloid PET, CSF tau and atrophy (15 years before onset), hypometabolism and episodic memory dysfunction (10 years before onset), and cognitive impairment (5 years before clinical diagnosis).

In familial FTD, atrophy patterns vary by genotype between carriers of *C9orf72*, *GRN* and *MAPT* variants [316]. For these mutation carriers, Staffaroni et al. predicted symptom onset using a joint Bayesian mixed effects model of longitudinal clinical assessments, regional brain volume and plasma neurofilament light chain (NfL) data [16]. Estimated disease onset ages were sampled from a prior distribution of carriers of the same mutations, and biomarker functions were fit with mutation-specific temporal shift and scale parameters. Using this method, regional brain atrophy and elevated plasma NfL levels were found to appear 10 to 40 years before noticeable symptomatic deterioration across genotypes [16].

Other studies have attempted to extrapolate models from genetic to sporadic disease. In a genetic AD cohort, Almkvist et al. fit curvilinear functions mapping years to expected clinical onset to various cognitive assessments [317]. If non-familial AD follows a similar clinical trajectory, inverting these relationships could be used to infer years to/since clinical onset from shared cognitive assessments. This calculated disease age did correlate better with CSF and imaging biomarkers than chronological age in non-familial mild cognitive impairment (MCI) and AD patients [318], with a bimodal distribution of onset age corresponding to early- and late-onset forms of sporadic AD.

It is important to test the assumptions of these extrapolations, and consider the extent to which familial and sporadic variants of a disorder are aligned in their pathological cascades. DIAD presents an opportunity to study the pre-symptomatic stage in carriers of risk variants who will go on to develop AD [311] with a somewhat predictable age of onset [313]. While similar trajectories of posterior cingulate amyloid deposition and memory decline have been noted in DIAD and sporadic AD patients, the latter display faster hippocampal atrophy [15] [305] [17] and an amyloid-independent medial temporal tauopathy [319]. A recent comparison of DIAD and sporadic early-onset AD clinical and biomarker progression reiterates that the former is more homogeneous, while the latter is more likely to exhibit atypical phenotypes [320]. For example, unlike sporadic AD, almost all DIAD patients exhibited an amnestic syndrome. Differences in genetic risk factors may drive the heterogeneity of sporadic AD [320], as well as potential later onset age, as more varied risk factor and comorbidities can accumulate over time.

Estimating disease onset in sporadic disorders

The pathological processes underlying sporadic neurodegenerative disorders such as AD and PD also begin decades before their characteristic symptoms [288] [299] [321]. Several early works used standardized clinical assessments to align subjects [322] [323]. In the Alzheimer's Disease Neuroimaging Initiative (ADNI) cohort, Yang et al. fit individual-specific functions to longitudinal cognitive scores with temporal offsets representing age of onset [324], and applied this subject ordering to other biomarkers. While the inferred ordering was consistent with the hypothetical cascade [54], this method did not account for subject-specific variability in rate of progression, which can be a major consideration in AD [325].

Subsequent DPMs have considered inter-individual variability in rate of progression [326]. In an exemplar study on the ADNI cohort, Jedynak et al. iteratively fit i) a subject-specific

DPS as a linear function of chronological age and ii) population biomarker curves as sigmoidal functions of DPS [326]. To simultaneously fit nonlinear population curves and subject-specific disease time, many studies use iterative or Bayesian approaches [310] [327] [310].

In contrast to the hypothetical biomarker cascade of Jack et al. [54], the Rey Auditory Verbal Learning Test was the first marker to become abnormal in the data-driven model of Jedynak et al., followed by hippocampal volume and CSF amyloid and tau concentrations [326]. Considering covariates, Ishida et al. found genotype-dependent timing of cognitive decline in female AD patients [327].

In addition to determining the timing of biomarker alterations, DPMs can be used to stage individual patients and predict the onset of clinical symptoms. Combining Bayesian inference with flexible logistic basis functions and stage-dependent rates of progression, Bilgel and Jedynak predicted age of dementia onset in the ADNI cohort with a root mean-squared error of 1.5 years [328]. The distributions of model-inferred disease times differ significantly between diagnostic classes in the AD spectrum [310]. Such estimates of latent disease time can be used to define clinical trial endpoints [16] and detect treatment effects using fewer participants [327]. DPM-inferred individualized disease time can also be the basis for data-driven probabilistic diagnosis and estimation of time to conversion [329]. Based on the DPM of Lorenzi et al., the transition from healthy to diseased state in AD largely corresponds to hypo-metabolism and temporal atrophy, with more advanced stages reflected by neuropsychological markers [329]. These results suggest that integrative, model-based disease time inference is particularly useful for early disease stages, when clinical symptoms are less evident. Furthermore, these DPMs can flexibly incorporate clinical, imaging, and fluid biomarkers, as well as other features such as topological properties of spatial brain maps [330].

Temporal associations between markers

Based on observational studies, the DPMs presented so far do not provide explicit evidence for causality. However, a simple yet critical epidemiological evidence of causality is temporality; presumed causes must precede their consequences. [331]. From this lens, the timing of biomarker alterations from DPMs can be used to evaluate disease hypotheses.

A major topic in AD research is the relationship between the two defining pathologies: amyloid and tau. Amyloid is believed to facilitate tau pathology, but the two proteinopathies also appear to have synergistic as well as independent effects [332] [333]. Developed for survival analysis, the framework of accelerated failure time (AFT) is a straightforward way to evaluate temporality via a common biomarker trajectory with individual-specific temporal shifts. Based on AFT analysis, model-inferred individual temporal shifts of amyloid and tau accumulation in the AD spectrum are better correlated with increasing proteinopathy burden than chronological age. *APOE ε4* genotype shifted both amyloid and tau curves earlier, by 6.1 and 2.6 years, respectively. These curves were also moderately correlated, with an average delay of 13.3 years between amyloid and tau accumulation [334]. While the AFT analysis does not demonstrate causation, it shows how the timing of amyloid and tau pathology are related and affected by covariates. Disentangling synergistic from independent effects of amyloid and tau requires more detailed mechanistic modeling, discussed in later sections.

Cerebrovascular disease (CVD) pathology also frequently co-exists in AD, suggesting a potential relation to proteinopathy accumulation. Comparing disease trajectories of CVD-associated white matter hyperintensities (WMH) and fractional anisotropy (FA) with AD-associated amyloid and tau PET imaging shows moderate within-disease temporal correlations between individualized timings of amyloid and tau accumulation (r=0.57) and WMH and FA

alterations (r=0.44) in the AD spectrum [335]. However, these imaging measures of CVD and AD pathology did not show strong correlations across disease measures nor with hippocampal volume, nor were associations with clinical symptoms considered. As a result, the authors propose that vascular and proteinopathy components in AD represent independent mechanisms [335]. However, interpretations are limited by the non-specificity of imaging measures to vascular pathophysiology, as well as aspects of vascular dysfunction not captured by WMH or FA.

Perfusion imaging modalities such as arterial spin labeling MRI can measure vascular function [336], which may be disrupted before structural alterations. Acknowledging the presence of diverse physiological alterations in late-onset AD, Iturria-Medina et al. fit multi-modal (structural, functional, metabolic, amyloid and tau) imaging, CSF and plasma mixed-effects models to infer biomarker abnormality as the distance between diseased and healthy trajectories [337]. Notably, vascular alterations (from arterial spin labeling MRI) preceded all other biomarker alterations, and memory deficit was observed early and continued to decline in parallel with neuroimaging- and biospecimen-based markers over disease progression.

Assumptions about trajectory shape

In addition to inter-subject variability in timing, assumptions about trajectory shape and biomarker dynamic range are important considerations in fitting empirical data. Using a non-parametric approach to fit monotonic splines to population trajectories in the ADNI cohort shows varying degrees of linearity and sigmoidal form among biomarkers [309], suggesting that some biomarkers did not capture the final, plateauing stage of a hypothetical sigmoidal disease trajectory. On the other hand, hippocampal volume had the highest signal-to-noise ratio at these

disease stages, in agreement with another non-linear mixed-effects model where it was the largest contributor to model-inferred disease time [309] [327].

A common assumption is that trajectories are monotonic, with markers progressing consistently from normal to diseased levels. It is important to note that biomarker progression may not conform to assumptions about trajectory shape, such as linearity, exponentiality, sigmoidal shape or even monotonicity, especially when considering features derived from topology [338] or dimensionality reduction [339]. Relaxing assumptions about mean trajectory shape apart from smoothness, Schmidt-Richberg et al. developed a probabilistic method based on vector generalized additive models (VGAMs) to estimate disease stage and rate of progression using quantile regression [340]. Using converter subjects that progressed to a worsened disease state, this method fits biomarker probability density functions for clinical assessments and low-dimensional projections of imaging data obtained using Laplacian eigenmaps [339], while handling missing data and non-monotonic biomarker trajectories. Addressing the common trajectory assumption, Guerrero et al. transitioned from mean population to individualized disease progression models by selecting a subpopulation of similar patients based on neighborhood in a low-dimensional projection [341]. The theory of fitting subject-specific trajectories as temporally re-parameterized, spatially-shifted variants of a group trajectory that is a geodesic on a Riemannian data manifold has also been mathematically developed [342], and applied to high-dimensional cortical thickness features [343] as well as neuropsychological data from ADNI [342].

Feature selection and inferring disease time from high-dimensional data

At a finer resolution than ROI-averaged features, other works have applied DPMs to voxel- or vertex-wise data. This higher-resolution characterization can help resolve pathological trajectories that may be regionally variable. Bilgel et al. [344] extended an earlier DPM [326] to voxel-wise amyloid PET data from the Baltimore Longitudinal Study of Aging (BLSA) cohort, finding the earliest amyloid accumulation in the precuneus despite its similar rate of change as other cortical regions, which is consistent with other studies [345]. Notably, their calculated DPS correlated better with mean cortical distribution volume ratio than subject-specific offset and rate of change parameters. Marinescu et al. developed Data-driven Inference of Vertex-wise Evolution (DIVE) [346], which was used to infer sigmoidal biomarker trajectories of vertex clusters in AD and posterior cortical atrophy (PCA) from cortical thickness MRI and amyloid PET data. By iteratively clustering vertices, estimating biomarker trajectories for each cluster, and inferring disease pseudo-time, DIVE can automatically segment the cortex into (potentially disconnected) regions sharing similar progression patterns.

Model scalability with large numbers of features is an important consideration for high-dimensional data from transcriptomics, proteomics and epigenomics. Analogous to DPMs, trajectory inference methods are commonly used in single-cell analyses to characterize dynamic cellular processes such as differentiation and life cycles from single-cell omics [347]. These concepts have also been applied to infer population trajectories from cross-sectional data [348] [349]. The general approach to trajectory inference is to fit a graph to individuals' data points in a reduced dimensional space, linking them along a continuum that can be used to calculate a pseudotime (which in this context is equivalent to a disease time or progression score).

Prioritizing variance between patients and controls during dimensionality reduction, a contrastive trajectory inference algorithm was applied to bulk tissue post-mortem brain and in vivo blood gene expression from cross-sectional cohorts of late-onset AD and HD patients [348]. This method used distance along a minimum spanning tree to healthy control references to calculate patients' pseudotimes, which are significantly correlated with the severity of neuropathologies (Cerad, Braak and Vonsattel stages) and cognitive performance. Another study on transcriptomics-based trajectory inference in the AD instead used a manifold learning approach that fits a nonlinear transformation to a low dimensional space where subjects have a tree structure. Pseudotimes calculated from this tree did correspond to neuropathological stages and diagnoses, and a "disease resistant state" was also found, consisting of subjects with disease-like transcriptomic profiles but no pathological diagnosis of AD [349]. In general, the choice of dimensionality reduction algorithms and graph structure can influence results, such as the ability to identify branching structure in the data [350]. Beyond transcriptomics, trajectory inference methods have also been applied to voxel-scale imaging data using latent embeddings from variational autoencoders (VAEs) [351].

The impact of disease variability on staging

In general, heterogeneity in biomarker trajectories can be a major confounding factor for staging. Acknowledging the symptomatic and physiological heterogeneity of neurodegenerative disorders, there have been many attempts to identify disease subtypes from clinical data, in vivo markers, and pathology [352]. While a detailed discussion of subtyping is outside the scope of this review, some methodological concerns are covered elsewhere [353]. Typically, subtyping involves unsupervised methods such as clustering or network community detection [354] applied to cross-sectional [355] or longitudinal [356] features. In AD, the consensus from imaging and

neuropathology points towards 3 subtypes, representing typical, limbic-predominant and hippocampal-sparing/minimal-atrophy spatial patterns [13] [357], while CSF proteomics-based clustering 5 subtypes with distinct molecular signatures that are identifiable from the pre-clinical phase [358]. However, disease stage can also exert significant influence on progression-naïve subtyping (e.g., in PD [359]), and distinguishing between effects due to disease progression and trajectory is important [348] [360].

To address both sources of variability simultaneously, expectation-maximization methods can be used iteratively to assign subjects to and construct biomarker trajectories for subtypes, with an initial subtyping solution provided by clustering. Applying this approach to a reduced dimensional fused network of multi-omics (transcriptomics, epigenetics, proteomics, and metabolomics) data identified 3 molecular subtypes in AD [360],

With the presence of disease subtypes, the interpretation of subtype-specific DPS can become more complicated. For example, when subtype-specific DPS reflects the distance from a subject to a healthy control reference population along its trajectory [360], can these scores be compared across subtypes? One way to anchor the subtypes would be to calibrate all subtype-specific DPS in reference to a clinical score threshold. However, this is likely not a major concern in practice, as accurately placing a patient along the expected trajectory of their identified subtype would be more relevant than comparing scores across subtypes.

Patients sharing the same clinical diagnosis may not be biologically homogeneous, and may follow distinct trajectories. To account for this variability, we have seen attempts to shift towards unsupervised discovery of subtypes [360] and individualized modeling [341]. Other studies have considered the effects of risk factors, such as *APOE* genotype, on model parameters [322]. While population disease trajectories are informative in understanding the stereotypical

sequence of biomarker alterations, it is important to consider the factors that may contribute to heterogeneity during modeling and analysis.

Sequences of alterations in event-based models

In contrast to the DPMs presented so far that assume a latent temporal continuum of disease progression, event-based models (EBMs) order biomarkers according to discrete transitions from normal to abnormal states. Because of this simplicity, EBMs can extract an intuitive biomarker ordering, depicted in Fig. 3.1c, using cross-sectional data from small datasets [361]. With this practical advantage, applications of EBMs to a variety of imaging, clinical, neuropathological and biospecimen features across diseases have provided data-driven insight into biomarker ordering and their subtype variability.

Discretizing disease stages

As with continuous-time DPMs, some of the earliest EBM studies addressed autosomal-dominant disorders, where carriers can be identified before symptom onset. An influential work by Fonteijn et al. [361] characterized the progression of regional atrophy and clinical diagnosis in familial AD and HD patients. At the core of EBMs are mixture models, a statistical approach to fitting data arising from multiple subpopulations. In the original EBM formulation of Fonteijn et al., a mixture of Gaussian and uniform distributions is fit to each event/biomarker. The Gaussian distribution corresponds to the likelihood of observing a biomarker value when the event has not occurred, while the uniform distribution corresponds to the likelihood given that the event has occurred [361]. An overall likelihood can then be calculated for each sequence of event orderings, and a Markov chain Monte Carlo (MCMC) algorithm is used to sample the posterior distribution of event orderings given biomarker data. A characteristic sequence of

events as well as their uncertainty estimates (represented by the gray elements in Fig. 3.1c) can then be calculated. In familial AD, hippocampal atrophy was the earliest imaging marker, occurring before MCI diagnosis, and soon followed by inferior parietal and precuneus atrophy. In HD, putamen, caudate, thalamus, posterior cingulate and superior frontal atrophy were the earliest markers.

Applications of EBMs to a variety of disorders have reproduced known aspects of disease progression while providing a quantitative staging system. Young et al. [362] extended the original EBM of Fonteijn et al. to sporadic AD, reproducing the early abnormality in CSF protein levels that is consistently observed, followed by regional atrophy rate, cognitive decline and decreased regional brain volume. Similar EBMs have been applied to anatomical connectivity-derived network measures in sporadic AD [363]. Combining a cross-sectional EBM with longitudinal differential equation modeling of multi-modal biomarkers in DIAD showed that many biomarker alterations accelerate with disease progression [364], in contrast to the sigmoidal plateauing hypothesized by many studies [54]. In DIAD, cortical and then subcortical amyloid accumulation was followed by p-tau, CSF amyloid and tau, neurodegeneration in the putamen and nucleus accumbens, cognitive decline, cerebral hypometabolism and finally other regional neurodegeneration [364]. Using gray and white matter, brainstem, cerebellar and ventricular volumes, Eshaghi et al. applied an EBM to transitions from normal to atrophic states of regional gray matter in multiple sclerosis (MS) patients [365]. Consistent with histopathology, primary-progressive and relapse-onset variants of MS showed similar orderings of regional atrophy. These prolific applications reflect the simplicity and generality of the EBM approach.

Estimating disease time from EBMs

Unlike continuous time DPMs, the standard EBM formulation infers only the relative ordering of biomarker alterations, but not any timing between events or global disease time. Variations such as the temporal event-based model (TEBM) assign both a stage and progression risk to individuals, thus placing them on a disease timeline [366]. Notably, TEBM predicts conversion time (when all cognitive biomarkers become abnormal) with more accuracy and precision than the standard EBM or a continuous time Gaussian process DPM. Acknowledging the noise in clinical diagnosis, Venkatraghavan et al. developed a discriminative EBM also incorporating timing between events [367]. This approach first fits PDFs for easily separable subsets of controls and AD patients. It then infers subject-specific orderings, generalizes these orderings to the populations, estimates relative temporal distances between events, and stages patients based on this ordering. Notably, model-derived patient stages from discriminative EBM better reflected the progression of AD patients than stage estimates from other contemporary EBM formulations [367]. In a "typical AD" subset consisting of amyloid-negative controls and amyloid-positive MCI and AD patients, p-tau becomes abnormal before the cognitive assessments. However, with the full dataset, CSF amyloid and cognitive alterations precede p-tau; in general, the biases introduced by inclusion criteria must be considered. Notably, hippocampal volume and other structural measures follow cognitive alterations, potentially due to the insufficient sensitivity of these imaging markers to early mild changes in this cohort [367].

Accounting for heterogeneity of event sequences

The original EBM formulation assumed a common monotonic trajectory for all biomarkers across the cohort. This assumption is likely more valid for certain subgroups, such as

patients of autosomal dominant disorders, or amyloid- and/or *APOE*-positive subjects who show less variability in event sequences [362]. Alternative formulations [368] allow heterogeneity in the temporal ordering of biomarkers using a probabilistic model. However, they considered the probability density functions of pre- and post-event classes to be independent Gaussian distributions for each biomarker, which likely exhibit correlation. Disentangling these distinct sources of variability, Subtype and Stage Inference (SuStaIn) simultaneously performs unsupervised subtyping and temporal disease staging using an iterative training procedure [369]. As a result, it has been able to derive data-driven subtypes based on progression patterns across many diseases.

Using structural MRI data, this method was able to identify known genotypes from imaging data of FTD patients, while proposing two distinct latent phenotypic subtypes linked to the *C9orf72* genotype [369]. In AD, three subtypes were identified based on regional origin of atrophy: i) the hippocampus and amygdala in the typical subgroup, ii) the nucleus accumbens, insula and cingulate in the cortical subgroup, and iii) the pallidum, putamen, nucleus accumbens and caudate in the subcortical subgroup [369]. These data-driven progression subtypes appear to correspond to the 3 neuropathologically observed subtypes of AD [357] [370]. SuStaIn also identified 4 distinct spatiotemporal trajectories of AD tau accumulation, corresponding to different clinical profiles and outcomes [242]. Modeling amyloid accumulation, SuStaIn found cortical and subcortical subtypes with the latter corresponding to more typical AD clinical presentation [371], while another study showed that cortical amyloid deposition is best explained by three subtypes defined by frontal, parietal and occipital initiation of abnormality [372]. Combining both proteinopathies in AD, SuStaIn also consistently reproduces complementary

"amyloid-first" and "tau-first" subtypes from separate modeling using in-vivo PET and neuropathological evaluation [373].

In TDP-43 proteinopathies, including ALS, FTD, and the recently characterized limbic-predominant age-related TDP-43 encephalopathy neuropathological change (LATE-NC) [374], an ordinal variant of SuStaIn has been used to define a more fine-grained data-driven subtyping, staging and disease classification based on neuropathological progression [375]. From atrophy progression in the ALS-FTD spectrum, SuStaIn subtyping found two cortical atrophy subtypes in addition to a normal-appearing group, and staging correlated well with clinical and neuropathological measures [376]. Using diffusion and neuromelanin-sensitive MRI measures in PD, SuStaIn suggested the presence of 2 distinct subtypes, with different clinical and pathological progression [377]. In MS patients, subtypes were defined by normal-appearing white matter, cortical and lesion subtypes, with the latter having the highest relapse rate and positive treatment response [378].

From sequences of alterations to interactions between biomarkers

In the past decade, both continuous time DPMs and discretized EBMs have helped characterize the sequence of physiological alterations in neurodegenerative disorders. These methods have attempted to account for inter-subject variability in timing, onset and trajectory, potential bias due to covariance between biomarkers, and differing trajectory shapes across biomarkers. DPMs have revealed a long prodromal period with multi-factorial alterations, such as the early roles of CSF amyloid accumulation in dominantly inherited AD [15], vascular dysregulation in AD [337], and atrophy and elevated NfL before symptom onset in FTD [16]. Furthermore, DPMs can integrate multiple data modalities to stage patients and estimate future progression [329], which may be particularly useful for pre-symptomatic individuals. While

DPMs and EBMs often assume a common population trajectory, formulations such as SuStaIn can identify patient subtypes from variability in progression ordering [369]. However, the typical optimization procedure constrains EBMs to a limited number of features, precluding their application to high dimensional (e.g., multi-omics) or high-resolution (e.g., whole-brain imaging), and thereby limiting mechanistic insight.

Mechanistically, similar pathological cascades seem to be shared between neurodegenerative diseases [379]. Data-driven subtyping and transdiagnostic clustering can help identify the distinct and shared mechanisms of different neurodegenerative disorders. To a limited extent, the ordering of disease alterations can be used to evaluate the temporality of pathogenic hypotheses [334, 335, 337]. However, the DPMs discussed account for relationships between biomarkers only implicitly, such as via joint probability distributions [16]. As such, while empirically validating hypothetical disease cascades is an important step towards understanding disease progression, biomarker timing only hints at the relationships between various neurobiological processes. In the following section, we discuss causal models that explicitly incorporate the interactions between multiple disease factors to evaluate hypotheses of disease pathogenesis and progression.

A Neuropathological staging from autopsy studies

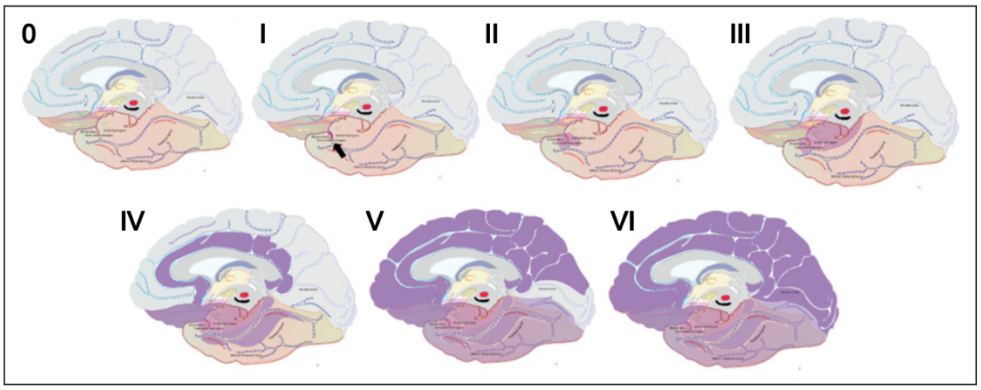

B Constructing biomarker trajectories from observational studies

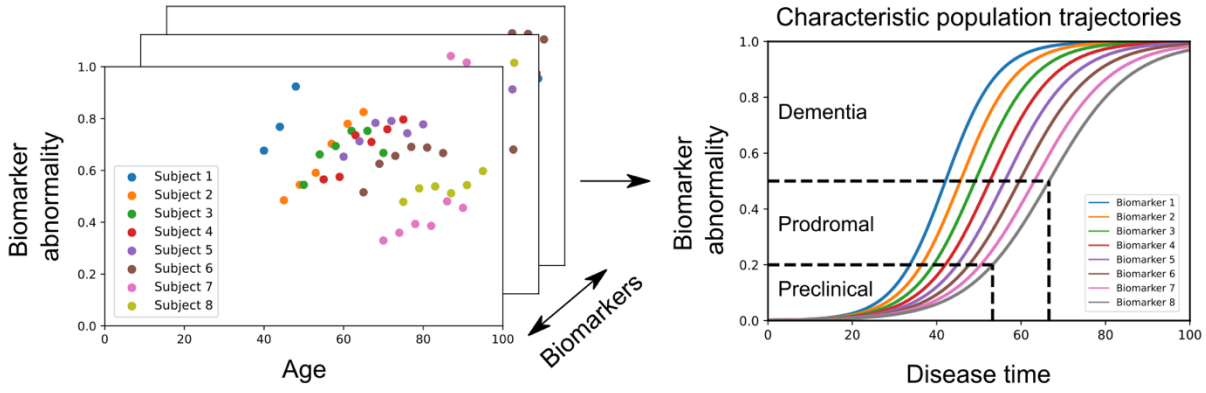

C Inferring subtypes of disease progression based on event order

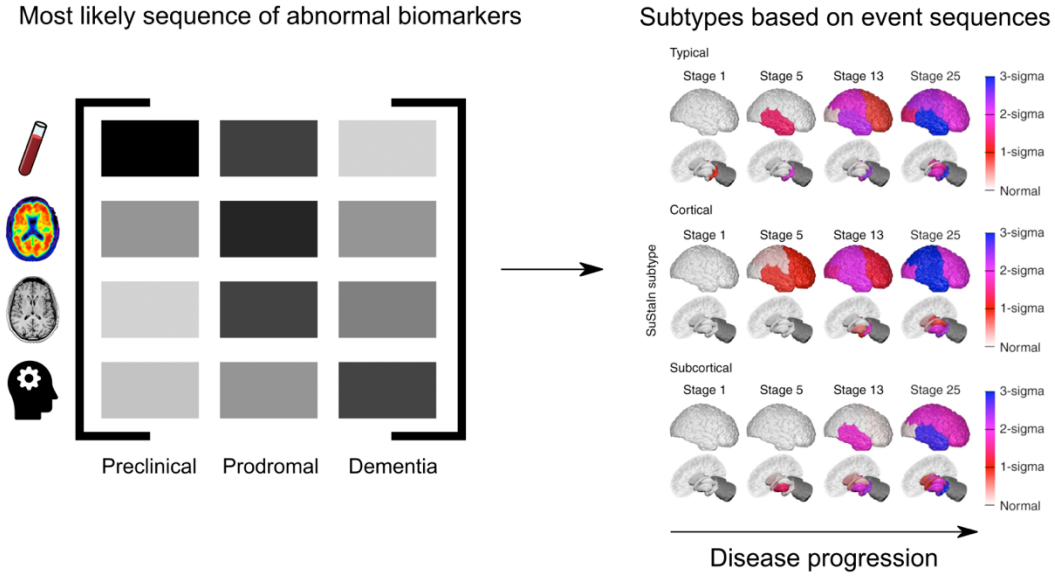

Figure 3.1. Data-driven biomarker trajectory inference and staging.

A) Neuropathological staging systems, such as the Braak stages for AD, represent the earliest attempts to identify characteristic pathophysiological progression patterns [302]. The accumulation of neurofibrillary tangles begins in transentorhinal regions (Stages I and II) and propagates along a stereotypical pattern to limbic (Stages III and IV) and neocortical (Stages V and VI) regions. The figure has been adapted with permission from [380]. B) Using in vivo (imaging, fluid and clinical) biomarkers from large observational studies, continuous-time disease progression models attempt to stitch together data points from many subjects to infer population trajectories along a latent disease time. With minimal a priori assumptions, these methods must account for inter-subject variability in disease onset and progression rate, as well as the potential existence of sub-populations with distinct trajectories. C) Event-based modeling is another approach to characterizing biomarker alterations over disease progression. (Left) This method does not explicitly model the trajectory along a latent temporal variable, but instead identifies the most likely sequences of biomarker alterations, along with their uncertainty represented by the gray elements in this positional variance diagram. These markers can be any combination of features from different brain regions and modalities. (Right) Event-based modeling is the basis for simultaneous Subtyping and Stage Inference (SuStaIn), a method that identifies sub-populations with varying event sequences. For example, SuStaIn identified 3 subtypes of AD atrophy progression, corresponding to typical, cortical-dominant and subcortical patterns. The figure was originally published in [369], is covered by the Creative Commons Attribution 4.0 International License (http://creativecommons.org/licenses/by/4.0/) and has been adapted to show only 4 disease stages.

Evaluating disease hypotheses using mechanistic and causal models

Neurodegenerative disorders are accompanied by a multitude of alterations. Aging is a major risk factor across neurodegenerative disorders, which share features such as genomic instability, loss of proteostasis and cellular senescence [4]. These related but distinct processes may represent the primary causes of damage (e.g., genomic instability) or compensatory responses that eventually result in physiological degradation (e.g., cellular senescence) [4]. A variety of genetic, environmental, pathogenic, lifestyle and dietary risk factors also contribute to sporadic disorders [2] [3] [22]. There is a notable vascular component to dementias, from AD [12] [22] to FTD [89]. The peripheral system [11] and gut-brain axis [381] also contribute to the onset and progression of PD. The integrity of the brain is thus multi-faceted, involving

supporting vascular, metabolic, inflammatory processes that support neuronal function. It is thus necessary to consider interactions between physiological factors and their causal directions, which may follow indirect, non-linear and complex pathways [382] (Fig. 3.2a), as well as inter-individual differences.

In this section, we shift away from the DPMs of the previous sections, which infer the order of biomarker alterations and event sequences but cannot resolve how these factors may influence each other. We now consider dynamical systems-based causal models of neurodegenerative disease progression. These methods explicitly employ interactions between disease factors. As a subset of these models with particular relevance to neurodegenerative diseases, we also consider network models of pathology propagation. With mechanistic interpretability and causal structure, these models are suited to testing disease hypotheses and inferring perturbational/treatment effects.

Model-inferred targets for combinatorial therapy in complex disorders

Given the unknown etiologies and heterogeneity of most neurodegenerative disorders, multiple therapeutic approaches are likely required [383]. However, identifying treatment targets is not trivial; disease-affected biomarkers do not necessarily translate to effective therapeutic targets [384]. Selecting candidate targets and designing clinical trials is likely to benefit from personalized and precision medicine approaches [385]. To this end, dynamical systems modeling using systems of coupled differential equations can characterize the spatio-temporal behaviour of key variables, impose causal structure on interactions, identify pathways involved in disease progression, and predict the outcomes of interventions.

Using a dynamical systems framework called multifactorial causal modeling (MCM), Iturria-Medina et al. fit whole-brain population models of structural, functional, metabolic, vascular, and amyloid alterations as functions of their local pairwise interactions and inter-region propagation along anatomical, vascular and functional networks [33]. Consistent with earlier DPM analysis [337], vascular followed by functional activity alterations were the most likely initial pathogenic events based on cross-sectional data. Such dynamical systems models are well suited to the rich mathematical tools of control theory, to determine perturbational inputs to guide the brain to a different state (Fig. 3.2a). These models can identify optimal treatment targets, doses and durations in various domains from molecular interaction networks [386] to brain stimulation [387]. In AD, MCM suggests that single-target therapy (e.g., targeting only amyloid accumulation or only vascular dysregulation) would be the least efficient way to return an advanced AD brain to a healthy state [33].

While cross-sectional data can be leveraged to select specific parameters to personalized using sensitivity analysis [388], applying MCM directly to individualized data can suggest biologically-based, patient-specific combination therapy to restore a healthy brain state [389]. Using a similar dynamical systems model, Zheng et al. note a stage-dependence on the relationship between physiological biomarkers and cognition; the amyloid parameter is most important at early disease stages but decreases in influence over time as neuronal degeneration has a stronger effect, further supporting combination therapy [388].

Network models of misfolded protein propagation

Neurotoxicity due to misfolded protein accumulation and inter-region propagation is a common theme across disorders, implicating pathogenic proteins with archetypal spreading patterns such as amyloid, tau, alpha-synuclein and TDP-43 [390]. In addition to the characteristic

patterns of proteinopathy, numerous studies have also co-localized structural and functional networks with disease-specific pathological alterations [391] [392], such as default mode network atrophy and hypometabolism in AD [393] and functional connectivity-associated tau accumulation in primary tauopathies [394]. These findings are the basis of the network degeneration hypothesis of neurodegeneration, depicted in Fig. 3.2b, which suggests that pathological changes propagate along brain networks [395] [396]. The convergence of empirical data and the emergent field of network neuroscience [397] has enabled extensive connectome-based modeling studies of neurodegenerative and other brain disorders [209] [398] [208].

A wide range of network propagation models have been applied to data from molecular neuroimaging. These models are defined and differentiated by their assumptions about seeding, clearance, propagation, and network organization. At the whole-brain level, simple isotropic diffusion is insufficient to explain the spatiotemporal spreading of pathological proteins across the brain. With diverse tissue types and long-range connections, the cytoarchitecture and connectome are likely determinants of propagation.

Investigating the consequences of purely diffusive propagation without regional specificity, Raj et al. developed a linear network diffusion model (NDM), with protein propagation along concentration gradients on a static structural connectome obtained from tractography [399] [400]. Certain eigenmodes of network diffusion patterns showed similarities to AD and behavioral variant FTD (bvFTD) atrophy patterns (Fig. 3.2c), and this model was also more predictive of end-stage atrophy and metabolic alterations than baseline imaging in the ADNI cohort, with inter-class differences in rate parameters [400]. Lacking a directed human connectome, Pandya et al. [401] extended the network diffusion model with regional analogues from the mouse connectome and examined the effects of directed connectivity on progressive

supranuclear palsy (PSP) atrophy. Both anterograde and retrograde propagation of purported tauopathy captured distinct topological patterns, suggesting the importance of propagation in both directions. Extensions of this approach attempted to infer seed regions of atrophy patterns [402], with most AD seed regions located in the temporal lobe, hippocampus and entorhinal cortex. Notably, model-derived seeds had a higher predictive power than assuming a common, hippocampal seeding, although no lower-dimensional latent structure was observed in the atrophy patterns and seeding regions. The importance of seed regions in determining eventual spatial spreading is emphasized by an anisotropic diffusion model, which recovers characteristic amyloid, tau, α-synuclein and TDP-43 deposition patterns based on different seed regions [403].

An important consideration in modeling protein propagation is chemical kinetics, such as the relationship between aggregation and clearing processes [207]. Garbarino and Lorenzi used Bayesian model comparison to evaluate different hypotheses of amyloid propagation in AD in silico [345]. Among increasingly complex dynamical systems models assuming i) constant diffusion of amyloid [399], ii) reaction-diffusion where aggregation and diffusion are simultaneous, and iii) non-linear accumulation, clearance and propagation, the latter performed best, where propagation is triggered by saturated aggregation rather than being a constant diffusive process.

Based on *in vitro*, animal and human studies, the aggregation of proteinopathy is believed to induce “prion-like” misfolding in normal proteins [301]. Compartmental models of interacting susceptible, infectious, and recovered (SIR) populations are commonly used to simulate infectious diseases, and such an epidemic spreading model (ESM) has been developed for intra-brain pathology propagation [404]. Initially applied to amyloid PET data from ADNI (Fig. 3.2d), there is a decrease in amyloid clearance rate and age of pathology appearance when going from

healthy controls to early and late MCI and finally AD patients [404]. Applications of this ESM to tau PET spreading patterns note that regions with high amyloid accumulation also display higher tau levels than predicted by connectivity-based spreading alone [241]. Other ESMs using MEG and tau PET data also demonstrated that functional connectivity predicts tau distribution patterns better than structural connectivity or simple diffusion [405], implicating dynamic activity as a substrate of pathological progression. In AD, amyloid accumulation is believed to form feedback loops with neurovascular uncoupling [406], and tau accumulation [55]. Causal mediation analysis suggests that amyloid positivity contributes to tau in the inferior temporal gyrus via a direct pathway as well as via medial temporal lobe tau levels [407], implying that both pathways would need to be targeted once an individual exhibits neocortical tau. Other, more detailed theoretical models (incorporating multiple forms of nucleation, elongation, etc.) also support the importance of amyloid-tau interactions and misfolded protein clearance, although available PET imaging data is unable to resolve all model mechanisms [408] [409]. Epidemiological models have also been combined with downstream modeling of neurotoxic proteinopathy effects result in atrophy (Fig. 3.2e) [410].

Competing hypotheses credit either connectivity-dependent intracellular or distance-dependent extracellular mechanisms for misfolded protein propagation. To compare these alternatives, Schäfer et al. [411] modeled longitudinal PET data using individualized network diffusion models. Although limited by the lack of follow-up imaging samples (with typically 3-4 visits per subject in ADNI), connectivity-based models seem to better match the longitudinal progression patterns observed in tau PET. Similar analyses using subject-specific Bayesian hierarchical modeling found statistically significant differences in average tau production rates and tau-dependent atrophy parameters between amyloid-positive and amyloid-negative

individuals [412] [413]. Other works suggest the importance of disease stage, with early spatiotemporal evolution of tau driven by propagation whereas local production dominates in later stages, with individual and regional factors explaining some variability [414] [415].

The model-inferred evidence for activity-dependent, connectome-driven and amyloid-enabled tau accumulation exemplifies the one application of causal modeling in evaluating disease hypotheses [405] [241] [407]. However, specific biological mechanisms of seeding, propagation and selective regional vulnerability remain unresolved [416]. Convincing answers to these mechanistic questions will likely require continued integration of macroscopic models dominant in the imaging community with microscopic aspects of chemical kinetics [207], cellular and molecular features [208], and clinical phenotype in dynamically-evolving models [209].

A Dynamical systems models of interacting physiological systems

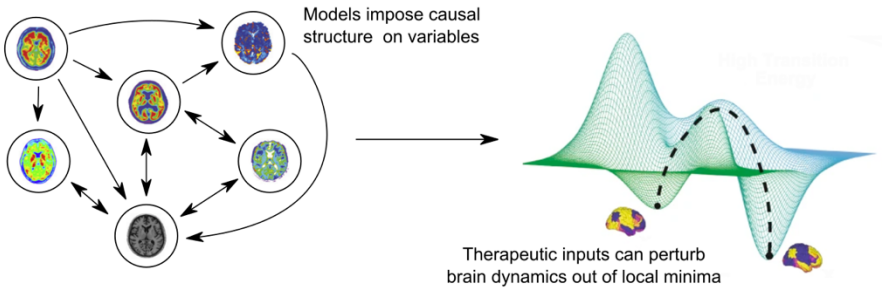

B Network models of connectome-driven pathophysiology propagation

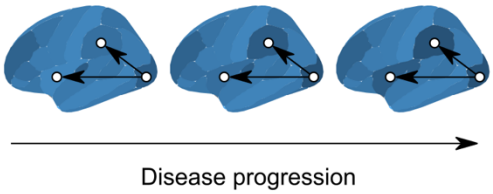

C Network eigenmodes resemble AD and bvFTD atrophy patterns

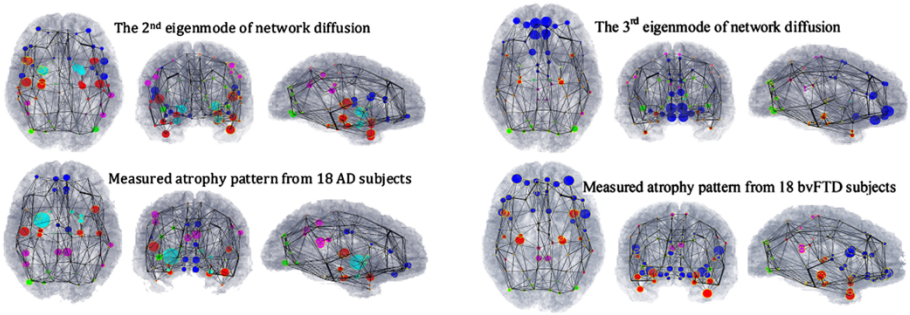

D Epidemiological model replicates amyloid propagation in the AD spectrum

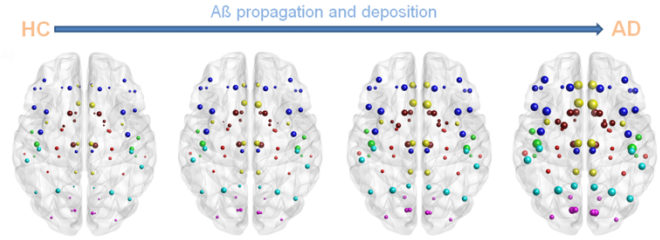

E Induced atrophy due to α-synuclein accumulation in PD

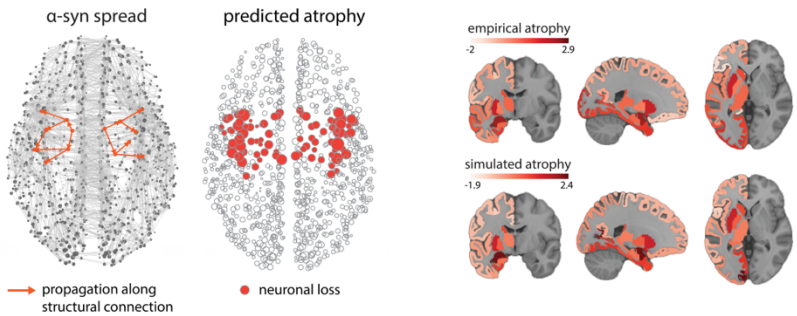

Figure 3.2. Mechanistic models of pathophysiological interactions and network propagation.

Dynamical systems-based models are used to explicitly represent intra-region interactions between different physiological systems, and inter-region propagation of pathophysiology. A) Dynamical systems models impose causal structure on the relationships between variables. They can be used to simulate the spatiotemporal evolution of brain dynamics, and to determine optimal therapeutic inputs. The figure on the right has been adapted from [417] and is under the Creative Commons Attribution 4.0 International License http://creativecommons.org/licenses/by/4.0/. B) Network models of connectome-driven pathophysiology propagation. These models consider the spatiotemporal propagation of disease factors, such as misfolded proteins, from regional epicenters along brain networks (e.g., structural, functional, or vascular connectomes). C) A network diffusion model noted the resemblance between eigenmodes of the structural connectome graph Laplacian and the disease-specific atrophy patterns observed in healthy ageing, AD and bvFTD. Figures have been adapted with permission from [399]. D) An epidemic spreading model (ESM) frames proteinopathy dynamics in terms of regional production, clearance, misfolding and propagation of misfolded proteins, and replicates spatial progression patterns observed from PET imaging. The figure has been adapted with permission from [404]. E) Although no approved α-synuclein PET tracer exists at the time of writing, this epidemiological model of neurotoxic protein propagation and subsequent atrophy in PD patients replicated empirical atrophy patterns. The figure has been adapted with permission from [410].

Molecular and cellular vulnerability to disease progression

Brain regions are differentiated by various molecular factors such as cytoarchitecture, neurochemistry, transcriptomics, and connectivity [418] [419], which render them selectively vulnerable in disease [301]. While the DPMs discussed so far can reconstruct biomarker trajectories and sequences, characterize spatial patterns of alterations and infer interactions between macroscopic neuroimaging features, the underlying molecular and cellular mechanisms are more difficult to ascertain.

Linking these biomarkers, which are often non-specific to pathophysiology [213] [420], to mechanistic pathways requires information about features such as gene expression and neurochemical organization. However, molecular data must typically be obtained post-mortem, limiting its spatial and temporal coverage, sample size, and availability for a disease population

of interest. Recently, many analyses have instead attempted to link spatiotemporal imaging pathology from neurodegenerative disease cohorts with template distributions of molecular features, such as mRNA expression for over 20,000 genes from the Allen Human Brain Atlas (AHBA) [421, 422], or neurotransmitter receptor densities from post-mortem autoradiography [423, 424] or PET imaging [425]. The growing body of research integrating neuroimaging-derived features with whole-brain molecular data (typically from averaged templates) has been termed the "molecular nexopathy paradigm" [426] or "imaging transcriptomics" [427, 428] (Fig. 3.3a). In this section, we summarize recent attempts to integrate molecular and cellular features in computational models of disease progression. We begin with several studies that show spatial correlations between imaging and molecular features. We then discuss how cellular and molecular features are used to augment mechanistic models, such as molecular-informed network propagation models and whole-brain dynamical models of coupled molecular and macroscopic physiological systems [429].

Neurochemical correlates of functional, perfusion and structural alterations

Neurotransmitter receptors are particularly relevant to behavioural function, interactions between physiological systems and pharmacological response. Neurotransmission dysfunction is implicated in many neurodegenerative disorders including AD and PD, and in their frequently co-occurring psychiatric symptoms [430] [23]. However, the expense of PET and the lack of in vivo radioligands [431] has impeded large-scale, case-control imaging studies for many receptor types in disease populations. Nevertheless, healthy template distributions of neurotransmitter

receptors are an informative proxy, and their physiological relevance to various populations has been supported by co-localization with macroscopic imaging signatures.

As the signaling system underlying neuronal activity, a natural first question is how neurotransmitter receptor architecture relates to spatial findings from functional and perfusion imaging. Cerebral blood flow (CBF) response to multiple drugs in young, healthy subjects is spatially correlated with autoradiography-derived receptor densities according to the corresponding drug-receptor affinity [432]. In the case of the dopaminergic D_2 receptor, antipsychotic CBF response was better explained by PET-derived receptor density maps than by the mRNA expression profile of the corresponding gene *DRD2* [433]. This is likely due to the many intermediary post-transcriptional steps separating gene expression from functioning receptors, supporting the complementary, but not identical, informativeness of these features. Acknowledging the multi-receptor binding of most psychedelic drugs and the complex interactions between various neurotransmitter systems, Luppi et al. found that pharmacologically-induce functional network reorganization is co-localized with neurotransmitter receptor expression [434], and regional susceptibility to cortical thinning in 11 neurological, developmental, and psychiatric disorders [434].

The impact of neurochemistry on structural vulnerability has also been supported by group-wise differences in the spatial correlation between receptor densities and disease-associated imaging features, such as atrophy patterns in schizophrenia patients with dyskinesia or parkinsonism [435], cortical thinning in PD patients with and without visual hallucinations [436], and white matter tract alterations in major psychiatric disorders (MPDs) [437]. In addition to patients with psychiatric symptoms, recent works have also co-localized healthy neurotransmitter receptor and transporter expression with structural and functional alterations in

neurodegenerative disorders. In behavioral variant FTD patients, reduced fractional amplitude of low frequency fluctuations (fALFF) in fronto-temporal and fronto-parietal regions correlated with the densities of serotonergic $5HT_{1B}$ and $5HT_{2A}$, $GABA_A$ and D_2 receptors as well as the norepinephrine transporter [438]. In particular, the strengths of the latter two associations correlated with symptom severity. In a PD cohort, fALFF alterations significantly associated with healthy D_2 and $5HT_{1B}$ receptor templates for both on and off levodopa conditions [439]. Voxel-wise gray matter volume differences spatially correlated with D_1 receptor and serotonin transporter densities in primary progressive aphasia (PPA) patients [440], and these spatial correlations are dependent on genotype and disease stage in FTD patients [441]. Specifically, prodromal *C9orf72* mutation carriers were associated with dopaminergic and cholinergic pathways, and *MAPT* carriers were linked to dopaminergic and serotonergic pathways, whereas no significant neurotransmission associations were found for prodromal *GRN* carriers. On the other hand, symptomatic FTD patients of all subtypes showed multi-receptor involvement including dopaminergic, serotonergic, glutamatergic and cholinergic pathways [441]. These studies suggest that the neurochemical architecture of the brain may influence the selective vulnerability of brain regions to structural and functional alterations, a topic that is further explored by mechanistic models discussed in later sections.

Transcriptomics correlates of imaging alterations

The spatial variation of gene expression in the brain and its relationship to imaging-derived features is also a topic of increasing interest [442]. Gene expression provides complementary molecular information to neurochemistry, and can be related to specific biological pathways using gene ontology. Correlative analyses using transcriptomic data have been applied to imaging signatures such as morphometric alterations in psychiatric disorders

[443] and inter-individual variability in healthy white matter functional connectivity [444]. The transcriptomic correlates of white matter tract alterations are consistent with genes associated with MPDs from other lines of evidence, such as genome-wide association studies (GWAS) [437].

The correspondence between specific, disease-associated genes and imaging measures can be disease- and pathology-specific; AD amyloid deposition shows a moderate positive correlation with the amyloid precursor protein gene *APP*, whereas neurodegeneration instead shows a similar association with the tau-associated gene *MAPT* [445]. In the main FTD genotypes, there is no significant correlation between atrophy patterns and *C9orf72*, *GRN* and *MAPT* expression [446]. However, genes associated with astrocytes and endothelial cells were overexpressed in regions with high atrophy, while neuronal- and microglial-associated genes were overexpressed in spread regions. In ALS patients, only *OPTN* showed a significant correlation with atrophy among disease-associated genes [447]. These correlative analyses can thus offer data-driven insight in addition to risk genes identified by GWAS.

Co-localization of imaging alterations and cell type expression

In addition to the contributions of diverse molecular pathways, the differential involvement of various cell types in neurodegenerative disorders is increasingly acknowledged [448] [449] [450]. Even characteristic disease genes, such as the *APOE* ε4 allele, appear to have cell type-specific effects [451], and mediation analysis suggests a pathway from tau pathology to cognitive decline via specific inhibitory neuronal, oligodendrocyte, astrocyte and endothelial cell populations [452]. In a case-control comparison of post-mortem tissue from AD patients and controls, the expression of cell type marker genes points to a decrease in excitatory neurons but an increase in inhibitory neurons and astrocytes in regions associated with AD cortical thinning

[453]. Whole-brain cell type proportion estimates from the AHBA gene expression data also indicate a correlation between the densities of non-neuronal cell types, particularly microglia and astrocytes, with atrophy across 11 neurodegenerative diseases including early and late onset AD, PD, ALS, FTD and dementia with Lewy bodies [454].

However, tissue heterogeneity is a notable limitation in bulk transcriptomics. As genomics progresses from bulk tissue to single-cell/nucleus sequencing and spatial transcriptomics [455] [456], and larger omics datasets such as the Seattle Alzhiemer's Disease Brain Cell Atlas (SEA-AD) become available [457], there is an increasing opportunity to integrate molecular information across scales and characterize regional and inter-individual variability [458] [459]. For example, Zeighami et al. combined the AHBA with single-cell gene expression from the middle temporal gyrus to compare the spatial expression patterns of disease-associated genes for 40 brain disorders, including neurodegenerative, developmental, psychiatric and movement disorders, and identify enrichment in specific cell types [460].

These applications represent some of the first efforts at resolving the cell type basis of neuroimaging alterations. Given the complicated and non-specific interpretation of many imaging measures (e.g., the influence of hemodynamics and afferent signals over regional activity on the BOLD signal [213]), the ability to disentangle the contributions of diverse cell types is a promising development.

Neurochemical and transcriptomic features in causal models

Molecular features can also be used to augment causal and network models discussed previously. Extensions of MCM have incorporated molecular mediation of interactions between pathological factors (Fig 3.3b) to improve the model explainability of structural, functional, metabolomic, cerebrovascular and proteinopathy alterations in the AD spectrum [461] [462]. In

these personalized models, inter-individual variability in receptor-mediated interactions terms closely correlated with symptom severity. In AD, two “disease axes", consisting of receptor-mediated biological interactions (e.g., between vascular and metabolic alterations), robustly correlated with inter-individual variability in i) executive dysfunction and ii) memory, language, and visuospatial symptoms [462]. Consistent with the dual syndrome hypothesis of PD [463], two distinct axes of model-inferred receptor-mediated interactions corresponded primarily to motor symptoms and secondarily to visuospatial, psychiatric and memory axis with a strong cholinergic component [464]. Likewise, inter-individual co-variability between transcriptomic contributions to imaging alterations and symptom severity in AD suggests the involvement of a wide variety of pathways, ranging from oxidative stress, immune/inflammatory response, G protein-coupled receptors, and mRNA splicing [461]. These findings support a biologically- and clinically relevant role of multiple neurotransmitter systems and diverse molecular pathways, informed by the neurochemical and transcriptomic organization of healthy brains.

The relative influence of local molecular vulnerability on connectome-driven propagation of proteinopathy (e.g., amyloid and tau in AD) remains an open question. Based on graph and network metrics in cognitively normal subjects, amyloid propagation co-localized with *CLU* expression and dendritic genes, whereas tau propagation was associated with *MAPT* expression and axonal genes, in addition to a shared association with lipid metabolism and the *APOE* gene [465]. Gradients of *APOE* and the glutamatergic synaptic gene *SLC1A2* expression are also implicated in the tau spreading network in cognitively unimpaired subjects [466]. However, an NDM suggests that gene expression alone does not explain pathology in AD; connectome-driven propagation predicts atrophy and hypometabolism better than the expression of single genes or principal components of multiple genes [467].

The pathways linking microscopic aggregation of α-synuclein with macroscopic functional activity and global brain network dysfunction in PD are also unresolved. Zheng et al. developed an epidemic spreading model of atrophy as a combination of α-synuclein mediated neurodegeneration and deafferentation (Fig 3.2e) [410]. Informed by evidence of gene function, the production and clearance of α-synuclein in this model were determined by the regional expression levels of *SNCA* and *GBA*, respectively. These transcriptomic features significantly improved model fit, with the substantia nigra identified as the region most likely to result in an epidemic spreading condition from an initial misfolded protein seeding. Similar dependence on structural brain networks and transcriptomic factors (*SNCA* and *GBA*) were also observed in the related synucleinopathies of isolated REM sleep behavior disorders using compartmental modeling [468]. Validating a computational network diffusion model in mice injected with α-synuclein, Henderson et al. found evidence for primarily retrograde transmission and dependence on *SNCA* expression [469]. In sporadic and genetic bvFTD, an agent-based spreading model implicated both network spreading effects as well as transcriptomic vulnerability in [470]; atrophy patterns from deformation-based morphometry (DBM) were correlated with the expression of FTD-associated *C9orf72* and *TARDP* genes. Epicenters varied between groups, potentially reflecting the convergence of multiple pathogenic factors to a common clinical syndrome mediated by network architecture [470]. These diverse applications demonstrate how transcriptomic data can be integrated into mechanistic models with or without prior knowledge of gene function.

Linking molecular features to model-inferred treatment needs

With regional variability in physiological interactions, connectome-based spreading of pathological factors, complex relationships between physiological and clinical biomarkers, and

cell type-specific vulnerability, clinical prognosis can be complicated. Notably, causal models such as MCM can solve the problem of optimal, personalized treatment using the mathematical tools of control theory [389]. Optimal controller design supports the efficiency of multi-factorial treatments, and notably, model-derived personalized therapeutic intervention fingerprints were found to better predict plasma gene expression than clinical assessments in the ADNI cohort [389]. In the PPMI cohort, imaging-derived therapeutic intervention fingerprints correlated significantly with genetic factors and plasma gene expression that also explain levodopa response [471].

The recently emerging body of work integrating molecular features with longitudinal imaging and clinical data indicates that connectivity, multiple transcriptomic pathways, diverse neurotransmitter systems and cytoarchitecture together determine regional vulnerability to physiological alterations in neurodegenerative disorders. As such analyses proliferate, it is important to note several sources of variability. Post-mortem data is rare and typically under-sampled compared to imaging data, and inter-subject or even inter-hemisphere variability is not fully characterized. At a more fundamental level, pleiotropic genes and polygenic traits complicate the reverse inference of genes responsible for imaging phenotypes [472]. Future work should aim to standardize methodology, for example microarray probe selection, the choice of brain atlas, interpolation, lateralization, within- and across-donor normalization, null brain maps, and open-access toolboxes [473] [474] [475] [476]. Nevertheless, the nascent field of imaging transcriptomics, using molecular data from representative populations [427], is a promising approach to linking in vivo macroscopic alterations with molecular pathways.

Biophysically constrained multi-scale dynamical models

Connectivity and interactions in the brain spans various scales, from local synapses and mesoscale circuits to long-range projections between distant brain regions [477]. As a result, there are complex relationships between microscopic molecular factors such as gene expression, cellular properties such as membrane potential and spike density, aggregation of neurotoxic pathology and neuronal activity, and macroscopic brain network dynamics. While the models discussed so far can hint at disease-relevant aspects of brain organization, the propagation of dysfunction up the hierarchy from microscopic to macroscopic scales has not explicitly addressed.

Biophysically constrained, whole-brain models of neuronal activity attempt to integrate data from multiple spatial scales to capture these relationships, typically with connectivity at the scales of i) cortical circuits comprising interacting excitatory and inhibitory neuronal populations and ii) long-range projections between macroscopic regions [478]. We distinguish these biophysically constrained models by their explicit modeling of multiple levels of brian organization. Simultaneously, these models must be detailed enough to provide mechanistic specificity, yet coarse-grained to be tractable. Microscopic properties of neural populations are typically averaged into spatiotemporal mean field or temporal neural mass models consisting of interacting populations of excitatory and inhibitory neurons, which contribute to macroscopic regional signals and network phenomena (Fig. 3.3c). By optimizing regional and global parameters to fit empirical data (e.g. fMRI or EEG/MEG signals), such approaches can evaluate the influence of cellular and molecular features on macroscopic alterations [479] [480] [481], and identify treatment targets for pharmacological interventions or brain stimulation [387].

Evaluating effective connectivity

Dynamical Causal Modeling (DCM) is a popular framework for model-based hypothesis testing [482], and has been used in many studies on task-based or resting state functional imaging (i.e., fMRI, EEG and MEG). At the core of DCM are individualized differential equation models of excitatory and inhibitory neural masses with local connections in cortical microcircuits as well as laminar-specific inter-regional projections. A forward model transforms this modeled neuronal activity into measured signal (e.g., BOLD signal for the fMRI models). Bayesian model comparison is then used to evaluate competing models [483], and DCM parameters can be compared across subjects and diagnostic classes. Unlike correlative measures (e.g., functional connectivity), DCM employs a causal model, and examining its parameters enables analysis of properties such as the effective connectivity of regional neuronal populations [484]. For example, DCM-inferred effective connectivity from the left dorsal premotor cortex to the left superior parietal cortex was (negatively) correlated with years to clinical onset in pre-symptomatic HD mutation carriers [485].

Neurotransmission modulates functional activity on a fixed structural connectome

A cognitively essential phenomenon that spans spatial scales and neurophysiological systems is the emergence of complex neuronal dynamics on a relatively fixed structural network via neurotransmitter modulation [486]. Multi-scale dynamical models are well suited to evaluating the effect of neurotransmission on the activities of local neuronal populations, as well as their hemodynamic or electrophysiological signatures (via observable BOLD or M/EEG signals).

The serotonergic system has several agonists of neuropsychiatric interest including psilocybin and LSD. Given the relatively fast action of these drugs, they offer a testbed for in silico dynamical modeling of pharmacological interventions. To investigate the effect of LSD on functional dynamics in a whole-brain, mean-field computational model, Deco et al. incorporated a single global gain parameter mediating the effect of local $5HT_{2A}$ receptor density on regional neuronal activity [487]. In this model, neuronal parameters were first fit to minimize the statistical distance between the temporal correlations of simulated and placebo condition functional connectivity matrices, and then tuned to the LSD condition using the global gain parameter. To simulate the effects of psilocybin intake on the BOLD signal, Kringelbach et al. instead used a dynamically coupled model of neuronal-neurotransmitter interaction [486]. Serotonin release is determined by neuronal activity, and vice versa, with regional $5HT_{2A}$ receptor density modulating the effect, and the model is fitted to features obtained by clustering the phase coherence between regional activity in a reduced dimensional space. The results support the importance of specific receptor density in both models; the $5HT_{2A}$ receptor distribution is significantly more informative to the pharmacological response of LSD [487] and psilocybin [486] than other serotonergic receptors or the serotonergic transporter. This molecular insight has therapeutic implications since pharmacological treatment of psychiatric disorders typically involves selective serotonin reuptake inhibitors (SSRIs) acting via the transporter.

Psychedelic drug response has also been associated with an increased entropy of electrophysiological signals, and the subjective experience of psychedelics and the increased firing rate entropy may relate to the consequential ease of achieving different dynamical states of activity. [488]. Herzog et al. fit mean-field models, with serotonergic gain modulation of neuronal firing rate, to fMRI data from subjects under the influence of LSD and controls, and

simulated resting state activity with and without $5HT_{-2A}$ agonism [489]. The regional increase in activity entropy due to LSD was explained well by a combination of local $5HT_{2A}$ receptor density and connectivity. Using network control theory informed by $5HT_{2A}$ receptor density, Singleton et al. quantified LSD, psilocybin and DMT response as a reduction in brain network control energy [417] [490], associated with reduced functional connectivity differentiation [491]. In a non-psychedelic scenario, Coronel-Oliveros et al. demonstrated the relevance of PET templates of cholinergic receptors and transporters to resting state and attentional task activity [492]. Whole-brain models based on neural masses were fit to EEG and BOLD signals from nicotine users. The model-inferred mechanistic effect of nicotine was reduced global coupling and local feedback inhibition. Furthermore, nodal functional connectivity changes correlated with $\alpha_4\beta_2$ receptor density [492].

Other multi-scale dynamical models have also incorporated aspects of neurotransmission. A mean field model links observable measures of functional integration/segregation with unobservable neurotransmitter kinetics (synaptic release and receptor binding) and its coupling with neuronal activity [493]. This model demonstrates that departures from an optimal E/I (i.e., glutamate/GABA) balance are associated with altered network measures of integration/segregation observed in functional connectivity analysis in neurological disorders [493]. A DCM study also integrated neurotransmitter concentrations from magnetic resonance spectroscopy (MRS) and resting state activity from MEG, to examine the specific connections affected by inter-individual differences in neurotransmitter concentrations in healthy subjects [494]. As expected, GABA concentrations influenced local recurrent inhibitory effective connectivity in the model, while glutamate levels influenced excitatory connections.

Mechanisms of excitatory-inhibitory imbalance and excitotoxicity in neural mass models

Electrophysiological data from M/EEG provides better temporal resolution at the expense of the spatial resolution of fMRI, and certain features such as attenuation of specific spectral bands are characteristic of AD [495]. In an early work combining neural mass modeling with a connectome template in AD, de Haan et al. simulated electrophysiological signals in healthy and diseased states with activity-dependent degeneration of synapses in response to spike density [496]. Compared to non-specific degeneration, activity-dependent degeneration better explained the structural and functional network alterations expected in AD, including oscillatory slowing, power spectrum attenuation, long-range desynchronization, hub vulnerability, and altered functional networks [496]. Notably, hub regions with high connectivity showed specific vulnerability as the sites of both higher amyloid deposition and increased neural activity. Although the symptomatic correlates of these alterations were not characterized, such models can be used to simulate expected macroscopic outcomes of interventions [497]. Counter-intuitively, excitatory neuronal stimulation was found to best preserve network activity. These findings highlight the complex response of the brain to simple perturbations, and the need for principled modeling of treatment effects. In AD patients, Sanchez-Rodriguez et al. used the framework of optimal control to determine stimulation target regions to steer the alpha band power spectrum towards a healthier, higher frequency state [387]. Notably, individuals with high anatomical connectivity (i.e., short path lengths and high global efficiency) had a lower stimulation energy cost.

Fitting MEG data from controls and MCI patients with amyloid pathology, van Nifterick et al. evaluated various mechanistic hypotheses of cellular alterations to excitatory and inhibitory

populations in AD [498]. Pyramidal neuronal hyperactivity, inhibitory neuronal hypoexcitability, increased excitatory-excitatory coupling and decreased inhibitory-excitatory coupling were linked to oscillatory slowing [498]. Similar neural mass models have been used to assess various candidate markers of excitation-inhibition (E/I) ratio [499].

Other works explicitly include local amyloid and tau levels and their pathological propagation in neural mass models. Alexandersen et al. assumed connectivity-driven propagation of tau and more diffuse spatial spreading of amyloid simultaneously from multiple epicenters [500]. This model showed an initial increase in alpha band power in simulated M/EEG signals followed by a decrease, as well as a slowing of alpha band oscillations due to a decrease in excitatory activity and increased global coupling.

With the advent of new imaging targets, dynamical models can incorporate several molecular factors simultaneously. Sanchez-Rodriguez et al. combined structural, functional, amyloid, tau and glial imaging, plasma markers and clinical data from 132 subjects on the AD spectrum from the Translational Biomarkers in Aging and Dementia (TRIAD) cohort in neural mass model [501]. The subject-specific influences on neuronal excitability (i.e., firing thresholds) of regional levels of amyloid, tau and their synergistic interaction were optimized to reconstruct individuals' BOLD signals. AD subjects were characterized by lower alpha power and increased theta power, with neuronal excitability differing based on amyloid status and Braak stage. Notably, model-inferred, latent neuronal hyperexcitability correlated with worsened cognitive symptoms and plasma tau biomarker concentrations [501].

The Virtual Brain (TVB) [502] is a multi-scale, whole brain mean field modeling framework that has been used to reproduce features of empirical fMRI and EEG signals [503], relate them to cellular-scale properties such as E/I balance [504], optimize lead placement for

deep brain stimulation [505] and predict functional connectivity outcomes of neurosurgery [506] [507]. In the context of neurodegenerative disorders, TVB has also been used to infer the macroscopic impact on EEG signals of amyloid modulation of neuronal dynamics [508] In AD patients, simulations reproduced properties of EEG signals, and reducing model weights (simulating the effects of the NMDA receptor antagonist memantine) partially reversed the characteristic oscillatory slowing [508]. Dynamical models such as TVB can also be used to infer relevant mechanistic alterations. Fitting resting state fMRI data in controls, amnestic MCI subjects and AD patients, statistically significant inter-subject correlations were observed between model parameters (representing excitatory-excitatory, excitatory-inhibitory, inhibitory-excitatory, and global coupling) and various cognitive domains [509]. These model parameters can differ between diagnostic categories and functional networks. For example, AD patients have significantly increased excitatory coupling in the default mode network, but it is reduced in the somatomotor network. The frontoparietal network, which is preserved in AD, involves alterations to all 4 TVB parameters in FTD [510].

Perturbational trajectories in low dimensional space

Low dimensional embeddings can be useful in capturing the salient structure of high dimensional brain states, such as neuronal activity or functional connectivity [511]. To compare the regional effects of external stimulation on different brain regions and across conditions, Sanz Perl et al. fit a phenomenological whole-brain model to the empirical functional connectivity of healthy controls, and AD and behavioral variant FTD patients [512]. Different waveforms of stimulation were applied to these models (specifically, to the bifurcation parameter, related to the excitatory-inhibitory balance). The resulting functional connectivity trajectories were visualized in a low dimensional space via variational autoencoders (VAEs), a non-linear dimensionality

reduction technique with a regularized latent space. While the parameters of this model themselves are difficult to interpret, proximity in the VAE latent space implies similar functional connectivity, and diagnostic classes clustered well in the latent space representation of functional connectivity. Perturbational trajectories in this latent space were then used to determine the proximity of different brain regions to the distribution in healthy controls. Depending on the waveform, stimulation to visual areas, the sensorimotor cortex, and the temporal lobe, including the hippocampus, perturbed AD subjects towards healthy latent representations. Meanwhile, frontal regions were the most important to behavioral variant FTD perturbations [512].

Multi-modal data integration in biophysical models

Dynamical models are a promising approach to understanding the molecular mechanisms behind macroscopic observations, and their associations with clinical variables at the group or individual level. Many dynamical models have incorporated molecular information, particularly neurotransmission and neurotoxic proteinopathy mechanisms, and explored the effects of external perturbation. More generally, other molecular drivers of regional susceptibility can also be incorporated, potentially informed by the models presented in the preceding sections. In contrast to the many dynamical models that simulate functional or electrophysiological activity, Khanal et al. developed a biophysical model of atrophy and brain deformation to generate realistic simulated atrophy patterns from longitudinal data in AD [513]. Accounting for the different mechanical properties of parenchyma and CSF, tissue remodeling minimizes internal mechanical stress due to neuronal death. A promising avenue of future work is the incorporation of other physical drivers of neurodegenerative brain alterations, including mechanical stress due to atrophy or inflammation, molecular influences on cellular properties, macroscopic influence on brain networks, and global effects of environmental factors. Looking beyond dynamical

models of neuronal activity and considering mechanical effects is a promising direction for multi-scale models [514].

A Spatial co-localization with imaging alterations

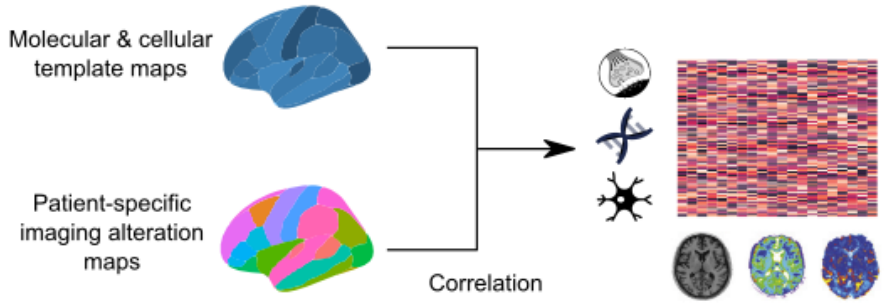

B Regional vulnerability in dynamical systems models

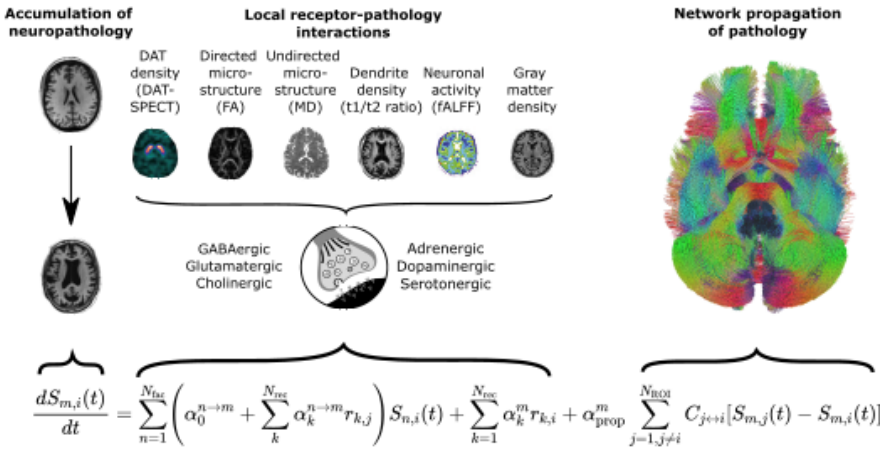

C Multi-scale biophysical models

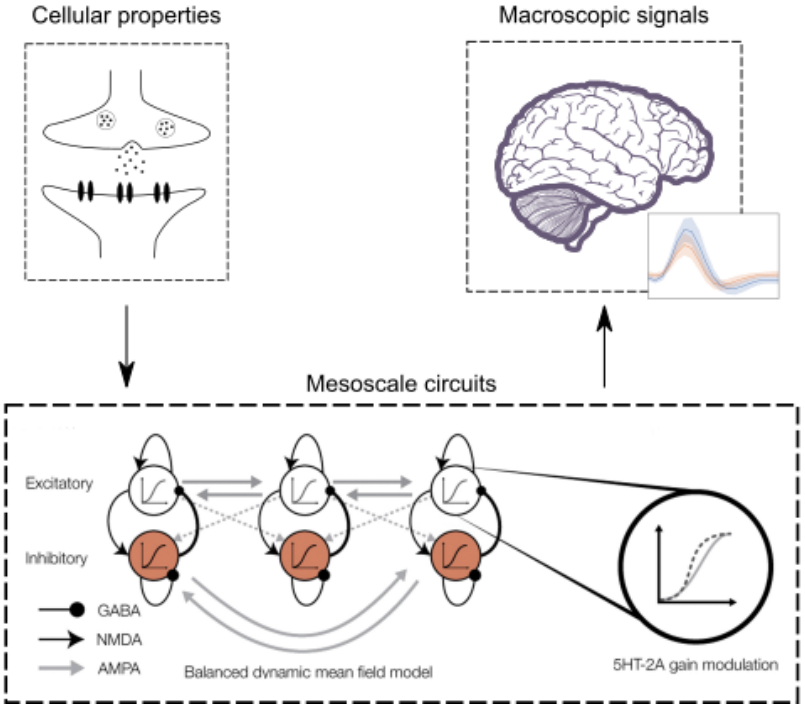

Figure 3.3. Understanding the role of cellular architecture and molecular mechanisms on large-scale brain alterations.

3) Imaging transcriptomics analyses use spatial correlations to identify cellular and molecular features co-localized with imaging alterations. B) Dynamical systems models can incorporate cellular architecture, for example, as mediators of physiological interactions. The figure has been adapted with permission from [464]. C) Biophysically constrained models consider the cellular, mesoscale circuit, and macroscopic network effects. These models can incorporate molecular mechanisms such as amyloid- and tau-mediated hyperexcitability [501] and serotonergic receptor-mediated gain modulation [487] at the appropriate scale. The figure has been adapted with permission from [487].

Category	Definition	Example method	Summary
Continuous-time disease progression models (DPMs)	DPMs are mathematical models that describe the temporal progression of one or more disease-associated markers (e.g., a clinical assessment, neuroimaging measure, CSF assay, etc.) either in individual patients or as population-averaged trajectories.	Mixed-effects model	Mixed effect models hierarchically model between- and within-subject variability via a combination of fixed and random effects. They are statistically suited to the correlated errors that arise from repeated and unevenly spaced measurements from observational studies [341] [337] [310].
		Quantile regression	Rather than estimating the mean of the dependent variable, quantile regression models different parts of the distribution (e.g., medians or quartiles). These methods can be flexible in the trajectories that can be modeled, while retaining interpretability (e.g., vector generalized additive model [340]).
		Trajectory inference	Analogous to its applications in single-cell analysis, trajectory inference algorithms arrange subjects according to disease severity, typically fitting trees in a low-dimensional space [348] [349].
Event-based models (EBMs)	A family of DPMs that estimates the most likely sequences of biomarker alterations from cross-sectional data. These methods assume that a mixture of sub-populations (patients and controls) underlies	Discriminative event-based model (DEBM)	DEBM expands on the standard EBM to estimate a central ordering across subjects from which a relative distance between events can be estimated [367].
		Subtype and Stage Inference (SuStaIn)	An EBM that simultaneously clusters subjects into subtypes following distinct disease trajectories [369].

	biomarker data [361] [362].		
Dynamical systems models (regional interactions)	Using coupled differential equations, these models impose causal structure on the interactions between variables. This may take the form of intra-region interactions between different biomarkers or inter-region propagation of pathophysiology.	Multifactorial causal model (MCM)	MCM models the interactions between various disease factors, as well as their propagation along (structural, functional, or vascular) brain networks [33]. Extensions of MCM have considered cellular and molecular features that may mediate these interactions, such as gene and receptor expression [461] [464] [462].
Dynamical systems models (network propagation)	Dynamical systems models are also used to represent the spatiotemporal propagation of pathological factors from an epicenter region.	Epidemic spreading model (ESM)	Based on epidemiological compartmental models, this network propagation model considers the spreading of pathological agents (typically misfolded proteins such as amyloid) following a susceptible-infectious-recovered (SIR) paradigm. Regions have an increased chance of developing more severe pathology after "infectious" seeding from a connected region [404].
		SIR model with gene expression and simulated atrophy	This model incorporates *GBA* and *SNCA* transcriptomics maps to inform regional α-synuclein production and clearance rates. Regional atrophy is a consequence of α-synuclein accumulation [410].
		Network diffusion model (NDM)	These models consider the spreading of pathology to follow a diffusion process along a connectome [399].
Multi-scale biophysical models	Biophysical models of whole-brain neuronal activity dynamics integrate cellular and molecular properties,	The Virtual Brain (TVB)	TVB is a multi-scale biophysical model and platform for simulating individualized EEG, MEG and BOLD data, and inferring inter-group differences in personalized model parameters (e.g., E/I balance) [502] [508] [510] [504] [509].

	mesoscale regional microcircuits, and large-scale connectivity. These models are typically fit to fMRI or EEG data and can evaluate inter-individual or inter-group differences in unobservable physiological parameters such as excitatory-inhibitory (E/I) balance.	Dynamic causal model (DCM)	Neuronal systems with (e.g., hemodynamic) forward models are used to simulate functional neuroimaging signals (i.e., fMRI, EEG, MEG, etc.). Bayesian model comparison is used to determine the neuronal mechanisms (e.g., effective connectivity) behind observed signals [485].
		Pathophysiological activity decoder	Regional levels of amyloid and tau affect local neuronal excitability, and their effects on BOLD signals are simulated using a hemodynamic model [501].
		Coupled neuronal-neurotransmitter model	Serotonergic neuromodulation and activity-driven neurotransmitter release is modeled explicitly. These models are fit to empirical functional activity data [486].

Table 3.1. Computational approaches to integrating multi-modal neuroimaging data to characterize disease progression and infer latent mechanisms.

Primary cohort	Modeling approach	Summary
Dominantly inherited Alzheimer's disease patients	Continuous-time DPM of CSF, blood, cognitive and imaging markers	The earliest biomarker alterations (decreased CSF amyloid levels) were found up to 25 years before expected symptom onset. This was followed by increased amyloid PET signal, CSF tau and atrophy. Finally, hypometabolism, episodic memory impairment and global cognitive impairment occur in the decade leading up to symptom onset [15].
Sporadic Alzheimer's disease patients	EBM with subtyping (SuStaIn) of tau PET	Four spatiotemporal trajectories of tau progression were identified, defined by limbic, medial temporal lobe-sparing, posterior and lateral temporal tau patterns [242].
Multiple sclerosis (MS) patients	EBM of gray matter atrophy	Relapse onset and primary-progressive MS patients follow distinct atrophy sequences that are consistent within each subtype [365].
Parkinson's disease patients with an elevated risk of dementia	EBM of clinical and imaging (quantitative susceptibility mapping and diffusion-weighted imaging) features	The classic prodromal symptoms of REM sleep behaviour and olfactory problems precede all other markers, and the earliest imaging markers are frontal and temporal iron concentrations [515].
Familial frontotemporal dementia patients	Continuous-time DPM of clinical assessments, regional brain volumes and plasma NfL	Biomarker trajectories are (*GRN*, *MAPT* and *C9orF72*) genotype-dependent [16].
Posterior cortical atrophy (PCA) patients	Longitudinal differential equation model and cross-sectional EBM of regional brain volumes and neuropsychological assessments	The characteristic occipital and parietal atrophy are followed by temporal lobe atrophy and ventricular expansion. Visuospatial processing declines rapidly in PCA compared to AD [516].

Table 3.2. Examples of data-driven characterization of biomarker alterations in neurodegenerative disease cohorts.

Discussion and conclusion

Summary

Despite varying genetic [2], environmental [3] and age-related [4] risk factors, causes of sporadic neurodegenerative disease onset remain unknown. Healthy brain function requires the coordination of multiple physiological systems, and neurodegenerative disorders can affect altered neuronal activity, proteinopathies, vascular dysfunction, neuroinflammation, metabolic alterations, cell death, and atrophy. In the preceding decade, computational models of these multi-factorial processes have proliferated. Continuous time DPMs and discretized EBMs have provided data-driven staging of biomarker abnormality, network propagation models have characterized pathology propagation across brain networks, the integration of molecular data sources has identified salient aspects of cyto-, receptor- and transcriptomic-architecture, and dynamical systems models have been used to reproduce and evaluate disease mechanisms.

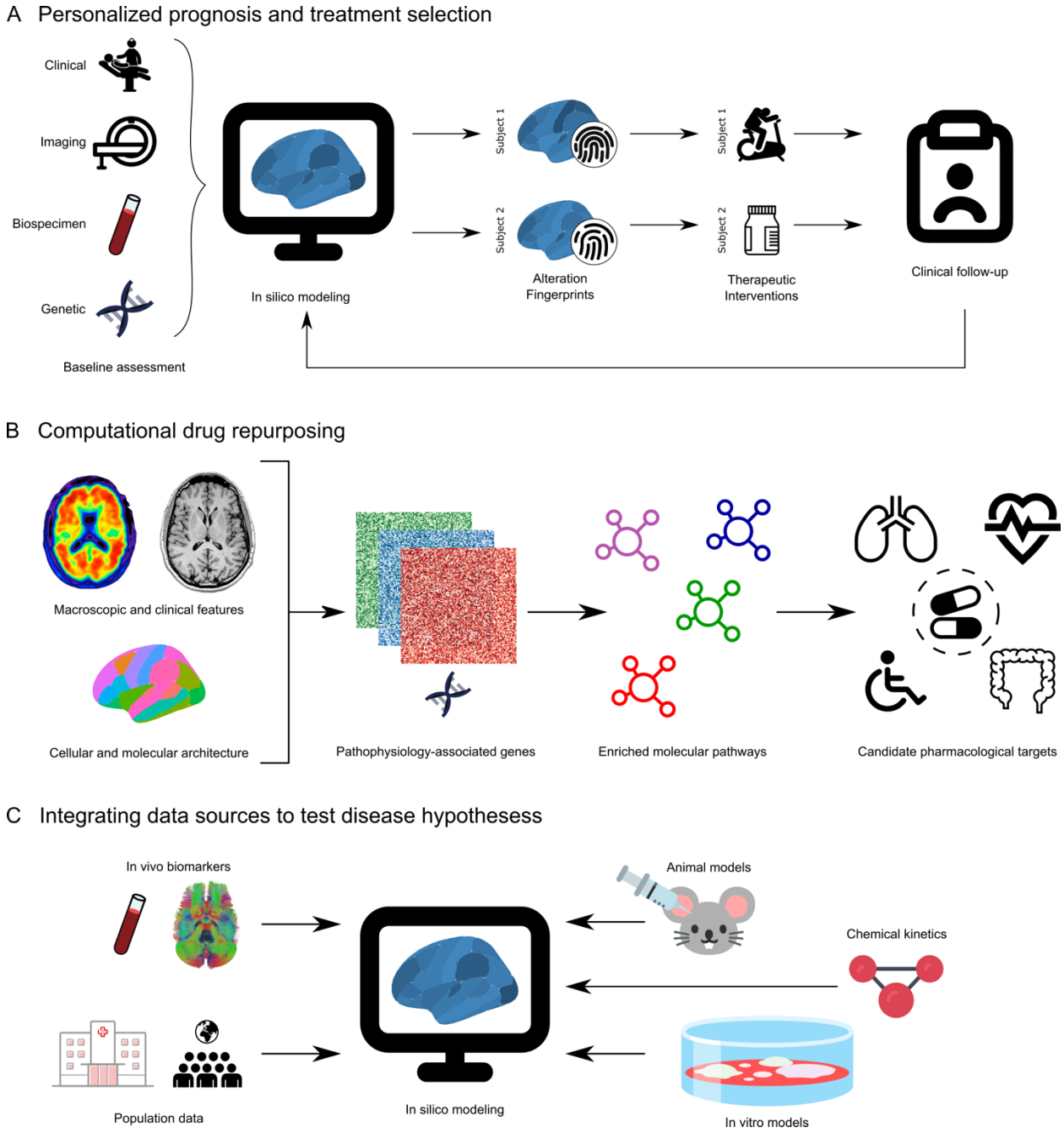

Figure 3.4. Using multi-factorial computational models to improve treatment selection and test mechanistic hypotheses.

Computational models of spatiotemporal pathophysiology progression can go beyond correlative analysis and infer disease-altered mechanisms. A) Integrative in silico modeling of the progression of multiple biomarkers can be used to predict future disease progression and infer optimal therapeutic interventions at an individualized level [389]. B) The role of the molecular architecture of the brain in various disease-affected alterations is an open question. Molecular pathways enriched in disease-affected tissue (e.g., where amyloid and tau accumulation alters functional activity) can be used to identify potential therapeutic targets

[517]. C) Computational modeling can benefit from diverse data sources, incorporating population-derived distributions of disease onset age with in vivo biomarker data [16], using homologous structures in other species to inform directed network propagation models [401], and validating model predictions using invasive experiments in animal models [518].

Causal inference using computational models

Yet, the central question remains: what are the causes of sporadic neurodegenerative disease onset, and how can they be treated? Over the 20th century, the post mortem clinico-anatomical method has been largely superseded by correlational in vivo neuroimaging studies [331], but this has not resulted in robust, disease-specific diagnostic or prognostic markers [519] [520]. Biomarker correlates of symptoms and treatment effects may be spurious, compensatory, or secondary to causal pathogenic mechanisms. The gold standard of causal evidence is the randomized controlled trial, requiring experimental intervention, in which studied populations, manipulated variables, and observed outcomes are carefully defined and individuals are blindly separated into control and treated groups. In the context of neurodegenerative pathogenesis in humans, this is often infeasible due to ethical concerns, the long temporal scale of disease progression, and the lack of appropriate counterfactuals.

Sufficient sample sizes can often be achieved only by multi-site observational studies, which can suffer from recruitment bias, missing data, patient drop-out, and varying protocols. Standardized workflows and validation in independent datasets may alleviate some of these issues, as well as harmonization to correct for technical and sample differences [521]. Nevertheless, large observational studies can still be leveraged for causal inference [522], and the Bradford Hill criteria provide a blueprint to design experiments and analyses to evaluate causality [331]. For example, DPM and EBM approaches can support or refute purported causal relationships between biomarkers via temporality, while dynamical systems approaches can

incorporate explicit causal structure and are well suited to modeling response to external perturbation. Other statistical techniques such as regression discontinuity design, differences-in-differences, Bayesian networks, and structural equation modeling are also appropriate for quasi-experimental causal inference [523]. Finally, we must be aware of the multiplicity of meaning behind the term "causal mechanism" in the literature, which can range in spatial scale from molecular interactions and cellular processes to circuit properties and abstract topological and network concepts [524].

In addition to considerations about causality, study design is often not explicitly considered or justified in computational models of observational data. In randomized experiments, there is a clear and well-defined distinction between pre-existing covariates, and outcomes after treatment. If the latter differ between the two groups significantly more than random chance, they are attributed to the treatment. However, this distinction between covariates and outcomes can be more blurred in observational studies. Well-designed observational studies should aim to approach characteristics of randomized experiments. One way to do so may include the definition of multiple control groups, to account for plausible alternatives [525].

On a related note, case-control studies may be sensitive to the precise selection criteria, particularly in the absence of robust biomarker disease categories. Often, inclusion criteria are intended to homogenize the studied population, but can introduce assumptions and biases. For example, amyloid-based definitions of "typical AD" can affect the results of downstream DPM analysis [367], and it is unclear whether patients with tau but no amyloid pathology should be considered to have early AD or non-AD pathology [526].

Although they are inherently limited by cohorts, study design, and collected data modalities, computational brain models can potentially resolve the "causality gap" [527], a

prerequisite for improving treatment target selection [528] [387]. Conversely, interventional studies can provide rich evidence to evaluate generative brain models and resolve causality. Autopsies [529] and biopsies conducted during standard treatment procedures (e.g., deep brain stimulation [530] or tumor [458] surgeries) can also be a valuable source of omics data with minimal modifications to routine clinical workflow. Phenotyping patients selected based on genotype also offers an alternative to the typical imaging transcriptomics workflow [472]. As the field continues to mature, closer links between experimental design, computational modeling and clinical considerations are imperative to resolving the unmet potential of neuroimaging-based modeling in clinical practice [520].

Clinical applications of computational models

Computational models also have rich applications outside of causal inference and scientific hypothesis testing. Suggested use cases of DPM-inferred latent disease time include defining endpoints [16], and inclusion criteria [327] [366] to reduce the number of subjects required to observe intervention effects in clinical trials. Personalized treatment design based on whole-brain dynamical models can also guide clinical interventions (Fig. 3.4a) [471] [33] [389] [531] [407], a paradigm that has wide applications from psychiatric disorders [532] [478] to epilepsy [533] [534]. While other applications are often focused on controlling pathological neuronal activity via stimulation, neurodegenerative disorders are likely to require multi-faceted treatment addressing the many affected physiological systems [33], with some responding slower than others. Indeed, current single-target, anti-amyloid monoclonal antibodies fail to cross the threshold of clinically important cognitive and functional benefit [27]. Model-inferred computational drug repurposing based on associated molecular pathways can also be used to

speed up the drug development process (Fig. 3.4b) [517]. Given potential limitations about the controllability of brain networks as well as practical implementations of such interventions, significant work is still needed to translate computational models into clinical practice [535].

Expanding current whole-brain models

There are several other methodological avenues for future work for whole brain computational models. Connectome-based modeling typically considers either structural or functional connectivity. However, a more complete picture may need to also consider metabolic, vascular, and molecular connectivity [33]. Comprehensive integration of multiple forms of connectivity and features driving local molecular vulnerability using causal, network and biophysical models is a promising avenue of research [536] [537].

Supporting these methodological extensions are technical advances providing new sources of molecular data. Causes of selective vulnerability, including cell type, can be further characterized throughout the cellular life cycle by single cell profiling and iPSC methods [448]. Given the differential contributions of genes associated with specific sub-cellular structures, the ever-improving spatial resolution of cellular profiling is a valuable development [465]. While in vitro and animal models cannot perfectly reproduce cognitive decline and other phenotypic aspects of neurodegenerative disorders [538], they can be used to validate new methods (Fig. 3.4c). In non-human animals, meso- and micro-scale features can be probed more invasively, and intervention effects can be tested more readily [539]. Computational models of protein propagation in rodents can image features such as directional [401] and meso-scale connectivity [518] [540], and microglial influence [541]. Other functionally relevant neuroanatomical features, such as laminar structure, may be further resolved by advances in human imaging [542].

Finally, an important consideration that is often overlooked in DPMs is the roles of genetic, sex, environmental, lifestyle and comorbid risk factors in sporadic disease onset and progression. One way to address this would be genome-wide association studies (GWAS) with imaging phenotypes and analysis of modifiable risk factors from large observational studies. For example, diabetes, air pollution and alcohol intake frequency were associated with structural degeneration of a vulnerable brain network [543]. Furthermore, DPMs have also noted genotype-specific progression patterns. In sporadic AD, an early EBM application noted more homogenized disease progression in *APOE* ε4 carriers [362], while a continuous-time DPM demonstrated sex differences in how genotype affects progression [327]. The main familial FTD genotypes also present distinct progression patterns [16]. Data-driven analysis of the impact of other non-autosomal dominant genetic risk factors on progression trajectories would address an important gap in our understanding of sporadic neurodegenerative diseases.

Bringing in vivo biomarkers to clinical practice

Although imaging and fluid measures have shown promise in research settings, we still lack definitive clinical biomarkers across neurodegenerative diseases, particularly in the early prodromal or preclinical stages [544] [545] [546]. Robust in vivo biomarkers are likely necessary for the detection of disorders in the pre-clinical phase, when treatment is most likely to succeed, as well as to monitor progression and treatment response [526] [547]. While there may be systematic factors hindering impact on clinical practice, such as a shortage of resources, physician unfamiliarity, non-standardized testing, lack of regulatory approval, incomplete validation, and inconsistent coverage by healthcare systems [548] [286], there are also technical limitations. In vivo biomarkers have varying but generally imperfect specificity and sensitivity to the underlying physiological process of interest. For example, the BOLD signal is merely a

proxy for functional brain activity [549], molecular imaging is susceptible to regionally-heterogeneous ligand uptake and off-target binding [526], and fluid markers are subject to variable protein kinetics [526]. As such, biomarkers (and any model-inferred features such as disease time) require extensive normative characterization, standardization across studies, replication across cohorts, and validation with neuropathology and clinical status [550].

Towards biomarker-based disease definitions

Even with clinical and neuropathological validation, there is room for disagreement about what (combination of) pathology constitutes a particular disorder due to the absence of definitive biological disease definitions. Individuals with tau but no amyloid pathology from PET imaging may be considered to have either early AD or non-AD pathology [526]. Furthermore, co-pathologies are potential sources of heterogeneity driving biological subtypes in disorders such as AD [13].

The knowledge gap between symptomatically defined neurodegenerative diseases and unknown pathogenic causes is a major impediment to drug development [551]. In general, the ratio of research and development expenses to FDA-approved drugs has been rising exponentially since the middle of the 20th century [552]. Yet, potential reversals to this trend may be occurring due to genomics-validated targets for rare diseases, where drug development benefits from biologically homogenized patient populations [553]. Until the recent anti-amyloid monoclonal antibodies, neurodegenerative disorders have suffered for decades from a lack of successful drug trials [547]. The typical pharmacological approach for these complex and heterogeneous diseases is fixated on a single target, usually reducing the insoluble form of a proteinopathy such as amyloid, tau, α-synuclein or TDP-43 [298] [554] [555] [556]. However,

looking beyond the usual proteinopathy suspects can reveal effective modifiable risk factors such as vascular health [89].

To this end, biological disease definitions are imperative, and likely involve molecular networks spanning multiple pathways [551]. A thorough molecular profiling of brain tissue or other biospecimens is needed to stratify biological heterogeneity [557] [360], along with combination therapy addressing the affected molecular networks and macroscopic physiological systems [547] [555]. The integrative computational modeling approaches discussed in this review can support these efforts to uncover the biological basis of clinical heterogeneity in transdiagnostic populations [558] [282].

Chapter 4. Personalized brain models identify neurotransmitter receptor changes in Alzheimer's disease

Ahmed Faraz Khan, Quadri Adewale, Tobias R. Baumeister, Felix Carbonell, Karl Zilles, Nicola Palomero-Gallagher, Yasser Iturria-Medina

Preface

Imaging and computational modeling studies support a multi-faceted view of AD, involving proteinopathy as well as vascular, metabolic, structural and functional alterations. However, the role of the brain's neurochemical organization in mediating the pathophysiological cascade had not been well characterized. This chapter presents the first application of the receptor-enriched multifactorial causal model (re-MCM) to AD, extending the original implementation of MCM to account for neurochemical features [33]. Using longitudinal data from ADNI for healthy controls, MCI subjects and AD patients, we fit personalized (i.e., subject-specific) models of 6 neuroimaging-derived variables representing regional brain integrity. The imaging variables are gray matter density, functional neuronal activity, CBF/perfusion, glucose metabolism and amyloid and tau distribution. These models are informed by the spatial distributions of 15 neurotransmitter receptors from autoradiography-derived templates. In this work, we verify that group-averaged autoradiography templates are informative to subject-specific models, and identify specific model-inferred physiological interactions associated with symptomatic decline.

This work was published in *Brain* on October 4, 2021 [462] and is accessible online: https://doi.org/10.1093/brain/awab375.

Abstract

Alzheimer's disease (AD) involves many neurobiological alterations from molecular to macroscopic spatial scales, but we currently lack integrative, mechanistic brain models characterizing how factors across different biological scales interact to cause clinical deterioration in a way that is subject-specific or personalized. Neurotransmitter receptors, as important signaling molecules and potential drug targets, are key mediators of interactions between many neurobiological processes altered in AD. We present a neurotransmitter receptor-enriched multifactorial brain model, which integrates spatial distribution patterns of 15 neurotransmitter receptors from *post-mortem* autoradiography with multiple *in-vivo* neuroimaging modalities (tau, amyloid-β and glucose PET, and structural, functional and arterial spin labeling MRI) in a personalized, generative, whole-brain formulation. Applying this data-driven model to a heterogeneous aged population (N=423, ADNI data), we observed that personalized receptor-neuroimaging interactions explained about 70% (± 20%) of the across-population variance in longitudinal changes to the six neuroimaging modalities, and up to 39.7% ($P<0.003$, FWE-corrected) of inter-individual variability in AD cognitive deterioration via an axis primarily affecting executive function. Notably, based on their contribution to the clinical severity in AD, we found significant functional alterations to glutamatergic interactions affecting tau accumulation and neural activity dysfunction, and GABAergic interactions concurrently affecting neural activity dysfunction, amyloid and tau distributions, as well as significant cholinergic receptor effects on tau accumulation. Overall, GABAergic alterations had the largest effect on cognitive impairment (particularly executive function) in our AD cohort (N=25).

Furthermore, we demonstrate the clinical applicability of this approach by characterizing subjects based on individualized 'fingerprints' of receptor alterations. This study introduces the first robust, data-driven framework for integrating several neurotransmitter receptors, multi-modal neuroimaging and clinical data in a flexible and interpretable brain model. It enables further understanding of the mechanistic neuropathological basis of neurodegenerative progression and heterogeneity, and constitutes a promising step towards implementing personalized, neurotransmitter-based treatments.

Introduction

Alzheimer's disease (AD) involves degenerative changes to several neurobiological processes spanning molecular to macroscopic scales, including proteinopathies, modified gene expression, synaptic alterations, vascular dysregulation, hypometabolism, and structural atrophy [25]. In AD, these processes begin decades before the manifestation of cognitive deterioration [559], with vast inter-patient heterogeneity in age of disease onset, spatial distribution of neuropathologies, progression patterns, and clinical presentation [560]. Currently, there are no effective disease-modifying treatments for AD, despite many expensive attempts [559] [560]. These failures may be attributed to: i) the use of a generalized medicine approach to treatment without considering the pathophysiological and clinical heterogeneity of the disease [561] [562] [563], ii) the focus on single disease factors (e.g. tau and amyloid) whereas most biological mechanisms in AD are multi-factorial [564], and, importantly, iii) an incomplete multi-scale understanding of how molecular and macroscopic factors interact to cause disease progression [565].

Recently, multi-modal neuroimaging models [566] [86] have unravelled the temporal ordering of macroscopic structural, functional, vascular and proteinopathy changes in AD.

Furthermore, personalized models of longitudinal neuroimaging data have been used to identify subject-specific alterations of neurobiological processes including tau and amyloid accumulation, blood flow, and neural activity at rest [567]. Nevertheless, such neuroimaging models lack a mechanistic basis in molecular and cellular processes. While these modalities may involve molecular imaging, such as amyloid or tau PET, their spatial resolution is limited in practice [227]. Identifying important pathways between truly microscopic-scale variables and observable macroscopic neuroimaging (i.e. molecular PET and MRI) in AD would both advance the understanding of the underlying biology and improve the selection of therapeutic targets tailored to an individual's particular disease subtype or presentation.

One particularly relevant class of molecules is neurotransmitter receptors, which regulate a variety of biological processes known to be dysfunctional in neurodegeneration. As neurotransmitter receptors are mediators of many relevant neurobiological factors, studying them is critical for a complete mechanistic understanding and the potential treatment of abnormal brain conditions such as neurodegeneration [25]. For example, dopamine receptors expressed by the cerebral microvasculature and glial cells appear to modulate the coupling between neural activity and vascular response [92], which is altered in AD [100]. As an organ, the brain consumes energy disproportionately to its mass [102]. A significant fraction of this energy expenditure is attributed to synaptic signalling and molecular synthesis, with approximately 37% of this associated with postsynaptic receptors and housekeeping processes [103]. The production and degradation of neurotransmitter receptors is a complex, dynamic process that is regulated in response to changes in many variables, such as receptor activation, gene expression, and external stimuli [105]. Since these processes are energy-intensive, changes to their concentrations are likely to indicate relevant biological alterations, making them a potential therapeutic target.

Although it is not primarily considered a neurotransmitter disease, AD is associated with dysfunction in several important neurotransmitter receptor systems. Particularly, acetylcholine and glutamate receptors are implicated in essential stages of a pathological neurodegenerative cascade, including cholinergic hydrolysis and glutamatergic excitotoxicity [25]. Neurotransmitter receptor alterations are also suspected of being a mechanistic pathway in healthy ageing [568]. Thus, integrating neurotransmitter receptors with macroscopic neuroimaging data has the potential to uncover molecular pathways important to ageing and disease progression. However, *in-vivo* neurotransmitter receptor imaging is difficult, due to the lack of specific *in-vivo* radiolabels [31]. Typically, receptor mapping has involved either post-mortem histology, or expensive positron emission tomography (PET) imaging for a limited set of molecules with available radionuclides. As such, large longitudinal *in-vivo* datasets for several receptors would be extremely expensive or technologically infeasible to collect. Consequently, alterations to neurotransmitter systems during disease progression are not well characterized [32].

Motivated by these concerns, we propose a whole-brain generative formulation integrating high resolution *in vitro* neurotransmitter receptor density maps and *in vivo* multi-modal neuroimaging. For the first time, this model allows a quantitative comparison of the causal role of different neurotransmitter receptors and neuroimaging modalities in healthy aging and neurodegeneration. Specifically, we fit subject-specific generative models of neuroimaging data in an aging population covering the AD spectrum (N=423, ADNI data), augmented with 15 whole-brain neurotransmitter receptor distribution patterns. We then treat the parameters of these personalized models as subject-specific measures representing latent receptor-neuroimaging interactions, and identify multi-scale interactions that explain mechanistic variability and cognitive heterogeneity between AD subjects. We find that receptor density maps and their

interactions with neuroimaging significantly improve the fit of neuroimaging models, providing a valid proxy for true, longitudinal *in-vivo* receptor imaging. Examining model parameters in AD patients, we found an axis of variability between receptor-imaging interactions and cognitive decline, primarily affecting executive function. Specifically, this axis is influenced by predictors of tau distribution and resting state neural activity, concordant with recent reports in late-onset AD [569] [570]. Via this axis, mechanisms of glutamatergic, cholinergic and GABAergic receptor interactions correlated significantly with cognitive decline in AD. In contrast, while receptor-imaging interactions in healthy individuals did not vary significantly with cognitive status, mechanisms affecting cerebral blood flow (CBF) changes and gray matter atrophy accounted for most of the inter-individual heterogeneity. This work represents the earliest attempt to integrate several neurotransmitter receptors and multi-modal neuroimaging data in a universal formulation, representing a notable advance towards implementing individually-tailored neurotransmitter-based diagnosis and treatment in neurodegeneration.

Materials and methods

Ethics statement

The study was conducted according to Good Clinical Practice guidelines, the Declaration of Helsinki, US 21CFR Part 50–Protection of Human Subjects, and Part 56–Institutional Review Boards, and pursuant to state and federal HIPAA regulations (adni.loni.usc.edu). Study subjects and/or authorized representatives gave written informed consent at the time of enrollment for sample collection and completed questionnaires approved by each participating site Institutional Review Board (IRB). The authors obtained approval from the ADNI Data Sharing and Publications Committee for data use and publication, see documents http://adni.loni.usc.edu/wp-

content/uploads/how_to_apply/ADNI_Data_Use_Agreement.pdf and http://adni.loni.usc.edu/wp-content/uploads/how_to_apply/ADNI_Manuscript_Citations.pdf, respectively.

Data description and processing

Study participants

This study used longitudinal data from N=423 participants (149 healthy, 151 early mild cognitive impairment (EMCI), 103 late mild cognitive impairment (LMCI), and 20 AD-diagnosed subjects at baseline) from the Alzheimer's Disease Neuroimaging Initiative (ADNI) (adni.loni.usc.edu). Demographic information is summarized in Supplementary Table S1. At least three different imaging modalities were acquired for each included subject (i.e. structural MRI, fluorodeoxyglucose PET, resting functional MRI, Arterial Spin Labeling and/or Amyloid-ß PET). The ADNI was launched in 2003 as a public-private partnership, led by Principal Investigator Michael W. Weiner, MD. The primary goal of ADNI has been to test whether serial magnetic resonance imaging (MRI), PET, other biological markers, and clinical and neuropsychological assessments can be combined to measure the progression of mild cognitive impairment (MCI) and early Alzheimer's disease (AD).

Structural MRI acquisition/processing

Brain structural T1-weighted 3D images were acquired for all N=423 subjects. For a detailed description of acquisition details, see http://adni.loni.usc.edu/methods/documents/mri-protocols/. All images underwent non-uniformity correction using the N3 algorithm [571]. Next, they were segmented into grey matter, white matter and cerebrospinal fluid (CSF) probabilistic maps, using SPM12 (fil.ion.ucl.ac.uk/spm). Grey matter segmentations were standardized to

MNI space [572] using the DARTEL tool [573]. Each map was modulated in order to preserve the total amount of signal/tissue. Mean grey matter density and determinant of the Jacobian (DJ) [573] values were calculated for the regions described in *Methods: Data description and processing: Receptor densities and brain parcellation.* For each region, obtained grey matter density and DJ values were statistically controlled for differences in acquisition protocols. Both measurements provided equivalent modeling results. All the results/figures presented in this study correspond to the DJ, which constitutes a robust local measure of structural atrophy.

Fluorodeoxyglucose PET acquisition/processing

A 185 MBq (5 $\pm$ 0.5 mCi) of [18F]-FDG was administered to each participant (N=418) and brain PET imaging data were acquired approximately 20 min post-injection. All images were corrected using measured attenuation. Also, images were preprocessed according to four main steps [574]: 1) dynamic co-registration (separate frames were co-registered to one another lessening the effects of patient motion), 2) across time averaging, 3) re-sampling and reorientation from native space to a standard voxel image grid space ("AC-PC" space), 4) spatial filtering to produce images of a uniform isotropic resolution of 8 mm FWHM, and 5) affine registration to the participant's structural T1 image. Next, using the registration parameters obtained for the structural T1 image with nearest acquisition date, all FDG-PET images were spatially normalized to the MNI space [572]. Regional standardized uptake value ratio (SUVR) values for the regions considered were calculated using the cerebellum as reference region.

Resting fMRI acquisition/processing

Resting-state functional images were obtained using an echo-planar imaging sequence on a 3.0-Tesla Philips MRI scanner for N=127 subjects. Acquisition parameters were: 140 time points, repetition time (TR)=3000 ms, echo time (TE)=30 ms, flip angle=80°, number of

slices=48, slice thickness=3.3 mm, in plane resolution=3 mm and in plane matrix=64×64. Pre-processing steps included: 1) motion correction, 2) slice timing correction, 3) alignment to the structural T1 image, and 4) spatial normalization to MNI space using the registration parameters obtained for the structural T1 image with the nearest acquisition date, and 5) signal filtering to keep only low frequency fluctuations (0.01–0.08 Hz) [575]. For each brain region, our model requires a local (i.e. intra-regional, non-network) measure of functional activity, in order to maintain mechanistic interpretability and to prevent data leakage of network information into local model terms (described further in *Receptor-Enriched Multifactorial Causal Model*). Due to its high correlation with glucose metabolism [576] and validation as an AD-sensitive metric [577] [219], we calculated regional fractional amplitude of low-frequency fluctuation (fALFF) [578] as a measure of functional integrity.

Furthermore, while our model uses structural connectivity as the network along which inter-region propagation occurs, we also calculated and used a functional connectome, as the average of the absolute Pearson correlation matrices across all healthy subjects with fMRI data (N=42). Based on this, we compared model performance using structural and functional connectivity, characterizing the choice of connectivity metrics (see *Multi-scale interactions involving neurotransmitter receptors are important to explaining multifactorial brain reorganization* and Supplementary Fig. S8).

ASL acquisition/processing

Resting Arterial Spin Labeling (ASL) data were acquired using the Siemens product PICORE sequence for N=195 subjects. Acquisition parameters were: TR/TE=3400/12 ms, TI1/TI2=700/1900 ms, FOV=256 mm, 24 sequential 4 mm thick slices with a 25% gap between the adjacent slices, partial Fourier factor=6/8, bandwidth=2368 Hz/pix, and imaging

matrix=64×64. For preprocessing details see ”UCSF ASL Perfusion Processing Methods” in adni.loni.usc.edu. In summary, main preprocessing steps included: 1) motion correction, 2) perfusion-weighted images (PWI) computation, 3) intensity scaling, 4) CBF images calculation, 5) alignment to the structural T1 image, and 6) spatial normalization to MNI space [572] using the registration parameters obtained for the structural T1 image with the nearest acquisition date, and 6) mean CBF calculation for each considered brain region.

Amyloid-ß PET acquisition/processing

A 370 MBq (10 mCi ± 10%) bolus injection of AV-45 was administered to each participant (N=422), and 20 min continuous brain PET imaging scans were acquired approximately 50 min post-injection. The images were reconstructed immediately after the 20 min scan, and when motion artifact was detected, another 20 min continuous scan was acquired. For each individual PET acquisition, images were initially preprocessed according to four main steps [574]: 1) dynamic co-registration (separate frames were co-registered to one another lessening the effects of patient motion), 2) across time averaging, 3) re-sampling and reorientation from native space to a standard voxel image grid space (“AC-PC” space), 4) spatial filtering to produce images of a uniform isotropic resolution of 8 mm FWHM, and 5) affine registration to the participant’s structural T1 image. Next, using the registration parameters obtained for the structural T1 image with the nearest acquisition date, all amyloid images were spatially normalized to the MNI space [572]. Considering the cerebellum as an Aß non-specific binding reference, SUVR values for the regions were calculated.

Tau PET acquisition/processing

A 370 MBq/kg bolus injection of tau specific ligand 18F-AV-1451 ([F- 18] T807) was administered to each participant (N=238), and 30 min (6 × 5 min frames) brain PET imaging

scans were acquired starting at 75 min post-injection (N = 200). Images were preprocessed according to four main steps [574]: 1) dynamic co-registration (separate frames were co-registered to one another lessening the effects of patient motion), 2) across time averaging, 3) re-sampling and reorientation from native space to a standard voxel image grid space ("AC-PC" space), 4) spatial filtering to produce images of a uniform isotropic resolution of 8mm FWHM, and 5) affine registration to the participant's structural T1 image. Next, using the registration parameters obtained for the structural T1 image with the nearest acquisition date, all tau images were spatially normalized to the MNI space [572]. Considering the cerebellum as a non-specific binding reference, SUVR values for the grey matter regions considered were calculated.

Receptor densities and brain parcellation

In-vitro quantitative receptor autoradiography was applied to measure the densities of 15 receptors in 44 cytoarchitectonically defined cortical areas spread throughout the brain [579]. These receptors span major neurotransmitter systems, and show significant regional variability across the brain. Brains were obtained through the body donor programme of the University of Düsseldorf. Donors (three male and one female; between 67 and 77 years of age) had no history of neurological or psychiatric diseases, or long-term drug treatments. Causes of death were non-neurological in each case. Each hemisphere was sliced into 3 cm slabs, shock frozen at -40C, and stored at -80C.

Receptors for the neurotransmitters glutamate (AMPA, NMDA, kainate), GABA ($GABA_A$, $GABA_A$-associated benzodiazepine binding sites, $GABA_B$), acetylcholine (muscarinic M_1, M_2, M_3, nicotinic $\alpha_4\beta_2$), noradrenaline (α_1, α_2), serotonin ($5\text{-}HT1_A$, $5\text{-}HT_2$), and dopamine (D_1) were labeled according to previously published binding protocols consisting of pre-incubation, main incubation and rinsing steps [579]. The ligands used are summarized in

Supplementary Table S3. Receptor densities were quantified by densitometric analysis of the ensuing autoradiographs, and areas were identified by cytoarchitectonic analysis in sections neighbouring those processed for receptor autoradiography, and which had been used for the visualization of cell bodies [580].

A brain parcellation was then defined with the aid of the Anatomy Toolbox [581] using 44 regions of interest for which receptor densities were available [253]. This parcellation was based on areas identified by cortical cytoarchitecture, as well as other cyto- and receptor-architectonically defined regions with receptor measurements (regions are summarized in Supplementary Table S4). These 44 regions were mirrored across left and right hemispheres for a total of 88 brain regions in our parcellation. For each receptor, regional densities were normalized using the mean and standard deviation across all 88 brain regions.

The structural T1 images of the Jülich [581] and Brodmann [582] brain parcellations were registered to the MNI ICBM152 T1 template using FSL 5.0's FLIRT affine registration tool [583], and the obtained transformations were used to project the corresponding parcellations to the MNI ICBM152 space (using nearest neighbor interpolation to conserve original parcellation values). In the MNI ICBM152 space, voxels corresponding to the cytoarchitectonically defined regions from [253] were identified from the regions in the Anatomy Toolbox, with the remaining Brodmann regions (Supplementary Table S4) filled in using the Brodmann brain atlas. The resulting parcellation of 88 brain regions in the common template space was then used to extract whole-brain multi-modal neuroimaging data and estimate the diffusion-based connectivity matrix, as described in *Materials and Methods: Multimodal neuroimaging data and Materials and Methods: Anatomical connectivity estimation*.

Anatomical connectivity estimation

The connectivity matrix was constructed using DSI Studio (http://dsi-studio.labsolver.org). A group average template was constructed from a total of 1065 subjects [584]. A multishell diffusion scheme was used, and the b-values were 990, 1985 and 2980 s/mm2. The number of diffusion sampling directions were 90, 90, and 90, respectively. The in-plane resolution was 1.25 mm. The slice thickness was 1.25 mm. The diffusion data were reconstructed in the MNI space using q-space diffeomorphic reconstruction [585] to obtain the spin distribution function [586]. A diffusion sampling length ratio of 2.5 was used, and the output resolution was 1 mm. The restricted diffusion was quantified using restricted diffusion imaging [587]. A deterministic fiber tracking algorithm [588] was used. A seeding region was placed at whole brain. The QA threshold was 0.159581. The angular threshold was randomly selected from 15 degrees to 90 degrees. The step size was randomly selected from 0.5 voxel to 1.5 voxels. The fiber trajectories were smoothed by averaging the propagation direction with a percentage of the previous direction. The percentage was randomly selected from 0% to 95%. Tracks with length shorter than 30 or longer than 300 mm were discarded. A total of 100000 tracts were calculated. A custom brain atlas based on cytoarchitectonic regions with neurotransmitter receptor data [253] was used as the brain parcellation, as described in *Materials and Methods*: *Data description and processing: Receptor densities and brain parcellation*, and the connectivity matrix was calculated by using count of the connecting tracks.

Multimodal neuroimaging data

After pre-processing ADNI neuroimaging data for all 6 modalities and extracting it for the cytoarchitectonically defined atlas described in *Materials and Methods: Data description and*

processing: Receptor densities and brain parcellation, subjects lacking sufficient longitudinal or multimodal data were discarded. The disqualification criteria were i) fewer than 4 imaging modalities with data, or ii) fewer than 3 longitudinal samples for all modalities. For the remaining subjects, missing neuroimaging modalities at each time point with actual individual data were imputed using trimmed scores regression with internal PCA [589]. Imputation accuracy was validated using 10-fold cross-validation, showing a strong capacity to recover the real data (correlation values: $r_{CBF} = 0.44$, $r_{amyloid} = 0.60$, $r_{neural\ activity} = 0.95$, $r_{gray\ matter} = 0.80$, $r_{metabolism} = 0.81$, $r_{tau} = 0.71$; all $P<10^{-6}$). Finally, a total of 423 subjects were left with all 6 neuroimaging modalities with an average of 4.75 (±2.71) time points. We used the mean and variance of each neuroimaging modality across all regions and healthy subjects to calculate z-scores of neuroimaging data across all (healthy, MCI, and AD) subjects. Please see Supplementary Tables S1-S2 for demographic characteristics, and *Materials and Methods: Multimodal neuroimaging data* and Supplementary Fig. S1 for a detailed flowchart of the selection and analysis of the participants.

Cognitive scores

We used multiple composite scores derived from the ADNI neuropsychological battery. Protocols for deriving each score are described in the respective ADNI protocols documentation or relevant publication for executive function [590], memory [590], language [591], visuospatial functioning [591], mini-mental state examination (MMSE) [592], and the Alzheimer's Disease Assessment Scale (ADAS11/13) [592]. With an average of 7.27 ± (2.55) evaluations per subject in our cohort (N=423), we calculated cognitive decline as the linear best fit rate of change of each cognitive score with respect to examination date. Thus, for each patient, cognitive decline was represented by a set of 7 rates of change.

Receptor-Enriched Multifactorial Causal Model (re-MCM)

Under the framework of the multifactorial causal model (MCM) introduced in [567], we consider the brain as a dynamical system of anatomically connected regions defined by interacting, neuroimaging-derived biological factors. These biological factors are tissue structure, neuronal activity, blood flow, metabolism, and the accumulation of misfolded proteins (amyloid, tau), quantified by structural MRI, functional MRI, ASL MRI, FDG PET, amyloid PET and tau PET, respectively. Each biological factor m at a particular brain region i is represented by a single variable $S_{m,i}$, whose rate of change is a function of i) local states of other factors, and ii) the propagation of the same factor across anatomically connected regions. Thus, in our model, pathological factors can propagate throughout the brain, but any direct interactions between factors must occur locally within a region.

In this study, for a given subject, and at each of the $N_{\text{ROI}} = 88$ brain regions, the system is defined by $N_{\text{fac}} = 6$ state variables or factors. Each factor $S_{m,i}$ represents the m^{th} neuroimaging modality at the i^{th} brain region. Factor dynamics can be decomposed into local effects due to factor-factor interactions and network propagation of the factor. In general, the differential equation describing this coupled system for a given subject is:

$$\frac{dS_{m,i}(t)}{dt} = \underbrace{f(\mathbf{S}_{*,i}(t))}_{\text{Local Effects}} + \underbrace{g(\mathbf{S}_{m,*}(t), C_{i\leftrightarrow *})}_{\text{Inter-region Propagation}}, \quad (1)$$

where f and g are functions that determine the effects of local multi-modal interactions and propagation, respectively, and $C_{i\leftrightarrow *}$ is the net connectivity of region i. Here, we extend the basic MCM formulation (Equation 1) to include the local effects of neurotransmitter receptors. With $\mathbf{R}$ being a $N_{\text{rec}} \times N_{\text{ROI}}$ matrix of spatial maps, composed of local densities $r_{k,i}$ of a receptor

k at a region i, and $\mathbf{R}_{*,i}$ being a $N_{\text{rec}} \times 1$ vector of all receptor densities in region i, we define the general form of the receptor-enriched MCM (re-MCM) as:

$$\frac{dS_{m,i}(t)}{dt} = f(\mathbf{S}_{*,i}(t), \mathbf{R}_{*,i}) + g(\mathbf{S}_{m,*}(t), C_{i\leftrightarrow *}).$$

(2)

The first term $f(\mathbf{S}_{*,i}(t), \mathbf{R}_{*,i})$ represents the local component, which is the interaction between the factor m and all other factors in region i, mediated by the local densities of receptors in that region. The second term $g(\mathbf{S}_{m,*}(t), C_{i\leftrightarrow *})$ represents the contribution due to network propagation of the factor m, mediated by the net anatomical connectivity $C_{i\leftrightarrow *}$ of the region i. The functions f and g in Equation 2 define the global imaging factor dynamics, which are valid for all brain regions. Thus, regional differences are due to different imaging factor states, receptor distributions and anatomical connectivity, but the mechanisms of their interactions, represented by f and g, are consistent across the whole brain.

Given the decades-long temporal scale of neurodegeneration compared to the relatively short few months between neuroimaging samples, we assume a locally linear, time-invariant dynamical system:

$$\frac{dS_i^m(t)}{dt} = \sum_{n=1}^{N_{\text{fac}}} \alpha^{n\to m} S_{n,i}(t) + \sum_{k=1}^{N_{\text{rec}}} \alpha_k^m r_{k,i} + \alpha_{\text{prop}}^m \sum_{j=1, j\neq i}^{N_{\text{ROI}}} \left[C_{j\to i} S_{m,j}(t) - C_{i\to j} S_{m,i}(t)\right],$$

(3)

where $C_{i\to j}$ is the directed anatomical connectivity from region i to j, and $\frac{dS_{m,i}(t)}{dt}$ was defined by the local rate of change of neuroimaging data for successive longitudinal samples at times t' and t:

$$\frac{dS_{m,i}(t)}{dt} = \frac{S_{m,i}(t) - S_{m,i}(t')}{t - t'}.$$

(4)

In this work, we expand the local effect term to include i) direct factor-factor effects, ii) interaction terms mediated by $N_{\text{rec}} = 15$ receptor types, and iii) direct receptor effects (Equation 3) on the neuroimaging factor rate of change $\frac{dS_{m,i}}{dt}$. The local factor effects term n Equation 3 is now expanded:

$$\alpha^{n\to m} = \underbrace{\alpha_0^{n\to m}}_{\text{Direct Factor-Factor Term}} + \underbrace{\sum_k^{N_{\text{rec}}} \alpha_k^{n\to m} r_i^k}_{\text{Interaction Term}}.$$

(5)

Although the receptor maps **R** are constant templates with spatial but no temporal variation, their interaction terms add a dynamic element, as they imply a regional heterogeneity to neuroimaging predictors that is not directly explained by the direct receptor term in Equation 3. For instance, we might notice that (hypothetically) the interaction between a glutamatergic receptor and functional activity is a significant predictor of gray matter atrophy. Whether or not functional activity or the glutamatergic receptor map are significant predictors on their own, the significance of the interaction term would imply that the spatial distribution template of the glutamatergic receptor is informative when combined with functional activity.

Additionally, for propagation, we consider only symmetric connectivity $C_{j\leftrightarrow i}$ between regions i and j, using a template connectivity matrix for all subjects, as described in *Anatomical connectivity estimation*, to give the propagation term

$$p_{m,i}(t) = \sum_{j=1, j\neq i}^{N_{\text{ROI}}} C_{j\leftrightarrow i} \left[S_{m,j}(t) - S_{m,i}(t)\right].$$

(6)

This reduces the net propagation of a factor m to a region i to a single propagation term. A more complete treatment may consider vascular connectivity as well [567] [561], as this

measure may be more relevant for different processes (such as functional activity, CBF and metabolism, respectively).

$$\frac{dS_{m,i}(t)}{dt} = \sum_{n=1}^{N_{\text{fac}}}\left(\alpha_0^{n\to m} + \sum_k^{N_{\text{rec}}} \alpha_k^{n\to m}\, r_{k,j}\right) S_{n,i}(t) + \sum_{k=1}^{N_{\text{rec}}} \alpha_k^m\, r_{k,i} + \alpha_{\text{prop}}^m p_{m,i}(t)$$

(7)

Formulated in this way, each model contains a set of $N_{\text{params}} = N_{\text{fac}} \times (1 + N_{\text{rec}}) + N_{\text{rec}} + 1 = 113$ parameters $\{\alpha\}_x^m$ for subject x and factor m (or 678 total parameters per subject). Apart from the propagation term, which is specific to the imaging modality output of the model, all predictors are identical for the 6 neuroimaging modalities. That is, a common set of receptor maps, multi-modal neuroimaging states, and pseudo-personalized receptor-imaging interactions are used as predictors. However, based on their respective effects on each output modality, we obtain 678 distinct biological parameters per subject, each with a distinct mechanistic interpretation (e.g. the effect of neural activity on metabolism or the effect of neural activity on CBF). We then perform linear regression, using the terms in Equation 7 as predictors with longitudinal ADNI neuroimaging samples $S_{m,i}(t)$ and receptor maps $\mathbf{R}$, to estimate subject- and modality-specific parameters $\{\alpha\}_x^m$ for each subject x and modality m. Separate regression models were built for i) each of the N=423 qualifying subjects, and ii) each of the 6 neuroimaging factors. These subjects were drawn from the ADNI dataset with at least 4 recorded neuroimaging modalities, and at least 3 longitudinal samples for at least one modality.

To evaluate model fit, we calculate the coefficient of determination (R^2) for each subject. This is summarized by modalities in Fig. 4.2. With the data vector $\mathbf{y}$ with elements $y_{m,i,t} = \frac{dS_{m,i}(t)}{dt}$, and model predictions $\hat{\mathbf{y}}$ with $\hat{y} = \hat{y}_{m,i,t}$, the coefficient of determination is

$$R^2 = 1 - \frac{\sum_{i,t}(\mathbf{y}_{m,i,t} - \hat{\mathbf{y}}_{m,i,t})^2}{\sum_{i,t}(\mathbf{y}_{m,i,t} - <\mathbf{y}_m>)^2},$$

(8)

where $< \mathbf{y}_m >$ is the mean of neuroimaging data for a particular modality m across all brain regions and longitudinal samples.

Statistical analysis

Model fit

Personalized model fit quantified by the coefficient of determination (R^2) was evaluated for each subject and neuroimaging modality. F-tests were used to compare receptor-neuroimaging (113 parameters per modality) and neuroimaging-only (8 parameters per modality) to fitting neuroimaging data in each subject (F-test with $p<0.05$). The model fit (R^2) was evaluated for each subjects' neuroimaging models using 1000 iterations of randomly permuted receptor maps (with receptor densities shuffled across regions independently for each receptor type), and we calculated the p-value of the true receptor data model R^2 compared to this distribution.

Biological parameters and relationship with cognition

We aimed to further clarify how the cognitive decline observed in AD progression is modulated by specific neurotransmitter receptor systems and their causal interactions with macroscopic biological factors (i.e. amyloid, tau, CBF, neural activity, glucose metabolism and gray matter density). As changes in several receptor densities are difficult to image in-vivo, we analyzed the receptor terms from our personalized re-MCM approach as a proxy for the importance of each particular receptor's distribution or interactions in predicting multi-domain cognitive deterioration in AD. To consider the inter-subject variability in the diseased population,

we used a combination of cognitive assessment scores as disease severity descriptors (i.e. executive function, memory, language, visuospatial functioning, MMSE, ADAS 11 and ADAS 13; see Materials and Methods: Cognitive Scores).

We aimed to robustly identify significant and relevant re-MCM parameters that represent molecular-neuroimaging interactions associated with cognitive decline, using a data-driven multivariate cross-correlation analysis in combination with a randomized permutation test to ensure the statistical stability of our results. By concurrently analyzing the multivariate changes across all re-MCM parameters, this multidimensional analysis searched for large clusters of functionally related receptor-neuroimaging interaction mechanisms statistically associated with AD-associated cognitive changes. In other words, the SVD method used here (and its associated permutation test) identified the specific set of receptors and/or imaging features that were maximally related to cognitive decline. To this end, we selected a clinical subgroup of interest (either N=112 cognitively healthy subjects or N=25 AD patients from the N=423 total subjects with sufficient multi-modal neuroimaging data), and performed the following procedure on the original set of 678 re-MCM parameters and 7 rates of cognitive decline per subject (executive function, memory, language, visuospatial functioning, MMSE, and ADAS11/13):

To identify correlated axes of variation, we performed principal component analysis (PCA) on all 678 biological parameters separately on the healthy and AD subjects, and ranked parameters based on the variance explained in the first principal component (PC).

To relate biological parameters to cognition, we performed singular value decomposition (SVD) on the cross-covariance matrix between significant parameters and rates of cognitive decline for AD patients, after adjusting for covariates (baseline age, education and gender). SVD allows us to simultaneously reduce the dimensionality of the 7 cognitive assessments and to rank

parameters by their variation with cognition. Where X is a matrix of z-scores of each re-MCM parameter for this clinical subgroup and Y is a matrix of the corresponding z-scores of the rates of clinical decline, the cross-covariance matrix $C = XY'$ is decomposed as

$$C = USV' \tag{9}$$

where U and V are orthonormal matrices of spatial loadings for the coefficients and cognitive scores, respectively, and S is a (diagonal) matrix of singular values $\{s_1, \dots, s_7\}$.

To evaluate the significance of SVD components, we performed permutation tests by shuffling the mapping between subjects' re-MCM parameters and cognitive scores, and repeating SVD. To compare permuted iterations, we performed a Procrustes transformation to align the axes of singular components. We kept only those singular components that are significant $p < 0.05$) compared to 1000 permutation iterations of SVD components.

We performed 1000 iterations of bootstrapping on the parameters X, and discarded the parameters with non-significant 95% confidence intervals.

For the remaining significant re-MCM parameters and SVD components, we computed the variance explained per parameter. We then summed the contribution of each significant parameter j to each significant SVD component i, weighted by the fraction of total variance explained by the i^{th} component

$$r_j^{2,\text{param,sig}} = \sum_i^{N_{\text{SVD,sig}}} \underbrace{\frac{U_{i,j}^2}{\sum_j U_{i,j}^2}}_{\substack{\text{Parameter} \\ \text{contribution}}} \underbrace{\frac{s_i^2}{\sum_j s_j^2}}_{\substack{\text{Singular value} \\ \text{contribution}}}. \tag{10}$$

Inter-subject mechanistic variability

To explore the potential clinical utility of our approach at the personalized level, we performed a quantitative comparison between diseased participants in terms of their inter-subject variability across different receptor systems. To this end, we defined individual-specific "fingerprints" of the alterations in receptor-modulated synergistic interactions. Specifically, for each participant *i* and receptor system *r*, we calculated the Mahalanobis distance $D_{i,r}$ of re-MCM parameters $\alpha_{i,r}$ associated with cognitive decline in our AD cohort (Fig. 4.4; Supplementary Table S5). This distance is calculated between subject's parameters $\alpha_{i,r}$, and the distribution of healthy subjects' parameters for receptor *r*, with means $\mu_{i,r}$ and a covariate matrix $\boldsymbol{S^{-1}}$,

$$D_{i,r} = \sqrt{(\alpha_{i,r} - \mu_{i,r})^T \boldsymbol{S^{-1}} (\alpha_{i,r} - \mu_{i,r})}. \quad (11)$$

To quantify the relationship between this summary metric of receptor alterations and specific cognitive domains, we performed multivariate linear regression on rates of cognitive decline (adjusted by age, gender, education level and APOE4 status; N=25) using the z-scores of the Mahalanobis distances for the 6 receptor systems. We also estimated the explanatory importance of each receptor system, as the percentage improvement in model fit (R^2) by including a particular receptor Mahalanobis distance.

Data and code availability

The three datasets used in this study are available from the ADNI database (neuroimaging and cognitive evaluations; http://www.adni.loni.usc.edu), the HCP database (tractography template for connectivity estimation; http://www.humanconnectomeproject.org/), and receptor density data published in [253]. We anticipate that the re-MCM method will be released soon as

part of our available and open-access, user-friendly software [593] (https://www.neuropm-lab.com/neuropm-box.html).

Results

Capturing receptor-mediated multifactorial brain reorganization

Here, we aimed to develop a multi-scale generative brain model linking regional receptor densities (for 15 neurotransmitter receptors) and multimodal neuroimaging-based factors (for six biological variables) in a flexible, unified formulation. We aimed to use this mathematical framework to infer receptor alterations associated with the long-term physiological changes of complex brain reorganization processes (namely aging and neurodegeneration) and their cognitive impact. Because changes in receptor concentrations are difficult to measure *in vivo*, our receptor density maps were composed of group-averaged templates, with spatial distributions of receptors but no inter-individual variability or intra-individual longitudinal progression. Consequently, we use the predictive importance of receptor distributions in generative models of abnormal neuroimaging-derived biological variables as a proxy for alterations in either receptor density or mechanistic interactions with other imaging-derived variables.

We proceeded to characterize the multifactorial brain dynamics of each participant using the developed *neurotransmitter receptor-enriched multifactorial causal model* (re-MCM; Fig. 4.1) and the quality-controlled, multi-modal longitudinal neuroimaging data (described in *Materials and Methods: Data description and processing*). For each participant with sufficient longitudinal and multi-modal data (N=423), the re-MCM was fit for all 6 neuroimaging modalities, to obtain receptor-imaging biological parameters reflecting local factor-factor interactions mediated by neurotransmitter receptor distributions (e.g. amyloid-tau interactions

modulated by NMDA receptors) and the spreading of effects via anatomical networks (e.g. amyloid and tau propagation along white matter connections).

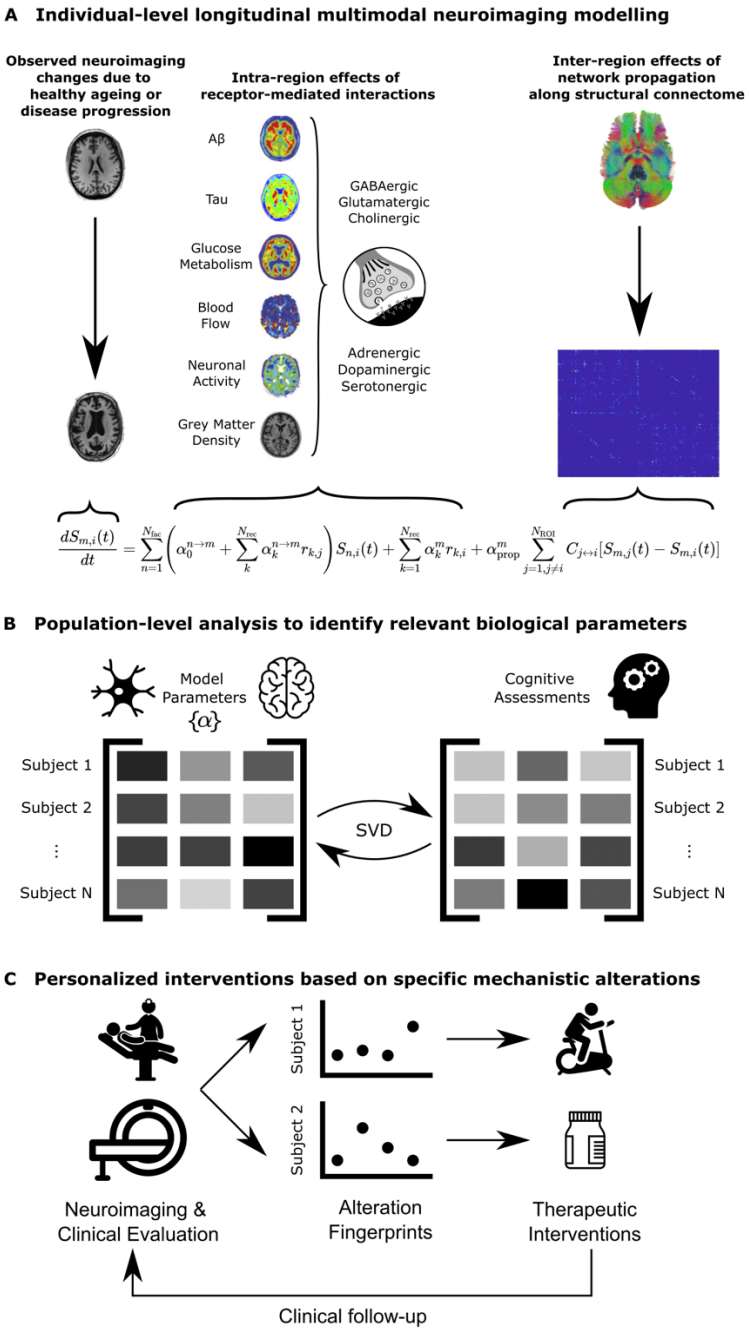

Figure 4.1. Neurotransmitter receptor-enriched multifactorial causal modeling.

a) For each subject with longitudinal neuroimaging data, changes between subsequent samples in each neuroimaging modality are decomposed into local synergistic effects due to i) the direct influence of all neuroimaging-quantified biological factors, ii) receptor density

distributions, and iii) multi-scale receptor-imaging interactions, and iv) global network-mediated intra-brain propagation. Combining this data across (N_{ROI}=88) brain regions and multiple neuroimaging samples results in a multivariate regression problem to identify the subject-specific parameters {α}. b) At a group level, these personalized model parameters are then compared to subjects' cognitive assessments (specifically, the rates of decline for 7 composite cognitive scores described in Materials and Methods: Cognitive scores) using a singular value decomposition (SVD) procedure on the cross-covariance matrix, to identify multi-scale receptor-neuroimaging interactions that are robustly correlated with the severity of cognitive symptoms in AD (outlined in Materials and Methods: Biological parameters and relationship with cognition). c) In the context of personalized applications, inter-subject variability in receptor-imaging interactions can be used as clinical "fingerprints" of molecular alterations representing different disease mechanisms. Patients can then receive individually tailored treatment plans to address their underlying etiology, based on their specific fingerprints. For example, patients with greater vascular alterations may benefit more from lifestyle interventions such as physical exercise, whereas patients with greater receptor alterations may require neurotransmitter-based medication (depending on the most affected receptor). Furthermore, treatment plans can be continually adjusted with follow-up visits.

Multi-scale interactions involving neurotransmitter receptors are important to explaining multifactorial brain reorganization

Firstly, we proceeded to evaluate the ability of the re-MCM approach to fit longitudinal neuroimaging data with and without receptor maps and multi-scale receptors-imaging interactions (Fig. 4.2a-b). For each of the six neuroimaging modalities per subject, we calculated the coefficient of determination (R^2) as a measure of model accuracy for explaining the real imaging-specific longitudinal changes. While model accuracy varied by imaging modality, we observed that the personalized models including receptor-neuroimaging interactions explained approximately 70% ($\pm$ 20%) of observed variance in all modalities (Fig. 4.2a).

Inter-region propagation in our model occurs along structural connectivity. While functional connectivity can be a better predictor of fMRI data, structural connectivity is a better measure of the actual physical substrate connecting brain regions. Nevertheless, to explore the effects of alternate connectivity measures, we repeated our modeling steps using functional connectivity in place of the structural connectivity derived from diffusion-MRI tractography.

While the connectivity matrices differed, we found almost no change in model fit or parameters across subjects, with a high correlation $r>0.99$ of model R^2 ($P<0.001$) across all modalities (Supplementary Fig. S8). We attribute this to the dominance of intra-regional effects in our model, with many interacting local receptor and neuroimaging predictors, and also to the shared information in structural and functional connectivity [594].

Next, to evaluate the relevance of receptor densities and receptor-mediated interactions between biological factors quantified by imaging (e.g. amyloid-tau interaction modulated by GABA), we compared the model fit of full re-MCM models (incorporating receptor-factor interactions as previously described) with restricted models (using only neuroimaging predictors and network propagation). The models including receptor maps and receptor-imaging interactions explained, on average, more than twice as much of the variance in longitudinal neuroimaging changes (Supplementary Table S7; $P<0.001$ with a two-sample t-test). To account for the greater explanatory power of a larger model with more parameters, we quantified the improvement in individual neuroimaging modeling due to the receptor terms, we conducted F-tests between the full re-MCM formulation (Fig. 4.2a) and the restricted model (Fig. 4.2b). As hypothesized, we observed that the inclusion of receptor maps and multi-scale (receptor-imaging) interaction terms significantly improved ($P<0.05$) the model accuracy for 86.8%-99.0% of the subjects (Fig. 4.2c) while accounting for the additional degrees of freedom in the model with receptors. While the inclusion of receptors and receptor-imaging interactions improved model performance for all subjects and modalities, this improvement was not always significant, most notably in 13.2% of gray matter atrophy models (Fig. 4.2c). We attribute this to the use of a shared, group-averaged set of neurotransmitter receptors templates (further tested below).

Having established that receptor maps and receptor-neuroimaging interactions do significantly improve personalized neuroimaging models, we then performed a permutation analysis on the receptor maps to test the informativeness compared model performance using averaged receptor templates to a set of null receptor maps. For each subject, the model fitting procedure was repeated using 1000 random permutations of the spatial receptor maps. Receptor densities were shuffled across regions of interest, independently for each receptor. We then compared the distribution of model fit (R^2) using these randomly permuted data with the R^2 obtained for the models using the true receptor templates. We observed that the significance of the improvement in model fitting over randomized receptor maps varied by imaging modality, for example, being lower for metabolism than for neural activity (Fig. 4.2d). Nevertheless, the true receptor templates perform significantly better in approximately 80%-98% of all subjects, depending on the modality. The gain in model performance by imaging modality is presented in Supplementary Table S8, and generally fell between 15.6% ± 13.3% ($p<0.0417$) for glucose metabolism to 22.3% ± 15.0% ($p<0.003$) for neural activity. Notably, the modalities for which true receptor data was the least informative (metabolism and gray matter atrophy), were also the ones for which augmenting the model with receptor data provided the least significant improvements across all subjects. Furthermore, we compared the proportion of subjects with significant improvements over null maps across diagnoses, shown in Supplementary Fig. S7. On average across modalities, 96.2% of healthy subjects' models were significantly improved, wheras this was progressively lower for MCI subjects (89.4% for early MCI and 89.8% for late MCI) and AD patients (78.3%).

We hypothesize that accentuated aging processes and neurodegeneration may alter receptor densities or interaction mechanisms in each individual, requiring the biological

parameters in our personalized models to compensate. Identifying these specific alterations is the subject of the remaining subsections.

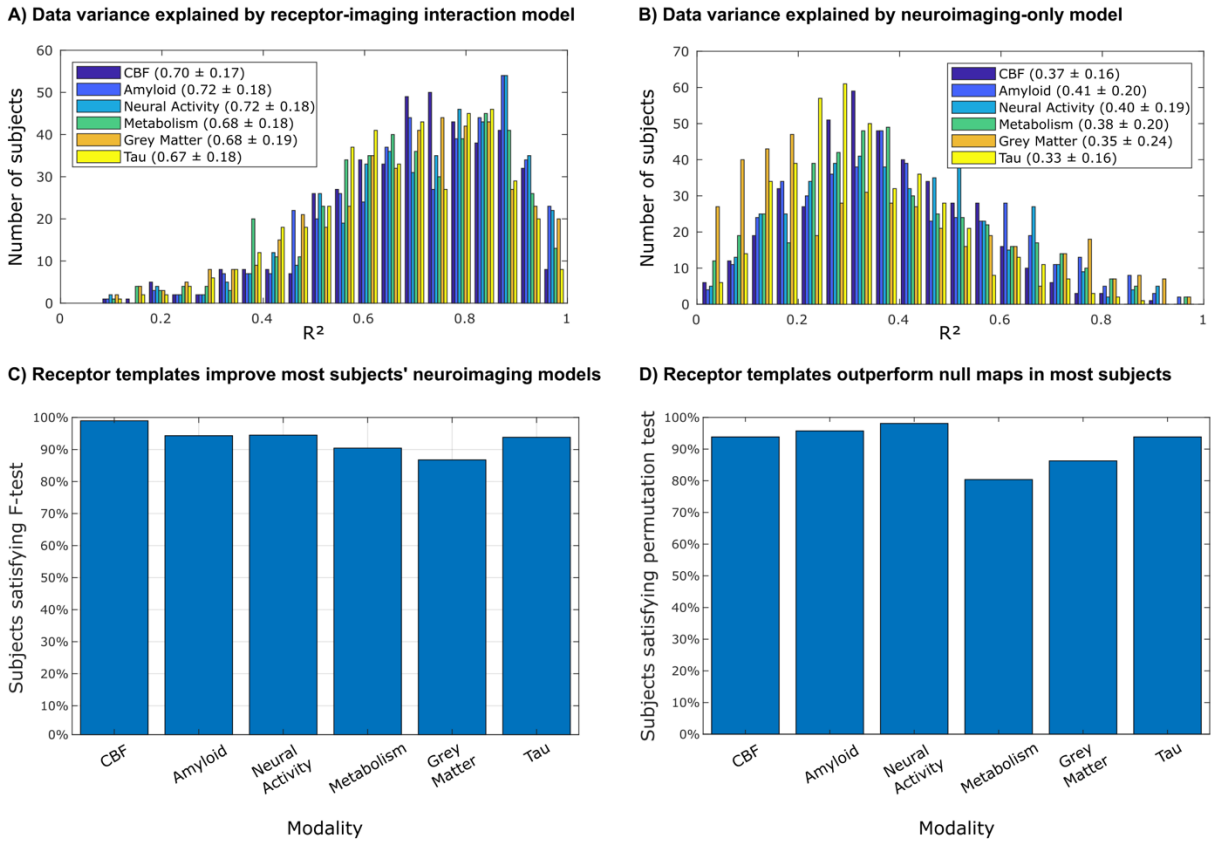

Figure 4.2. Receptor density templates and multi-scale receptor-neuroimaging interactions significantly improve individual longitudinal neuroimaging models.

The improvement in neuroimaging modeling was evaluated in terms of i) including direct receptor terms and receptor-neuroimaging interactions in the model, and ii) using true receptor density maps compared to randomized, spatially permuted maps. The histograms in (a) and (b) show the distribution of the coefficient of determination (R^2) of N=423 individual models of neuroimaging changes including (a) and excluding (b) receptor predictors. Subject-specific linear models fit neuroimaging changes reasonably well, with a significant improvement by including receptor terms. This is confirmed by the F-test between subject models with and without receptor densities and receptor-imaging interactions (113 and 8 parameters, respectively). The proportion of subjects for whom the F-statistic is above the critical threshold is shown in (c). This critical threshold corresponds to a statistically significant ($P<0.05$) improvement due to the receptor terms in the re-MCM model, accounting for the increase in adjustable model parameters. Furthermore, to validate the benefit of the receptor templates over randomized null maps, re-MCM models were fit with 1000 spatially-shuffled receptor maps for each subject. The p-value of the model fit (R^2) using true receptor templates compared to the distribution of R^2 of models using randomized templates was calculated for each subject. The proportion of subjects for whom the true receptor maps resulted in a statistically significant

improvement in model fit ($P<0.05$) is shown in (d). The results of these two analyses in (c) and (d) validate the use of averaged receptor templates in personalized neuroimaging models.

Characterizing receptor-imaging interaction variability in healthy aging and AD

We aimed to characterize the variability in receptor-mediated brain reorganization in the studied healthy aging (N=112) and AD subpopulations (N=25). In the healthy population, we performed a principal component analysis (PCA) on all re-MCM biological parameters (678 in total) across the 6 neuroimaging modalities, finding that the first principal component (PC1) is able to explain 97.3% of the group's variance. The most variable parameters contributing to PC1 belonged to CBF and gray matter models (Fig. 4.3a). That is, if current CBF in a region becomes less important (relative to other re-MCM predictors) to predicting its future change, gray matter density also becomes less important to predicting future atrophy, whereas the current level of amyloid becomes more important to predicting future accumulation. These results suggest that, in the absence of an influential disease process (e.g. neurodegeneration), inter-individual differences in the long-term brain reorganization are mechanistically driven by receptor-mediated processes affecting CBF and gray matter density. Most prominently, these include the CBF effects due to interactions between the dopaminergic D_1 receptor and amyloid distribution (2.9%), the adrenergic α_1 receptor and gray matter density (2.7%), the $GABA_A$ benzodiazepine site and neural activity ($GABA_A$/BZ; 2.0%), and the $GABA_A$ receptor and gray matter density (1.8%). Additionally, the interaction between the glutamatergic AMPA receptor and amyloid distribution as a predictor of gray matter atrophy (2.3%) are also notably variable.

In the AD group (N=25), with the presence of a neurodegenerative condition, the first PC of the re-MCM biological parameters only explained 26.2% of the population variability (with

subsequent PCs explaining less than 10% each). Along this main axis of variability, inter-individual differences are primarily due the effects of neural activity as a direct or receptor-mediated predictor of tau accumulation (Fig. 4.3b; 7.9% of PC1 via the direct term, 7.3% via adrenergic $\alpha_1$receptors, 5.7% via serotonergic $5HT_{1A}$ receptors, 4.0% via dopaminergic D_1 receptors, and 3.7% via cholinergic $\alpha_4\beta_2$ receptors). The next subsection covers a deeper analysis of the AD group.

Interestingly, in the healthy subpopulation, when the individually small contributions of all receptor-terms for each target neuroimaging modality were summed (Fig. 4.3c), we observed that the receptor mechanisms that affect CBF changes, gray matter atrophy and amyloid accumulation were the most variable, with GABAergic and serotonergic mechanisms dominating. For example, combined variability due to GABAergic (9.7% of PC1), serotonergic (8.7% of PC1) and adrenergic (primarily α_1 receptors; 7.3% of PC1) interactions predicting CBF changes accounted for approximately a quarter of variability across all 6 neuroimaging modalities and 678 total parameters (25.7% of PC1). As seen in Fig. 4.3b, the main sources of biological parameter variability in AD (Fig. 4.3d) involved neural activity predictors of tau accumulation. Predictors of tau accumulation involving adrenergic (9.9% of PC1), serotonergic (9.6%), cholinergic (6.6%) and dopaminergic (4.7%) interactions were the most variable.

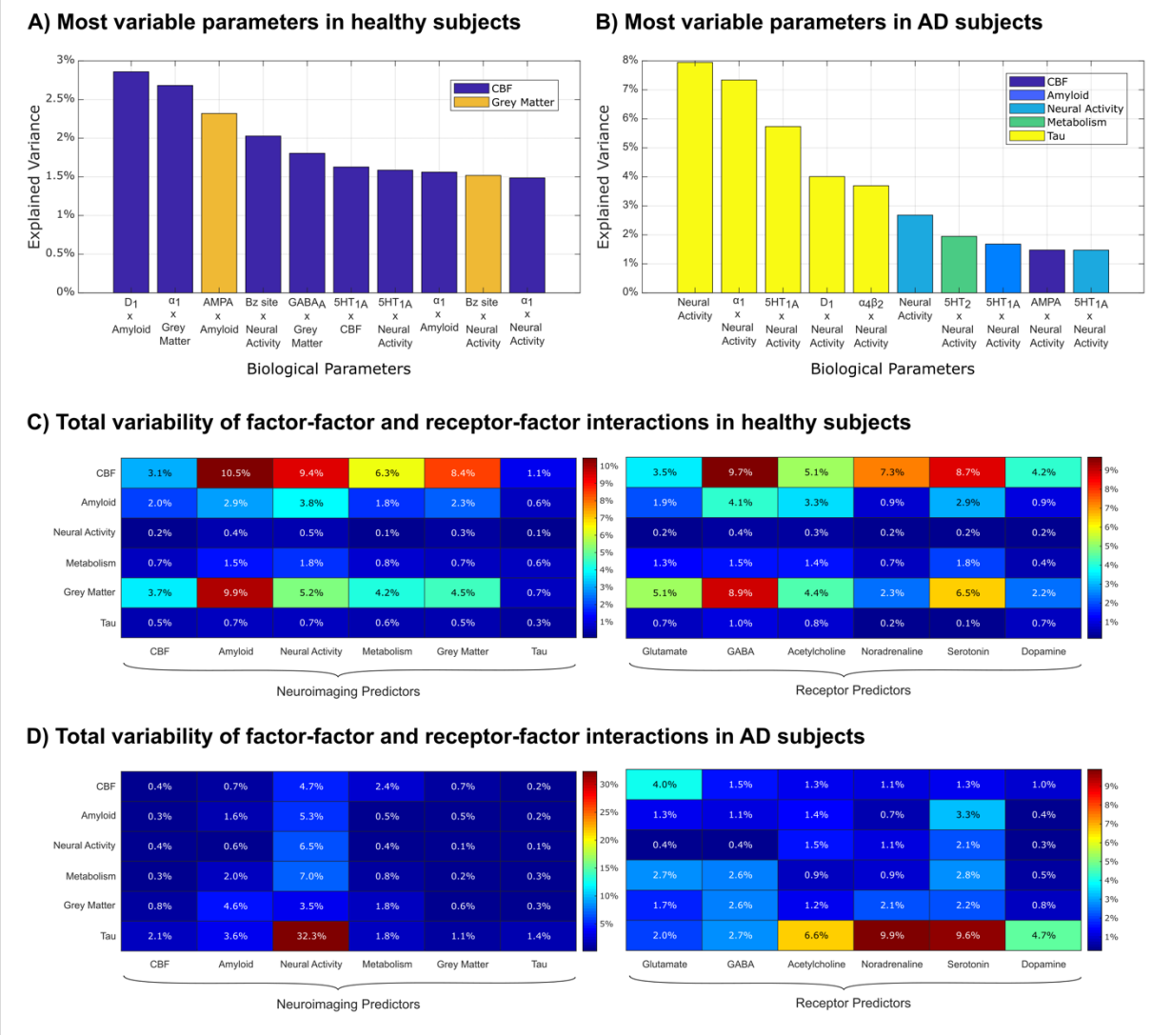

Figure 4.3. Variability of biological parameters across healthy and AD subjects.

a-b) PCA-based sources of variability in the 678 re-MCM parameters across healthy subjects (N=112) and AD patients (N=25), respectively. The first principal component (PC1) captured 97.3% of the variance across parameters in healthy subjects, and 26.2% in AD patients. The top 10 biological parameters and their contributions to PC1 are plotted (with their target neuroimaging models in the legend), highlighting the receptor-imaging interactions that characterize the main axis of variability in each clinical subgroup. In healthy subjects, a multi-factorial combination of receptor-imaging interactions affecting atrophy and CBF changes were the most variable parameters along PC1. Notably, for AD patients, the top parameters were direct or receptor-mediated effects of neural activity on various (but especially tau) imaging models. c-d) To evaluate the relative importance of receptor- and factor-factor interactions, we then aggregated the importance of all direct or interaction terms involving a given predictor class (factor or receptor type) along PC1, for healthy subjects (c) and (d) for AD patients, respectively. Note that the percentage variation across all parameters is shown. As such, there is an overlap in terms between the two heat maps (receptor-factor interaction terms contribute to both), and they should be interpreted separately.

Receptor-imaging alterations underlying cognitive deterioration in AD

To determine the receptor-neuroimaging alterations underlying multiple cognitive variations in AD, we performed a multivariate cross-correlation analysis between the rate of changes of the selected cognitive descriptors and the biological parameters across all AD subjects (*Materials and Methods: Biological parameters and relationship with cognition*). Notably, we found that just the first component of the identified biological parameters can explain up to 39.7% ($P<0.004$, FWE-corrected) of the inter-individual variability in AD cognitive deterioration (Fig. 4.4a). Furthermore, we identified the specific cognitive domains that are correlated with receptor-neuroimaging alterations (Fig. 4.4c), with executive dysfunction being the most salient cognitive feature with respect to receptor-neuroimaging parameters. Finally, Fig. 4.4d presents a detailed pathway of 95 receptor-imaging interactions significantly associated with cognitive decline based on feature bootstrapping, and their associated neuroimaging modalities mediating AD-related symptom severity. These results show that a multi-factorial set of molecular alterations are relevant to cognitive decline in AD. Cumulative effects of different neuroimaging interactions and receptor subtypes from the same family are summarized in Fig. 4.5, quantified by the total cognitive variance explained by all parameters of the relevant category via the significant SVD component.

Gray matter density (2.1%) and CBF (1.5%) changes as predictors of neural activity dysfunction, and CBF (1.3%) and glucose metabolism (1.0%) as predictors of tau distribution were the most cognitively-significant pathways between imaging modalities, although tau as a

predictor of amyloid distribution (0.7%), neural activity dysfunction (0.7%) and glucose metabolism (1.2%) was also significant. Overall, as predictors, biological parameters involving CBF, tau and gray matter density were the most significant in relation to the cognitive severity of AD. The neuroimaging models of neural activity dysfunction and tau accumulation were the major sources of cognitively-significant biological parameters.

In terms of receptor systems, glutamatergic, GABAergic and cholinergic alterations were significant to cognitive decline, as summarized in Supplementary Table S6. Alterations to glutamatergic predictors of resting state functional activity (2.5%), GABAergic predictors of amyloid deposition (1.4%), and cholinergic predictors of tau distribution (1.4%) were the dominant receptor effects.

Furthermore, while the second component was borderline non-significant ($p<0.051$), it explained 23.4% of the variance between model parameters and cognitive decline ($r=0.89$, $p<10^{-8}$; Supplementary Fig. S10). In this axis, receptor-imaging parameters predicting neural activity were less prominent, with CBF and metabolism model parameters contributing more. Cognitively, this second component corresponded to non-executive function domains, primarily memory, language and visuospatial function.

As a control case, we performed an equivalent cross-correlation analysis in the healthy population, notably finding the first principal component relating re-MCM parameter with rates of cognitive decline in health to be non-significant (Supplementary Fig. S3), although the second principal component explaining a small amount of cognitive variance was significant (15.5% variance explained, $p<0.02$; Supplementary Fig. S4). Furthermore, we found no significant component in amyloid-negative healthy subjects ($p>0.2$ for all components). We attribute this

effect to the lack of consistent cognitive decline in the analyzed healthy population, in contrast to the large variability observed for AD.

To test the sensitivity of our findings to genetic covariates, we repeated our analyses both with and without APOE ε4 allele status and a polygenic hazard score (PHS) [595] as covariates in the SVD analysis, in addition to age, gender and education in both cases. To overcome the low number of AD subjects, we expanded our criteria to include MCI and AD subjects (N=177 for APOE status, N=161 for PHS). Importantly, we confirmed that the previously identified AD-related significant latent variables and parameters are robust to the inclusion of APOE status and PHS (Supplementary Fig. S5 and S6). Finally, to further restrict our analysis to subjects on the amyloid-mediated AD spectrum, we repeated the SVD analysis in amyloid positive subjects with MCI and AD (N=52). As was the case in the initial AD group, we found one significant principal component (44.3% variance explained, $p<0.003$) with a high correlation between model parameters and cognitive decline (mainly executive function; $r=0.76, p<0.001$). The main receptor-imaging interactions along this axis were analogous to those in the AD group, namely cholinergic predictors of tau accumulation, although parameters of the neural activity model were less prominent in favour of predictors of metabolism (particularly for adrenergic and cholinergic systems; see Supplementary Fig. S9).

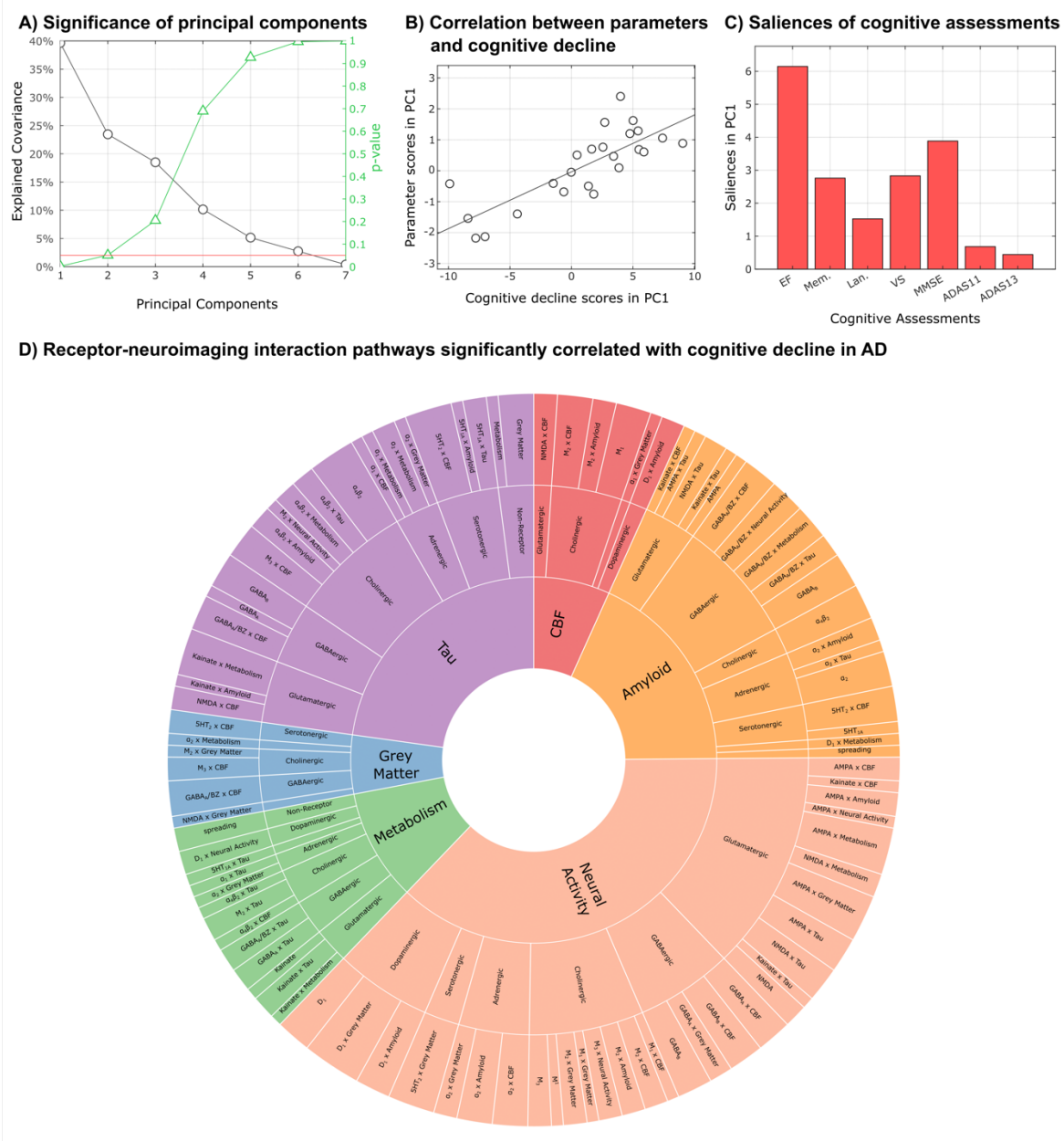

Figure 4.4. Significant neurotransmitter receptor-imaging interactions underlying AD clinical severity.

a) The latent cross-correlation components are ranked by the fraction of cognitive decline variance explained by re-MCM biological parameters (along with the reported p-values based on the permutation analysis; see Biological parameters and relationship with cognition). In this case, only a single latent component was significant (39.7% variance explained, p<0.004, FWE-corrected). b) A notable correlation (r=0.80; P<10-8) between the projections of statistically stable re-MCM parameters and rates of cognitive decline in the principal component space was observed, with the removal of an outlier subject more than 3 median absolute deviations from the median. c) Saliences of cognitive decline to this first latent component, providing a relative ranking of cognitive domains. These saliences are proportional to the

contribution of each term relative to every other term, for example showing that executive dysfunction is most correlated with alterations to receptor-imaging interactions in AD. d) Receptor-imaging pathways that are significantly correlated with cognitive decline, arranged by neuroimaging model and receptor type (Supplementary Table S5). The angle of each sector is proportional to the contribution of the corresponding parameter to explaining the variance in the rates of cognitive decline. The inner sectors represent the 6 neuroimaging modalities that together comprise each personalized re-MCM model. Within each modality, the intermediate sectors represent the neurotransmitter system involved, while the outer sector consists of the specific two-way receptor-neuroimaging interactions or direct predictor terms in the model. Notably, while receptors appear only as predictors in the outer sector, neuroimaging modalities appear both as predictors and as model outputs in the inner sectors. Thus, the relative importance of each neuroimaging modality to explaining cognitive differences is not fully represented by the angle of each inner sector.

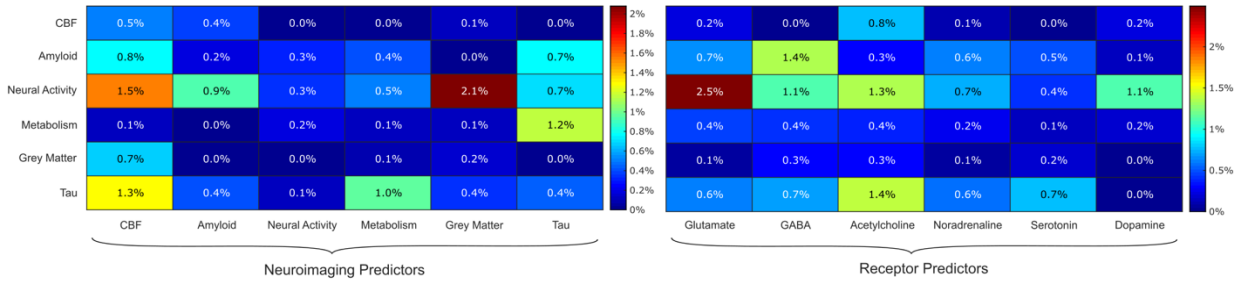

Figure 4.5. Contributions of mechanistic pathways to the severity of cognitive decline in AD.

To better visualize the importance of neuroimaging factors and neurotransmitter receptor systems, heatmaps of the cumulative cognitive variance explained by each predictor category in each neuroimaging model are shown. These variances are the percentages of total cognitive variance that are explained by significant biological parameters of each category via the first significant SVD component. As such, the rows of the heatmap on the left replicate the inner sector of Fig. 4.4d, while the columns show the importance of each imaging modality or receptor family as predictors, with CBF and tau predictors explaining the most variance in cognitive decline.

Clinically similar subjects have different underlying receptor alterations

Finally, for each participant and receptor family, we defined a summary metric quantifying how much receptor-based mechanisms differ from clinically healthy subjects (see *Statistical analysis: Inter-subject mechanistic variability*). For example, a given subject's

glutamatergic Mahalanobis distance is a combined measure of the "unhealthiness" of receptor-based interactions and spatial distributions involving NMDA, AMPA and kainate, while accounting for the variation of these mechanisms in healthy subjects.

Although a simplified summary metric, the receptor Mahalanobis distances explained a large proportion of cognitive variance in the AD population, with 71.4% for executive function ($p<0.0004$), 43.3% for memory ($p<0.08$), 18.7% for language ($p<0.66$), 40.1% for visuospatial function ($p<0.10$), 43.8% for MMSE ($p<0.08$) and 33.8% for ADAS11 ($p<0.22$). Figure 4.6a shows the effects of each receptor family on cognitive domains, as well as the percentage improvement in explaining cognitive variance due to each receptor family. We note the large negative effects of GABAergic alterations on executive function and the MMSE, and dopaminergic alterations on memory. Interestingly, cholinergic alterations showed a moderate positive effect and explanatory importance towards executive function.

In Figure 4.6b-c, we illustrate how two AD patients with similar cognitive symptoms present distinct receptor alteration fingerprints, with primarily glutamatergic and cholinergic mechanisms respectively. Importantly, this result suggests that even subjects with identical clinical diagnoses present distinctive underlying spatiotemporal molecular alterations, and supports the use of whole-brain generative models to uncover patient-specific receptor and potential disease mechanisms to target clinically.

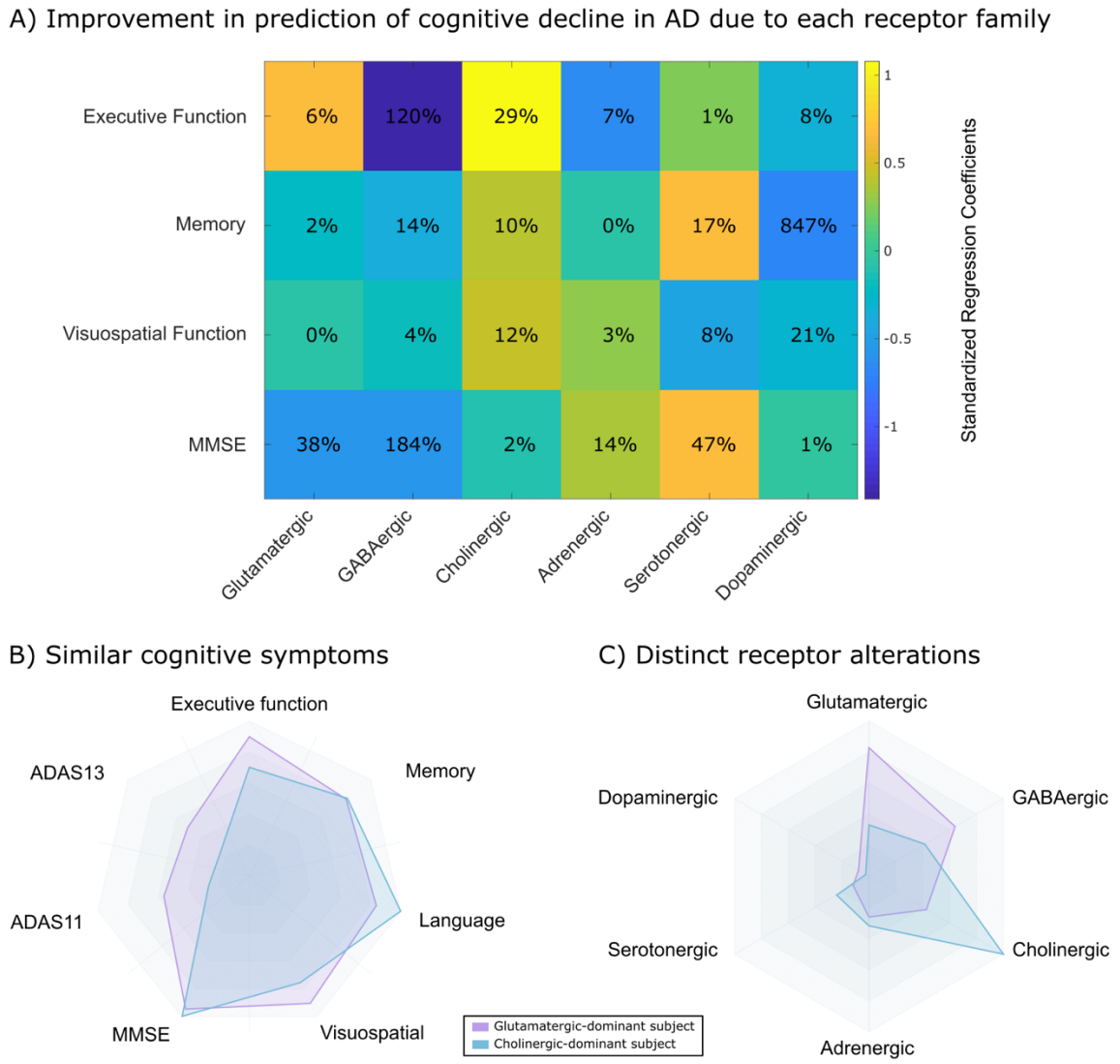

Figure 4.6. Receptor alterations underlying inter-individual disease heterogeneity.

a) In AD patients (N=25), we quantified the relative effect sizes of standardized Mahalanobis distances of receptor mechanisms on different cognitive domains. We also standardized the regression coefficients within each cognitive domain before visualizing to facilitate comparison across cognitive domains, and the percentage improvement in model fit (R2) due to each receptor system is also shown. For example, the explanation of inter-subject variability in executive function decline by glutamatergic, cholinergic, adrenergic, serotonergic and dopaminergic Mahalanobis distances is improved by 120% (i.e. more than doubled) by the inclusion of GABAergic Mahalanobis distance as well. b-c) We show two AD subjects, with similar symptoms across a variety of cognitive domains. For these subjects, we calculated the Mahalanobis distance to the distribution of all healthy subjects (N=112), along mechanisms involving each receptor family. The subjects show distinct receptor alterations based on their longitudinal neuroimaging changes, despite their shared designation as AD patients and similar cognitive profiles.

Discussion

In this work, we have presented a personalized, whole-brain and generative multi-modal neuroimaging model incorporating receptor-neuroimaging interactions using *in-vivo* data. Subsequent analyses on the resulting models have allowed, for the first time, the identification of i) variability in receptor-neuroimaging interactions in healthy subjects and AD patients, and ii) specific pathways of receptor-neuroimaging interactions that are important to cognitive decline in AD patients. This exploratory analysis provides a bridge between molecular-level mechanisms and observable macroscopic neuroimaging biomarkers of healthy aging and AD, revealing which neurotransmitter receptor systems mediate dysfunctional interactions between neurobiological processes such as cerebral blood flow, amyloid and tau deposition, gray matter atrophy, neural activity and metabolism.

Due to the difficulty of comprehensive, personalized *in vivo* receptor imaging for a large cohort, receptor maps were not specific to each subject, but instead the averaged templates of 4 post-mortem brain samples. Post-mortem *in vitro* autoradiography allowed the imaging of a large number of receptor types, even those without *in vivo* radioligands. Firstly, our work demonstrates that i) multi-scale interaction terms involving the spatial distributions of neurotransmitter receptors are highly informative to models of neuroimaging progression, and ii) even group-averaged receptor map templates can significantly improve the personalized model fit in nearly all subjects when combined with personalized neuroimaging predictors. Specifically, incorporating receptor maps and multi-scale receptor-imaging interactions to personalized models with multi-modal neuroimaging predictors improves the average data variance explained from approximately 40% to 70% (Fig. 4.2a, b). This improvement is statistically significant (F-test with $P<0.05$) in almost all subjects (Fig. 4.2c), even after accounting for the additional

predictive power of the larger, multi-scale models. Including only receptor maps without receptor-imaging interactions also resulted in a more modest yet significant improvement in the vast majority of subjects across all imaging modalities (Supplementary Fig. S2). This is a particularly strong result, validating the use of a group-averaged receptor template, given the large improvement and the stringent criterion accounting for additional model parameters.

Additionally, models using the true receptor templates perform significantly better ($P<0.05$ of R^2) than models using randomly permuted, null receptor maps in almost all subjects (Fig. 4.2d; 80.4%-98.1%, depending on the modality), although this improvement was less evident with disease progression (Supplementary Fig. S7). These results, along with the consistency of regional receptor densities across the 4 (aged but healthy) brains used to produce the templates compared to inter-region variability [253], support the applicability of receptor templates to a wider population. Receptor mapping studies across more diverse clinical groups of patients would help validate or augment our modeling approach. Nevertheless, given the difficulty of acquiring a wide variety of *in-vivo* molecular data, due to a limited number of appropriate radioligands, and the high cost of longitudinal molecular imaging, these results on model accuracy are a promising validation for the combination of other molecular templates (such as gene expression atlases) with personalized neuroimaging predictors. These "pseudo-personalized" molecular-imaging predictors can then be incorporated into neuroimaging models and used to infer mechanistic alterations in a group of subjects. If these personalized models are sufficiently accurate, as in this work, the weights of their biological parameters then serve as proxies for individual-specific alterations to receptor-mediated mechanisms.

While interpreting these parameters, it is important to distinguish between the types of biological mechanisms they represent, which include (for each neuroimaging model) i) direct

neuroimaging effects, ii) direct receptor density effects, iii) receptor-imaging interactions, iv) network propagation and v) offset terms representing an intrinsic rate of change for the neuroimaging modality. We hypothesize that ageing and neurodegeneration alter the spatial distributions of and functional interactions involving neurotransmitter receptors, which would lead to subject-specific model parameters to compensate in the absence of inter-subject variability in receptor data. Thus, model parameters are a proxy for alterations to spatial maps of receptors or their interactions with neurobiological processes (represented by direct model receptor density terms and receptor-imaging interaction terms in the model, respectively). In our parameter analyses in *Receptor-imaging alterations underlying cognitive deterioration in AD*, direct receptor density terms represent alterations to the spatial distribution of a particular receptor. Each interaction biological parameter value can be interpreted as the effect of the corresponding receptor or imaging factor on the brain reorganization process, as measured by neuroimaging changes, given "normal" (i.e. spatial mean) values of all related predictors involving the same receptor or imaging term, respectively. For example, we consider the case where the interaction term between a glutamatergic receptor and amyloid in the CBF model is significantly related to cognitive decline. This implies that, under normal levels of amyloid and the glutamatergic receptor individually, a functional alteration in this mechanism (quantified by the re-MCM parameter weight) is correlated with faster cognitive deterioration.

Biological parameters were evaluated for principal axes of variability in Fig. 4.3 and the cognitively relevant variability in Fig. 4.4. The former method was used to identify linear combinations of biological parameters that accounted for inter-individual differences in receptor and/or neuroimaging interaction strengths in healthy and AD subjects. On the other hand, the goal of the latter analysis was to identify biological parameters that were robustly correlated with

multivariate measures of cognitive decline in AD. The purpose of these analyses was not to compare effects sizes between predictors, but rather to explore inter-subject differences in receptor-imaging interactions in relation to cognitive decline. For example, if regional amyloid accumulation strongly predicts changes in functional activity, but this biological parameter is consistent across subjects with different clinical and cognitive states, it would not be significant to our analysis. Rather than using clinical diagnosis, which is subject to large variability due to patient presentation and clinician bias, we used a combination of cognitive test scores. Ultimately, cognitive performance is the phenotype of interest in neurodegeneration. Our SVD analysis allows us to identify parameters associated with cognitive scores, rather than simply those with a large variability between individuals due to other causes.

Sources of variability in healthy and AD subjects (Fig. 4.3) reflect alterations to mechanisms of receptor-imaging interaction that predict the same or another imaging modality. Here, we observed that a single PCA component explains 97.3% of the inter-individual variability in healthy subjects. Along this axis, a multi-faceted combination of receptor-imaging interaction predictors of CBF alterations (e.g. the interaction between dopaminergic D_1 receptors and amyloid) and gray matter atrophy (e.g. the interaction between glutamatergic AMPA receptors and amyloid) account for the majority of variability (Fig. 4.3a, c). Interestingly, there is relatively low variability in the biological parameters of receptor influence on neural activity, glucose metabolism and tau distribution in healthy individuals (Fig. 4.3c). In healthy subjects, the receptor-imaging mechanisms affecting these factors are comparatively consistent, whereas the mechanisms behind atrophy, CBF regulation and amyloid accumulation display more inter-subject heterogeneity.

In contrast, the first principal component of AD subjects' biological parameters explained only 26.2% of the total variance, but this was dominated by neural activity as a (receptor-modulated) predictor of tau accumulation (as well as other neuroimaging modalities; Fig. 4.3b,d). Receptor mechanism variability was largely explained by adrenergic and serotonergic predictors, for example the interactions of α_1 and $5HT_{1A}$ receptors with neural activity to predict tau accumulation. As tau is primarily present in axonal microtubules, the exacerbation of tau pathology has been linked to enhanced neural activity [596]. Conversely, tau is also believed to suppress and silence neural activity [570]. Thus, the principal component of variability in AD subjects may represent variability in an activity-dependent tau accumulation via adrenergic α_1, serotonergic $5HT_{1A,}$ dopaminergic D_1, and cholinergic $\alpha_4\beta_2$ receptors. This would be consistent with the observed mediation of tau hyperphosphorylation by adrenergic and serotonergic receptors in animal models [159] [597].

From the inner sectors of Fig. 4.4d, inter-individual differences in cognitive decline are most correlated with biological parameters of the neural activity, tau and amyloid models, and least correlated with biological parameters of the CBF, gray matter density and glucose metabolism models. In other words, differences in receptor-imaging interactions affecting CBF changes are less relevant to cognitive symptom severity in AD than those affecting resting state functional activity. While neural activity is not a cognitively important predictor of other neuroimaging modalities, many predictors of neural activity dysfunction are correlated with cognitive severity in AD (Fig. 4.5). Conversely, predictors of CBF do not vary significantly with cognition, whereas CBF itself is an important predictor of many other neuroimaging modalities. This may imply a causal ordering, with CBF alterations preceding dysfunctional activity.

The glutamatergic system is implicated in cognitive decline via its role as the major excitatory mediator of neural activity [598] [599] [600]. In AD, the glutamatergic system is involved in excitotoxicity due to calcium ion influx via NMDA receptors [598], resulting in synaptic loss and neuronal cell death [599]. Tau and amyloid are involved via an overactivation of NMDA receptors [124]. The synaptic activation of NMDA receptors is linked to specific neurophysiological conditions, particularly activity-dependent synaptic plasticity, as well as behavioural symptoms of multiple brain disorders including AD [601]. In addition, AMPA receptors are involved in synaptic scaling, and consequently learning and memory. Reductions in AMPA receptor levels have been observed in mouse models of AD [602], as well as in the entorhinal cortices [603] of AD patients, with a differential preservation of certain subunits in the hippocampus [604], and AMPA receptor endocytosis has been linked to the phosphorylated tau signaling cascade [605]. Thus, the established AD-related alterations and cognitive roles of the glutamatergic NMDA and AMPA receptors would be consistent with their significant modulation of resting state functional activity in relation to cognitive decline in AD via interactions with CBF, glucose metabolism and tau.

From the columns of Fig. 4.5, CBF changes are the largest neuroimaging driver of cognitively relevant dysfunction in other modalities, consistent with its precedence among AD imaging biomarkers [86]. Closely coupled to neural activity, CBF is mediated by several neuronal factors, including vasodilatory neurotransmitters, and vascular dysregulation is implicated in the pathogenesis of AD [606]. CBF interactions with a multitude of receptors were correlated to cognitive severity via amyloid, neural activity, gray matter density and tau models. This is consistent with the amyloid-dependent relationship of CBF to memory performance [607], and the link to tau pathology via gene expression alterations in AD [608].

Furthermore, inter-individual differences in the effects of tau on other imaging modalities are also major contributors to AD-associated cognitive decline, as seen in Fig. 4.5. These include glutamatergic interactions affecting neural activity and amyloid accumulation, and a multifactorial set of receptor interactions affecting metabolism. Cognitive decline in AD is accompanied by changes in the role of regional tau concentration as a predictor of amyloid distribution, suggesting synergistic or mediation effects such as the tau axis hypothesis [609]. Tau is believed to mediate amyloid toxicity [609], which may explain the significant role of tau as a predictor of amyloid accumulation (Fig. 4.5). Multimodal PET imaging has shown a region-dependent relationship between tau burden and hypometabolism in AD [610]. Furthermore, alterations to glucose metabolism in mice brains were found to lead to abnormal tau hyperphosphorylation [611]. Along with the established neural activity dysfunction due to tau accumulation [612], these mechanisms are consistent with the cognitively significant role of tau as a predictor of other neuroimaging modalities.

Along with NMDA, acetylcholine is the neurotransmitter system most associated with Alzheimer's disease and its clinical treatment [613]. Based on the cholinergic hypothesis, dysfunction in acetylcholine-producing basal forebrain regions would eventually lead to synaptic deafferentation in the cortical regions to which they project [614], with cognitive implications [615]. This is consistent with the significant role of cholinergic predictors of tau distribution, which appear to be more correlated with cognitive severity of AD than amyloid distribution (Fig. 4.5).

Although GABAergic receptors were not initially linked to AD, recent evidence has uncovered disease-related alterations, contributions to pathogenesis, and a potential therapeutic role in AD [152]. The disruption of the excitatory/inhibitory balance maintained by GABAergic

signaling has been implicated in the cognitive symptoms of AD, such as an increase in epileptic seizures [616]. Electrophysiological activity has found a functional remodeling of GABAergic neurons in AD, showing reduced currents and a faster rate of desensitization [617]. The presence of amyloid was also found to affect the expression of the α_6 subunit of the $GABA_A$ receptor [152]. Furthermore, a role for tau has been proposed in the regulation of GABAergic function and synaptic plasticity to maintain normal cognition [616]. Additionally, it has recently been found that the administration of benzodiazepine in mouse brains leads to tau hyperphosphorylation [618]. Such drugs potentiate GABAergic neurotransmission by binding to the benzodiazepine binding site of $GABA_A$ receptors. As such, this may indicate a mechanistic pathway for the induction of tau pathology involving GABAergic receptors, based on the tau and gray matter sectors of Fig. 4.4d. From Fig. 4.4d, the $GABA_A$-associated benzodiazepine site is particularly involved in cognitively significant interactions affecting amyloid accumulation. $GABA_A$ and $GABA_B$ receptors play a notable cognitive role by affecting neural activity dysfunction, and all three GABAergic targets included in this work are involved via tau accumulation.

Finally, we introduced a summary metric of alterations to receptor-mediated interactions with reference to their normal variation in healthy ageing. Particularly, we found that GABAergic alterations had the largest effect on cognitive impairment in AD patients, significantly affecting executive function and the MMSE (Fig. 4.6a). Furthermore, we showed that subjects with identical clinical diagnosis and similar cognitive symptoms can have distinct underlying dynamics and receptor alteration fingerprints (Fig. 4.6b-c). These results highlight the clinical utility of our dynamical modeling approach. By fusing *in vitro* receptor templates with longitudinal neuroimaging data and modeling the underlying dynamics of receptor-mediated

neurobiological interactions, we are able to infer subject-specific mechanistic alterations despite the lack of subject-specific receptor data. As a demonstrative example, we summarized subject-specific alterations at the scale of receptor families. However, in a clinical context, subject-specific alterations at the broad scale of receptor families, the finer scale of specific receptors, or even specific receptor-neurobiological interactions (e.g. NMDA × CBF interactions) can be used to design personalized, precision treatments, which will be a topic of future work.

The whole-brain re-MCM models used cytoarchitectonically identified cortical regions of interest, neglecting sub-cortical structures for which no receptor distribution data was available. Many neurotransmitter alterations relevant to neurodegeneration occur in these regions, notably dopamine deficiencies in the basal ganglia in Parkinson's disease and early cholinergic neuronal death in AD. As such, including sub-cortical regions may better characterize important molecular pathways. Nevertheless, some effects of these phenomena are captured via projections to cortical neurons that are covered by our regions of interest. Additionally, future work will aim to integrate CSF into the model.

In this work, we used fractional amplitude of low-frequency fluctuation (fALFF) [578] as the regional measure of functional integrity. Low frequency (0.01-0.08 Hz) oscillations in the blood oxygenation level-dependent (BOLD) signal reflect the intensity of spontaneous activity in the resting brain, primarily in the default mode network [578]. When the amplitude of low frequency fluctuations (ALFF) is normalized by the overall power spectrum of the BOLD signal to calculate fALFF, the effects of physiological noise are suppressed [578]. However, compared to ALFF, fALFF significantly amplifies the signal from some non-default mode network regions (namely temporal-parietal regions and the precentral gyrus) [578], reducing its desired specificity to resting state activity. Nevertheless, fALFF shows high temporal stability over the course of

fMRI scans [619], long-term (i.e. about 6 month) test-retest reliability [620], and high sensitivity to AD progression [577] [219]. Alternative fMRI-based metrics include regional homogeneity (ReHo) [621] or graph theoretic metrics such as functional connectivity degree [622]. Comparing fALFF, ReHo, and graph-based metrics using simultaneous resting state fMRI/PET scans, Aiello et al. found functional connectivity degree to be the least correlated to glucose uptake, while the difference in correlation to glucose uptake between fALFF and ReHo was not significant [576]. Furthermore, as an intentional consideration to maintain model interpretability, our modeling framework avoids graph theoretic fMRI metrics in order to separate local, intra-region effects from inter-region effects due to network propagation. Although graph theoretic features can have biophysical interpretation, such as weighted degree representing transneural propagation or regional participation coefficients reflecting metabolic demands, they integrate information from multiple regions, which causes a leakage of network information into the intra-regional component of our model. Thus, as fALFF is a local fMRI measure that has been found to be at least as informative as ReHo in reflecting metabolic activity and validated as a measure sensitive to AD progression by multiple studies [577] [219], all the analyses and results presented in this study correspond to fALFF as the measure of resting state functional integrity. It is, however, important to note that all available fMRI metrics have limitations in reflecting actual neuronal activity or integrity. Here, our choice of metric is aligned with the “neurocentric” resting-state fMRI model [623], which assumes that the spontaneous fluctuations in BOLD signal reflect ongoing neuronal processes. Multiple limitations to this model have been pointed out, including the lack of clear neurophysiological interpretability [623], suggesting that interpretations of resting state fMRI-based findings (including ours) should be taken with caution.

In addition to intra-region effects, our model considered network propagation along the tractography-derived white matter structural connectome. However, functional, metabolic [624] and vascular connectivity define complementary biophysical networks that may also contribute to the propagation of neurodegenerative pathology. For simplicity and to focus on local, receptor-mediated interactions, we restricted our model to structural connectivity. The structural connectome is the physical substrate for the axonal propagation of pathology, and the scaffolding for the more abstract functional network. However, to estimate the effect of our choice of connectivity, we repeated our model fitting with functional connectivity, finding no significant change in model fit (*Multi-scale interactions involving neurotransmitter receptors are important to explaining multifactorial brain reorganization* and Supplementary Fig. S8). We attribute this to (i) the dominance of intra-regional effects in our model, with a relatively low contribution due to propagation effects and (ii) the shared information between anatomical and functional connectivity [594]. While this work has focused on local interactions between biological processes, dynamical interactions also occur at a network level. For example, structural connectivity [625] and the vascular network [626] are two of the factors that shape functional connectivity, and modeling the dynamic interactions between these networks may be a potential direction for future work.

The dynamical system modeling approach in this work relies on longitudinal and multi-modal neuroimaging data in order to fit personalized models. Consequently, our results would benefit from larger cohorts with more longitudinal samples of multi-modal data. Additionally, receptor map templates of patients at different stages of aging and disease progression would improve the characterization of salient alterations. While we have attempted to uncover causal molecular-macroscopic mechanisms, due to the lack of personalized, longitudinal receptor maps,

some identified biological model parameters may in fact reflect a molecular alteration (i.e. a change in either spatial distribution or functional alteration of a receptor) in response to a change in a macroscopic biological variable. As such, the exploratory interpretation of our results in relation to cognitive decline in AD should account for both possible causal directions between a given biological parameter and its target modality. For example, α_1 receptors interacting with tau to predict functional activity represents a 3-way interaction, which may in fact reflect a causal direction from functional activity to adrenergic alteration. Furthermore, we have assumed a direct relationship between each imaging modality and an underlying neurobiological process. For instance, CBF in our model was derived from ASL MRI, the temporal resolution of which is limited by the relaxation time of blood. However, recent work on venous blood flow using BOLD perfusion lag-mapping has shown significant age-related changes outside the temporal resolution of ASL MRI [627]. As new or improved imaging biomarkers are developed for AD, their future inclusion in the re-MCM framework would improve the coverage of potential disease-related mechanisms.

Nevertheless, these results offer interpretable results via molecular targets and mechanisms of action. We find that receptor distributions mediate interactions between macroscopic biological factors that significantly affect cognitive decline in AD. Specifically, inter-individual differences in cognitive deterioration correlate with the modulation of neural activity dysfunction primarily by glutamatergic receptors, amyloid accumulation by GABAergic receptors, and tau buildup by glutamatergic, GABAergic and cholinergic receptors. Traditionally, the accumulation of misfolded proteins, namely amyloid and tau, has been implicated in the pathogenesis of AD. However, our results suggest a multi-factorial, and heterogeneous set of

mechanisms involved in disease. Furthermore, our personalized, data-driven approach allows us to account for inter-subject heterogeneity in biological pathology and clinical presentation.

A growing body of evidence supports the critical role of neurotransmitter receptors in AD symptoms severity and their subsequent potential as therapeutic targets [628] [629]. Neurotransmitter-based drugs such as the acetylcholinesterase inhibitor donepezil and the NMDA antagonist memantine have long been proposed as potential treatments for AD patients. However, these drugs have shown limited efficacy and adverse side effects [32] [124]. We propose that using personalized and multi-scale modeling can identify patient-specific alterations and therapeutic needs, by stratifying patients based on the biological parameter weights corresponding to the underlying, cognitively significant mechanisms (Figs. 4.1c and 4.6). This information can then be used to design individually tailored multi-factorial therapies to slow the process of cognitive decline in both diseased and normally-ageing individuals.

Funding

This research was undertaken thanks in part to funding from: the *Canada First Research Excellence Fund*, awarded to McGill University for the *Healthy Brains for Healthy Lives Initiative*, the Canada Research Chair tier-2, *Fonds de la recherche en santé du Québec* (FRQS) Junior 1 Scholaship and Weston Brain Institute (Rapid Response AD program 2018) awards to YIM, the *Brain Canada Foundation* and *Health Canada* support to the McConnell Brain Imaging Center at the Montreal Neurological Institute, and the *European Union's Horizon 2020 Framework Programme for Research and Innovation* under the Specific Grant Agreements 785907 (Human Brain Project SGA2) and 945539 (Human Brain Project SGA3) awarded to NPG and KZ. Multimodal imaging and clinical data collection and sharing for this project was funded by ADNI (National Institutes of Health Grant U01 AG024904) and DOD ADNI

(Department of Defense award number W81XWH-12-2-0012). ADNI is funded by the National Institute on Aging, the National Institute of Biomedical Imaging and Bioengineering, and through generous contributions from the following: AbbVie, Alzheimer's Association; Alzheimer's Drug Discovery Foundation; Araclon Biotech; BioClinica, Inc.; Biogen; Bristol-Myers Squibb Company; CereSpir, Inc.; Eisai Inc.; Elan Pharmaceuticals, Inc.; Eli Lilly and Company; EuroImmun; F. Hoffmann-La Roche Ltd and its affiliated company Genentech, Inc.; Fujirebio; GE Healthcare; IXICO Ltd.; Janssen Alzheimer Immunotherapy Research & Development, LLC.; Johnson & Johnson Pharmaceutical Research & Development LLC.; Lumosity; Lundbeck; Merck & Co., Inc.; Meso Scale Diagnostics, LLC.; NeuroRx Research; Neurotrack Technologies; Novartis Pharmaceuticals Corporation; Pfizer Inc.; Piramal Imaging; Servier; Takeda Pharmaceutical Company; and Transition Therapeutics. The Canadian Institutes of Health Research is providing funds to support ADNI clinical sites in Canada. Private sector contributions are facilitated by the Foundation for the National Institutes of Health (www.fnih.org). The grantee organization is the Northern California Institute for Research and Education, and the study is coordinated by the Alzheimer's Disease Cooperative Study at the University of California, San Diego. ADNI data are disseminated by the Laboratory for Neuro Imaging at the University of Southern California.

Competing Interests

The authors report no competing interests.

Supplementary material

Category	All re-MCM subjects	Healthy Aging	AD
Total subjects	423	112	25
Female	194 (45.9%)	56 (50.0%)	9 (36.0%)
Mean age (years)	71.8 (±7.0)	73.8 (±6.0)	72.0 (±5.5)
Mean education (years)	16.4 (±2.7)	16.5 (±2.8)	16.4 (±2.8)
APOE4 positive	175 (41.4%)	35 (31.2%)	8 (32.0%)

Supplementary Table 4.1. Summary of demographic data for ADNI subjects.

Summary of demographic data for subjects included in 3 analysis: i) all re-MCM models, ii) healthy subjects that did not progress to MCI or AD, and iii) subjects that developed AD.

Category	All re-MCM subjects	Healthy Ageing	AD
CBF	195 (46.1%)	39 (34.8%)	16 (64.0%)
Amyloid	422 (99.8%)	112 (100.0%)	25 (100.0%)
Neural Activity	127 (30.0%)	32 (28.6%)	6 (24.0%)
Metabolism	418 (98.8%)	109 (97.3%)	24 (96.0%)
Gray Matter	423 (100.0%)	112 (100.0%)	25 (100.0%)
Tau	238 (56.3%)	82 (73.2%)	14 (56.0%)

Supplementary Table 4.2. Proportion of subjects with multi-modal neuroimaging data by clinical subgroup.

Neurotransmitter	Receptor	Ligand	Type
Glutamate	AMPA	[^{3}H]-AMPA	Agonist
	NMDA	[^{3}H]-MK-801	Antagonist
	Kainate	[^{3}H]-Kainate	Agonist
GABA	$GABA_A$	[^{3}H]-Muscimol	Agonist
	$GABA_B$	[^{3}H]-CGP 54626	Antagonist
	$GABA_A$-associated benzodiazepine binding site ($GABA_A$/BZ)	[^{3}H]-Flumazenil	Antagonist
Acetylcholine	M_1	[^{3}H]-Pirenzepine	Antagonist
	M_2	[^{3}H]-Oxotremorine-M	Agonist
	M_3	[^{3}H]-4-DAMP	Antagonist
	Nicotinic $\alpha_4\beta_2$	[^{3}H]-Epibatidine	Agonist
Noradrenaline	α_1	[^{3}H]-Prazosin	Antagonist
	α_2	[^{3}H]-RX 821002	Antagonist
Serotonin	5-HT_{1A}	[^{3}H]-8-OH-DPAT	Agonist
	5-HT_2	[^{3}H]-Ketanserin	Antagonist
Dopamine	D_1	[^{3}H]-SCH 23390	Antagonist

Supplementary Table 4.3. Autoradiography ligands and receptor targets.

Lobe	Anatomical subdivision	Jülich area	Region name
Occipital lobe	Visual cortex	hOc1	Brodmann's area 17 / V1
		hOc2	Brodmann's area 18 / V2
		hOc4d	V4
		hOc3d	V3d
		hOc3v	V3v
		hOc4v	V4
	Extrastriate cortex	FG1	Part of Brodmann area 19
		FG2	Part of Brodmann area 19
Parietal lobe	Somatosensory cortex	1	Brodmann's area 1
		2	Brodmann's area 2
		3a	Brodmann's area 3a
		3b	Brodmann's area 3b
	Superior parietal lobule	5L	Brodmann's area 5L
		5M	Brodmann's area 5M
		7A	Brodmann's area 7A
	Inferior parietal lobule	PGa	Anterior inferior parietal area
		PGp	Posterior inferior parietal area
		PFt	Temporal inferior parietal area
		PFm	Medial inferior parietal area
Temporal lobe	Auditory cortex	Te1	Temporal area 1 (part ofBrodmann's area 41)
		Te2	Temporal area 2 (part of Brodmann's area 41)
	Hippocampus	CA+dentate	Cornu ammonis + fascia dentata
	Entorhinal cortex	Ent	Brodmann's area 28
		20	Brodmann's area 20
		21	Brodmann's area 21

		22	Brodmann's area 22
		36	Brodmann's area 36
		37	Brodmann's area 37
		38	Brodmann's area 38
Frontal lobe	Agranular premotor cortex	6	Brodmann's area 6
	Primary motor cortex	4p	Brodmann's area 4p
	Broca's region	44	
		45	
	Frontopolar cortex	Fp1	Frontopolar area (part of Brodmann area 10)
		Fp2	Frontopolar area (part of Brodmann area 10)
	Orbitofrontal cortex	Fo1	Orbitofrontal area (part of Brodmann area 11)
	Lateral prefrontal	46	Brodmann's area 46
		47	Brodmann's area 47
		8	Brodmann's area 8
		9	Brodmann's area 9
Cingulate regions (multiple lobes)	Anterior cingulate	p24ab	Pregenual cingulate areas p24a & p24b
		p32	Pregenual cingulate area p32
	Posterior cingulate	23	Brodmann's area 23
		31	Brodmann's area 31

Supplementary Table 4.4. Jülich histological atlas regions. Note that regions are defined by cytoarchitecture, and thus do not correspond perfectly with functional regions.

Neuroimaging Modality	Model Parameter	Receptor Type	Explained Variance
CBF	NMDA × CBF	Glutamatergic	0.22%
	M_2 × CBF	Cholinergic	0.30%
	M_2 × Amyloid	Cholinergic	0.17%
	M_1	Cholinergic	0.30%
	α_1 × Gray Matter	Adrenergic	0.11%
	D_1 × Amyloid	Dopaminergic	0.22%
Amyloid	Kainate × CBF	Glutamatergic	0.10%
	AMPA × Tau	Glutamatergic	0.15%
	NMDA × Tau	Glutamatergic	0.18%
	Kainate × Tau	Glutamatergic	0.10%

	AMPA	Glutamatergic	0.13%
	$GABA_A$/BZ × CBF	GABAergic	0.33%
	$GABA_A$/BZ × Neural Activity	GABAergic	0.26%
	$GABA_A$/BZ × Metabolism	GABAergic	0.26%
	$GABA_A$/BZ × Tau	GABAergic	0.22%
	$GABA_B$	GABAergic	0.29%
	$\alpha_4\beta_2$	Cholinergic	0.29%
	α_2 × Amyloid	Adrenergic	0.19%
	α_2 × Tau	Adrenergic	0.11%
	α_2	Adrenergic	0.31%
	$5HT_2$ × CBF	Serotonergic	0.34%
	$5HT_{1A}$	Serotonergic	0.13%
	D_1 × Metabolism	Dopaminergic	0.15%

	Neural Activity	Non-Receptor	0.04%
	spreading	Non-Receptor	0.14%
Neural Activity	AMPA × CBF	Glutamatergic	0.24%
	Kainate × CBF	Glutamatergic	0.15%
	AMPA × Amyloid	Glutamatergic	0.16%
	AMPA × Neural Activity	Glutamatergic	0.14%
	AMPA × Metabolism	Glutamatergic	0.36%
	NMDA × Metabolism	Glutamatergic	0.15%
	AMPA × Gray Matter	Glutamatergic	0.42%
	AMPA × Tau	Glutamatergic	0.29%
	NMDA × Tau	Glutamatergic	0.30%
	Kainate × Tau	Glutamatergic	0.13%

	NMDA	Glutamatergic	0.15%
	$GABA_A$ × CBF	GABAergic	0.27%
	$GABA_B$ × CBF	GABAergic	0.35%
	$GABA_A$ × Gray Matter	GABAergic	0.23%
	$GABA_B$	GABAergic	0.27%
	M_1 × CBF	Cholinergic	0.11%
	M_2 × CBF	Cholinergic	0.17%
	M_2 × Amyloid	Cholinergic	0.16%
	M_3 × Neural Activity	Cholinergic	0.20%
	M_1 × Gray Matter	Cholinergic	0.14%
	M_2 × Gray Matter	Cholinergic	0.23%

	M_1	Cholinergic	0.12%
	M_3	Cholinergic	0.23%
	α_2 × CBF	Adrenergic	0.26%
	α_2 × Amyloid	Adrenergic	0.32%
	α_2 × Gray Matter	Adrenergic	0.15%
	$5HT_2$ × Gray Matter	Serotonergic	0.42%
	D_1 × Amyloid	Dopaminergic	0.29%
	D_1 × Gray Matter	Dopaminergic	0.49%
	D_1	Dopaminergic	0.31%
Metabolism	Kainate × Metabolism	Glutamatergic	0.11%
	Kainate × Tau	Glutamatergic	0.18%
	Kainate	Glutamatergic	0.14%
	$GABA_A$ × Tau	GABAergic	0.20%

	$GABA_A$/BZ × Tau	GABAergic	0.22%
	$\alpha_4\beta_2$ × CBF	Cholinergic	0.11%
	M_2 × Tau	Cholinergic	0.16%
	$\alpha_4\beta_2$ × Tau	Cholinergic	0.11%
	α_2 × Gray Matter	Adrenergic	0.11%
	α_1 × Tau	Adrenergic	0.14%
	$5HT_{1A}$ × Tau	Serotonergic	0.14%
	D_1 × Neural Activity	Dopaminergic	0.17%
	spreading	Non-Receptor	0.16%
Gray Matter	NMDA × Gray Matter	Glutamatergic	0.07%
	$GABA_A$/BZ × CBF	GABAergic	0.28%
	M_3 × CBF	Cholinergic	0.21%
	M_2 × Gray Matter	Cholinergic	0.10%
	α_2 × Metabolism	Adrenergic	0.07%

	$5HT_2$ × CBF	Serotonergic	0.18%
Tau	NMDA × CBF	Glutamatergic	0.16%
	Kainate × Amyloid	Glutamatergic	0.10%
	Kainate × Metabolism	Glutamatergic	0.36%
	$GABA_A$/BZ × CBF	GABAergic	0.29%
	$GABA_A$	GABAergic	0.12%
	$GABA_B$	GABAergic	0.27%
	M_3 × CBF	Cholinergic	0.33%
	$\alpha_4\beta_2$ × Amyloid	Cholinergic	0.17%
	M_2 × Neural Activity	Cholinergic	0.10%
	$\alpha_4\beta_2$ × Metabolism	Cholinergic	0.18%

	$\alpha_4\beta_2 \times$ Tau	Cholinergic	0.25%
	$\alpha_4\beta_2$	Cholinergic	0.36%
	$\alpha_1 \times$ CBF	Adrenergic	0.12%
	$\alpha_1 \times$ Metabolism	Adrenergic	0.11%
	$\alpha_2 \times$ Metabolism	Adrenergic	0.24%
	$\alpha_2 \times$ Gray Matter	Adrenergic	0.10%
	$5HT_2 \times$ CBF	Serotonergic	0.40%
	$5HT_{1A} \times$ Amyloid	Serotonergic	0.15%
	$5HT_{1A} \times$ Tau	Serotonergic	0.20%
	Metabolism	Non-Receptor	0.08%
	Gray Matter	Non-Receptor	0.25%

Supplementary Table 4.5. Biological parameters most correlated with cognitive decline in AD, and the percentage of cognitive decline variance explained.

Receptor Type	Total Variance Explained
Glutamatergic	4.47%
GABAergic	3.85%
Cholinergic	4.46%
Adrenergic	2.34%
Serotonergic	1.96%
Dopaminergic	1.63%

Supplementary Table 4.6. Total cognitive variance explained by receptor type in AD patients (via the significant SVD component).

Imaging Modality	Average Gain in R^2	P-value
CBF	125% ± 123%	P<0.001
Amyloid	119% ± 141%	P<0.001
Neural Activity	123% ± 150%	P<0.001
Metabolism	133% ± 200%	P<0.001
Gray Matter	234% ± 389%	P<0.001
Tau	141% ± 142%	P<0.001

Supplementary Table 4.7. Performance gain due to the inclusion of receptor maps, and the p-value from a two-sample t-test for each modality.

Imaging Modality	Average Gain in R^2	P-value
CBF	19.5% ± 13.7%	P<0.01
Amyloid	20.5% ±15.3%	P<0.01
Neural Activity	22.3% ± 15.0%	P<0.01
Metabolism	15.6% ± 13.3%	P<0.04
Gray Matter	20.2% ± 18.4%	P<0.03
Tau	21.5% ± 13.0%	P<0.01

Supplementary Table 4.8. Performance gain due to true receptor distributions over null maps, and p-value of the true receptor data model belonging to the null distribution.

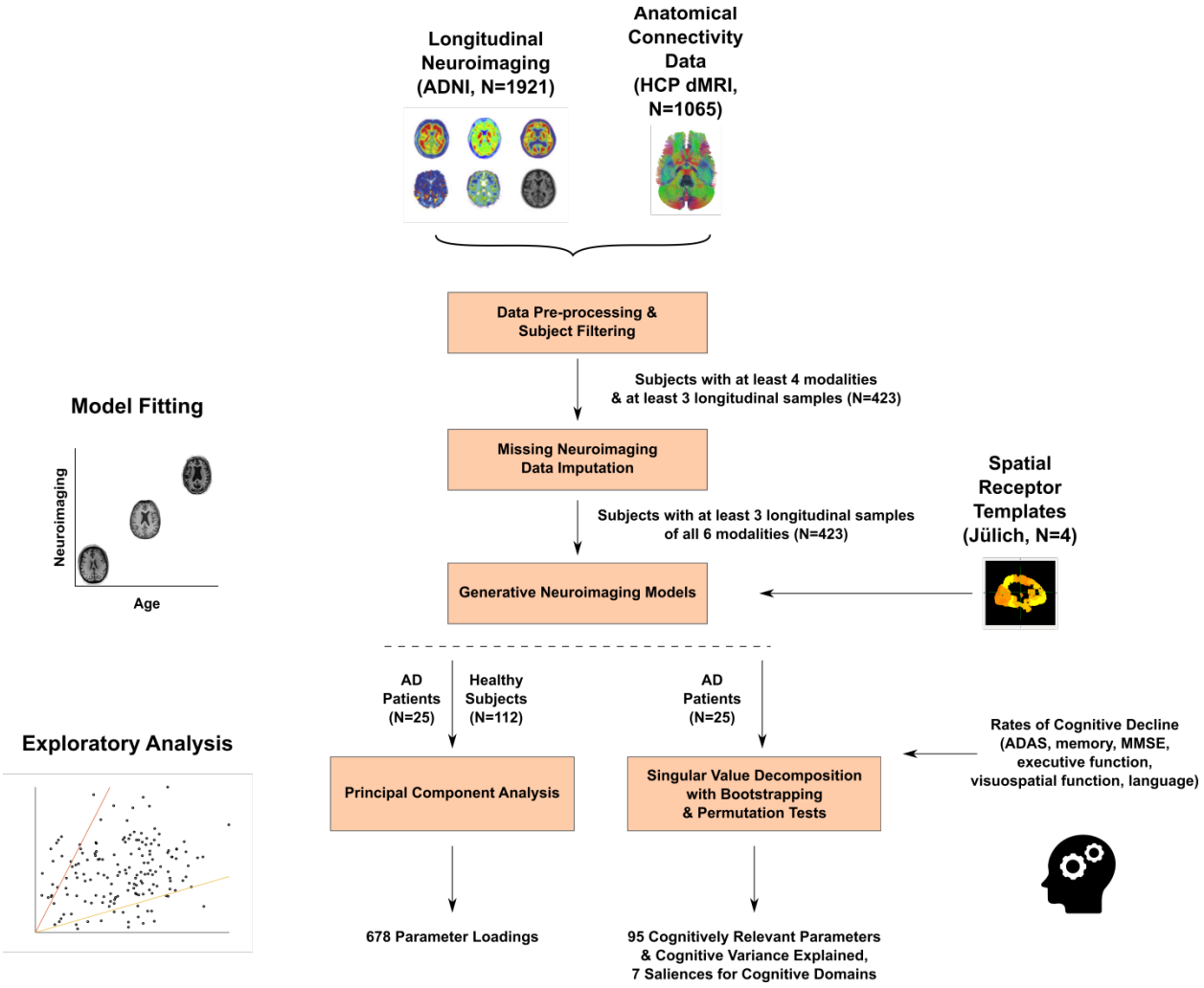

Supplementary Figure 4.1. Modeling and analysis pipeline.

First, multi-modal neuroimaging data, neurotransmitter receptor maps and tractography-derived connectivity matrices are used to fit personalized neuroimaging models. PCA was used to identify biological parameters contributing to inter-individual variability in healthy and AD subgroups. Subsequently, model parameters were compared to the subject-wise variation of cognitive decline in the AD subgroup using singular value decomposition. SVD allows the ranking of parameters based on the variance explained, allowing the identification of prominent alterations.

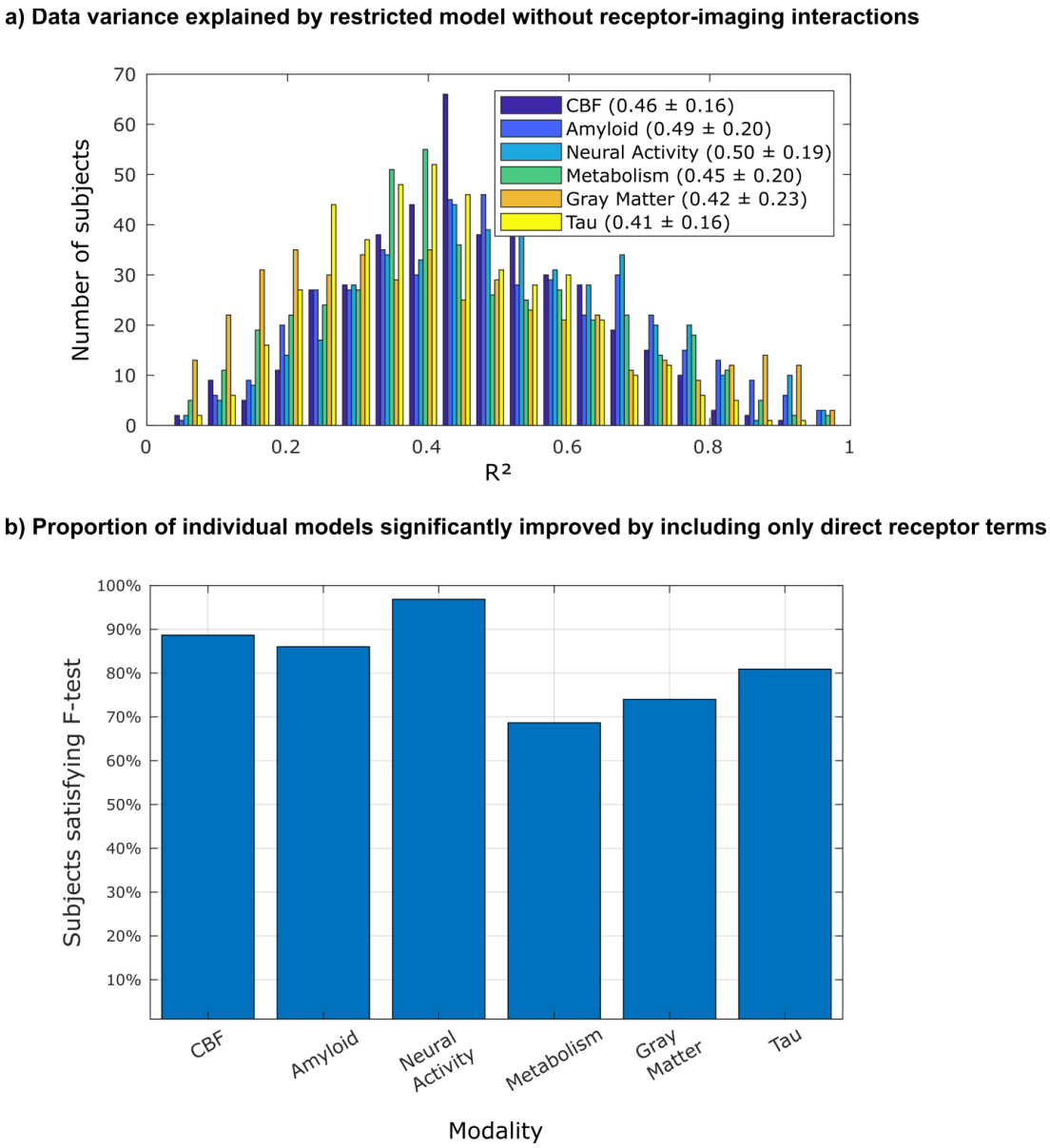

Supplementary Figure 4.2. Receptor maps improve neuroimaging model accuracy.

In all (N=423) subjects, we fit personalized neuroimaging models using receptor maps and neuroimaging data, but excluding receptor-neuroimaging interactions. a) The distribution of R^2 shows a moderate improvement over the restricted model with no receptor data (Fig. 2b). b) The majority of subjects showed a significant ($P<0.05$) improvement in R^2, based on an F-test between the restricted, interaction-free model (with receptor maps) and the neuroimaging-only model of Fig. 2b.

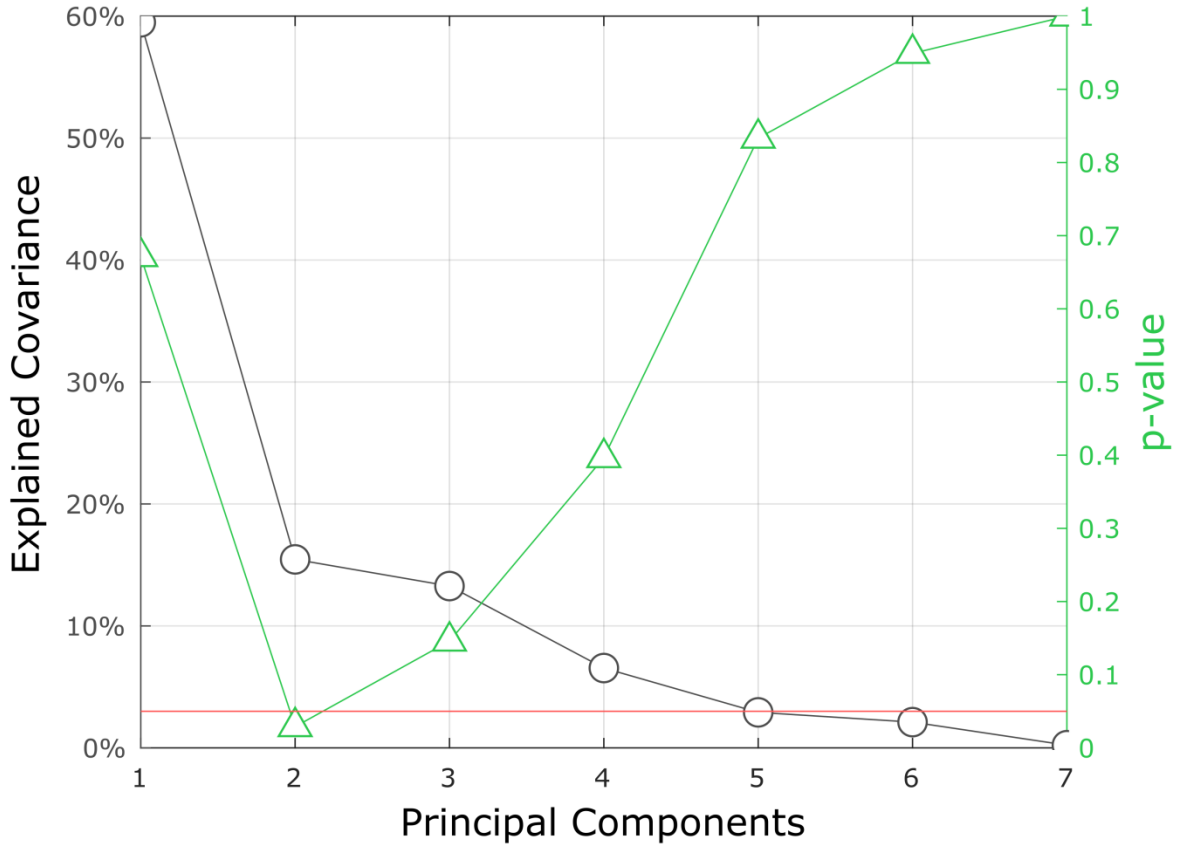

Supplementary Figure 4.3. Secondary significant component links biological parameters to cognitive decline in healthy ageing.

We performed singular value decomposition linking biological parameters to rates of cognitive decline in N=112 healthy subjects. The latent components are ranked by the fraction of cognitive decline variance explained, and p-value based on the permutation analysis outlined in Biological parameter cognitive significance analysis. A minor SVD component linking re-MCM parameters to rates of cognitive decline was significant ($p<0.02$ for the second component).

Supplementary Figure 4.4 Significant neurotransmitter receptor-imaging interactions underlying cognitive decline in healthy aging.

Receptor-imaging interactions significantly correlated, via the second principal component, to cognitive decline in healthy aging are shown (PC2; 15.5% variance explained, p<0.02; N=112).

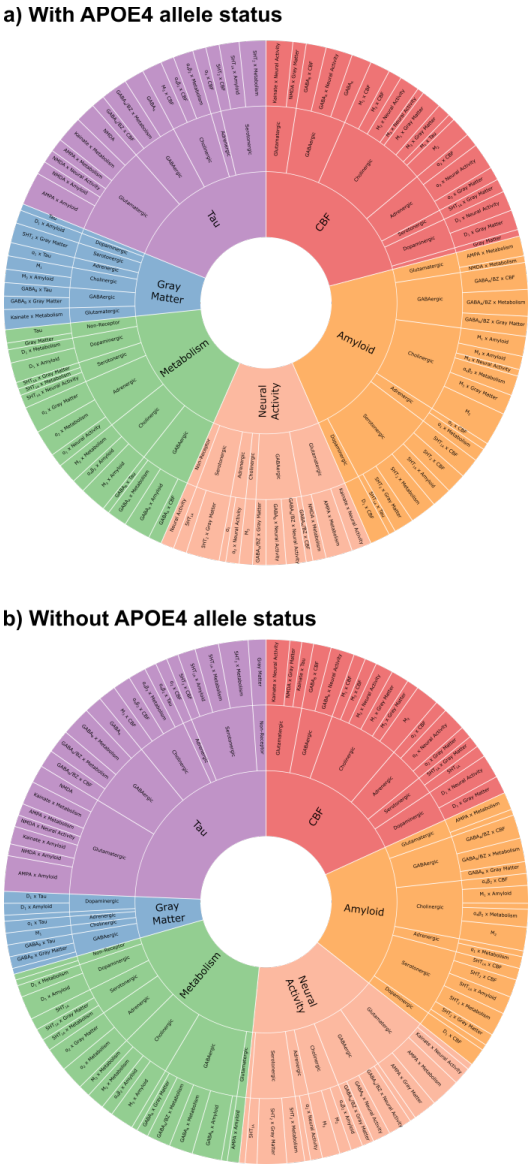

Supplementary Figure 4.5. Effect of APOE4 status on significant neurotransmitter receptor-imaging interactions underlying cognitive decline in MCI and AD subjects (N=177).

a) Cognitive decline variance explained by significant receptor-imaging interactions identified after covariate adjustment of subjects' model parameters by APOE ε4 allele status, for the first principal component (40.2% variance explained, p<0.001). b) Significant interactions identified without covariate adjustment by APOE status in the same subgroup, for the first principal component (41.9% variance explained, p<0.001).

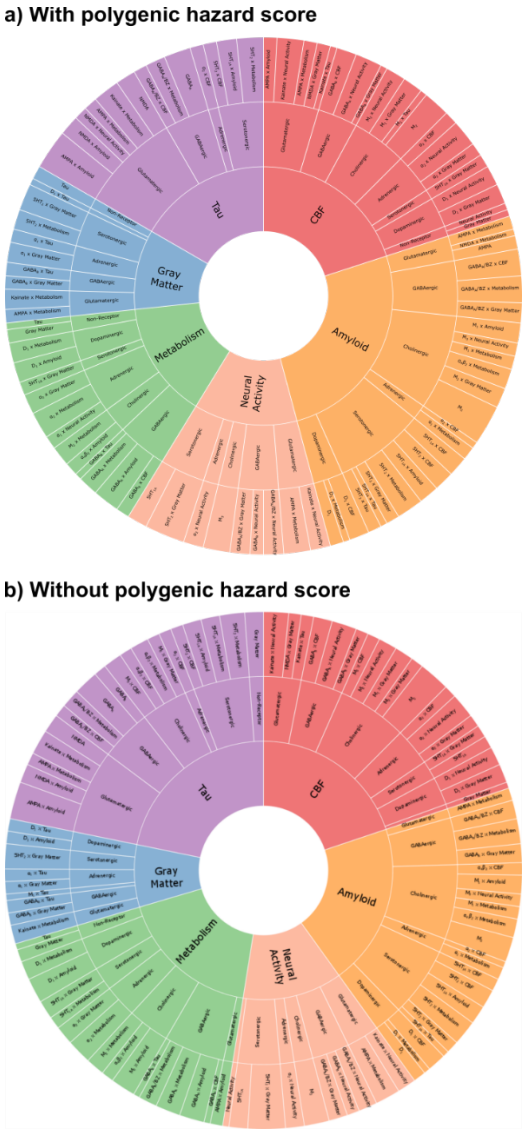

Supplementary Figure 4.6. Effect of polygenic hazard score (PHS) on significant neurotransmitter receptor-imaging interactions underlying cognitive decline in MCI and AD subjects (N=161).

a) Cognitive decline variance explained by receptor-imaging interactions identified after covariate adjustment of subjects' model parameters by polygenic hazard scores, for the first principal component (40.6% variance explained, p<0.001). b) Significant interactions identified without covariate adjustment by polygenic hazard score in the same subgroup, for the first principal component (42.2% variance explained, p<0.001).

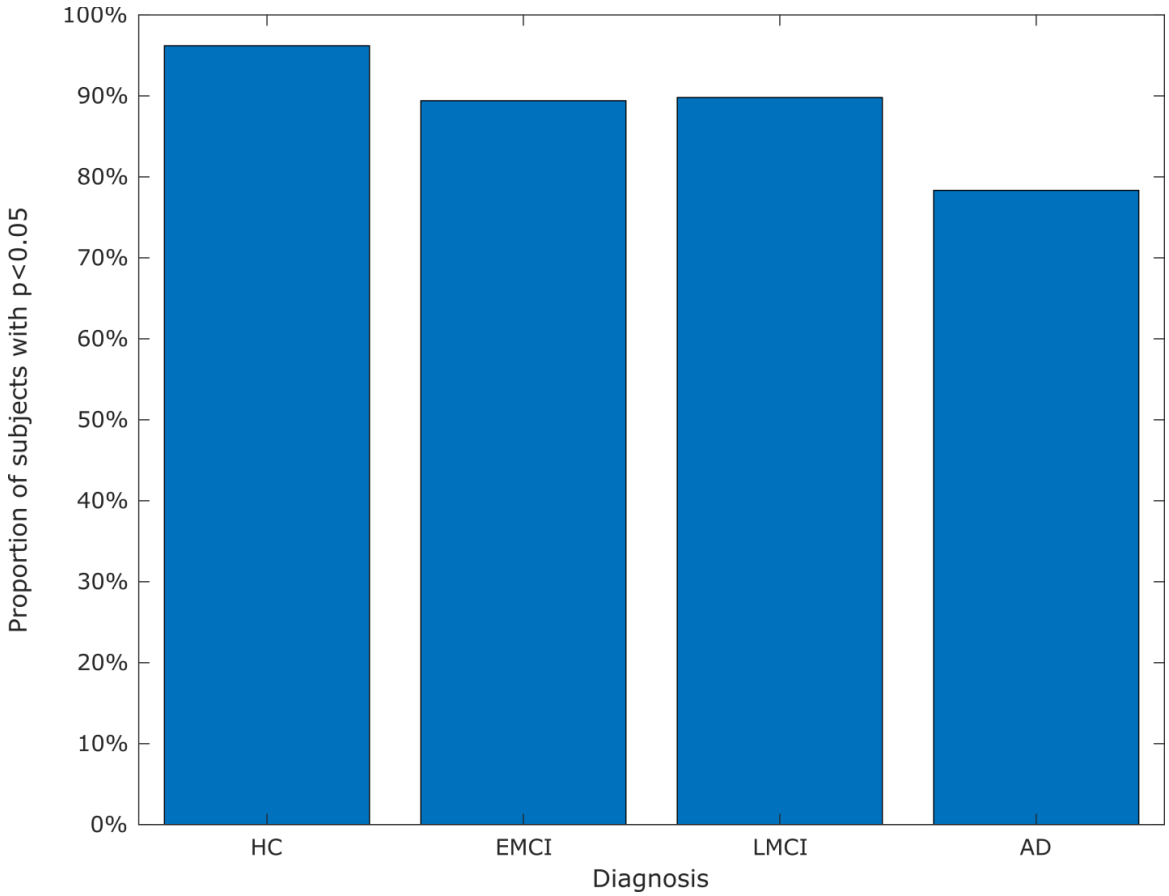

Supplementary Figure 4.7. Distribution of significantly improved receptor template model fit by diagnoses (N=423).

The average number of subjects (across all 6 modalities) for whom the true receptor maps resulted in significantly better model fit ($p<0.05$) than the randomly permuted receptor maps. The receptor template is most informative for healthy subjects, and progressively less for MCI and AD subjects.

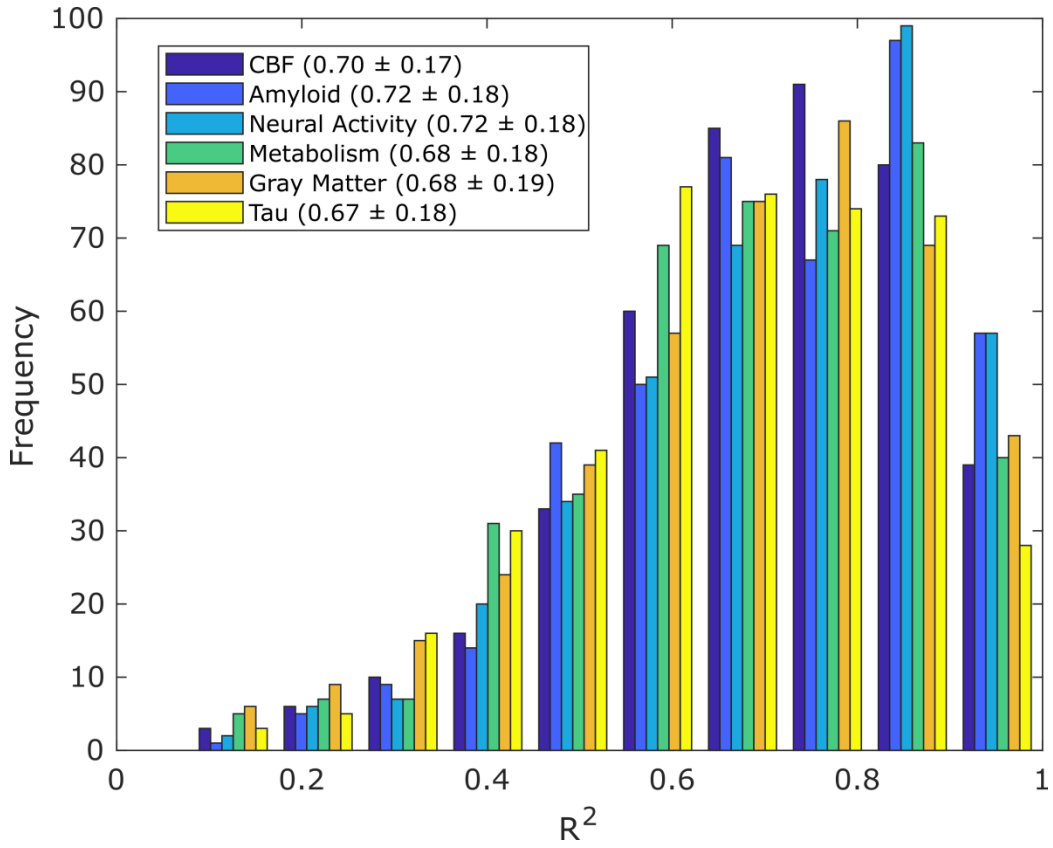

Supplementary Figure 4.8. Distribution of model fit (R^2) for re-MCM models using functional connectivity (N=423).

The model performance is virtually indistinguishable from the structural connectivity model (Fig. 2; r>0.99 for all modalities).

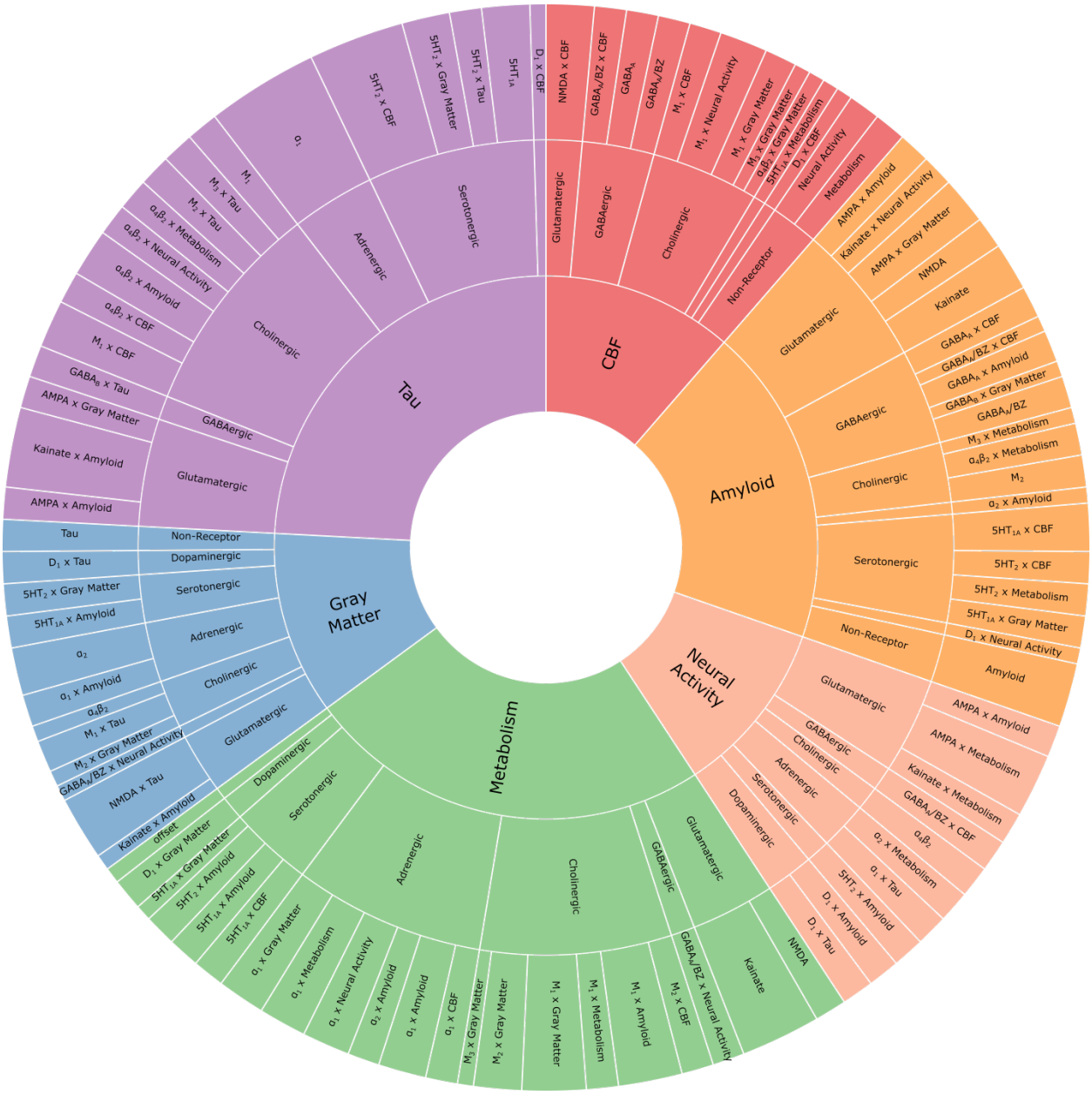

Supplementary Figure 4.9. Model parameters significant to cognitive decline in amyloid-positive MCI and AD subjects (N=52).

Cognitive decline variance explained by receptor-imaging interactions, for the first principal component (44.3% variance explained, $p<0.003$; $r=0.76$, $p<10\text{-}8$ after removing outliers more than 3 MAD from the projections of model parameters and cognitive scores, $p<0.001$).

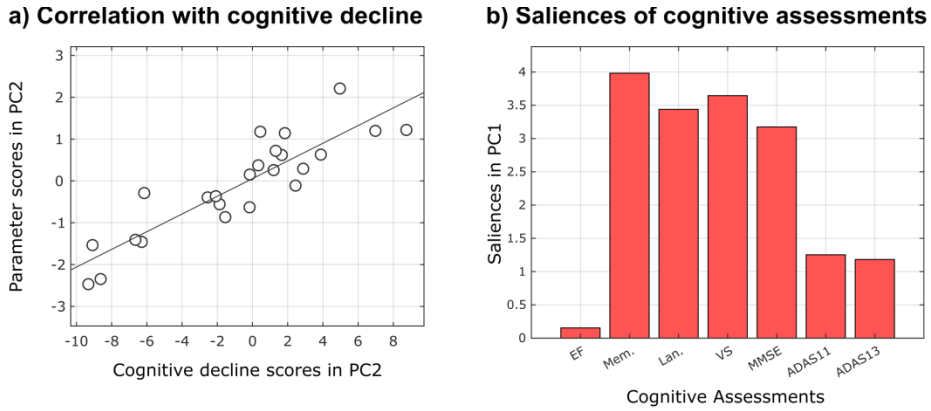

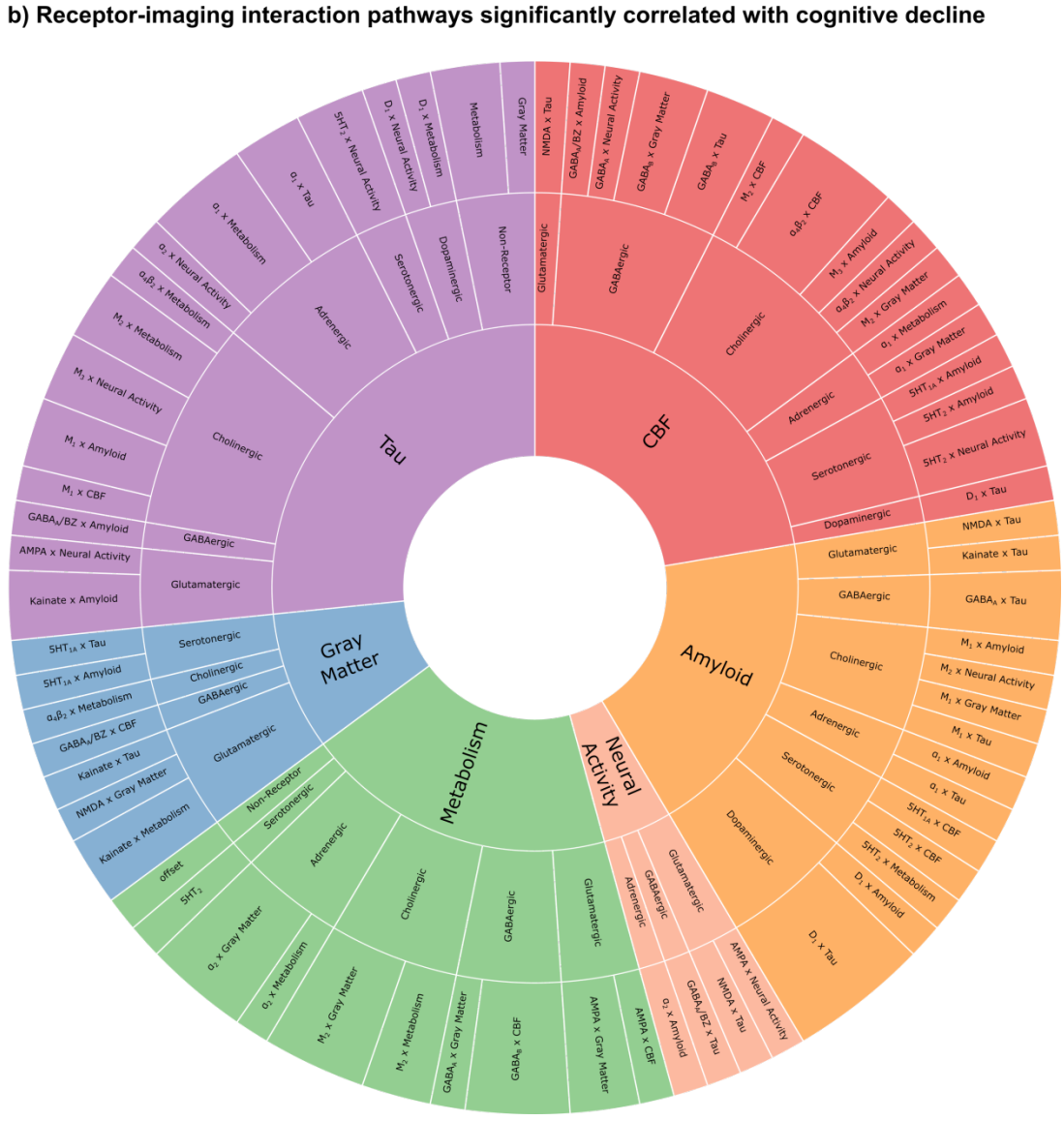

Supplementary Figure 4.10. Second component of receptor-cognitive variance in AD (N=25).

Contributions of receptor-imaging interactions to explaining the inter-subject variance between model parameters and cognitive scores projected to the second principal component (23.4% variance explained, $p<0.051$). a) The second component also showed a high correlation between model parameters and cognitive scores ($r=0.890$, $p<10^{-8}$). b) Cognitive variance in this axis showed a lower contribution of executive dysfunction. c) Receptor-imaging interactions in the second component showed a lower contribution due to neural activity model parameters, and a greater contribution due to CBF and metabolism models.

Chapter 5. Patient-specific models link neurotransmitter receptor mechanisms with motor and visuospatial axes of Parkinson's disease

Ahmed Faraz Khan, Quadri Adewale, Sue-Jin Lin, Tobias R. Baumeister, Yashar Zeighami, Felix Carbonell, Nicola Palomero-Gallagher, Yasser Iturria-Medina

Preface

Two centuries after being described by James Parkinson, a critical challenge for the treatment of Parkinson's Disease (PD) is posed by its remarkable multifactorial complexity. The classic dopaminergic circuit does not sufficiently explain PD's neuropathological and symptomatic variability, and many other neurotransmitter systems appear to be involved. Patients present a broad and heterogeneous set of motor, cognitive, psychiatric, sleep and sensory symptoms, and often do not respond well to dopaminergic medication. Improved treatment requires a comprehensive understanding of the various neurotransmission pathways underlying physiological degeneration and associated with symptomatic variability. However, the lack of suitable radioligands and the high cost of in vivo molecular imaging are a critical impediment to identifying molecular mechanisms involved in the disease.

Here, we develop and validate the first patient-centered approach to quantify neurotransmitter receptor involvement in PD neurodegeneration and symptomatic variability. Using advanced mathematical modeling integrating 15 important neurotransmitter receptor spatial distributions, 6 clinically-sensitive neuroimaging modalities, structural brain connectivity, and 11 clinical assessments from the Parkinson's Progression Markers Initiative (PPMI), we identify

receptor-mediated mechanisms of interaction between several measures of brain alterations (gray matter density, resting-state functional activity, dopamine transporter SPECT imaging, mean diffusivity, fractional anisotropy and t1/t2 ratio). We note that regional receptor architecture explains a large fraction of neurodegenerative changes in our cohort (N=71 PD patients), with multiple receptor families involved. Furthermore, correlating model-derived patient-specific receptor mechanisms with motor, psychiatric and cognitive clinical assessments, we discover two distinct, parallel disease axes representing motor symptoms with a strong GABAergic component, and cholinergically-dominant visuospatial symptoms. Importantly, we also identify specific brain regions of high receptor influence in PD-caused brain reorganization.

The multi-faceted nature of PD is increasingly acknowledged. To facilitate our evolving understanding of the disorder, our work presents the first integrative model linking multiple neurotransmitter receptors with macroscopic brain alterations and clinical symptoms. Importantly, estimating patient-specific, receptor involvement addresses an urgent clinical need by laying the foundation for model-based personalized treatment design. Furthermore, the novel methodology of using non-individualized receptor templates to infer patient-specific receptor involvement has broad applications in computational modeling when individualized imaging is infeasible.

The work presented in this chapter was published in *Nature Communications* on September 26, 2023, and is available online: https://doi.org/10.1038/s41467-023-41677-w.

Abstract

Parkinson's disease involves multiple neurotransmitter systems beyond the classical dopaminergic circuit, but their influence on structural and functional alterations is not well understood. Here, we use patient-specific causal brain modeling to identify latent

neurotransmitter receptor-mediated mechanisms contributing to Parkinson's disease progression. Combining the spatial distribution of 15 receptors from post-mortem autoradiography with 6 neuroimaging-derived pathological factors, we detect a diverse set of receptors influencing gray matter atrophy, functional activity dysregulation, microstructural degeneration, and dendrite and dopaminergic transporter loss. Inter-individual variability in receptor mechanisms correlates with symptom severity along two distinct axes, representing motor and psychomotor symptoms with large GABAergic and glutamatergic contributions, and cholinergically-dominant visuospatial, psychiatric and memory dysfunction. Our work demonstrates that receptor architecture helps explain multi-factorial brain re-organization, and suggests that distinct, co-existing receptor-mediated processes underlie Parkinson's disease.

Introduction

Parkinson's disease (PD) is primarily associated with a nigrostriatal dopamine deficit resulting in the characteristic motor symptoms of tremor, rigidity, and bradykinesia. However, the involvement of other brain circuits is now widely recognized [630], and the majority of patients also present numerous non-motor symptoms such as dementia, depression, sleep disorders, or apathy [631]. For this multi-system disease with significant inter-patient heterogeneity in pathology, symptoms and treatment response [632] [24] [633], consistent links between genetic, neuropathological and clinical subtypes remain elusive [634]. With no cure [635], symptomatic pharmacological treatment (e.g. levodopa) is at best partially effective [123] and may result in undesired side effects with chronic administration [126]. Given that diagnostic accuracy in untreated or medication non-responder PD patients is as low as 26% [636], an improved understanding of biological mechanisms and potential therapeutic targets underlying

pathological and symptomatic heterogeneity is imperative to bridging the treatment gap in PD [637] [638] [639].

Neurotransmission underlies many disease-related mechanisms as well as pharmacological response [123] [124]. Regional variability in neurotransmitter receptor gene expression correlates with altered macroscopic interactions such as neurovascular [117] and structural-functional decoupling [118]. Multiple non-dopaminergic nuclei are affected in PD [640] [122], with specific neurotransmitter systems linked to symptoms such as cholinergic freezing of gait and dementia [119], serotonergic depression and tremor [120], and adrenergic postural symptoms [121]. The dual syndrome hypothesis of PD [122] proposes a dichotomy between dopamine-mediated fronto-striatal executive impairment and a cholinergically-mediated prodromal visuospatial dementia. To better characterize the role of neurotransmission in mediating neurodegenerative brain reorganization, an integrative model linking multiple receptor systems, macroscopic brain reorganization and clinical symptoms would be essential. However, we are limited by the absence of whole-brain spatial distribution maps of neurotransmitter receptors in PD patients [123].

On the other hand, neuroimaging supports the multi-factorial and heterogeneous view of PD [641]. Various modalities are routinely used to support differential diagnosis [642] [637] [643] and evaluate treatment effects [644]. Multi-modal modeling of neuroimaging alterations can elucidate the temporal ordering, disease trajectories, and interactions of various pathologies in neurodegeneration [566] [86], and link these macroscopic observations with underlying genetic and transcriptomic determinants [645]. Multifactorial causal modeling (MCM) is a mechanistic modeling approach that is able to identify contributions of interacting factors to longitudinal changes [567], which can be used in a personalized medicine context to design

optimal therapeutic interventions [561]. Combining multi-modal neuroimaging with spatial distribution templates of 15 neurotransmitter receptors from post-mortem autoradiography [253] in an MCM-based approach significantly improved the explanation of degenerative changes in individual patients' neuroimaging data, and linked specific receptor-pathology interactions to clinical symptoms in Alzheimer's disease (AD) [646]. Furthermore, this approach was able to estimate individualized receptor alterations based on inter-subject differences in receptor-neuroimaging interactions.

Here, we extend previous molecular-phenotypic PD characterizations in four fundamental ways: i) by combining spatial distribution maps of 15 key neurotransmitter receptors derived from post-mortem autoradiography [253] with longitudinal neuroimaging data in a personalized modeling framework to infer the individualized importance of various receptor-mediated interactions (N=71, PPMI data), ii) by demonstrating the improved ability of receptor-enriched multifactorial causal modeling (re-MCM) to explain imaging-measured neurodegeneration and identify consistent mechanistic changes across patients, iii) by characterizing inter-patient heterogeneity, specifically linking receptor-based mechanistic alterations to two main axes of motor, cognitive and psychiatric symptoms, iv) quantitatively mapping brain regions with high receptor influence on PD neurodegeneration.

Results

Model-based approach to inferring personalized neurotransmitter receptor alterations

To characterize neurotransmitter receptor contributions to the multifaceted neurodegenerative processes of PD, we fit receptor-informed individualized generative

computational models to the longitudinal alterations of 6 biological factors. Each biological factor is associated with neurodegeneration in PD, namely atrophy, dysregulated functional activity, dopaminergic deficiency, directed and microstructural damage, and dendrite loss, represented by the neuroimaging-derived measures of gray matter density (GM), fractional amplitude of low frequency fluctuations (fALFF), dopamine transporter SPECT (DAT-SPECT), fractional anisotropy (FA), mean diffusivity (MD), and t1/t2 ratio [184] [185]. Neuroimaging data was acquired over multiple imaging scans for N=71 PD patients (PPMI data, Methods: Data description and processing). In addition, regional densities for 15 neurotransmitter receptors (from glutamatergic, GABAergic, cholinergic, adrenergic, serotonergic, and dopaminergic families) were derived from averaged templates (Methods: Data description and processing: Receptor densities and brain parcellation), and anatomical connectivity was estimated from the high-resolution Human Connectome Project template (HCP-1065; Methods: Anatomical connectivity estimation).

The neurotransmitter receptor-enriched multifactorial causal model (re-MCM; Fig. 5.1) decomposes the spatiotemporal evolution of pathology of multiple biological factors into localized receptor- and network-mediated effects (Fig. 5.1a). Model parameters explicitly represent distinct biological mechanisms, namely i) direct and ii) receptor-mediated pairwise interactions between imaging-derived biological factors (dopaminergic deficiency, functional activity, microstructural damage, dendrite density, and atrophy), iii) effects of local neurotransmitter receptor densities on factor-specific longitudinal deterioration, and iv) spreading of pathology to and from anatomically connected regions. Notice that, in the absence of true personalized longitudinal receptor imaging, model weights of specific receptor-mediated biological mechanisms compensate to fit individualized trajectories of neurodegeneration. Thus,

inter-subject variability in model weights serves as a proxy for the corresponding receptor densities or receptor-pathology interactions. Specifically, i) the improvement of model fit by the inclusion of healthy aged receptor templates validates their application to this clinical population, ii) biological mechanisms that are statistically stable across subjects represent mechanistic pathways shared by all PD patients in our cohort, iii) inter-patient co-variability between biological mechanisms and clinical symptoms represents overlapping disease processes (Fig. 5.1b), and iv) inter-region variability in the model fit improvement due to receptor templates can identify regions differentially affected by neurotransmitter receptor alterations in PD (Fig. 5.1c).

a Individualized causal modeling of interacting pathological factors

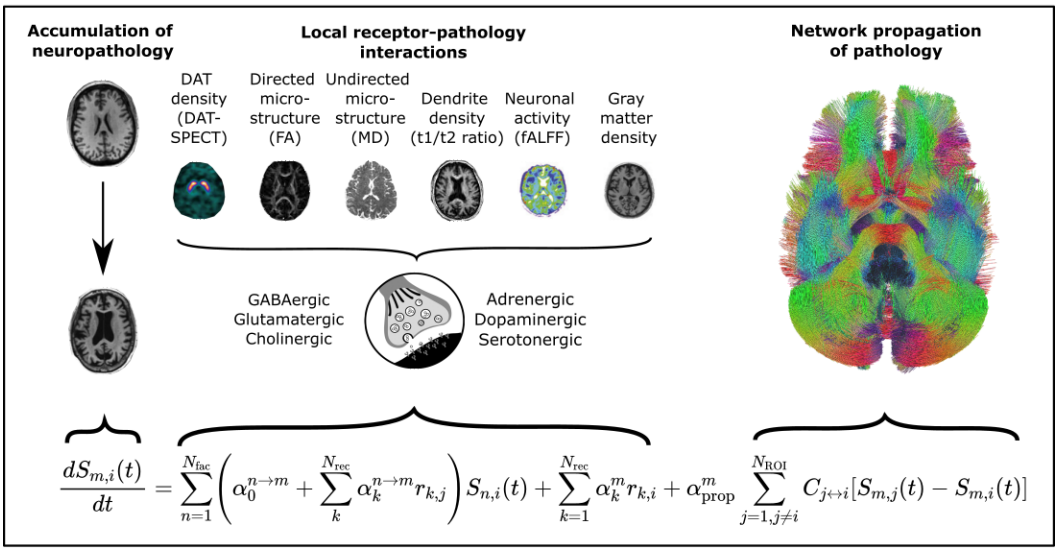

b Population-level association of model-derived mechanisms and clinical symptoms

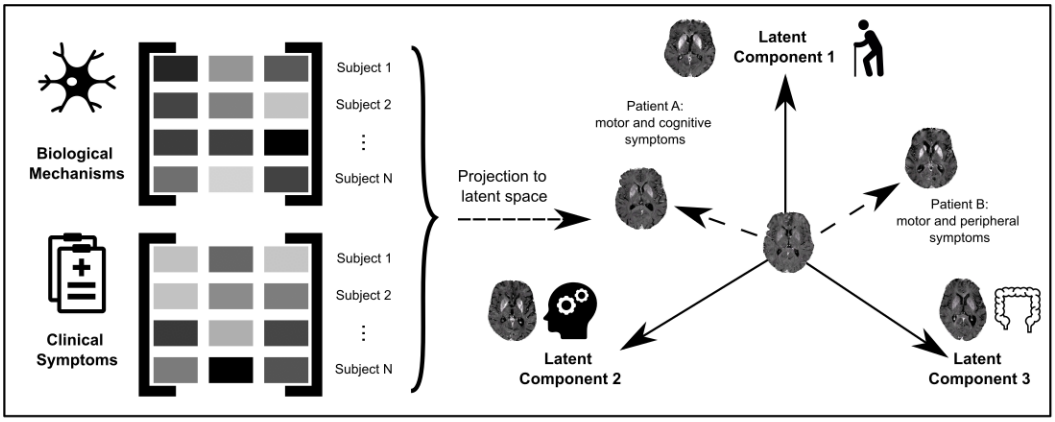

c Population-level estimation of regional receptor influence

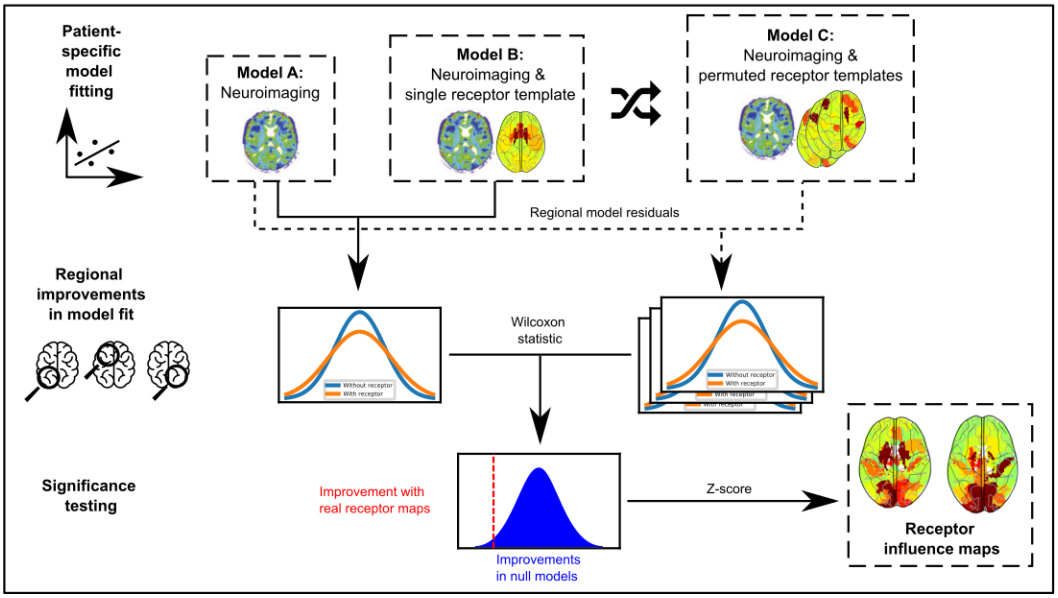

Figure 5.1. ***Neurotransmitter receptor-enriched multifactorial causal modeling.***

a) *Each patient's longitudinal pathological progression is decomposed into local effects due to: i) direct influence of every imaging-derived biological factor (e.g., atrophy on resting state functional activity), ii) receptor density distribution (e.g., D_1 receptor density on DAT loss), and iii) receptor-pathology interactions (e.g., D_1 receptors × DAT interactions on functional activity), in addition to iv) network-mediated inter-region propagation. Combining this data across (N_{ROI}=95) brain regions and multiple visits results in a multivariate regression problem to identify the patient-specific parameters {α}.* ***b)*** *Decomposing the covariance matrix of patients' model-derived biological mechanism weights and clinical scores (specifically, the rates of decline of composite clinical scores; Methods: Clinical scores) identifies multivariate axes of receptor-factor interactions that are robustly correlated with the severity of combinations of clinical symptoms in PD (Methods: Biological parameters and relationship with cognition).* ***c)*** *The regional contributions of receptor interactions to neurobiological changes are estimated by a feature importance analysis. We fit individualized models for every biological factor with and without each receptor map and performed permutation tests on the improvement in regional model residuals due to the inclusion of receptor maps. The resulting improvements are the significant regional influence of receptors on each target biological factor model.*

Neurotransmitter receptor maps significantly improve the explanation of multi-factorial brain reorganization in PD

Before proceeding to identify relevant model-derived biological mechanisms in PD, we first aimed to validate that re-MCM robustly fits patient-specific neuroimaging data. For each of the 6 biological factors and all subjects (N=71), we calculated the coefficient of determination (R^2) as a measure of the data variance explained. On average, re-MCM explained 74% ± 18% of the variance in rate of pathology accumulation (Fig. 5.2a), although model fit varied by biological factor, with neural activity dysfunction (fALFF; 81% ± 11%), dopaminergic degeneration (DAT-SPECT; 80% ± 13%) and dendrite loss (t1/t2 ratio; 80% ± 12%) being explained better than gray matter atrophy (GM; 58% ± 14%), or microstructural damage (MD; 70% ± 14%, and FA; 0.74 ± 0.13). For validation, we repeated the model-fitting without receptor-pathology interactions or direct local receptor density effects. On average, neuroimaging-only models without receptor data explained 52% ± 20% of the variance in neuroimaging rate of change (Fig. 5.2b), and the inclusion of receptor templates improves the data variance explained by 42.3%. Dopaminergic loss (DAT-SPECT) was the least improved by the addition of receptor maps, with imaging-only models explaining 60% ± 17%, a drop of 20% of variance on average compared to the full re-MCM. On the other hand, gray matter atrophy (GM: 22% ± 17% variance explained without receptor maps) was the most reliant on receptor data. While DAT-SPECT scans themselves already image the density of presynaptic dopaminergic transporters, gray matter atrophy models benefit more from regional differentiation based on receptor expression.

Figure 5.2c presents the improvement in each participant's model fit due to receptor mechanisms, compared to the restricted, neuroimaging-only models. Accounting for the

increased model size from 8 to 113 parameters, the F-statistics of 80.3% (MD) to 100% (DAT-SPECT) of patients is significant ($p<0.05$ red dotted line in Fig. 5.2c). We then performed a permutation test for the significance of the informativeness of receptor maps, by randomly shuffling each receptor map across brain regions 1000 times and fitting the re-MCM with each set of permuted maps.

The resulting distribution of model fit (R^2) was used to calculate significance levels for re-MCM with true receptor data from Figure 5.2a. For each biological factor, we plotted the number of subjects with significantly better model fit ($p<0.05$) compared to the null distribution in Fig. 5.2d. Notably, nearly all patients' biological factor models are significantly improved by the inclusion of receptor maps, except for undirected microstructural damage (MD; 67.6% or 48 subjects). Across all participants, Fisher's method gives χ^2 statistics in the range of $800< \chi^2 < 2300$ (depending on the biological factor), corresponding to a near-zero combined P-value. These analyses validate the use of averaged receptor templates in patient-specific PD models.

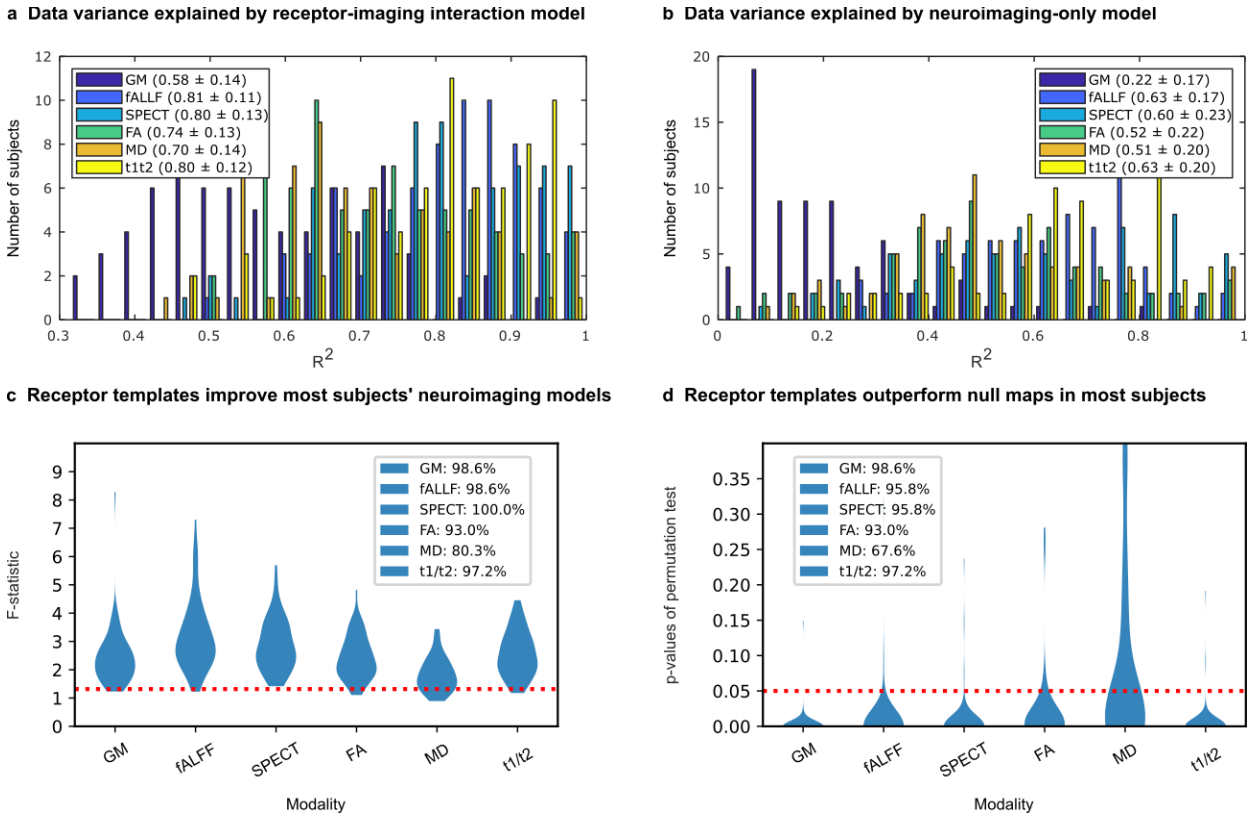

Figure 5.2. ***Contribution of receptor distributions to explaining multimodal brain reorganization in PD.***

Pathological factors are quantified by 6 neuroimaging-derived metrics: gray matter density (GM), neuronal activity (fractional amplitude of low frequency fluctuations; fALFF), dopamine transporter density (DAT) from SPECT, directed microstructure (fractional anisotropy; FA), undirected microstructure (mean diffusivity; MD), and dendrite density (t1/t2 ratio). The improvement in modeling the accumulation of pathology was evaluated in terms of i) the additional explanatory power due to receptor information, and ii) the significance of true receptor maps compared to null distributions. The histograms show the distribution of the coefficient of determination (R^2) of N=71 individual models of longitudinal neuroimaging changes including (a) and excluding (b) receptor predictors. Notably, including receptor terms improves model fit for all biological factors, although to varying extents. (c) Subject-wise F-tests between models with and without receptor maps (113 and 8 parameters, respectively) show proportions of subjects for whom the F-statistic is above the critical threshold (red dotted line). This critical threshold corresponds to a statistically significant ($P<0.05$) improvement due to the receptor terms in the re-MCM model, accounting for the increase in adjustable model parameters. Furthermore, to validate the benefit of the receptor templates over randomized null maps, re-MCM models were fit with 1000 spatially permuted receptor maps for each subject. The p-value of the model fit (R^2) using true receptor templates compared to the distribution of R^2 of models using randomized templates was calculated for each subject. (d) Proportion of subjects for whom the true receptor maps resulted in a statistically significant improvement in model fit ($P<0.05$; red dotted line).

Identifying stable neurobiological mechanisms and receptor-pathology interactions in PD

We proceeded to identify biological mechanisms consistently involved in structural, functional, and dopaminergic brain alterations in PD. For this, 99% confidence intervals for each re-MCM parameter across all patients were calculated and used to identify stable predictors. Since all predictors were standardized before data fitting, model weights are the relative effect sizes of different biological mechanisms on the rate of change of their target biological factor over the course of PD progression. Specifically, these neurobiological mechanisms are i) direct effects of local pathology, ii) direct effects of local receptor densities, iii) local receptor-pathology interactions, and iv) network propagation of pathology (Methods: Receptor-Enriched Multifactorial Causal Model).

Figure 5.3a shows the relative effective sizes of stable biological mechanisms. The most influential stable predictors of each biological factor's rate of change are the direct effects of local alterations to the same modality. Propagation of pathology along the structural connectome is also a minor yet stable predictor for all data modalities except functional activity (fALFF) and directed microstructural damage (FA), with a much lower effect than the local evolution of neurodegeneration. Notably, from Figure 5.3b, functional brain alterations (fALFF) do not appear to drive structural alterations (GM and MD), instead interacting bidirectionally with dendritic density (t1/t2).

Nevertheless, local interactions between imaging-based biological factors, whether direct or receptor-mediated, constitute a significant driver of PD neurodegeneration in all cases, and

form a complex network with potentially bidirectional influences (Fig. 5.3b). While comparatively smaller for functional activity, dopaminergic transporter density and directed microstructural integrity (FA), receptor-mediated interactions constitute approximately half the model effects for gray matter atrophy (GM), overall microstructural integrity (MD) and dendrite density (t1/t2).

We observed that a relatively sparse set of receptors is involved in stable interactions for each biological factor (Fig. 5.4). The muscarinic M_2 and nicotinic $\alpha_4\beta_2$ receptors contribute significantly to gray matter atrophy, neuronal activity dysfunction, and dopaminergic loss. The Bz site is also prominently associated with neuronal activity dysfunction and dopaminergic loss. The serotonergic $5HT_2$ receptor is involved in functional and undirected microstructural alterations, while glutamatergic effects are marked by NMDA affecting gray matter atrophy, AMPA and kainate affecting directed microstructure and kainate affecting dendrite density, respectively.

Generally, the dopaminergic, cholinergic, serotonergic, glutamatergic and GABAergic systems broadly affect (micro-)structural alterations (GM, MD and t1/t2). Serotonergic mechanisms are most associated with undirected microstructural alterations (MD), and secondarily dysfunctional neural activity (fALFF). Cholinergic receptors are prominent predictors of atrophy, microstructural damage and loss of dendrites (GM, MD and t1/t2), with minor influence on functional activity and dopaminergic transporter density. Glutamatergic receptors have a moderate influence across structural modalities (GM, MD, FA and t1/t2). GABAergic influence is minor yet stable across functional (fALFF and SPECT) and (micro-)structural (MD and t1/t2) modalities. Adrenergic and dopaminergic receptors are the least involved in stable neurobiological mechanisms, with α_2 adrenergic receptor modulating directed

microstructural damage (FA), and the D_1 dopaminergic receptors mediating the effect of atrophy on microstructure (MD).

For atrophy (GM), functional activity (fALFF) and microstructure (MD) models, the direct effects of specific receptor density maps reflect local susceptibility to neurodegeneration. The densities of the muscarinic M_2 and nicotinic $\alpha_4\beta_2$ cholinergic receptors help explain inter-region variability in the rate of gray matter atrophy, while M_2 and the serotonergic $5HT_2$ receptor densities are stable predictors of both altered activity (fALFF) and microstructural damage (MD).

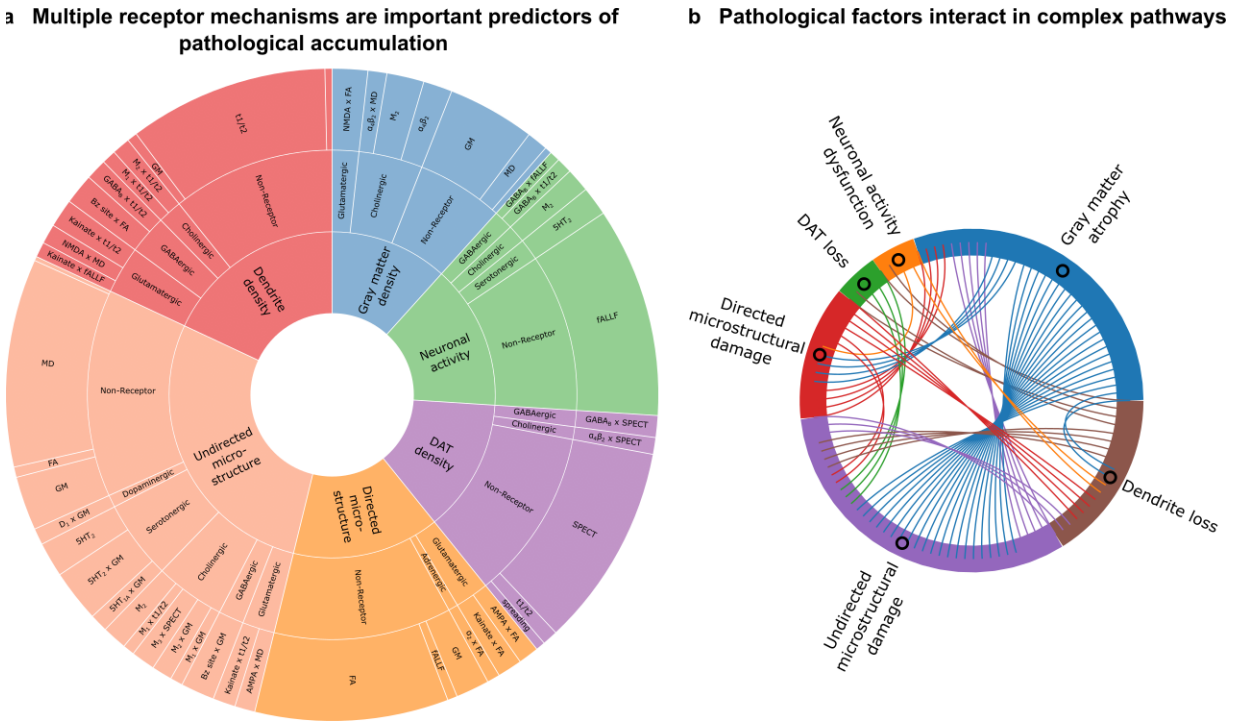

Figure 5.3. ***Receptor-mediated interactions explaining longitudinal neurodegeneration in PD.***

A) Statistically stable biological mechanisms in PD show significant receptor-mediated contributions. The angle of each outer sector is proportional to the mean weight of each stable (99% confidence interval) re-MCM model weight across the PD patients. The inner sectors represent the 6 modeled biological factors. Within each factor, the intermediate sectors represent the neurotransmitter system involved, while the outer sector consists of the specific two-way receptor-pathology interactions or direct predictor terms in the model. Notably, biological factors may appear as both model predictors (outer sector) and targets (inner sector).

B) Effect size (number of chords) of statistically stable interactions between any pair of biological factors modeled in PD.

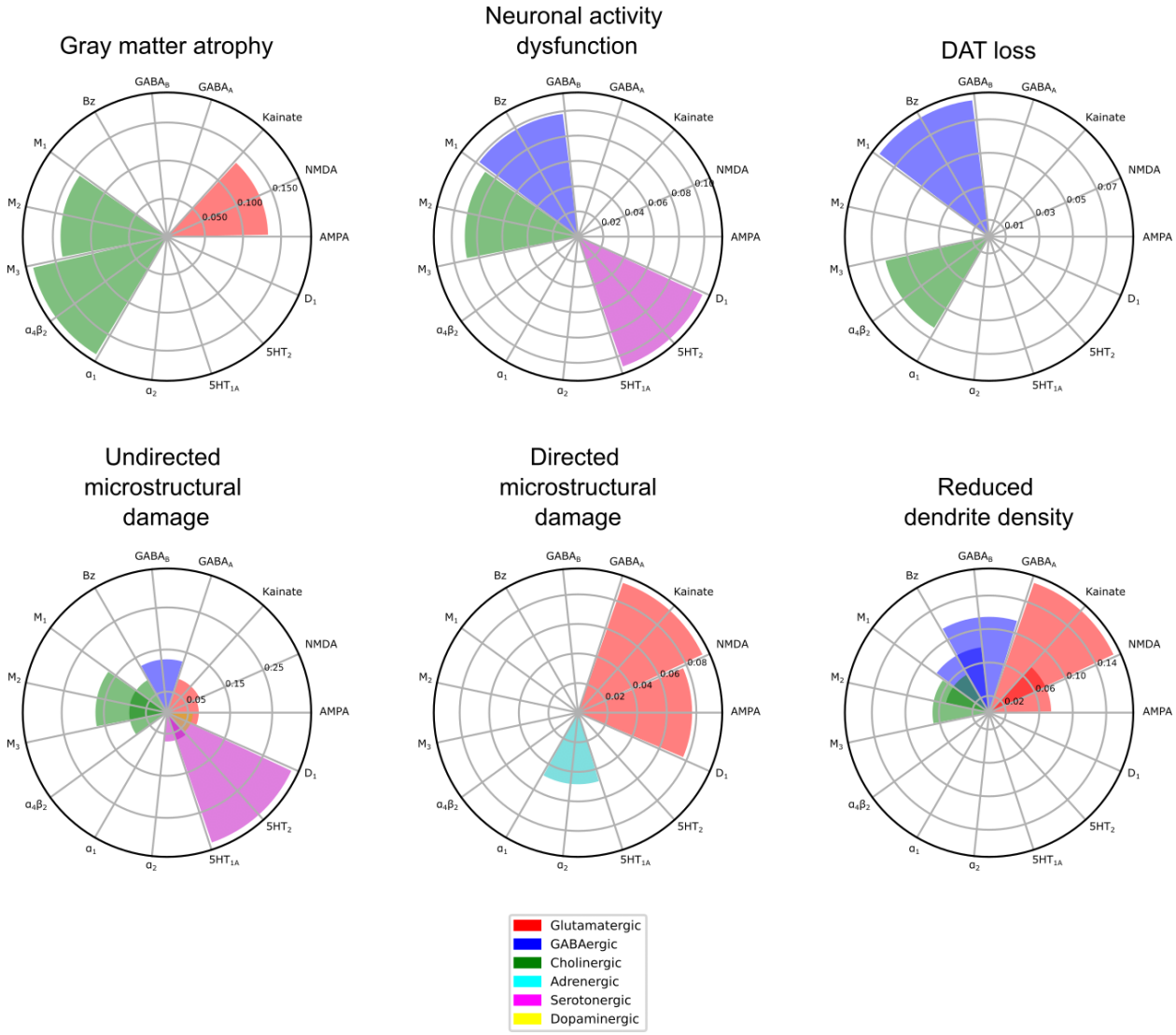

Figure 5.4. ***Receptors mediating degenerative alterations to different macroscopic biological factors in PD.***

The combined statistically stable model effects of each receptor type on each biological factor are shown. The muscarinic M_2 and nicotinic $\alpha_4\beta_2$ receptors contribute significantly to gray matter density, neuronal activity and dopamine transporter alterations. The Bz site is prominently associated with activity and dopamine transporter alterations. The serotonergic $5HT_2$ receptor is involved in functional and microstructural (MD) alterations, while glutamatergic effects are marked by NMDA affecting gray matter atrophy, AMPA and kainate affecting directed microstructural damage (FA) and kainate affecting dendrite density (t1/t2), respectively. Notably, the D_1 receptor distribution is relatively homogeneous and not marginally informative in the presence of DAT imaging.

Two axes of receptor-pathology alterations underlie clinical symptoms in PD

To link model-derived receptor-mediated neurobiological mechanisms with clinical presentation in PD, we identified shared axes of covariance between re-MCM-derived biological mechanisms and motor, non-motor, cognitive and psychiatric symptoms (Methods: Clinical scores). Partial least squares (PLS) regression using singular value decomposition (SVD) across all patients (N=71) was used to identify multivariate and overlapping relationships between identified biological parameters and clinical symptoms (Methods: Covariance of biological mechanisms with clinical symptoms) via projections to a latent space. Two latent components were relevant based on permutation tests, explaining 48.4% (P=0.001, FWE-corrected) and 13.2% (P=0.069, FWE-corrected) of the population co-variance, respectively. Projections of biological mechanisms and clinical scores to these components show moderate to high correlations of r=0.70 ($P=3.11\times10^{-11}$; Fig. 5.5a) and 0.86 ($P=3.75\times10^{-21}$; Fig. 5.5b).

Interestingly, the first component (primary axis; Fig. 5.5c) largely corresponds to variance of the MDS-UPDRS Parts 1-3 scores (composed of cognitive, psychiatric and motor aspects of daily living, as well as a motor exam), and SDM (assessing attention, perceptual speed, motor speed, and visual scanning [647]). On the other hand, the second component (secondary axis; Fig. 5.5d) is associated with the BJLOT (visuospatial judgment), LNS (working memory), STAIAD (anxiety) and the GDS (depression in older adults). The statistically stable biological mechanisms contributing to each axis are summarized in Figure 5.6. Both components show that inter-subject symptom variability is associated with multiple receptor-mediated biological mechanisms and neuropathological changes. The primary axis is largely driven by GABAergic alterations (explaining 5.97% of the total covariance via this component), although

glutamatergic (4.85%), cholinergic (4.77%), and serotonergic (3.77%) alterations are also prominent. The secondary axis is instead associated primarily with cholinergic alterations (1.74%), although GABAergic (1.24%) and glutamatergic (1.19%) alterations also play a role.

While the local (regional) evolution of pathology in each considered biological factor and its network propagation are prominent stable predictors of PD neurodegeneration (Fig. 5.3), the influence of these mechanisms does not co-vary prominently with symptom severity. Instead, we find a broad array of receptors with clinical effects along both latent axes, as shown in Fig 5.5. For example, the mainly motor symptoms of the primary axis are associated with inter-subject variability in glutamatergic and GABAergic interactions affecting microstructural integrity (MD and FA) and dendrite density (t1/t2). In contrast, the visuospatial, psychiatric and memory dysfunction of the secondary axis is associated more with inter-subject variability in cholinergic interactions affecting microstructure (MD) and dendritic density (t1/2), as well as changes to GM density.

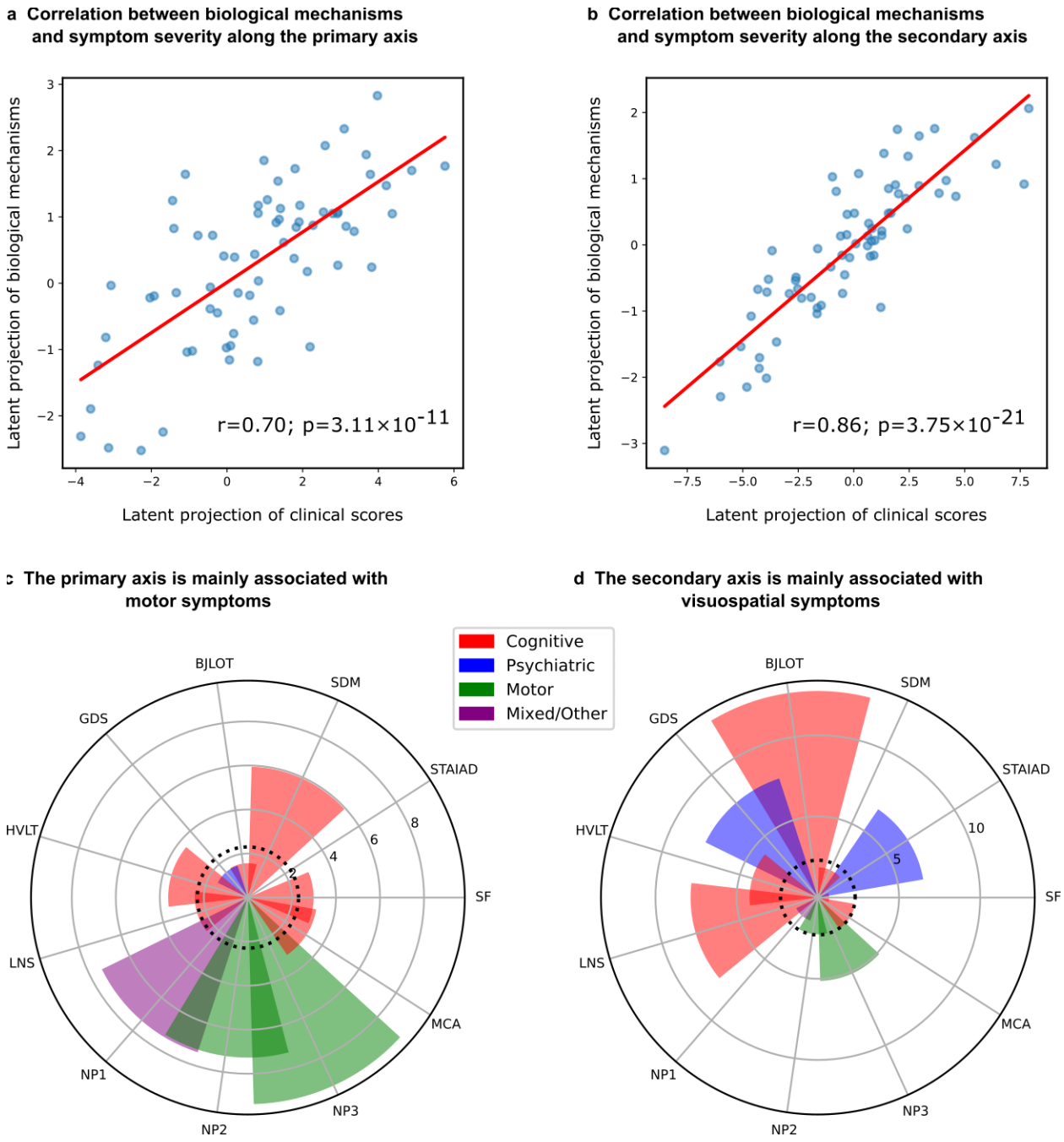

Figure 5.5. Two axes of covariance between biological mechanisms and symptom severity in PD.

a) Based on a permutation analysis, two latent SVD components were significant or near-significant, explaining 48.4% (P=0.001, FWE-corrected) and 13.2% (P=0.069, FWE-corrected) of the covariance respectively. a,b) High correlations of r=0.70 (P=3.11×10-11) and 0.86 (P=3.75×10-21), between the projections of statistically stable (based on 95% confidence intervals from bootstrapping) biological mechanisms and rates of clinical decline onto the latent components were observed. c,d) Bootstrap ratios of each clinical assessment to the two latent components, providing a relative ranking of motor, nom-motor, psychiatric and cognitive

domains. These saliences are proportional to the contribution of each term relative to every other term, for example showing that MDS-UPDRS scores, SDM and HVLT scores are the top contributors to the primary axis. Details about specific scores can be found in Methods: Clinical scores.

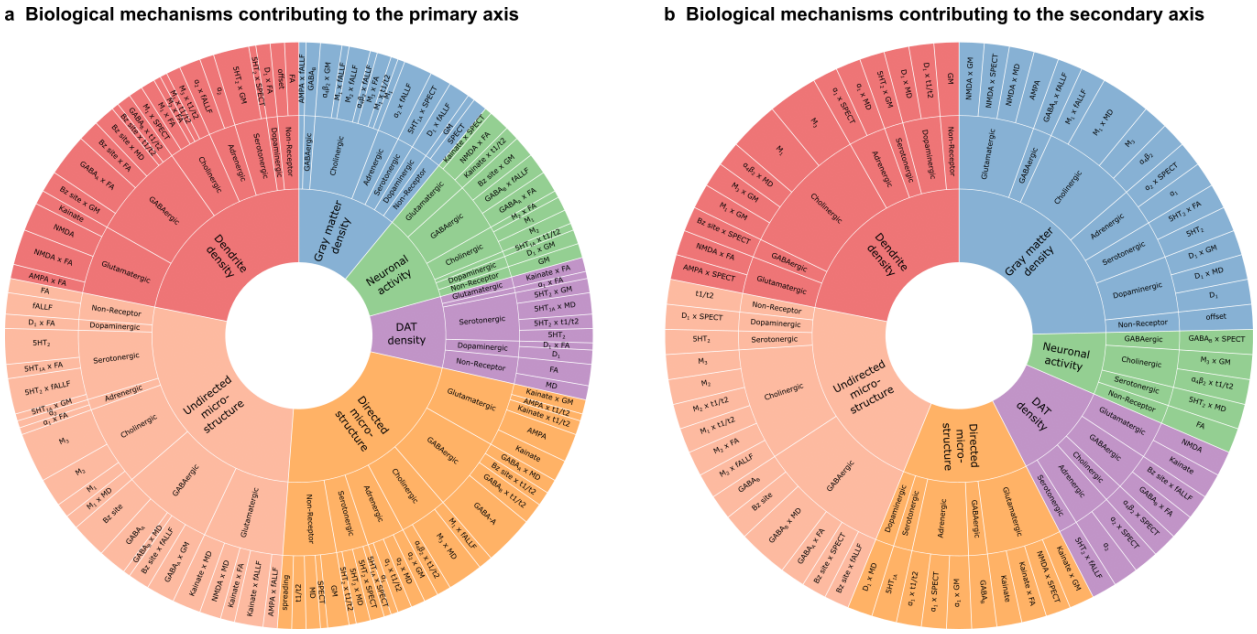

Figure 5.6. Distinct combinations of receptor-mediated interactions are associated with the two axes of clinical symptoms.

Biological mechanisms correlated with clinical severity in PD via the a) motor/psychomotor and b) visuospatial/memory/psychiatric axes are plotted. Representing the effects of receptor densities, local pathology, receptor-pathology interactions, and network propagation of pathological factors, combinations of patient-specific mechanisms co-vary with specific clinical symptoms. Sector colours represent the output pathological factor of each model, named in the inner (central) sectors. For each mechanism, the angle is proportional to the percentage of mechanistic-clinical covariance explained. The outer sector contains the specific mechanisms, while the middle sector is grouped by receptor families and the inner sector by target biological factor.

Mapping receptor influence in PD

Finally, we inferred the degree of receptor influence on multi-modal PD neurodegeneration at different brain regions, by identifying brain regions where the inclusion of a specific receptor predictor consistently improves the explanation of a particular type of neuropathology across all subjects. For each receptor, we fit individualized, single receptor-enriched models, and compared their ability to explain the accumulation of pathology at each brain region with restricted, neuroimaging-only models (see Methods: Regional influence). At each brain region, we studentized residuals across all patients, with each residual representing the unexplained pathology in a region at a given imaging visit. Then, for all regions, we computed the Wilcoxon rank sum statistics of the population residuals from the two models, and repeated the model-fitting procedure with 1000 randomly shuffled receptor maps to obtain a null distribution of Wilcoxon statistics. We used this permutation test to filter brain regions with significant residual improvements ($P<0.05$) over the null distributions. These maps do not represent the regions with the highest pathological severity, but rather those where longitudinal alterations are significantly better explained by the inclusion of a particular receptor distribution. In Figure 5.7, we summarize the receptor influence maps for the top 4 receptor-pathology pathways (Fig. 5.3a): $5HT_2$ and M_2 on microstructural alterations (MD), $\alpha_4\beta_2$ on gray matter atrophy (GM), and kainate on dendrite density (t1/t2). Receptor influence maps for all biological factors are presented in Supplementary Figures S1-S6.

Among other regions, the $5HT_2$ receptor most prominently influences microstructure (MD) in the anterior and medial thalamus, left posterior cingulate region (Brodmann area 31), anterior prefrontal cortex, left primarily motor cortex, right premotor cortex and supplementary motor area (Brodmann area 6). The muscarinic M2 receptor influences microstructural

alterations in the somatosensory cortex, left distal visual area V3d, right primary motor cortex, left hippocampus (CA), right primary somatosensory cortex (Brodmann area 2), lateral prefrontal cortex (Brodmann areas 46 - left and 47 - right), and entorhinal cortex (Brodmann areas 36-right and 37-left). The nicotinic $\alpha_4\beta_2$ receptor influences gray matter atrophy in the (left and right) thalamus, primary somatosensory cortex (Brodmann area 2), right temporal inferior parietal area, left caudate nucleus and entorhinal cortex (left Brodmann region 22). Kainate influences dendrite density in a broad set of regions, focused on the thalamus, visual areas (V1, V2 and the ventral parts of V3 and V4 in the right hemisphere, and V1 and ventral V4 in the left hemisphere), and prefrontal areas.

Across biological factors, glutamatergic receptors contribute significantly to explaining neurodegeneration in fronto-temporal regions (Supplementary Fig. S1). Particularly, both AMPA and kainate receptors contribute strongly to most factors (except for dopamine transporter loss) in frontal regions. The influences of $GABA_A$ receptors, $GABA_B$ receptors and the benzodiazepine binding site (Bz site) generally follow their distribution (Supplementary Fig. S2), peaking at visual, visual-parietal and fronto-temporal areas, respectively. Notably, dendrite loss is most pronounced at subcortical and fronto-temporal regions for all GABAeric receptors.

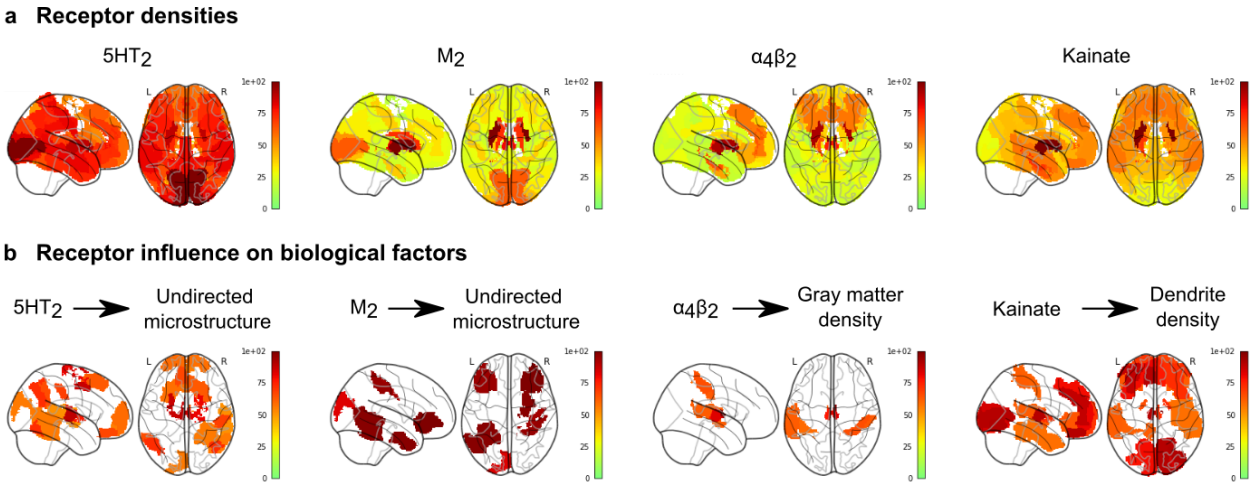

Figure 5.7. ***Model-derived maps of receptor influence on PD neurodegeneration****.*

We compared the (a) receptor densities and (b) influence maps. Influence maps show the brain regions where specific receptors are consistently informative to explaining the neuropathological changes across all PD subjects, and are re-scaled to arbitrary units for visualization. They represent the population-wide improvement in model residuals at each region due to the inclusion of receptor density maps and receptor-pathology interactions as model predictors for each PD patient. Receptor influences are calculated as the Wilcoxon rank-sum statistics of each model's residuals for a region, and the maps show only regions with significant z-scores ($P<0.05$) of Wilcoxon rank-sum statistics relative to the null distributions.

Discussion

The complex pathophysiology of PD involves multiple difficult-to-map neurotransmitter systems, and the selective vulnerability of various non-dopaminergic nuclei [24]. We apply a personalized, causal brain modeling approach that combines longitudinal neuroimaging data and clinical assessments with averaged spatial receptor templates, to infer the previously uncharacterized roles of receptor-mediated interactions in PD neurodegeneration and symptomatic heterogeneity.

In PD, dopaminergic neuroimaging is common [648], and some non-dopaminergic targets such as acetylcholinesterase have been characterized [649]. However, the expense of PET imaging and the lack of suitable in vivo radioligands have impeded the study of many other receptor alterations in a PD population. Our method circumvents this limitation by inferring the importance of receptor interactions in individualized models of brain reorganization. We note that the different receptor maps are not very correlated with each other (Supplementary Fig. S1-S6) and the "multi-receptor fingerprint" of each (cyto-architectonically defined) brain region is distinct, particularly differing across the functional hierarchy [253]. In vitro multi-receptor autoradiography of the caudate nucleus and midcingulate area 24 of progressive supranuclear palsy (PSP) patients showed differentiation of patients from age-matched controls, as well as diverging alterations in clinical subgroups of PSP [650]. In this related movement disorder, notable, previously unknown receptor associations (to kainate and adenosine type 1 receptors) were discovered, supporting the case for more thorough receptor mapping studies in neurodegenerative populations.

Lacking in vivo or in vitro receptor mapping data in PD patients, we attempted to use in silico modeling to infer regional susceptibility to neurodegeneration based on receptor

expression, and characterize the relationship between inter-individual variability in receptor-mediated neurodegeneration and symptomatic variability. Recent works in Alzheimer's disease (AD) have demonstrated that model parameters from personalized brain models can represent otherwise unobservable, latent mechanisms that relate to phenotype better than raw imaging data [651] [646] [652].

While we used autoradiography-derived templates of receptor density, receptor gene expression may be used as a proxy [653]. For example, the Allen Human Brain Atlas (http://human.brain-map.org) gene expression template has been used to identify transcriptomic pathways mediating neurodegeneration in AD [652]. However, several translational and trafficking steps separate gene expression and synaptically integrated receptors. Although receptor densities and gene expression are correlated for selected receptor subunit genes and across certain cytoarchitectonically-defined regions [654], this is not universally true [655]. Low correlations are also observed between gene expression and in vivo PET imaging of dopamine transporters [656]. Other works combining unimodal neuroimaging from disease cohorts with PET- and SPECT-derived healthy neurotransmitter receptor and transporter templates have uncovered the co-localization of specific neurotransmitter systems with PD resting state fMRI alterations [657], dyskinesia- and parkinsonism-associated atrophy in schizophrenia patients [658], gray matter atrophy in symptomatic FTD and its genetic subtypes [659], and functional alterations in behavioral variant FTD [660]. Furthermore, our averaged autoradiography-derived receptor templates are correlated with neurobiological processes such as drug-induced cerebral blood flow changes [661]. Additionally, in vitro autoradiography allows access to a broader class of receptors (without in vivo ligands) at a sub-millimeter resolution (as low as 0.3mm slice width per receptor [253]) compared to PET with its theoretical bound of ~2mm spatial resolution [662].

Future work will extend the presented results with voxel-scale whole brain receptor maps rather than macroscopically averaged values.

We incorporated several neuroimaging-derived measures sensitive to PD progression [663], from structural MRI-based gray matter density (GM) and dendrite density (t1/t2 ratio), diffusion-based measures of microstructural integrity (MD and FA) [664], functional neuronal activity (fALFF) and presynaptic dopamine transporter availability (DAT-SPECT). Resting-state fMRI-derived metrics such as fALFF can distinguish PD patients from controls [220], with fALFF being able to explain up to 25% of variability in MDS-UPDRS scores [665]. While initially proposed as a quantitative measure of demyelination from routine MRI scans, t1/t2 ratio has since been demonstrated to have a stronger correlation with dendritic density [184] [185], particularly relevant to synaptic integrity and receptor activity. Furthermore, our flexible modeling approach can be extended to incorporate other relevant modalities.

Although receptor maps were averaged from neurologically healthy aged brains, earlier work has demonstrated their utility in other cohorts, namely healthy aged subjects, mildly cognitively impaired subjects, and AD patients from the Alzheimer's disease Neuroimaging Initiative (ADNI) [646]. Extending this validation to the PPMI cohort, we note an approximately 42.3% improvement in the explanation of neuropathology accumulation in receptor-enriched models. These improvements are statistically significant for well over 90% of subjects ($P<0.05$ in both F-tests and permutation tests; Fig. 5.2c, d) for all biological factors with the exception of undirected microstructural damage (MD). We used a non-parametric permutation to generate null receptor distributions, which does not consider any spatial autocorrelation in the receptor maps [666]. The lack of voxel-scale receptor maps and the inclusion of subcortical regions in our

parcellation would preclude both cortical surface rotation-based methods as well as parametrized models requiring autocorrelation information in other, more typical statistical analyses.

For a third of all subjects, the improvement in model fit of undirected microstructure was not significantly better than permuted null distributions of receptors. While diffusion MRI can be sensitive to aspects of gray matter microstructure [667] [668], it is less accurate than in white matter due to the heterogeneity of tissues and their (lack of) organization [669]. Yet, despite the limitation of partial volume effects in gray matter ROIs [200], receptor-enriched models fit longitudinal alterations to microstructure reasonably well (average $r^2 = 0.70$ for undirected MD and $r^2 = 0.74$ for directed FA; Fig. 5.2).

Differential neurotransmitter and receptor expression may underpin the selective vulnerability of several neuronal populations, from the dopaminergic substantia nigra to the adrenergic locus coeruleus and serotonergic raphe nuclei, and their cortical projections [26]. Furthermore, PD neurodegeneration may alter both the spatial distributions as well as functional interactions of specific dopaminergic and non-dopaminergic receptors, with symptomatic consequences [124]. In our mechanistic modeling framework, each model weight is interpretable as the importance of specific neurobiological mechanism. Receptors contribute to neurodegeneration in re-MCM either as i) direct effects representing regional susceptibility to neurodegeneration based on receptor expression, or ii) receptor-mediated interactions involving a source and target biological factor. Additionally, biological factors have i) local effects on themselves and other factors, and ii) intra-factor network effects due to propagation of pathology along the structural connectome. Lacking inter-subject variability in receptor data, our model compensates by assigning weights differently across subjects. Consistent trends in model weights

reflect the importance of the corresponding neurobiological mechanism across the PD population, while co-variability with symptoms suggests clinical relevance.

First, we identified specific mechanisms affecting neurodegeneration across the PD cohort (Fig. 5.3). We observed a complex network of interactions between biological factors, with distinct receptor profiles affecting each factor. The large contributions of receptor-mediated inter-factor interactions (Fig. 5.3a) supports the multi-system view of PD. Fewer receptors are statistically stable predictors of longitudinal changes to functional activity (fALFF), directed microstructural damage (FA) and dopaminergic neurotransmission (SPECT), while gray matter atrophy (GM), dendrite density (t1/t2 ratio) and undirected microstructural changes (MD) show greater influence from a more diverse set of receptors.

Notably, the D_1 receptor map is not a stable predictor of DAT alterations. While presynaptic DAT density and postsynaptic dopaminergic receptor distributions are strongly related under normal conditions, they may be affected differently by disorders. For example, while D_2 receptor availability is reduced in alcoholism, DAT availability is preserved [670]. In PD, DAT-SPECT and receptor PET imaging have distinct clinical interpretations [671], and increased dopamine turnover early at symptom onset has implicated presynaptic mechanisms at this disease stage [672]. Furthermore, healthy aged D_1 receptor expression is relatively uninformative as it is comparatively homogeneous across cortical regions (Supplementary Fig. S6) and likely redundant to the model in the presence of individualized DAT imaging. On the other hand, DAT density also peaks in striatal regions, and DAT-SPECT is not able to resolve cortical radiotracer uptake as well as DAT-PET [673]. SPECT is currently more prevalent clinically for DAT imaging, and was thus the modality used in a large, multi-center study such as

PPMI. Nevertheless, it must be noted that DAT-SPECT is limited in its ability to resolve cortical alterations, and this is likely reflected in its under-emphasis in our results.

Network degeneration hypotheses of PD pathogenesis implicate various mechanisms from the propagation of neurotoxic alpha-synuclein [674] to the structural and functional neurodegeneration following striatal denervation [675]. We note that propagation is only a small contributor to the accumulation of pathology, and is dwarfed by local effects in our models (Fig. 5.3a). These findings may potentially reflect distinct disease phases. Our cohort was composed entirely of PD patients, for whom propagative, disease seeding processes may have already occurred, and neurodegeneration may now be driven by local effects. Furthermore, white matter tractography may not completely capture the connectivity between our cyto- and receptor-architectonically defined regions. A more complete treatment may consider vascular connectivity as well [567] [561], which may also be a substrate for pathology propagation.

We find notable glutamatergic effects on multiple (micro-)structural factors (Supplementary Fig. S1): gray matter atrophy (NMDA), directed microstructural damage (AMPA and kainate), and dendrite density (kainate and NMDA). As NMDA and AMPA receptors are postsynaptic targets of glutamate, these mechanisms likely reflect the structural consequences of excitotoxicity and cell death [676]. On the other hand, kainate is believed to modulate synaptic transmission and plasticity [677], which may affect dendritic density. In our models, NMDA receptor influence is focused on occipital and temporal regions, AMPA influence is highest in frontal regions, and kainate influences mainly dendrite loss in both frontal and occipital regions. Among glutamatergic receptors, influence on microstructure of the motor cortex (MD, FA and t1/t2) is prominent, although it is more limited for atrophy or functional alterations.

The stable roles of GABAergic receptors (Fig. 5.3a) suggest their involvement via altered neuronal activity inhibition, interaction with the dopaminergic system, and potential regional vulnerability to microstructural degradation or dendrite loss. Inter-subject variability along the primary, mainly motor axis correlates with GABAergic mechanisms affecting microstructure (FA, MD and t1/t2) and functional activity. Furthermore, a magnetic resonance spectroscopy (MRS) study found reduced levels of GABA in the visual cortex of PD patients [678], consistent with the regions of maximal influence of $GABA_A$ and $GABA_B$ receptors in our model.

Due to the necessity for sufficient longitudinal and multi-modal scans, no healthy subjects met our inclusion criteria. As each individualized model is fit independently, we account for the confounding effects of healthy ageing on model-derived mechanisms by performing a multivariate correlation with 11 assessments representing various symptomatic domains, with age as a covariate. Presently, PD is defined primarily by clinical symptoms, and thus any combination of model mechanisms robustly correlated with multi-domain symptoms can be considered as contributing to the spectrum of PD rather than healthy (i.e. non-symptomatic) aging.

Various non-dopaminergic neurotransmitter systems have been associated with specific symptoms in PD, including cholinergic memory defects, adrenergic impairment of attention, and serotonin-driven depression [679] and visual hallucinations [680] [681]. Comparing model-derived receptor mechanisms and clinical assessments across PD patients, we observe two main axes of co-variability. The primary component represents motor/psychomotor symptoms associated prominently with GABAergic mechanisms, with secondary contributions from glutamatergic, cholinergic, and serotonergic systems (Supplementary Table S7). The secondary component is defined by visuospatial, memory and psychiatric symptoms, with the cholinergic

system being the dominant receptor family. Mechanisms affecting microstructure (FA and MD) are more prominent in the primary component, while those affecting gray matter density are greater in the secondary component. Nevertheless, receptor mechanisms affecting microstructure and dendrite density (t1/t2) contribute strongly to both axes.

The secondary component is consistent with the cholinergically-driven visuospatial aspect of the dual-syndrome hypothesis of PD [122]. Stable cholinergic mechanisms are also present for every biological factor except directed microstructure (FA), most notably the contributions to dendrite loss (t1/t2), undirected microstructural damage (MD) and gray matter atrophy (Fig. 5.3a). Specifically, we note prominent muscarinic M_2 and nicotinic $\alpha_4\beta_2$ receptor influences (on MD and GM, respectively) on the primary somatosensory cortex, a site of reduced activation in PD (Fig. 5.7) [682]. Our model suggests that nicotinic and muscarinic cholinergic systems strongly affect PD symptoms along specific pathways primarily involving dendritic density, atrophy, and degradation of microstructure (Fig. 5.6b). While typically associated with cognitive impairment and dementia in PD, cholinergic degeneration is also linked to depressive mood, apathy, olfaction, sleep disorder, and postural and gait disorder [683]. Epidemiological studies of smokers suggest a neuroprotective role for nicotinic receptors [684], which experience widespread decrease in PD [685]. The cholinergic and dopaminergic systems interact at biochemical, circuit and functional levels [679], tightly coupled by nicotinic receptors expressed on striatal dopaminergic neurons and acetylcholine [679] [686] modulate dopaminergic neurotransmission. An imbalance of cholinergic and dopaminergic neurotransmission may thus underlie PD cognitive dysfunction [679]. Our results suggest that cholinergic receptor distributions contribute to both motor and non-motor axes, albeit via distinct pathways (Fig. 5.6a, b).

We note the mild motor phenotype of the PD patients from PPMI included in this work (mean MDS-UPDRS Part III score, Supplementary Table S1). Potential low variability in these scores in combination with the poor cortical signal in DAT-SPECT may have under-emphasized the dopaminergic-motor axis of PD. Nevertheless, the dopaminergic relationship with motor symptoms is reproduced in the primary, mainly motor component, with DAT-SPECT appearing as a target imaging modality. In addition to the classical dopaminergic-motor axis, our work presents a multi-modal perspective of PD, associating multivariate combinations of receptor distributions with macroscopic imaging-derived pathological alterations, and motor and non-motor symptoms.

In addition to mediating inter-factor interactions, dysfunctional interactions between receptors may also be involved in neurodegeneration. Neurotransmitter release is regulated by presynaptic auto- and hetero-receptors [687], which in PD is potentially impaired in the dopaminergic system [688] and in GABAergic inhibition of the motor cortex [689]. Where possible, concurrent receptor or transporter imaging in a PD cohort would help clarify the role of neurotransmission balance in neurodegeneration.

We attempted to cover a broad variety of (particularly structural) disease-sensitive neuroimaging modalities. Yet, PD neurodegeneration is complex and likely also involves changes to surface morphology [690] [691], such as gyrification. However, to include the basal ganglia and thalamus in our model using the same set of features, we did not include surface-based measures.

Despite the prevalence of PD, the causes of this neurodegenerative condition remain unknown, and treatment is limited to symptomatic therapy complicated by individual variability in clinical presentation, side effects and treatment response [692]. Our work sheds light on the

complex, especially non-dopaminergic neurotransmitter receptor-mediated mechanisms underlying brain reorganization and symptomatic variability in PD. As longitudinal data collection progresses in large cohorts, model-derived mechanisms may help differentiate mechanisms distinct to PD and its (genetic or clinical) subtypes, Parkinson-plus syndromes, other neurodegenerative diseases, and healthy ageing. Since neurotransmitter receptors are clinically efficacious drug targets [693], future work will explore the use of our personalized modeling approach to design personalized receptor-based therapy.

Methods

Ethics statement

This work has been conducted in accordance with ethical guidelines and regulations. Neuroimaging and clinical data in this study was acquired through the multi-center Parkinson's Progression Markers Initiative (PPMI; ppmi-info.org). Following good clinical practices and in accordance with the Declaration of Helsinki guidelines, study subjects and/or authorized representatives gave written informed consent at the time of enrollment for sample collection and completed questionnaires approved by each participating site Institutional Review Board (IRB). The authors obtained approval from the PPMI for data use and publication, see documents https://www.ppmi-info.org/documents/ppmi-data-use-agreement.pdf and https://www.ppmi-info.org/documents/ppmi-publication-policy.pdf, respectively.

Data description and processing

Study participants

This study used longitudinal data from N=71 participants from the PPMI from 12 international sites, with a clinical diagnosis of PD. Demographic information is summarized in Supplementary Table S1. The inclusion criterion was the presence of at least 3 different imaging modalities (i.e. structural MRI, resting functional MRI, diffusion MRI and/or dopamine SPECT) over at least 3 visits at the time of our analysis.

Structural MRI acquisition/processing

Brain structural T1- and T2-weighted 3D images were acquired for all N=71 subjects. A detailed description of acquisition details can be found from the PPMI procedures manuals at http://www.ppmi-info.org/. T1- and T2-weighted images from 3T scanners were acquired as a 3D sequence with a slice thickness of 1.5 mm or less, under three different views: axial, sagittal and coronal. All images underwent non-uniformity correction using the N3 algorithm [571]. Next, they were segmented into gray matter probabilistic maps using SPM12 (version 12, https://fil.ion.ucl.ac.uk/spm). Gray matter segmentations were standardized to MNI space [572] using the DARTEL tool [573]. Each map was modulated to preserve the total amount of signal/tissue. Mean gray matter density [573] values were calculated for the regions described in Methods: Data description and processing: Receptor densities and brain parcellation.

Resting fMRI acquisition/processing

Resting-state functional images were obtained using an echo-planar imaging sequence on 3T MRI scanners for N=71 subjects. For a detailed description of acquisition protocols, please see http://www.ppmi-info.org. Acquisition parameters were: 140 time points, repetition time

(TR)=2400 ms, echo time (TE)=25 ms, flip angle=80°, number of slices=40, slice thickness=3.3 mm, in plane resolution=3.3 mm and in plane matrix=68×66. Pre-processing steps included: 1) motion correction, 2) slice timing correction, 3) alignment to the structural T1 image, and 4) spatial normalization to MNI space using the registration parameters obtained for the structural T1 image with the nearest acquisition date, and 5) signal filtering to keep only low frequency fluctuations (0.01–0.08 Hz) [575]. For each brain region, our model requires a local (i.e., intra-regional, non-network) measure of functional activity, to maintain mechanistic interpretability and to prevent data leakage of network information into local model terms (described further in Receptor-Enriched Multifactorial Causal Model). Due to its high correlation with glucose metabolism [694] and disease progression in PD [220] , we calculated regional fractional amplitude of low-frequency fluctuation (fALFF) [578] as a measure of functional integrity.

Diffusion MRI acquisition/processing

Diffusion MRI (dMRI) images were acquired using standardized protocol on 3T MRI machines from 32 different international sites. Diffusion-weighted images were acquired along 64 uniformly distributed directions using a b-value of 1000 s/mm^2 and a single b = 0 image. Single shot echo-planar imaging (EPI) sequence was used (116 × 116 matrix, 2 mm isotropic resolution, TR/TE 900/88 ms, and twofold acceleration). An anatomical T1-weighted 1 mm^3 MPRAGE image was also acquired. Each patient underwent two baseline acquisitions and a further two one year later. More information on the dMRI acquisition and processing can be found online at http://www.ppmi-info.org/. Preprocessing steps included: 1) motion and eddy current correction [695], 2) EPI distortion correction, 2) alignment of the T1-weighted image to the b0 image based on mutual information, 3) calculation of the deformation field between the diffusion and T1-weighted images, 4) calculation of the voxelwise diffusion tensors, 5)

alignment to the structural T1 image, and 6) spatial normalization to MNI space [572] using the registration parameters obtained for the structural T1 image with the nearest acquisition date, and 6) calculation of mean values of summary metrics (FA and MD) for each considered brain region.

Dopamine SPECT acquisition/processing

A 111-185 MBq (3-5 mCi) bolus injection of I-123 FB-CIT was administered to each participant (N=71), and the SPECT scan was performed 4 hours post-injection. Raw projection data was acquired as a 128x128 matrix and the SPECT image was reconstructed. Attenuation correction and Gaussian blurring with a 3D 6mm filter were applied. The reconstructed and corrected SPECT images were normalized and registered to MNI space [572], and average values were calculated for all considered regions of interest.

Receptor densities and brain parcellation

In-vitro quantitative receptor autoradiography was applied to measure the densities of 15 receptors in 57 cytoarchitectonically defined cortical areas spread throughout the brain [579]. These receptors span major neurotransmitter systems and show significant regional variability across the brain. Brains were obtained through the body donor programme of the University of Düsseldorf. Donors (three male and one female; between 67 and 77 years of age) had no history of neurological or psychiatric diseases, or long-term drug treatments. Causes of death were non-neurological in each case. Each hemisphere was sliced into 3 cm slabs, shock frozen at -40C, and stored at -80C.

Receptors for the neurotransmitters glutamate (AMPA, NMDA, kainate), GABA ($GABA_A$ $GABA_A$-associated benzodiazepine binding sites, $GABA_B$), acetylcholine (muscarinic M_1, M_2, M_3, nicotinic $\alpha_4\beta_2$), noradrenaline (α_1, α_2), serotonin ($5\text{-}HT_{1A}$, $5\text{-}HT_2$), and dopamine

(D_1) were labeled according to previously published binding protocols consisting of pre-incubation, main incubation and rinsing steps [579]. The ligands used are summarized in Supplementary Table S3. Receptor densities were quantified by densitometric analysis of the ensuing autoradiographs, and areas were identified by cytoarchitectonic analysis in sections neigbouring those processed for receptor autoradiography, and which had been used for the visualization of cell bodies [580].

A brain parcellation was then defined with the aid of the Anatomy Toolbox [581] using 57 regions of interest for which receptor densities were available [253]. This parcellation was based on areas identified by cortical cytoarchitecture, as well as other cyto- and receptor-architectonically defined regions with receptor measurements (regions are summarized in Supplementary Table S4). These 57 regions were mirrored across left and right hemispheres for a total of 114 brain regions in our parcellation. For each receptor, regional densities were normalized using the mean and standard deviation across all brain regions.

The structural T1 images of the Jülich [581], Brodmann [582], AAL3 [696] and DISTAL [697] brain parcellations were registered to the MNI ICBM152 T1 template using the FSL (version 6.0) FLIRT affine registration tool [698], and the obtained transformations were used to project the corresponding parcellations to the MNI ICBM152 space (using nearest neighbor interpolation to conserve original parcellation values). In the MNI ICBM152 space, voxels corresponding to the cytoarchitectonically-defined regions from [253] were identified from the regions in the Anatomy Toolbox, with the remaining Brodmann regions filled in using the Brodmann brain atlas. Supplementary Table S4 summarizes the ROI maps used to create the Brain atlas for regions with receptor data. The resulting parcellation of 114 brain regions in the common template space was then quality controlled, and small regions under 50 voxels were

excluded. The resulting atlas with 155 bilateral brain regions (95 of which had receptor data) was used to extract whole-brain multi-modal neuroimaging data and estimate the diffusion-based connectivity matrix, as described in Methods: Multimodal neuroimaging data fusion and Methods: Anatomical connectivity estimation.

Anatomical connectivity estimation

The connectivity matrix was constructed using DSI Studio (March 8, 2019 build; http://dsi-studio.labsolver.org). A group average template was constructed from a total of 1065 subjects [584]. A multi-shell diffusion scheme was used, and the b-values were 990, 1985 and 2980 s/mm^2. The number of diffusion sampling directions were 90, 90, and 90, respectively. The in-plane resolution was 1.25 mm. The slice thickness was 1.25 mm. The diffusion data were reconstructed in the MNI space using q-space diffeomorphic reconstruction [585] to obtain the spin distribution function [586]. A diffusion sampling length ratio of 2.5 was used, and the output resolution was 1 mm. The restricted diffusion was quantified using restricted diffusion imaging [587]. A deterministic fiber tracking algorithm [588] was used. A seeding region was placed at whole brain. The QA threshold was 0.159581. The angular threshold was randomly selected from 15 degrees to 90 degrees. The step size was randomly selected from 0.5 voxel to 1.5 voxels. The fiber trajectories were smoothed by averaging the propagation direction with a percentage of the previous direction. The percentage was randomly selected from 0% to 95%. Tracks with length shorter than 30 or longer than 300 mm were discarded. A total of 100000 tracts were calculated. A custom brain atlas based on cytoarchitectonic regions with neurotransmitter receptor data [253] was used as the brain parcellation, as described in Methods: Data description and processing: Receptor densities and brain parcellation, and the connectivity matrix was calculated by using count of the connecting tracks.

Multimodal neuroimaging data fusion

After pre-processing PPMI neuroimaging data for all 6 modalities, data harmonization was performed using ComBat (commit 91f8bf3, https://github.com/Jfortin1/ComBatHarmonization) [699]. Each site used the same scanner for all subjects, and our harmonization procedure corrected for batch effects due to sites while preserving variance due to clinical diagnosis, age, education level, sex and (left or right) handedness. After extracting harmonized neuroimaging data for the cytoarchitectonically defined atlas described in Methods: Data description and processing: Receptor densities and brain parcellation, subjects lacking sufficient longitudinal or multimodal data were discarded. The disqualification criteria were i) fewer than 4 imaging modalities with data, or ii) fewer than 3 longitudinal samples for all modalities. For the remaining subjects, missing neuroimaging modalities (primarily FA, MD and t1/t2 ratios) at each visit were imputed using trimmed scores regression. Finally, a total of N=71 subjects were left with all 6 neuroimaging modalities with an average of 3.59 (± 0.50) time points. We used the mean and variance of each neuroimaging modality across all regions to calculate z-scores of neuroimaging data for all subjects. Please see Supplementary Table S1 for demographic characteristics.

Clinical scores

We used multiple composite scores derived from the PPMI clinical (motor, non-motor, psychiatric, cognitive, etc.) testing battery, namely the Benton Judgment of Line Orientation Test (BJLOT [700]), Geriatric Depression Scale (GDS [701]), Hopkins Verbal Learning Test (HVLT [702]), Letter Number Sequencing (LNS [703]), Movement Disorders Society – Unified Parkinson's Disease Rating Scale (MDS-UPDRS [704]) Parts 1 (non-motor aspects of daily

living; NP1), 2 (motor aspects of daily living; NP2), and 3 (motor exam; NP3), the Montreal Cognitive Assessment (MoCA [705]), semantic fluency (SF), State-Trait Anxiety Inventory for Adults (STAIAD [706]), and Symbol Digit Modalities (SDM [707]) tests. Protocols for deriving each score are described in the respective PPMI protocols documentation. We calculated symptomatic decline as the rate of change (linear slope) of the 11 clinical scores with respect to examination date. Average numbers of longitudinal evaluations per clinical score are summarized in Supplementary Table S2.

Receptor-Enriched Multifactorial Causal Model (re-MCM)

Multifactorial causal modeling is a generalized framework [567] [646] that treats the brain as a dynamical system of ROIs characterized by multiple interacting neuroimaging-quantified biological factors. Pathology may develop over time in each factor, affecting other factors locally and propagating to neigbouring regions via anatomical connections. We introduce the receptor-enriched multifactorial causal model (re-MCM), in which the local densities of various neurotransmitter receptors mediate interactions between biological factors at each brain region.

In this work, the biological factors are gray matter density, neuronal activity, presynaptic dopamine, demyelination/dendritic density and two measures of white matter integrity, derived from structural T1 MRI, resting state functional MRI (rs-fMRI), DAT-SPECT, T1/T2 ratio, FA and MD, respectively. For any given subject and at a particular brain region i, the level of pathology of each biological factor m is represented by a single variable $S_{m,i}$, calculated as the deviation from the neuroimaging signal at the baseline visit. The temporal evolution of pathology $S_{m,i}$ in modality m at brain region i is given by following differential equation:

$$\frac{dS_{m,i}(t)}{dt} = \underbrace{f(\mathbf{S}_{*,i}(t), \mathbf{R_i})}_{\text{Local Effects}} + \underbrace{g(\mathbf{S}_{m,*}(t), \mathbf{C}_{i\leftrightarrow *})}_{\text{Inter-region Propagation}}.$$

(1)

The functions f and g govern the global biological factor dynamics that are consistent across all brain regions. The local component $f\left(S_{,i}(t), R_{,i}\right)$ is the cumulative effect of all biological factors on factor m within region i mediated by $\boldsymbol{R}_i$, composed of local densities $r_{k,i}$ of a receptor k at a region i. The propagation term g represents the net spreading of pathology in factor m along anatomical connections $C_{i\leftrightarrow *}$ of the region i. Since the inter-visit interval of approximately 6 months is significantly shorter than the temporal scale of neurodegeneration, we assume a locally linear, time-invariant dynamical system:

$$\frac{dS_i^m(t)}{dt} = \sum_{n=1}^{N_{\text{fac}}} \alpha^{n\to m} S_{n,i}(t) + \sum_{k=1}^{N_{\text{rec}}} \alpha_k^m r_{k,i} + \alpha_{\text{prop}}^m \sum_{j=1, j\neq i}^{N_{\text{ROI}}} \left[C_{j\to i} S_{m,j}(t) - C_{i\to j} S_{m,i}(t)\right],$$

(2)

where $C_{i\to j}$ is the directed anatomical connectivity from region i to j, and $\frac{dS_{m,i}(t)}{dt}$ the local rate of change of neuroimaging data for successive longitudinal samples at times t' and t:

$$\frac{dS_{m,i}(t)}{dt} = \frac{S_{m,i}(t) - S_{m,i}(t\prime)}{t - t\prime}.$$

(3)

Local effects include i) direct factor-factor effects, ii) interaction terms mediated by $N_{\text{rec}} = 15$ receptor types, and iii) direct receptor effects on the biological factor rate of change $\frac{dS_{m,i}}{dt}$ (the second term in Equation 2). The first term in Equation 2 is expanded as:

$$\alpha^{n\to m} = \underbrace{\alpha_0^{n\to m}}_{\text{Direct Factor-Factor Term}} + \underbrace{\sum_k^{N_{\text{rec}}} \alpha_k^{n\to m} r_i^k}_{\text{Interaction Term}}.$$

(4)

The propagation term assumes symmetric connectivity $C_{j\leftrightarrow i}$ between regions i and j, using a template connectivity matrix for all subjects, as described in Anatomical connectivity estimation, so we define the propagation component as:

$$p_{m,i}(t) = \sum_{j=1,j\neq i}^{N_{\text{ROI}}} C_{j\leftrightarrow i}\left[S_{m,j}(t) - S_{m,i}(t)\right].$$

(5)

Thus, for each subject, the evolution of pathology in each biological factor m at region i is described by:

$$\frac{dS_{m,i}(t)}{dt} = \sum_{n=1}^{N_{\text{fac}}}\left(\alpha_0^{n\to m} + \sum_k^{N_{\text{rec}}} \alpha_k^{n\to m}\, r_{k,j}\right) S_{n,i}(t) + \sum_{k=1}^{N_{\text{rec}}} \alpha_k^m\, r_{k,i} + \alpha_{\text{prop}}^m p_{m,i}(t).$$

(6)

Each model contains a set of $N_{\text{params}} = N_{\text{fac}} \times (1 + N_{\text{rec}}) + N_{\text{rec}} + 1 = 113$ parameters $\{\alpha\}_x^m$ for subject x and factor m (or 678 total parameters per subject), each with a distinct neurobiological interpretation (e.g. the effect of reduced white matter integrity on gray matter atrophy mediated by glutamatergic receptor density). We perform linear regression, using the terms in Equation 6 as predictors with longitudinal PPMI neuroimaging samples $S_{m,i}(t)$ and receptor maps R, to fit parameters $\{\alpha\}_x^m$ for each subject x and modality m. Separate regression models were built for i) each of the N=71 qualifying subjects, and ii) each of the 6 neuroimaging factors. These subjects were drawn from the PPMI dataset with at least 3 recorded neuroimaging modalities, and at least 3 longitudinal samples for at least one modality.

We then calculate the coefficient of determination (R^2 for each model to evaluate model fit, summarized in Figure 5.2. With the true neuroimaging-derived data $y_{m,i,t} = \frac{dS_{m,i}(t)}{dt}$, subject-wise mean imaging data $< \mathrm{y}_m >$ for modality m across all brain regions and longitudinal samples, and model predictions $\hat{y}_{m,i,t}$, the coefficient of determination is

$$R^2 = 1 - \frac{\sum_{i,t}(y_{m,i,t} - \hat{y}_{m,i,t})^2}{\sum_{i,t}(y_{m,i,t} - <y_m>)^2} \quad .$$

(7)

Model fit

For each subject and neuroimaging modality, we evaluated the quality of model fit by calculating the coefficient of determination (R^2). Secondly, to evaluate the improvement in model fit due to receptor and receptor-mediated interaction terms while accounting for the difference in model size for each subject, we used F-tests ($p<0.05$) to compare the model fit of the full, receptor-neuroimaging interaction models (113 parameters per modality) with restricted, neuroimaging-only (8 parameters per modality) models.

Finally, we evaluated the significance of the improvement in model fit (R^2) due to actual receptor distributions with a permutation test using 1000 iterations of randomly permuted receptor maps (with receptor densities shuffled across regions independently for each receptor type), calculating the p-value of the model R^2 with the true receptor data compared to the null distribution.

Covariance of biological mechanisms with clinical symptoms

To identify multivariate links between receptor-mediated biological mechanisms and to clinical symptoms in PD, we performed a data-driven partial least squares (PLS) regression analysis. Using singular value decomposition (SVD) to factorize the population covariance matrix between re-MCM parameters and clinical assessments (summarized in Methods: Clinical scores) to its eigenvectors, we identify multivariate axes of co-varying features. Different axes represent orthogonal disease processes affecting symptom severity. Permutation tests and

bootstrapping ensure the statistical significance of the axes and the stability of identified mechanisms and symptoms, respectively. The algorithm is summarized as follows:

We performed SVD on the cross-covariance matrix between all 678 re-MCM parameters and rates of clinical decline for N=71 PD patients, adjusted for covariates (baseline age, education, and sex). SVD simultaneously reduces the dimensionality of features, and ranks them by their contribution to each axis. The cross-covariance matrix $C = XY'$ of the z-scores of re-MCM parameters X and the z-scores of the clinical decline rates Y is decomposed as

$$C = USV' \quad (8)$$

where U and V are orthonormal matrices of spatial loadings for the parameters and clinical scores, respectively, and S is a diagonal matrix of singular values $\{s_1, \dots, s_7\}$.

We then performed permutation tests by shuffling the mapping between subjects' re-MCM parameters and clinical scores, and repeating Step 1 for 1000 iterations, to evaluate the significance of latent components. We performed a Procrustes transformation to align the axes of singular components in order to compare components from permuted iterations. We retained only those significant ($p<0.05$ with respect to the permuted distribution) singular components.

To discard non-stable re-MCM parameters and clinical assessments in each axis, we performed 1000 iterations of bootstrapping on the parameters X and clinical scores Y. To compare permuted iterations, we performed a Procrustes transformation to align the axes of singular components. We discarded the parameters with non-stable 95% confidence intervals.

For the remaining stable re-MCM parameters and clinical scores, and significant latent components, we computed the variance explained per parameter j along each axis i:

$$r_{i,j}^2 = \underbrace{\frac{U_{i,j}^2}{\sum_j U_{i,j}^2}}_{\substack{\text{Parameter} \\ \text{contribution}}} \quad (9)$$

Regional influence

To infer the spatial patterns of receptor involvement in neurodegeneration, we examined the improvement in neuroimaging models due to the inclusion of each receptor map. For each biological factor m, receptor k and brain region i, we fit a restricted, single-receptor version of the model

$$\frac{dS_{i,k}^m(t)}{dt} = \sum_{n=1}^{N_{fac}} \left(\alpha_0^{n\to m} + \alpha_k^{n\to m} r_{k,j}\right) S_{n,i}(t) + \alpha_k^m r_{k,i} + \alpha_{\text{prop}}^m \sum_{j=1, j\neq i}^{N_{ROI}} \left[C_{j\to i} S_{m,j}(t) - C_{i\to j} S_{m,i}(t)\right], (10)$$

where the longitudinal rate of change of each factor is predicted by its network propagation, direct factor effects, the local density of a single receptor k, and factor interactions with the density of only receptor k. We compare this model with a restricted, neuroimaging-only model excluding receptor density and interactions:

$$\frac{dS_{i,k}^m(t)}{dt} = \sum_{n=1}^{N_{fac}} \alpha^{n\to m} S_{n,i}(t) + \alpha_{\text{prop}}^m \sum_{j=1, j\neq i}^{N_{ROI}} \left[C_{j\to i} S_{m,j}(t) - C_{i\to j} S_{m,i}(t)\right]. (11)$$

To generate brain maps representing receptor influence on neuroimaging changes,

for each subject, we fit the single receptor and neuroimaging-only models for all biological factors and receptors, and studentize the residuals across regions and time points,

we combine the studentized residuals corresponding to each region across subjects and time points, and calculate the Wilcoxon rank sum statistic $w_{i,k}^m$ between studentized residuals of the two models,

we compute a null distribution of the Wilcoxon statistic by repeating Steps 1-2 with 1000 randomly permuted receptor maps per imaging modality and receptor,

to estimate the significance of the Wilcoxon maps of each receptor across all 6 imaging modalities, we calculate the z-scores $z_{i,k}^{m}$ of the Wilcoxon statistic $w_{i,k}^{m}$ to its null distribution.

Data availability

The three datasets used in this study are publicly available. The PPMI database (neuroimaging and clinical evaluations; https://www.ppmi-info.org/) is available to access after completing a data use agreement and submitting an online application (https://www.ppmi-info.org/access-data-specimens/download-data). The HCP database (HCP-1065 [584]; tractography template for connectivity estimation; http://www.humanconnectomeproject.org/) is available at https://brain.labsolver.org/hcp_template.html, and receptor autoradiography data published in [253] is available at https://github.com/AlGoulas/receptor_principles.

Code availability

The PLS-SVD code is available at https://github.com/neuropm-lab/svd_pls. The re-MCM method (implemented in Matlab 2019b) will be incorporated as a part of our open-access, user-friendly software (https://www.neuropm-lab.com/neuropm-box.html) [593] .

Acknowledgements

The authors would like to acknowledge the integral role of the late Prof. Dr. Karl Zilles in collecting the receptor autoradiography data. This research was undertaken thanks in part to funding from: the Parkinson's Canada graduate training award to AFK, the *Canada First Research Excellence Fund*, awarded to McGill University for the *Healthy Brains for Healthy Lives Initiative*, the Canada Research Chair tier-2, *Fonds de la recherche en santé du Québec* (FRQS) Junior 1 Scholarship, Natural Sciences and Engineering Research Council of Canada (NSERC) Discovery Grant, and Weston Brain Institute awards to YIM, the *Brain Canada Foundation* and *Health Canada* support to the McConnell Brain Imaging Center at the Montreal Neurological Institute, and the *European Union's Horizon 2020 Framework Programme for Research and Innovation* under the Specific Grant Agreements 785907 (Human Brain Project SGA2) and 945539 (Human Brain Project SGA3) awarded to NPG and KZ. Multimodal imaging and clinical data collection and sharing for this project was funded by PPMI (www.ppmi-info.org/data). A public-private partnership, PPMI is funded by the Michael J. Fox Foundation for Parkinson's Research and funding partners, including AbbVie, Allergan, Amathus Therapeutics, Avid Radiopharmaceuticals, Biogen, BioLegend, Bristol Myers Squibb, Celgene, Denali Therapeutics, GE Healthcare, Genentech, GlaxoSmithKline plc., Golub Capital, Handl Therapeutics, Insitro, Janssen Neuroscience, Eli Lilly and Company, Lundbeck, Merck Sharp &

Dohme Corp., Meso Scale Discovery, Neurocrine Biosciences, Pfizer Inc., Piramal Group, Prevail Therapeutics, Roche, Sanofi Genzyme, Servier Laboratories, Takeda Pharmaceutical Company Limited, Teva Pharmaceutical Industries Ltd., UCB, Verily Life Sciences, and Voyager Therapeutics Inc. The full list of funding partners is available at www.ppmi-info.org/about-ppmi/who-we-are/study-sponsors.

Author contributions

A.F.K. helped conceptualize the project, preprocessed the data, implemented the model, conducted the analysis, and wrote the manuscript. Q.A. and S.-J.L. helped preprocess the data. T.R.B. and F.C. contributed statistical methods. Y.Z. helped preprocess the data. N.P.-G. collected the receptor data. Y.I.-M. conceptualized and supervised the project. All authors helped interpret the results and revise the manuscript.

Competing Interests

The authors declare no competing interest.

Supplementary material

Category	PD subjects
Mean MDS-UPDRS Part III score	18.8 ± 8.7
Female patients	20 (28.2%)
Mean age (years)	59.6 ± 9.8
Mean education (years)	15.5 ± 2.8
Non-white patients	0
Right handed patients	64 (90.1%)

Supplementary Table 5.1. Summary of demographic data for N=71 PD patients.

Category	Number of evaluations
BJLOT	7.62 ± 1.13
GDS	8.27 ± 1.09
HVLT	7.65 ± 1.14
LNS	7.63 ± 1.12
LXF	0.79 ± 0.56
NP1	15.0 ± 1.9
NP2	15.0 ± 1.9
NP3	19.5 ± 4.0
NP4	9.94 ± 3.0
MoCA	7.63 ± 1.12
SF	7.62 ± 1.11
STAIAD	8.28 ± 1.08
SDM	7.66 ± 1.15

Supplementary Table 5.2. Mean and standard deviation of the number of clinical evaluations per subject.

Neurotransmitter	Receptor	Ligand	Type
Glutamate	AMPA	[^{3}H]-AMPA	Agonist
	NMDA	[^{3}H]-MK-801	Antagonist
	Kainate	[^{3}H]-Kainate	Agonist
GABA	$GABA_A$	[^{3}H]-Muscimol	Agonist
	$GABA_B$	[^{3}H]-CGP 54626	Antagonist
	$GABA_A$-associated benzodiazepine binding site ($GABA_A$/BZ)	[^{3}H]-Flumazenil	Antagonist
Acetylcholine	M_1	[^{3}H]-Pirenzepine	Antagonist
	M_2	[^{3}H]-Oxotremorine-M	Agonist
	M_3	[^{3}H]-4-DAMP	Antagonist
	Nicotinic $\alpha_4\beta_2$	[^{3}H]-Epibatidine	Agonist
Noradrenaline	α_1	[^{3}H]-Prazosin	Antagonist
	α_2	[^{3}H]-RX 821002	Antagonist
Serotonin	5-HT_{1A}	[^{3}H]-8-OH-DPAT	Agonist
	5-HT_2	[^{3}H]-Ketanserin	Antagonist
Dopamine	D_1	[^{3}H]-SCH 23390	Antagonist

Supplementary Table 5.3. Autoradiography ligands and receptor targets.

Lobe	Anatomical subdivision	Jülich area	Region name	Atlas source
Occipital lobe	Visual cortex	hOc1	Brodmann's area 17 / V1	Jülich
		hOc2	Brodmann's area 18 / V2	Jülich
		hOc4d	V4	Jülich
		hOc3a	V3a	Jülich
		hOc3d	V3d	Jülich
		hOc3v	V3v	Jülich
		hOc4v	V4	Jülich
	Extrastriate cortex	FG1	Part of Brodmann area 19	Jülich
		FG2	Part of Brodmann area 19	Jülich
Parietal lobe	Somatosensory cortex	1	Brodmann's area 1	Jülich
		2	Brodmann's area 2	Jülich
		3a	Brodmann's area 3a	Jülich
		3b	Brodmann's area 3b	Jülich
	Superior parietal lobule	5L	Brodmann's area 5L	Jülich
		5M	Brodmann's area 5M	Jülich
		7A	Brodmann's area 7A	Jülich
	Inferior parietal lobule	PGa	Anterior inferior parietal area	Jülich
		PGp	Posterior inferior parietal area	Jülich
		PFt	Temporal inferior parietal area	Jülich

		PFm	Medial inferior parietal area	Jülich
Temporal lobe	Auditory cortex	Te1	Temporal area 1 (part of Brodmann's area 41)	Jülich
		Te2	Temporal area 2 (part of Brodmann's area 41)	Jülich
	Hippocampus	CA	Cornu ammonis	Jülich
		DG	Dentate gyrus	Jülich
	Subiculum	Subiculum	Subiculum	Jülich
	Entorhinal cortex	Ent	Brodmann's area 28	Jülich
		20	Brodmann's area 20	Brodmann
		21	Brodmann's area 21	Brodmann
		22	Brodmann's area 22	Brodmann
		36	Brodmann's area 36	Brodmann
		37	Brodmann's area 37	Brodmann
		38	Brodmann's area 38	Brodmann
Frontal lobe	Agranular premotor cortex	6	Brodmann's area 6	Jülich
	Primary motor cortex	4p	Brodmann's area 4p	Jülich
	Broca's region	44		Jülich
		45		Jülich
	Frontopolar cortex	Fp1	Frontopolar area (part of Brodmann area 10)	Jülich
		Fp2	Frontopolar area (part of Brodmann area 10)	Jülich

	Orbitofrontal cortex	Fo1	Orbitofrontal area (part of Brodmann area 11)	Jülich
	Lateral prefrontal	46	Brodmann's area 46	Brodmann
		47	Brodmann's area 47	Brodmann
		8	Brodmann's area 8	Brodmann
		9	Brodmann's area 9	Brodmann
Cingulate regions (multiple lobes)	Anterior cingulate	p24ab	Pregenual cingulate areas p24a & p24b	Jülich
		p32	Pregenual cingulate area p32	Jülich
	Posterior cingulate	23	Brodmann's area 23	Brodmann
		31	Brodmann's area 31	Brodmann
Basal ganglia	Striatum	Putamen	Putamen	AAL
		Caudate	Caudate nucleus	AAL
	Pallidum	Globus pallidus	Globus pallidus	DISTAL
	Subthalamic nucleus	STN	Subthalamic nucleus	DISTAL
Forebrain	Thalamus	Thalamus (anterior)	Thalamus (anterior)	AAL
		Thalamus (medial)	Thalamus (medial)	AAL
		Thalamus (lateral)	Thalamus (lateral)	AAL

Supplementary Table 5.4. Brain regions with receptor data, and the corresponding atlas used to extract the ROI map.

Note that regions are defined by cytoarchitecture, and thus do not correspond perfectly with functional regions.

Neuroimaging Modality	**Model Parameter**	**Receptor Type**	**Explained Variance**
GM	AMPA x fALLF	Glutamatergic	0.12%
	$GABA_B$	GABAergic	0.18%
	$\alpha_4\beta_2$ x GM	Cholinergic	0.31%
	M_1 x fALLF	Cholinergic	0.10%
	M_2 x fALLF	Cholinergic	0.31%
	$\alpha_4\beta_2$ x fALLF	Cholinergic	0.10%
	M_3 x FA	Cholinergic	0.16%
	M_1 x t1/t2	Cholinergic	0.12%
	M_1	Cholinergic	0.10%
	α_2 x fALLF	Adrenergic	0.42%
	$5HT_{1A}$ x SPECT	Serotonergic	0.29%
	D_1 x fALLF	Dopaminergic	0.29%
	GM	Non-Receptor	0.14%
	SPECT	Non-Receptor	0.20%
fALFF	Kainate x SPECT	Glutamatergic	0.10%
	NMDA x FA	Glutamatergic	0.33%
	Kainate x t1/t2	Glutamatergic	0.24%
	Bz site x GM	GABAergic	0.31%
	$GABA_B$ x fALLF	GABAergic	0.29%
	$GABA_A$ x FA	GABAergic	0.27%

	M_2 x FA	Cholinergic	0.13%
	M_1	Cholinergic	0.18%
	M_2	Cholinergic	0.21%
	$5HT_{1A}$ x t1/t2	Serotonergic	0.08%
	D_1 x GM	Dopaminergic	0.19%
	GM	Non-Receptor	0.16%
SPECT	Kainate x FA	Glutamatergic	0.15%
	α_1 x FA	Adrenergic	0.12%
	$5HT_2$ x GM	Serotonergic	0.18%
	$5HT_{1A}$ x MD	Serotonergic	0.25%
	$5HT_2$ x t1/t2	Serotonergic	0.23%
	$5HT_2$	Serotonergic	0.21%
	D_1 x FA	Dopaminergic	0.14%
	D_1	Dopaminergic	0.21%
	FA	Non-Receptor	0.31%
	MD	Non-Receptor	0.19%
FA	Kainate x GM	Glutamatergic	0.22%
	AMPA x t1/t2	Glutamatergic	0.13%
	Kainate x t1/t2	Glutamatergic	0.18%
	AMPA	Glutamatergic	0.36%
	Kainate	Glutamatergic	0.28%
	$GABA_A$ x MD	GABAergic	0.20%

	Bz site x t1/t2	GABAergic	0.20%
	$GABA_B$ x t1/t2	GABAergic	0.30%
	$GABA_A$	GABAergic	0.67%
	M_1 x fALLF	Cholinergic	0.15%
	M_3 x MD	Cholinergic	0.48%
	$\alpha_4\beta_2$ x t/1t2	Cholinergic	0.19%
	α_2 x GM	Adrenergic	0.25%
	α_2 x MD	Adrenergic	0.23%
	α_1 x t1/t2	Adrenergic	0.16%
	α_1	Adrenergic	0.13%
	$5HT_{1A}$ x SPECT	Serotonergic	0.08%
	$5HT_2$ x SPECT	Serotonergic	0.18%
	$5HT_2$ x MD	Serotonergic	0.17%
	$5HT_2$ x t1/t2	Serotonergic	0.12%
	GM	Non-Receptor	0.28%
	SPECT	Non-Receptor	0.12%
	MD	Non-Receptor	0.21%
	t1/t2	Non-Receptor	0.23%
	spreading	Non-Receptor	0.17%
MD	AMPA x fALLF	Glutamatergic	0.23%
	Kainate x fALLF	Glutamatergic	0.37%
	Kainate x FA	Glutamatergic	0.20%

	NMDA x MD	Glutamatergic	0.25%
	Kainate x MD	Glutamatergic	0.38%
	$GABA_A$ x GM	GABAergic	0.41%
	Bz site x fALLF	GABAergic	0.31%
	$GABA_B$ x MD	GABAergic	0.11%
	$GABA_A$	GABAergic	0.35%
	Bz site	GABAergic	0.50%
	M_1 x MD	Cholinergic	0.18%
	M_1	Cholinergic	0.21%
	M_2	Cholinergic	0.43%
	M_3	Cholinergic	0.67%
	α_1 x FA	Adrenergic	0.10%
	α_2	Adrenergic	0.13%
	$5HT_{1A}$ x GM	Serotonergic	0.12%
	$5HT_2$ x fALLF	Serotonergic	0.54%
	$5HT_{1A}$ x FA	Serotonergic	0.22%
	$5HT_2$	Serotonergic	0.45%
	D_1 x FA	Dopaminergic	0.15%
	fALLF	Non-Receptor	0.29%
	FA	Non-Receptor	0.24%
t1/t2	AMPA x FA	Glutamatergic	0.21%
	NMDA x FA	Glutamatergic	0.55%

	NMDA	Glutamatergic	0.38%
	Kainate	Glutamatergic	0.16%
	Bz site x GM	GABAergic	0.31%
	$GABA_A$ x FA	GABAergic	0.62%
	Bz site x FA	GABAergic	0.27%
	Bz site x MD	GABAergic	0.35%
	Bz site x t1/t2	GABAergic	0.13%
	$GABA_B$ x t1/t2	GABAergic	0.20%
	M_1 x SPECT	Cholinergic	0.21%
	M_1 x FA	Cholinergic	0.15%
	M_2 x FA	Cholinergic	0.08%
	M_1 x t1/t2	Cholinergic	0.13%
	M_3 x t1/t2	Cholinergic	0.18%
	α_2 x fALLF	Adrenergic	0.28%
	α_2	Adrenergic	0.21%
	$5HT_2$ x GM	Serotonergic	0.52%
	$5HT_2$ x SPECT	Serotonergic	0.14%
	D_1 x FA	Dopaminergic	0.19%
	offset	Non-Receptor	0.25%
	FA	Non-Receptor	0.19%

Supplementary Table 5.5. Biological parameters most correlated with clinical symptoms in PD via the primary component, and the percentage of clinical score covariance explained via this component.

Neuroimaging Modality	**Model Parameter**	**Receptor Type**	**Explained Variance**
GM	NMDA x GM	Glutamatergic	0.06%
	NMDA x SPECT	Glutamatergic	0.10%
	NMDA x MD	Glutamatergic	0.05%
	Kainate x MD	Glutamatergic	0.04%
	AMPA	Glutamatergic	0.08%
	NMDA	Glutamatergic	0.04%
	$GABA_A$ x GM	GABAergic	0.04%
	$GABA_A$ x fALLF	GABAergic	0.09%
	$GABA_A$ x FA	GABAergic	0.05%
	$GABA_A$ x MD	GABAergic	0.05%
	M_1 x fALLF	Cholinergic	0.07%
	M_1 x MD	Cholinergic	0.19%
	M_3	Cholinergic	0.08%
	$\alpha_4\beta_2$	Cholinergic	0.08%
	α_2 x SPECT	Adrenergic	0.11%
	α_1	Adrenergic	0.07%
	$5HT_2$ x FA	Serotonergic	0.13%
	$5HT_2$	Serotonergic	0.06%
	D_1 x GM	Dopaminergic	0.10%
	D_1 x MD	Dopaminergic	0.07%

	D_1	Dopaminergic	0.06%
	offset	Non-Receptor	0.06%
	t1/t2	Non-Receptor	0.04%
fALFF	$GABA_B$ x SPECT	GABAergic	0.06%
	M_3 x GM	Cholinergic	0.06%
	$\alpha_4\beta_2$ x t1/t2	Cholinergic	0.05%
	$5HT_2$ x MD	Serotonergic	0.08%
	$5HT_{1A}$ x t1/t2	Serotonergic	0.03%
	GM	Non-Receptor	0.04%
	FA	Non-Receptor	0.06%
	t1/t2	Non-Receptor	0.04%
SPECT	AMPA	Glutamatergic	0.04%
	NMDA	Glutamatergic	0.08%
	Kainate	Glutamatergic	0.12%
	$GABA_B$ x GM	GABAergic	0.05%
	Bz site x fALLF	GABAergic	0.05%
	$GABA_B$ x FA	GABAergic	0.07%
	$\alpha_4\beta_2$ x SPECT	Cholinergic	0.14%
	α_1 x SPECT	Adrenergic	0.04%
	α_2 x SPECT	Adrenergic	0.07%
	α_2	Adrenergic	0.09%
	$5HT_2$ x fALLF	Serotonergic	0.09%
	D_1 x FA	Dopaminergic	0.03%

FA	Kainate x GM	Glutamatergic	0.10%
	NMDA x SPECT	Glutamatergic	0.10%
	Kainate x FA	Glutamatergic	0.09%
	Kainate	Glutamatergic	0.12%
	$GABA_A$ x SPECT	GABAergic	0.04%
	$GABA_B$	GABAergic	0.07%
	α_1 x GM	Adrenergic	0.06%
	α_2 x fALLF	Adrenergic	0.05%
	α_1 x SPECT	Adrenergic	0.09%
	α_1 x t1/t2	Adrenergic	0.06%
	$5HT_{1A}$	Serotonergic	0.08%
	D_1 x MD	Dopaminergic	0.07%
MD	Kainate x MD	Glutamatergic	0.04%
	Bz site x fALLF	GABAergic	0.06%
	Bz site x SPECT	GABAergic	0.07%
	$GABA_A$ x FA	GABAergic	0.07%
	Bz site x FA	GABAergic	0.04%
	$GABA_B$ x MD	GABAergic	0.16%
	Bz site	GABAergic	0.06%
	$GABA_B$	GABAergic	0.06%
	M_2 x fALLF	Cholinergic	0.05%
	M_1 x SPECT	Cholinergic	0.03%
	M_2 x FA	Cholinergic	0.07%

	M_1 x t1/t2	Cholinergic	0.06%
	M_2 x t1/t2	Cholinergic	0.06%
	M_2	Cholinergic	0.06%
	M_3	Cholinergic	0.09%
	α_2 x fALLF	Adrenergic	0.04%
	$5HT_{1A}$ x GM	Serotonergic	0.05%
	$5HT_{1A}$ x t1/t2	Serotonergic	0.04%
	$5HT_2$	Serotonergic	0.06%
	D_1 x SPECT	Dopaminergic	0.07%
	t1/t2	Non-Receptor	0.06%
t1/t2	AMPA x SPECT	Glutamatergic	0.07%
	NMDA x FA	Glutamatergic	0.07%
	$GABA_A$ x GM	GABAergic	0.04%
	$GABA_B$ x GM	GABAergic	0.04%
	Bz site x SPECT	GABAergic	0.06%
	$GABA_B$ x SPECT	GABAergic	0.05%
	M_1 x GM	Cholinergic	0.08%
	M_3 x GM	Cholinergic	0.14%
	M_2 x SPECT	Cholinergic	0.04%
	$\alpha_4\beta_2$ x MD	Cholinergic	0.06%
	M_1	Cholinergic	0.16%
	M_3	Cholinergic	0.15%
	α_1 x GM	Adrenergic	0.03%

	α_1 x SPECT	Adrenergic	0.07%
	α_1 x FA	Adrenergic	0.04%
	α_1 x MD	Adrenergic	0.08%
	$5HT_2$ x GM	Serotonergic	0.07%
	$5HT_2$ x MD	Serotonergic	0.05%
	D_1 x MD	Dopaminergic	0.06%
	D_1 x t1/t2	Dopaminergic	0.07%
	GM	Non-Receptor	0.06%

Supplementary Table 5.6. Biological parameters most correlated with clinical symptoms in PD via the secondary component, and the percentage of clinical score covariance explained.

Receptor Type	Total variance explained in the primary component	Total variance explained in the secondary component
Glutamatergic	4.85%	1.19%
GABAergic	5.97%	1.24%
Cholinergic	4.77%	1.74%
Adrenergic	2.02%	0.88%
Serotonergic	3.77%	0.75%
Dopaminergic	1.16%	0.53%

Supplementary Table 5.7. Total MCM parameter-clinical co-variance explained by receptor type in PD patients (via each SVD component).

Imaging Modality	Average Gain in R^2	P-value
GM	35.6% ± 10.8%	$P=1.16\times10^{-27}$
fALFF	18.8% ± 8.0%	$P=7.22\times10^{-13}$
SPECT	20.2% ± 12.4%	$P=1.38\times10^{-9}$
FA	21.7% ± 11.8%	$P=5.87\times10^{-11}$
MD	19.0% ± 9.1%	$P=1.69\times10^{-9}$
t1/t2	17.1% ± 9.3%	$P=5.83\times10^{-9}$

Supplementary Table 5.8. Performance gain due to the inclusion of receptor maps, and the p-value from a two-sample t-test for each modality, across all (N=71) subjects.

Imaging Modality	Average Gain in R^2	P-value
GM	13.4% ± 5.3%	$P=2\times10^{-16}$
fALFF	7.3% ± 4.5%	$P=2\times10^{-16}$
SPECT	6.7% ± 4.3%	$P=2\times10^{-16}$
FA	7.5% ± 5.3%	$P=2\times10^{-16}$
MD	5.3% ± 4.0%	$P=2\times10^{-16}$
t1/t2	6.0% ± 3.5%	$P=2\times10^{-16}$

Supplementary Table 5.9. Performance gain due to true receptor distributions over null maps, and p-value of the true receptor data model belonging to the null distribution, using Fisher's method to combine p-values across all (N=71) subjects.

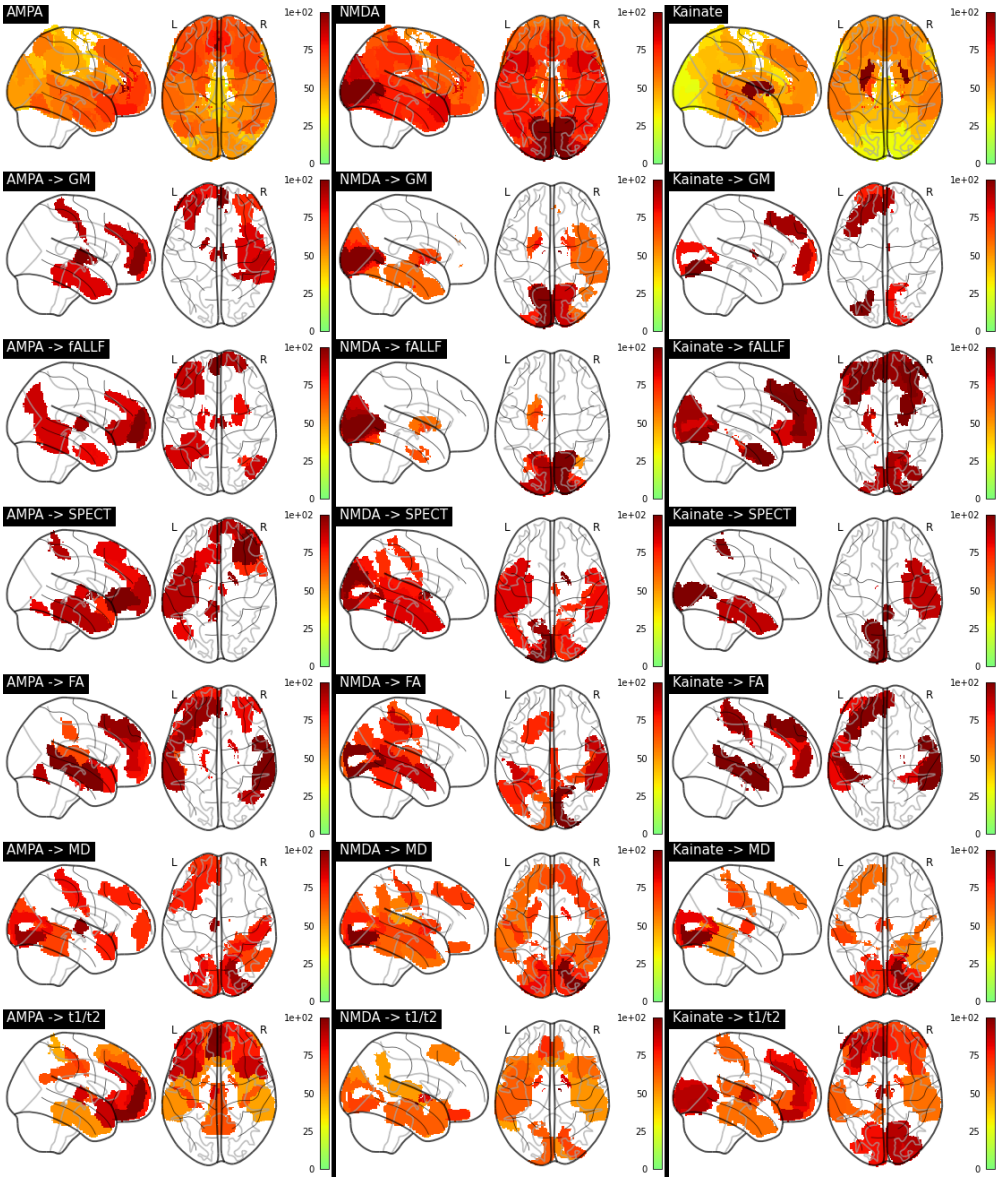

Supplementary Figure 5.1. Glutamatergic receptor influence maps.

The first row shows the densities of AMPA, NMDA and kainate receptors, with remaining rows showing their influence on gray matter density (GM), fractional amplitude of low frequency fluctuations (fALFF) from rs-fMRI, dopaminergic transporter (DAT) SPECT density, fractional anisotropy (FA), mean diffusivity (MD) and t1/t2 ratio. All maps are re-scaled to arbitrary units for visualization, and show only regions with significant z-scores ($P<0.05$) of Wilcoxon rank-sum statistics relative to the Wilcoxon statistics due to null distributions (1000 iterations with permuted receptor maps).

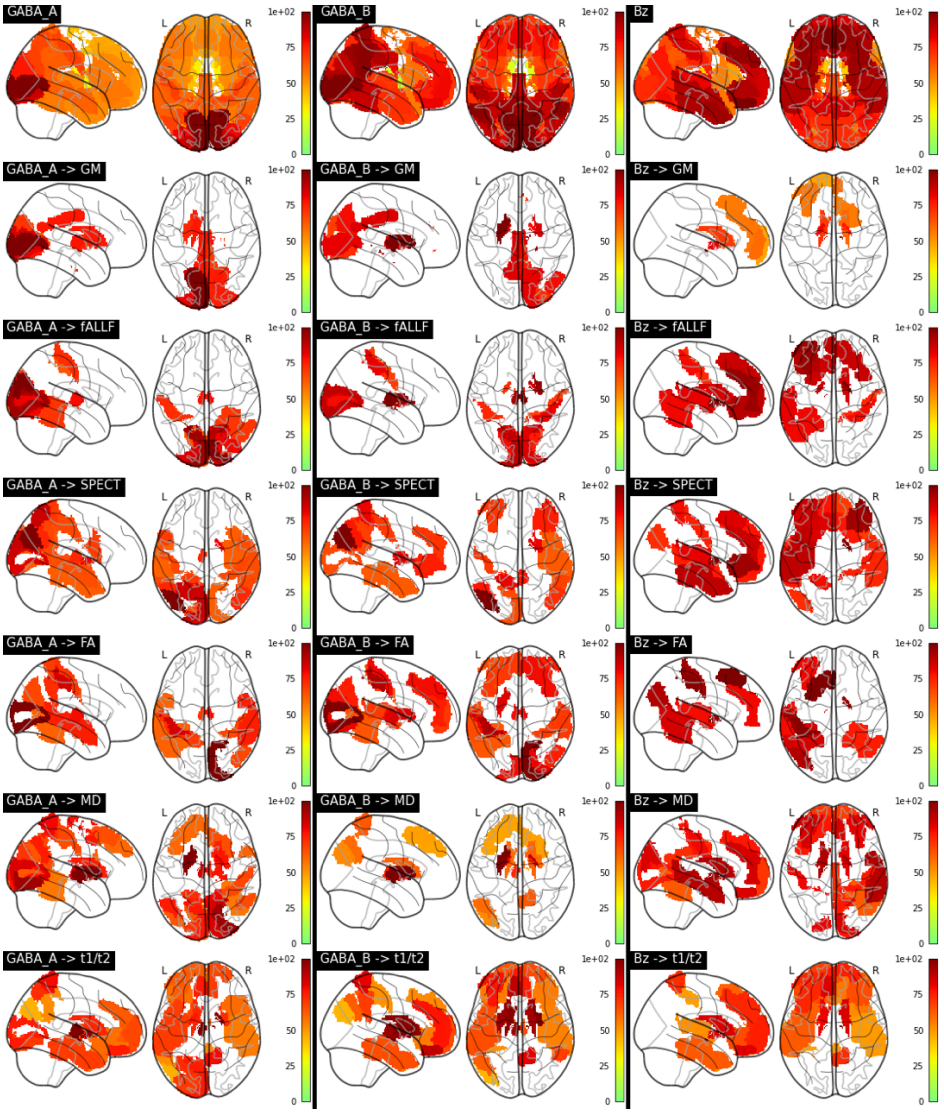

Supplementary Figure 5.2. GABAergic receptor influence on imaging modalities.

The first row shows density maps for $GABA_A$, $GABA_B$ and the Bz binding site, with remaining rows showing receptor influence maps for each imaging modality, including gray matter density (GM), fractional amplitude of low frequency fluctuations (fALFF) from rs-fMRI, dopaminergic transporter (DAT) SPECT density, fractional anisotropy (FA), mean diffusivity (MD) and t1/t2 ratio. All maps are re-scaled to arbitrary units for visualization, and show only regions with significant z-scores ($P<0.05$) of Wilcoxon rank-sum statistics relative to the Wilcoxon statistics due to null distributions (1000 iterations with permuted receptor maps).

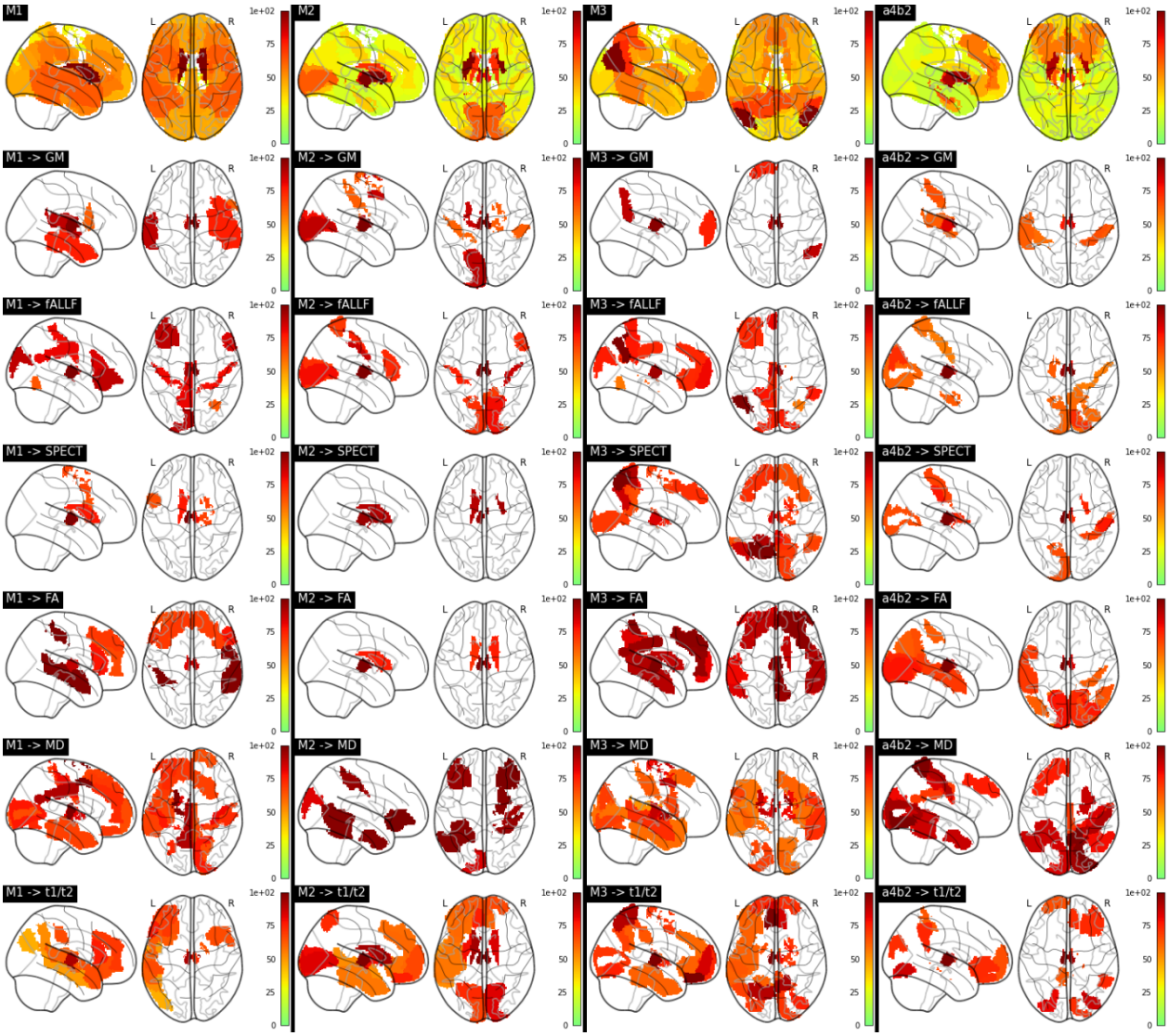

Supplementary Figure 5.3. Cholinergic receptor influence maps.

The first row shows the densities of the muscarinic M_1, M_2 and M3, and cholinergic $\alpha_4\beta_2$ receptors, with remaining rows showing receptor influence maps for each imaging modality, including gray matter density (GM), fractional amplitude of low frequency fluctuations (fALFF) from rs-fMRI, dopaminergic transporter (DAT) SPECT density, fractional anisotropy (FA), mean diffusivity (MD) and t1/t2 ratio. All maps are re-scaled to arbitrary units for visualization, and show only regions with significant z-scores ($P<0.05$) of Wilcoxon rank-sum statistics relative to the Wilcoxon statistics due to null distributions (1000 iterations with permuted receptor maps).

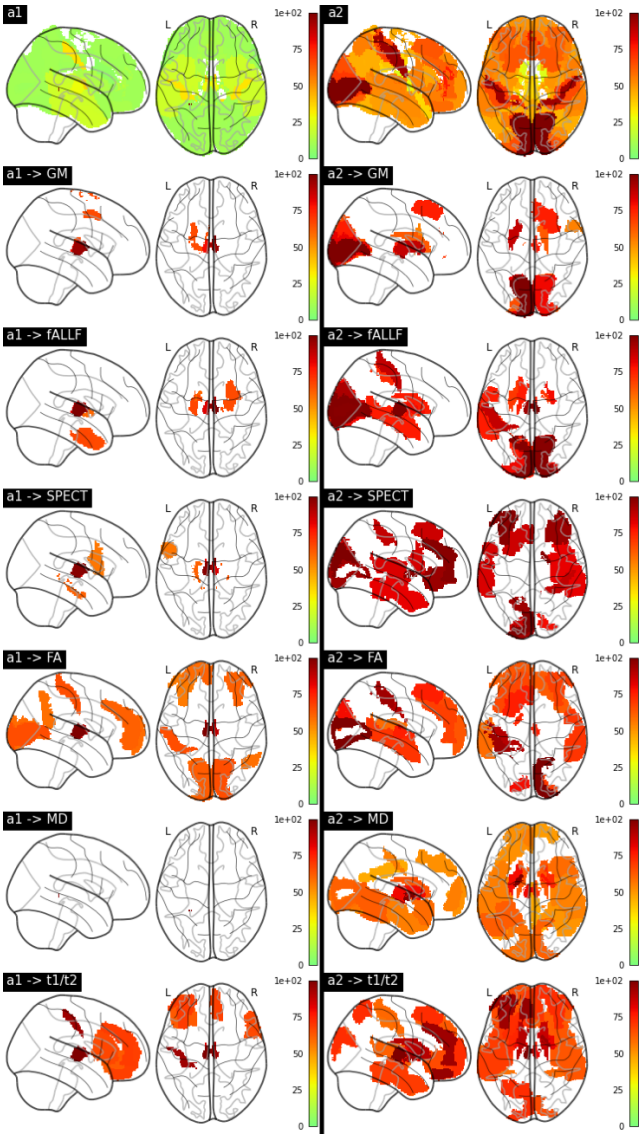

Supplementary Figure 5.4. Adrenergic receptor influence maps.

The first row shows α_1 and α_2 receptor density maps. with remaining rows showing receptor influence maps for each imaging modality, including gray matter density (GM), fractional amplitude of low frequency fluctuations (fALFF) from rs-fMRI, dopaminergic transporter (DAT) SPECT density, fractional anisotropy (FA), mean diffusivity (MD) and t1/t2 ratio. All maps are re-scaled to arbitrary units for visualization, and show only regions with significant z-scores ($P<0.05$) of Wilcoxon rank-sum statistics relative to the Wilcoxon statistics due to null distributions (1000 iterations with permuted receptor maps).

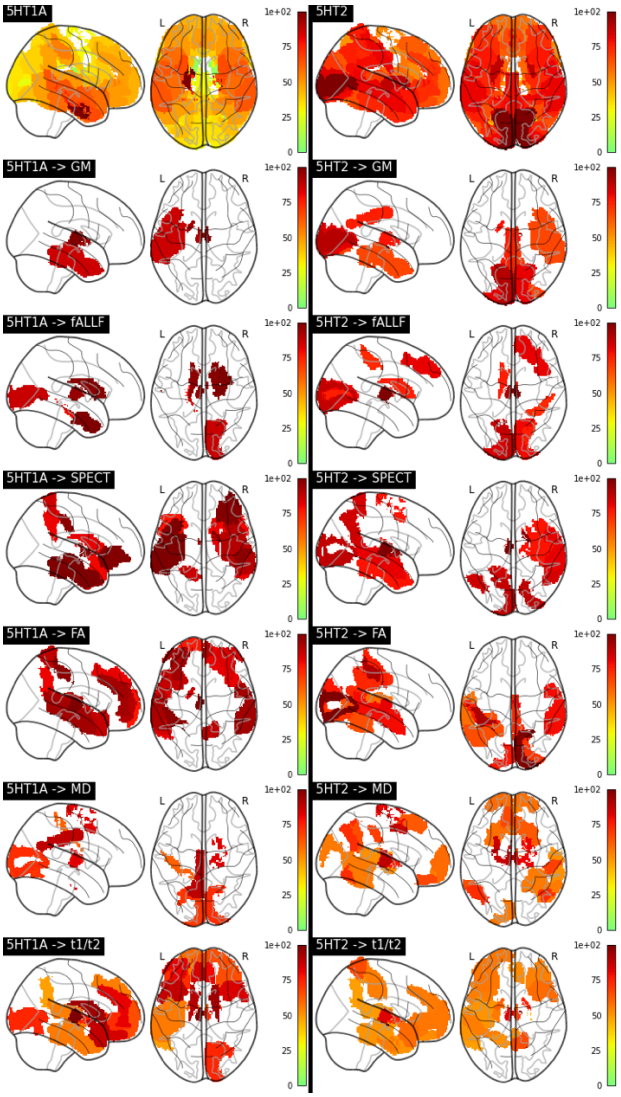

Supplementary Figure 5.5. Serotonergic receptor influence maps.

The first row shows the $5HT_{1A}$ and $5HT_2$ serotonergic receptor density maps, with remaining rows showing receptor influence maps on gray matter density (GM), fractional amplitude of low frequency fluctuations (fALFF) from rs-fMRI, dopaminergic transporter (DAT) SPECT density, fractional anisotropy (FA), mean diffusivity (MD) and t1/t2 ratio. All maps are re-scaled to arbitrary units for visualization, and show only regions with significant z-scores ($P<0.05$) of Wilcoxon rank-sum statistics relative to the Wilcoxon statistics due to null distributions (1000 iterations with permuted receptor maps).

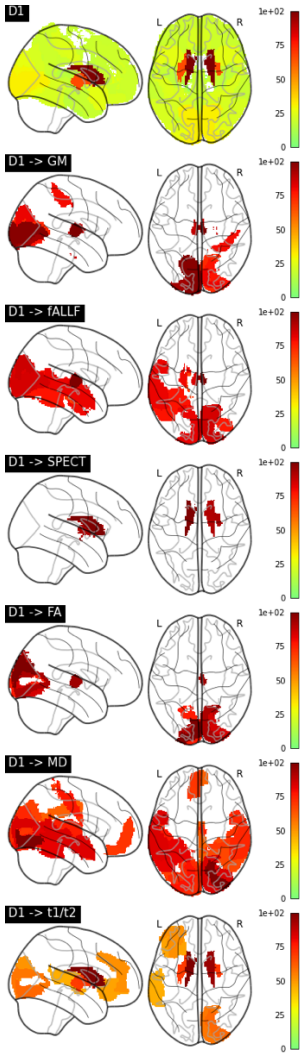

Supplementary Figure 5.6. Dopaminergic receptor influence maps.

The first row shows the D_1 dopaminergic receptor density, with remaining rows showing its influence on each imaging modality, which include gray matter density (GM), fractional amplitude of low frequency fluctuations (fALFF) from rs-fMRI, dopaminergic transporter (DAT) SPECT density, fractional anisotropy (FA), mean diffusivity (MD) and t1/t2 ratio. All maps are re-scaled to arbitrary units for visualization, and show only regions with significant z-scores ($P<0.05$) of Wilcoxon rank-sum statistics relative to the Wilcoxon statistics due to null distributions (1000 iterations with permuted receptor maps).

Chapter 6. Discussion

Summary of findings

Neurodegenerative disorders such as AD and PD involve multi-factorial physiological alterations, from dysregulated neuronal activity and perfusion changes to atrophy and proteinopathy accumulation. Altered neurotransmission has been implicated in many of these physiological changes [25] [24], but the role of multi-neurotransmitter dysfunction and its association with multi-domain symptomatic variability has not been sufficiently characterized.

To address this key gap in our knowledge of disease biology, this thesis has attempted to link the spatiotemporal progression of neurodegenerative changes with the neurotransmitter receptor architecture of the brain. Using longitudinal multi-modal imaging markers in combination with receptor autoradiography and diffusion tractography templates, personalized whole-brain computational models with interpretable parameters are fit to healthy aged subjects, individuals on the AD spectrum and PD patients. These model parameters represent the subject-specific roles of mechanisms, such as local receptor-mediated interactions between physiological systems (e.g., blood flow and atrophy) and the network propagation of abnormalities. Notably, using a data-driven inter-subject comparison with multi-domain symptom severity, we identify 2 distinct and co-occurring “disease axes” in both AD and PD with distinct symptomatic profiles. These results suggest that disorders such as AD and PD may involve the overlap of separate disease processes, that additively or synergistically result in the observed clinical progression.

Modeling approach

Chapter 4 introduces re-MCM, a dynamical system model where the state variables are regional measures of gray matter density, functional activity, CBF, glucose metabolism, and amyloid and tau levels. These variables are quantified by structural, functional and perfusion MRI as well as FDG, AV-45 and AV-1451 PET. Chapter 5 presents an application of re-MCM to PD, examining the receptor-mediated interactions between gray matter atrophy, functional activity dysregulation, microstructural changes, and dopaminergic loss. These factors are quantified using T1-derived gray matter density, t1/t2 ratio, fALFF, MD, FA and DAT density maps, from structural, functional, and diffusion MRI and DAT SPECT. For each individual subject, the regional rate of change in each physiological variable is decomposed into i) within-region interactions with other variables (both direct and mediated by the local concentrations of 15 neurotransmitter receptors), and ii) inter-region propagation of abnormality along the structural connectome.

Receptor template maps are informative to the individualized progression of pathophysiology

In a heterogeneous aged population (consisting of healthy aged subjects, MCI individuals and AD patients), re-MCM explains an average of ~70% (± 20%) of longitudinal variance in imaging rate of change, including a ~20% improvement due to (direct and interaction) receptor effects (Supplementary Table S8). In PD patients, the inclusion of regional receptor concentrations improved the model variance explained by ~42.3% on average. These improvements are significant for almost all subjects after accounting for increased model size, and compared to permuted null models.

Overall, there are widespread interactions between different forms of structural and functional degradation (Chapter 5, Figure 5.3), with distinct contributions attributed to the spatial patterns of neurotransmitter receptor distribution (Chapter 5, Figure 5.4). Receptor distributions contribute especially strongly to gray matter atrophy, undirected microstructural damage (MD), and dendrite loss (t1/t2).

These findings support the hypothesis of this work, that even group-averaged templates of molecular data are relevant features determining local vulnerability to neurodegenerative changes.

Inter-subject variability in model mechanisms is linked to multi-domain symptomatic profiles

Lacking definitive biological disease definitions, clinical symptoms are the variable of interest with which we attempted to validate model-inferred mechanistic differences between subjects. Notably, inter-subject variability in model parameters is significantly and robustly correlated with multi-domain cognitive symptoms using PLS-SVD cross-decomposition. In AD (N=25), there are two prominent latent components. The first component ($p<0.003$, FWE-corrected) explains 39.7% of parameter-symptom co-variability with its main cognitive contribution from executive dysfunction. Prominent cognitively associated receptor effects include glutamatergic disruption of functional activity, GABAergic mediation of amyloid accumulation, and cholinergic mediation of tau accumulation. There is also a secondary component (23.4% co-variance explained, Supplementary Figure S10) with a similarly high correlation between projections of model parameters and cognitive scores ($r=0.890$, $p<10^{-8}$). In

this secondary component, memory, language and visuospatial dysfunction correlate mainly with model predictors of perfusion changes, metabolic alterations and proteinopathy accumulation.

While healthy ageing (N=112), there is less consistent cognitive variability. Nevertheless, a statistically significant and stable secondary PLS-SVD component was observed (15.5% co-variance explained, $p<0.02$), mainly linked to tau accumulation, followed by atrophy, CBF, functional activity and metabolic alterations. Notably, predictors of amyloid accumulation did not correlate with cognitive decline in healthy ageing.

In PD patients (N=71), there are two significant and stable components (explaining 48.4% and 13.2% of the co-variance, respectively). In each of these components, the latent projections of parameters and clinical rates of decline are strongly correlated ($r=0.70$ and $r=0.86$, respectively). These components correspond to motor symptoms and cognitive processing speed, and visuospatial function along with working memory, depression and anxiety (Chapter 5, Figure 5.5c-d). The two disease axes have distinct model-inferred mechanistic contributions; for example, GABA and glutamate receptor distributions drive t1/t2 ratio changes in the primary component, while the cholinergic system plays the largest role in the secondary component. The results correspond closely to the dual syndrome hypothesis of PD [122], which postulates dopaminergic executive impairment and cholinergic visuospatial dysfunction. However, as noted in Chapter 5, *Discussion*, the dopaminergic maps in our models are relatively uninformative due to their spatial homogeneity, complementary information with DAT-SPECT, and early depletion in PD patients [708].

Finally, to derive spatial information from these subject-level model parameters, we inferred the importance of receptor templates to explaining the physiological alterations at different brain regions in PD.

The distance of patients' neurotransmission mechanisms from a normative distribution is correlated with symptomatic decline

By comparing receptor parameters between AD patients and a normative distribution from healthy controls, an overall "receptor alteration fingerprint" is obtained. These 6 features (one per neurotransmitter family) explained 71.4% of the variance in executive function scores, and 43.8% of the variance in MMSE scores for AD patients (Chapter 4, Figure 4.6). Particularly, i) executive dysfunction seemed to be explained by GABAergic and cholinergic alterations, ii) memory scores largely depended on dopaminergic alterations, and iii) MMSE is associated with a combination of glutamatergic, GABAergic and serotonergic scores. Finally, we demonstrate that subjects with similar clinical scores can have different model-inferred neurotransmission dysfunction (e.g., more cholinergic vs. more glutamatergic alterations), providing a grounding for model-based treatment selection.

Inferring latent mechanisms from model parameters

The work presented in this thesis fits personalized (i.e., subject-specific) models where each α model parameters in Equations 4.7 or 5.6 has a biological interpretation: i) direct effects between the physiological processes behind imaging measures (e.g., the effect of local amyloid accumulation on gray matter atrophy), ii) receptor-mediated interactions (e.g., NMDA-mediated effects of amyloid accumulation on gray matter atrophy), iii) direct receptor effects (e.g., local

vulnerability to gray matter atrophy based on NMDA receptor expression), and iv) network propagation of pathophysiology (e.g., amyloid propagation to neighboring regions, or transneuronal degeneration leading to atrophy).

These parameters are then compared across subjects, to identify mechanisms consistently associated with symptom severity. More generally, computational models with interpretable parameters can be used to infer mechanistic differences between individuals or groups that may not be directly observable. The most prominent example of this approach is the incorporation of amyloid-facilitated neuronal hyperexcitability and disrupted excitatory-inhibitory (E/I) balance in biophysical models of EEG or fMRI activity, with the influence of external (network) input on local populations modulated by an optimized global coupling factor (G).

In the personalized models of Stefanovski et al., a network of regional Jansen-Rit neural mass models (which consists of excitatory and inhibitory interneurons in addition to excitatory pyramidal cells) produce simulated EEG output [508]. PET-derived amyloid load determines the inhibitory time constant. Qualitative features in the bifurcation diagrams of neural mass model input-output relationships (e.g., the presence of limit cycles) at varying amyloid burden reflect model-inferred differences between diagnostic classes. Interestingly, regional variation in amyloid burden was associated with oscillatory slowing in AD patients, but the opposite occurs in cognitively normal individuals [508]. Simulated therapy using memantine (an NMDA receptor antagonist) increases mean EEG frequency, suggesting a mechanistic explanation for the symptomatic benefits of the drug [508].

Using a similar model, Patow et al. note inter-class differences in amyloid- and tau-driven scaling parameters. Amyloid influences neuronal activity more in the early stages of the AD spectrum (i.e., in MCI patients), while tau dominates later [709]. Zimmerman et al. note that

personalized biophysical model parameters correlate better with cognition than more direct, imaging-derived measures such as structural or functional connectivity [651]. Sanchez-Rodriguez et al. observe increased synergistic effects of amyloid and tau burden on neuronal activity with disease progression [501].

There studies support i) the importance of intra-individual, inter-region influence of pathological factors on neural activity, and ii) the inter-individual differences in model parameters between diagnostic classes. The design of such in silico models may be informed by suspected disease mechanisms, and, conversely, it may guide other molecular or interventional studies.

However, while the interaction parameters capture a subject-specific effect (i.e., the NMDA-functional activity interaction parameter in the atrophy model represents the effects of spatial variability in this variable if NMDA density and functional activity were at their spatial mean values), it is unclear whether this may be due to an altered receptor distribution, dysfunctional receptor activity, or some other, potentially molecular or cellular factor. Instead, the parameters provide clues for more detailed molecular investigation (e.g., in vitro or animal studies).

Evaluating mechanistic hypotheses

Identifying causal mechanisms of disease onset and progression is an overarching goal in ageing and neurodegeneration research. Causal mechanisms are particularly important in neurodegeneration, where upstream targets for effective disease-modifying treatment have not been identified (resulting in the “causality gap” [527]). However, “causal mechanism” can be a nebulous term, referring to a variety of abstractions from the molecular, cellular, circuit, network,

system or behavioral level [710]. In the context of this thesis, a mechanism refers to the biological interpretations of model parameteters summarized in the previous subsection.

By inferring latent biological mechanisms and their inter-subject differences, computational models such as re-MCM can support the search for mechanistic hypotheses even with observational data. Although this work relies on observational data (with the model structure being causal), the Bradford Hill criteria for causation provide a multi-dimensional guideline to evaluate such studies based on effect size, reproducibility, specificity of findings, temporal order of proposed cause and effect, a dose-dependent gradient of effects, consistency with known mechanisms, and coherence between different types of studies (e.g., replicating mechanisms between computational models and in vitro studies) [331].

So, while these individualized model parameters have biological interpretations, this work is exploratory. Definitive conclusions about disease biology, and robust translation to therapy would require replication of observed associations from other imaging cohorts, as well as thorough validation of the identified molecular mechanisms.

Limitations

Modeling requires longitudinal and multi-modal imaging data

The work presented in this thesis has attempted to characterize the progression of and interactions between multiple imaging modalities in individual subjects. Naturally, the availability of sufficient multi-modal and longitudinal data has limited the number of qualifying subjects (N=25 AD and N=71 PD patients), particularly lacking controls from the PPMI cohort. The number of longitudinal imaging visits per subject determined the sample size in subject-specific model fitting, while the number of subjects with sufficient data determined the sample

size for downstream analysis. Therefore, simple linear techniques (linear regression and PLS-SVD) were used in these steps. Nevertheless, imaging models as well as stable and significant PLS-SVD components captured a substantial amount of data variance.

To ensure that all neuroimaging modalities could be included in the model, missing longitudinal neuroimaging data was imputed when necessary. If assumptions about the underlying mechanism of missingness (e.g., data missing at random) are not valid, imputation may introduce bias. Imputation may also reduce effective sample size and underestimate data variability.

The models were also fit to a broader range of subjects from ADNI (N=423 total, including cognitively unimpaired individuals, MCI subjects and AD patients). While this allowed the characterization of parameter variability and provided a normative distribution for receptor parameters (Chapter 4, *Clinically similar subjects have different underlying receptor alterations*), symptom severity is milder and AD-specific phenotype is more difficult to ascertain.

On the other hand, more data was available for PD patients compared to controls in the PPMI cohort. However, PPMI aimed to recruit subjects who had recently been diagnosed with PD and had not yet been treated [306]. The subjects likely represent an early motor phase of PD, a transitionary period between the earliest non-motor manifestations and the more severe disease progression to come. Longitudinal studies with pre-symptomatic individuals that converted to PD may be informative in potential differences in model-inferred mechanisms over progressive disease stages. Likewise, characterization of more advanced PD patients may be informative to understanding the receptor basis of diverging clinical subtypes.

Finally, for practical clinical applications of such dynamical systems models, it would be desirable to perform system identification with as few time points as possible and using the least invasive modalities.

Receptor distributions are from averaged templates

A major motivation for this work was to infer the involvement of multiple neurotransmitter systems in physiological alterations over the course of ageing and neurodegenerative disease progression, in the absence of individualized receptor distribution data. It must be noted that longitudinal receptor mapping for over a dozen neurotransmitter receptors would be prohibitively expensive. Instead, post-mortem autoradiography templates were used, which were based on the neurotransmitter receptor profiles of healthy aged individuals (72-77 years old) with no neurological or psychiatric conditions [423]. The usage of post-mortem autoradiography data allowed the inclusion of receptor types without in vivo radioligands, and many recent studies (summarized in Chapter 3) have examined the spatial correlation of patients' neuroimaging features with molecular template data (from PET, autoradiography or the Allen Human Brain Atlas post mortem gene expression).

The models presented in this thesis assume that the receptor architecture of healthy aged brains is representative of the molecular environment at the onset of ageing and neurodegeneration. Despite using averaged data from a different set of subjects, this work demonstrates that the aged brain's neurotransmitter receptor architecture is informative to understanding individualized interactions between various physiological systems. Receptor templates provided statistically significant improvements in almost all subjects' imaging models (between 15.6% and 22.3% average improvement among ADNI subjects, and 42% average improvement in PD), after accounting for increased model size and compared to spatial null

models (Chapter 4, *Multi-scale interactions involving neurotransmitter receptors are important to explaining multifactorial brain reorganization* and Chapter 5, *Neurotransmitter receptor maps significantly improve the explanation of multi-factorial brain reorganization in PD*).

However, receptor architecture is not static, and is itself affected by neurodegeneration as well as normal ageing. Receptor PET binding studies in animal models and AD and PD patients [711] [123] as well as post mortem assessment of neurotransmitter metabolites [712] point towards alterations of neurotransmitters, transporters and receptors. The dynamics of these features over the ageing and neurodegenerative process would need to be better characterized. Biophysical modeling to infer specific mechanisms of neurotransmission dysfunction (e.g., presynaptic neurotransmitter or transporter alterations or post-synaptic receptor modifications) would be a promising avenue of future work with pharmacological relevance.

Receptor data has limited spatial resolution

The regionally averaged receptor autoradiography data constrained the analysis to a custom brain parcellation [579]. While some recent studies have used whole-brain PET templates or gene expression maps to spatially correlate imaging alterations with molecular features (summarized in Chapter 3), the three data modalities not strongly correlated [655]. They likely represent different views of the underlying biological processes. The latter is arguably closer to the relevant biological feature (functional proteins), with a theoretically higher spatial resolution than PET [227].

As these regions are defined by cyto- and receptor-architecture, they are consistent in terms of receptor expression. However, there may be partial volume effects in imaging modalities, due to overlapping tissue types, as well as potential blurring effects in small volume regions and lower spatial resolution imaging modalities. Registration of the histological data to

3D brain maps would allow more fine-grained analysis, i) at the voxel scale, ii) using different brain atlases, and iii) with the spatial distributions of specific cell types [454].

Imaging abnormalities are physiologically non-specific

A major limitation in interpreting neuroimaging-based features as distinct physiological mechanisms is their non-specificity. Broadly, fMRI has strong influence from non-neuronal processes, diffusion MRI and T1/T2 ratio have unclear microstructural origin, and molecular PET imaging can suffer from off-target binding and heterogeneous uptake [526]. Below, some specific limitations of imaging markers used in this thesis and caveats about interpretation are highlighted.

Interpreting microstructure

Diffusion MRI measures are typically interpreted in terms of axonal integrity and myelination in white matter (Chapter 2). However, in the primarily gray matter regions of our atlas, diffusion is assumed to be more isotropic. In Chapter 5, over-interpretation of the underlying alterations has been avoided by considering FA and MD to reflect “directed” and “undirected” microstructure, respectively.

As an alternative underlying source for the diffusion scalar maps, a study comparing in vitro imaging of a ferritin-loaded phantom with in vivo data suggests that gray matter diffusion MRI measures may instead be associated with ferritin-bound iron [713]. Iron accumulates in gray and white matter with age in specific patterns, potentially as a consequence of factors such as increased blood-brain barrier permeability, neuroinflammation, and disrupted iron homeostasis [714] [715]. The distribution and concentration of brain iron may change in

neurodegenerative diseases [713], which offers yet another interpretation for the diffusion scalar maps. However, further validation of diffusion MRI metrics in these regions is necessary.

Even in purely white matter regions, interpretation of FA is further complicated by the "crossing fibers problem". A decrease in FA is assumed to reflect the loss of directed white matter microstructure, but it is estimated that 63%-90% of white matter voxels contain multiple fiber bundles of different orientations [716]. As a result, FA cannot distinguish between the lack of directed microstructure and the presence of directed microstructure with orthogonal orientations. In the latter case, the selective degeneration of white matter fiber bundles along one orientation can counter-intuitively increase the anisotropy of a voxel [193]. This is intrinsic to the complex organization of brain tissue, and not an artifact of technical limitations [717]. As an aggregate measure of diffusivity along all axes, MD is expected to be more robust to the "crossing fibers problem" [193]. Alternatively, fixel-based analysis could disentangle the signal due to each fiber bundle [718].

Finally, while the T1/T2 ratio is often associated with myelin [181], comparison with other imaging measures, such as myelin water fraction (MWF), diffusion scalars and magnetization transfer ratio, suggests a non-myelination component [182] [183]. In Chapter 5, the T1/T2 ratio has been interpreted as a measure of dendrite density, due to its strong correlation (at least in MS patients) [185] . While the precise underlying microstructural source for the T1/T2 signal is unresolved, it provides an additional picture that is distinct from diffusion MRI [182].

Partial volume effects

Partial volume effects may introduce bias into certain imaging modalities. A single voxel may contain multiple tissue types (e.g., gray and white matter as well as CSF) or orientations

(such as crossing fibers) [719]. These varied tissue types can have vastly different properties, such as the 2-5 times higher perfusion of gray matter compared to white matter (with CSF not being perfused) [720]. In the gray matter regions of the atlas, this may particularly affect the interpretation of diffusion MRI measures.

Furthermore, atrophy may lead to an overestimation of gray matter MD [721], and ASL-measured perfusion [720] alterations. The direct effect of gray matter alterations on MD in Chapter 5, Figure 5.3a may reflect atrophy-related changes (which are much smaller than MD changes not associated with atrophy) . These specific biases are somewhat mitigated in our models, where multiple imaging and neurochemical features are considered simultaneously. However, more broadly, the effects of partial volume effects would need to be robustly characterized to validate mechanistic conclusions from MCM, potentially by using voxel-scale receptor atlases.

Functional activity alterations

The BOLD signal is an indirect measure of neuronal activity; it contains contributions from metabolic and vascular processes, as well as other non-neuronal factors such as cardiac and respiratory noise and cerebral autoregulation [722]. Furthermore, hemodynamic response has spatiotemporal variation [723], and modulatory neurotransmission can break the conventional interpretation of BOLD response as reflecting neuronal activity. For example, local inhibitory circuits may suppress the inputs from projection neurons, resulting in a BOLD response without the accompanying neuronal activity [549]. Thus, it would be more accurate to consider the BOLD signal as a measure of regional synaptic input and local activity [549].

Of particular interest to this thesis is the resting state BOLD signal, in the absence of task stimulus. The origins of intrinsic resting state dynamics are an open question, potentially arising

from sodium and potassium ion concentration dynamics [724] or the anatomically-facilitated coupling between oscillatory activity across brain regions [725]. It has been suggested that resting state activity reflects some sort of "functional capacity" that can be affected in disease [726].

The models presented in this thesis used the fALFF as the measure of regional functional integrity, which may suppress physiological noise by focusing on low frequency (0.01-0.08 Hz) BOLD oscillations [578]. Unlike functional connectivity (FC) and related measures such as regional homogeneity (ReHo), fALFF does not incorporate information from outside the ROI, which is a desired property of for the interpretability of state variables in re-MCM. Furthermore, it exhibits intra-scan temporal stability [619], test-retest reliability [620], and sensitivity to AD and PD progression [577] [219] [220] [665]. It also shows a higher correspondence to glucose uptake compared to other fMRI measures, thus potentially better reflecting neuronal activity [576]. While there is an association between resting state BOLD and electrophysiological measurements, the latter explains only around 10% of the BOLD signal variability [623]. Thus, while it appears to be relevant to disease progression, these caveats must be noted in interpreting fALFF as a measure of neuronal activity.

Finally, we must note the limited temporal limitations of perfusion and functional MRI. Veins (and capillaries) are the major contributors to the BOLD signal, and they dilate more slowly than arteries [723]. However, the flow of dilation is too fast to be temporally resolved by fMRI [723]. The temporal delay between neuronal activity and the corresponding BOLD spike (more precisely, the full width at half maximum of the hemodynamic response function) is estimated to be around ~5 seconds [727]. Similarly, ASL would not be able to resolve processes faster than the longitudinal relaxation time of blood [627] [728].

Important disease processes may not be captured by the imaging modalities

While this thesis has attempted to cover a wide range of physiological processes, it is likely that several important factors have been missed. Although it is believed to be a significant factor in AD and PD [21] [74] [75], an imaging marker of neuroinflammation has only recently emerged in the form of translocator protein (TSPO) PET [76]. Ongoing efforts to develop and validate PET tracers for TDP-43 [729] and α-synuclein [730] would also enable in vivo assessment of their contribution to disease progression. As large, multi-site longitudinal studies incorporate such emerging imaging markers, we will have an opportunity to expand computational models such as re-MCM to study new processes.

Applications and extensions to the model

Connectivity

In this work, we considered a combination of local, receptor-mediated interactions and network propagation of pathophysiology. The substrate for this network was the white matter structural connectome. However, the spreading of physiological dysfunction may occur along other networks, such as functional, vascular, metabolic and molecular connectivity [33] [536] [731] [537], as well as nearby brain regions (e.g., diffusion in extracellular space). How these different forms of connectivity are interrelated is also an important question; structural and vascular connectivity both seem to determine functional connectivity [625] [626]. Furthermore, while directional connectivity cannot be inferred from diffusion tractography, analogous regions from tracer-derived animal connectomes may be an informative proxy [401].

Finally, more detailed biophysical modeling of multi-scale connectivity and interactions may be a promising direction. Incorporating receptors in regional microcircuits [486] [501] and

incorporation of protein aggregation kinetics [207] may elucidate better mechanistic insight. For example, a computational model of spatiotemporal amyloid distribution suggests that propagation may be driven by regional differences in capacity for the misfolded protein [732].

Cell types

One of the defining features of neurodegenerative diseases is the selective loss of specific cellular populations. As discussed in Chapter 2, non-neuronal cell types are linked with many of the interactions considered in this work, such as astrocyte reactivity modulating tau hyperphosphorylation [80]. There is evidence for the differential vulnerability of various cell types in neurodegeneration [733]. Voxel-scale whole brain cell type atlases, derived from gene expression, would help resolve potential cell-specific effects [454], and could be used as complementary or alternative molecular features in MCM. In general, complementary cellular and molecular information would clarify whether receptor mechanisms or other spatially correlated features underlie the associations observed in this thesis.

Data-driven transdiagnostic categorization using model parameters

Despite diverging phenotype, neurodegenerative diseases share the defining features of progressive and selective neuronal loss followed by cognitive and functional decline. There is notable genetic, pathological, imaging, and clinical overlap between neurodegenerative diseases, and with psychiatric disorders [734] [165] [735]. This psychiatric component is evident in the role of depression and anxiety in the secondary PD axis in Chapter 5: *Two axes of receptor-pathology alterations underlie clinical symptoms in PD*.

Most PD patients with dementia have AD pathology [261]. Other conditions (e.g., PD dementia, LBD or vascular dementia) can often be confused for AD, and around 15% of ALS

patients meet the clinical criteria for FTLD [558] [736]. A meta-analysis suggests that the best-case diagnostic accuracy for PD (by movement disorder specialists) is around 80% and has not significantly improved since the 1980s despite advances in imaging [262]. Similarly, up to 23% of patients clinically diagnosed with AD do not have autopsy-confirmed AD pathology [263] (with the remainder often having mixed pathology [59] [275]). Misdiagnosis may be particularly likely in the early stages and mild phenotypes, where atypical presentations and treatment response (two criteria often used to distinguish diseases) are less evident [737] [263] [261]. These estimates may also be affected by the inconsistency of disease definitions; either neuropathological evaluation, consensus criteria (e.g., UK Parkinson's Disease Society Brain Bank Research Center criteria or the MDS Clinical Diagnosis Criteria) or refined diagnosis by experts may be used as the ground truth diagnosis.

One possible interpretation of mixed pathology can be the co-occurrence of independent (but possibly interacting) age-related disorders. It is possible that mixed pathology may additively or synergistically contribute to symptomatic clinical disease, despite each pathology individually being at "subclinical" levels [261]. To disentangle the contributions of different disease processes, a biological taxonomy of neurodegenerative disorders based on affected anatomical pathways, vulnerable cell populations and molecular features [738] may be necessary.

To support these efforts, integrative, transdiagnostic analysis using mechanistic models such as MCM could be used to identify shared and distinct underlying biological mechanisms from in vivo data. The identification of multiple "disease axis" for AD (Chapter 4: *Receptor-imaging alterations underlying cognitive deterioration in AD*) and PD (Chapter 5: *Two axes of receptor-pathology alterations underlie clinical symptoms in PD*) from patient-specific

computational models is a demonstration of this approach. Combining existing large studies across disease cohorts may be feasible start, with data-driven analysis using clinical symptoms rather than case-control comparisons based on diagnosis. However, the lack of shared biomarkers and clinical (e.g., simultaneous cognitive and psychiatric) assessments can be an impediment in practice.

Biological definitions of AD and PD using model parameters

In addition to the transdiagnostic overlap among neurodegenerative diseases, there is notable within-disease heterogeneity in disorders such as AD and PD [13] [739]. While they have historically been defined by a combination of symptoms and neuropathological features, it is acknowledged that a biological (as opposed to clinical) disease definition for living patients is needed [708]. Biomarker-based categorizations would ideally allow biologically homogenized groups of patients to be selected for clinical studies. Recently, efforts along these lines have spread from AD to other conditions (e.g., the ATN [236] and SynNeurGe [294] frameworks for AD and PD, respectively). However, these are evolving concepts [740] and the precise combinations of biological factors underlying disease remain to be determined. Interpretable models such as MCM can support these efforts by resolving latent mechanisms and "deeper" biophenotype that may differ between clinically similar patients; such as the dysfunction of specific neurotransmitter systems (Chapter 4: *Clinically similar subjects have different underlying receptor alterations*) or physiological interactions.

Neurotransmission imbalance in neurodegenerative diseases

Besides their canonical role in neuronal signal transduction, neurotransmitters are involved in maintaining essential processes such as neurovascular coupling [91] [92].

Conversely, optimal neurotransmission requires the coordination of multiple (neuronal and non-neuronal) cell types [136], and cell dysfunction or death may impact neurotransmission. Furthermore, neurotransmitter systems interact not just with other processes, but also with each other [109]. Dopamine can influence the excitability of cholinergic neurons [146], nicotinic cholinergic receptors generally seem to have a modulatory role [127], and serotonin modulates glutamatergic and GABAergic neurotransmission in several brain regions [741].

Consequently, neurotransmission balance is a critical to healthy brain function. Multi-receptor "fingerprints" of various brain areas are distinct [424] [423]. The excitatory/inhibitory balance between glutamatergic and GABAergic systems has a strong influence on cortical dynamics, and the cholinergic and adrenergic systems maintain the balance between segregation and integration [742]. The cholinergic system allows segregation by modulating multiplicative gain selectively, the noradrenergic system allows integration by broadly affecting response gain.

Disease can thus involve neurotransmission dysfunction bidirectionally and in complex ways, including loss of function and compensatory upregulation (e.g., M_1 cholinergic receptors are upregulated in temporal cortex of DLB patients [130]). However, as alluded earlier, the present formulation of re-MCM does not explicitly model alterations in receptor distributions, nor can it conclude whether receptor parameters reflect altered distributions or functional interactions. Incorporating neurotransmission (as some combination of transmitters, receptors and transporters) as state variables in detailed biophysical models, particularly where individualized PET data is available, may be a promising avenue to resolve the directionality of interactions with other physiological processes [486].

Clinically, the synergistic roles of multi-neurotransmitter system alterations in AD and PD may help explain the molecular and cellular basis of neurotransmitter therapy side effects and non-response [123] [126] [743] [25].

Validation of treatment response

Coupled differential equations are suited to modeling complex systems composed of interacting factors. Particularly relevant for clinical applications, input response can be simulated, and optimal (e.g., minimum dose) combinatorial therapeutic interventions can be determined using control theory [33] [387]. However, these models typically rely on certain assumptions, such as linear time-invariance in the case of this thesis. While this allows a well-developed mathematical framework to be applied [744], its biological validity would need to be verified in living organisms. Nevertheless, we note that the temporal scales considered in this work (~6 month follow ups for generally less than 5 years) may justify the assumption of local linearity, relative to the long temporal scale of neurodegeneration. Furthermore, we note the relatively high model fit using this approach (e.g., ~70% average explained variance in the ADNI cohort).

In the interpretation of mathematical models of biological systems, it is important to avoid the “prediction-explanation fallacy”; prediction-optimized models that fit the data well do not necessarily replicate the same data-generating processes [745]. An important validation of dynamical systems models such as re-MCM would be the accurate simulation of interventions (e.g., treatment response). While this thesis lacked intervention effects, they would be an important validation. In animal models, more invasive interventional studies can be performed (e.g., injection of misfolded proteins or localized brain stimulation) to validated model-predicted input response.

Finally, the precise implementations of as well as theoretical assumptions behind brain network controllability [746] [535] [747] remain unverified in living organisms.

Guiding clinical practice and personalized medicine

Neurotransmitter-based medications have been at the core of clinical treatment for decades, from levodopa for PD to cholinesterase inhibitors and glutamatergic antagonists for dementias [711] [32]. However, they provide only symptomatic therapy, often with non-response or side effects. Furthermore, while recent anti-amyloid monoclonal antibody treatments have shown some improvements in symptomatic progression, the clinical importance is a subject of debate [27] [28]. We propose that these failures are due to i) the use of generalized medicine without consideration for the vast heterogeneity in pathology and symptoms between patients and ii) the focus on single targets whereas the disrupted pathways in AD and PD are multi-factorial. Personalized computational models allow us to account for both of these reasons, to infer combinatorial and individual-specific therapeutic needs [562] [563].

Clinically, misdiagnosis can occur due to the overlap in early symptoms and lack of definitive biomarkers. A critical consequence of misdiagnosis is an inappropriate treatment plan. One-fifth to one-third of patients misdiagnosed with AD may be receiving inappropriate medication, which typically involves acetylcholinesterase inhibitors or glutamate blockers (especially during these studies prior to the approval of anti-amyloid monoclonal antibodies) [263]. With sufficient validation in diverse clinical cohorts, model-based inference of individualized neurotransmission dysfunction may better resolve specific latent mechanisms to be targeted (Chapter 4, *Clinically similar subjects have different underlying receptor alterations*), and dynamical system models can be used to design optimal combinatorial therapy [33].

In addition to localized effects of brain stimulation [387] or manipulation of macroscopic imaging-derived variables [33], incorporating pharmacokinetics may be necessary to accurately model drug response [661]. This may be particularly relevant to oral neurotransmitter-based medication, where factors such the blood-brain barrier (impermeable to large molecules and most small molecules) must be considered [230]. Modelling treatment response may be one avenue to resolve open questions after the current wave of anti-amyloid therapy, such as the optimal timing, duration and dose of treatment [37] [51]. Given the importance of peripheral and systemic risk factors in neurodegeneration [89], extensions may even consider how cardiovascular and metabolic systems influence spatiotemporal brain degeneration.

Given the multiple physiological systems affected and the vast heterogeneity within neurodegenerative disorders such as AD and PD [13] [743], personalized and precision medicine approaches may be necessary to determine effective targets, doses, durations and timing for combinatorial therapy. Practically, personalized medicine requires large datasets with sufficient diversity to capture rare disease subtypes, selection of participants at the suitable disease stages and appropriate harmonization across sites and cohorts [748].

Chapter 7. Conclusion

There is a scientific and clinical need for an integrative and comprehensive systems-level understanding of the role of neurotransmission dysfunction in multi-scale neurodegenerative changes [29]. This thesis has presented a dynamical system model of multi-factorial physiological alterations in AD and PD, mediated by the receptor architecture of the brain. This constitutes first computational model considering several physiological processes, multi-neurotransmitter dysfunction and multi-domain symptomatic decline in AD and PD.

This work supports the claim that the neurotransmitter receptor architecture of brain helps explain regional vulnerability to various neurodegenerative changes. Inter-individual differences receptor-mediated interactions correlate strongly with distinct disease axes in both AD and PD, supporting the perspective that these disorders are multi-factorial and involve widespread neurotransmission dysfunction. Comparisons with normative distributions suggest that model-inferred mechanisms of overall neurotransmission dysfunction are relevant correlates of clinical severity. The potential spatial variability in these dysfunctional interactions, and other potential cellular/molecular drivers of neurodegeneration are promising avenues of immediate extension. This work sets the stage for an integrative computational modeling incorporating cellular/molecular template atlases and individualized neuroimaging data to ultimately infer optimal treatment targets for neurodegenerative disease patients.

Bibliography

[1] B. Dugger and D. Dickson, "Pathology of neurodegenerative diseases," *Cold Spring Harbor perspectives in biology,* vol. 9, no. 7, p. a028035, 2017.

[2] L. Pihlstrøm, S. Wiethoff and H. Houlden, "Genetics of neurodegenerative diseases: an overview," *Handbook of clinical neurology,* vol. 145, pp. 309-323, 2018.

[3] M. Chin-Chan, J. Navarro-Yepes and B. Quintanilla-Vega, "Environmental pollutants as risk factors for neurodegenerative disorders: Alzheimer and Parkinson diseases," *Frontiers in cellular neuroscience,* vol. 9, p. 124, 2015.

[4] Y. Hou, X. Dan, M. Babbar, Y. Wei, S. Hasselbalch, D. Croteau and V. Bohr, "Ageing as a risk factor for neurodegenerative disease," *Nature Reviews Neurology,* vol. 15, no. 10, pp. 565-581, 09 September 2019.

[5] R. Nussbaum and C. Ellis, "Alzheimer's disease and Parkinson's disease," *New england journal of medicine,* vol. 348, no. 14, pp. 1356-1364, 2003.

[6] R. Mayeux and Y. Stern, "Epidemiology of Alzheimer disease," *Cold Spring Harbor perspectives in medicine,* vol. 2, no. 8, p. a006239, 2012.

[7] L. De Lau and M. Breteler, "Epidemiology of Parkinson's disease," *The Lancet Neurology,* vol. 5, no. 6, pp. 525-535, 2006.

[8] E. Nichols, J. Steinmetz, S. Vollset, K. Fukutaki, J. Chalek, F. Abd-Allah, A. Abdoli, A. Abualhasan, E. Abu-Gharbieh, T. Akram and H. Al Hamad, "Estimation of the global prevalence of dementia in 2019 and forecasted prevalence in 2050: an analysis for the Global Burden of Disease Study 2019," *The Lancet Public Health,* vol. 7, no. 2, pp. e105-e125, 2022.

[9] E. Dorsey, A. Elbaz, E. Nichols, N. Abbasi, F. Abd-Allah, A. Abdelalim, J. Adsuar, M. Ansha, C. Brayne, J. Choi and D. Collado-Mateo, "Global, regional, and national burden of Parkinson's disease, 1990–2016: a systematic analysis for the Global Burden of Disease Study," *The Lancet Neurology,* vol. 17, no. 11, pp. 939-953, 2018.

[10] A. Tahami Monfared, M. Byrnes, L. White and Q. Zhang, "The humanistic and economic burden of Alzheimer's disease," *Neurology and therapy,* vol. 11, no. 2, pp. 525-551, 2022.

[11] N. Titova, C. Padmakumar, S. J. G. Lewis and K. R. Chaudhuri, "Parkinson's: a syndrome rather than a disease?," *Journal of Neural Transmission,* vol. 124, pp. 907-914, 27 December 2016.

[12] J. De la Torre, "Alzheimer disease as a vascular disorder: nosological evidence," *Stroke,* vol. 33, no. 4, pp. 1152-1162, 2002.

[13] D. Ferreira, A. Nordberg and E. Westman, "Biological subtypes of Alzheimer disease: A systematic review and meta-analysis," *Neurology,* vol. 94, no. 10, pp. 436-448, 2020.

[14] D. Berg, P. Borghammer, S. Fereshtehnejad, S. Heinzel, J. Horsager, E. Schaeffer and R. Postuma, "Prodromal Parkinson disease subtypes—key to understanding heterogeneity," *Nature Reviews Neurology,* vol. 17, no. 6, pp. 349-361, 2021.

[15] R. Bateman, C. Xiong, T. Benzinger, A. Fagan, A. Goate, N. Fox, D. Marcus, N. Cairns, X. Xie, T. Blazey and D. Holtzman, "Clinical and biomarker changes in dominantly inherited Alzheimer's disease," *New England Journal of Medicine,* vol. 367, no. 9, pp. 795-804, 2012.

[16] A. Staffaroni, M. Quintana, B. Wendelberger, H. Heuer, L. Russell, Y. Cobigo, A. Wolf, S. Goh, L. Petrucelli, T. Gendron and C. Heller, "Temporal order of clinical and biomarker changes in familial frontotemporal dementia," *Nature medicine,* vol. 28, no. 10, pp. 2194-2206, 2022.

[17] V. Villemagne, S. Burnham, P. Bourgeat, B. Brown, K. Ellis, O. Salvado, C. Szoeke, S. Macaulay, R. Martins, P. Maruff and D. Ames, "Amyloid β deposition, neurodegeneration, and cognitive decline in sporadic Alzheimer's disease: a prospective cohort study," *The Lancet Neurology,* vol. 12, no. 4, pp. 357-367, 2013.

[18] S. Gauthier, H. Zhang, K. Ng, T. Pascoal and P. Rosa-Neto, "Impact of the biological definition of Alzheimer's disease using amyloid, tau and neurodegeneration (ATN): what about the role of vascular changes, inflammation, Lewy body pathology?," *Translational neurodegeneration,* vol. 1, no. 1-7, p. 7, 2018.

[19] X. Yan, Y. Hu, B. Wang, S. Wang and X. Zhang, "Metabolic dysregulation contributes to the progression of Alzheimer's disease," *Frontiers in neuroscience,* vol. 14, p. 530219, 2020.

[20] S. Cunnane, S. Nugent, M. Roy, A. Courchesne-Loyer, E. Croteau, S. Tremblay, A. Castellano, F. Pifferi, C. Bocti, N. Paquet and H. Begdouri, "Brain fuel metabolism, aging, and Alzheimer's disease," *Nutrition,* vol. 27, no. 1, pp. 3-20, 2011.

[21] J. Kinney, S. Bemiller, A. Murtishaw, A. Leisgang, A. Salazar and B. Lamb, "Inflammation as a central mechanism in Alzheimer's disease," *Alzheimer's & Dementia: Translational Research & Clinical Interventions,* vol. 4, pp. 575-590, 2018.

[22] M. Sweeney, A. Montagne, A. Sagare, D. Nation, L. Schneider, H. Chui, M. Harrington, J. Pa, M. Law, D. Wang and R. Jacobs, "Vascular dysfunction—the disregarded partner of Alzheimer's disease," *Alzheimer's & Dementia,* vol. 15, no. 1, pp. 158-167, 2019.

[23] A. Schapira, K. Chaudhuri and P. Jenner, "Non-motor features of Parkinson disease," *Nature Reviews Neuroscience,* vol. 18, no. 7, pp. 435-450, 2017.

[24] N. Titova, S. Lewis, C. Padmakumar and K. Chaudhuri, "Parkinson's: a syndrome rather than a disease?," *Journal of Neural Transmission,* vol. 124, no. 8, 2017.

[25] P. T. Francis, M. J. Ramírez and M. K. Lai, "Neurochemical basis for symptomatic treatment of alzheimer's disease," *Neuropharmacology,* vol. 59, no. 4-5, p. 221–229, 2010.

[26] H. Fu, J. Hardy and K. Duff, "Selective vulnerability in neurodegenerative diseases," *Nature Neuroscience,* vol. 21, no. 10, pp. 1350-1358, 2018.

[27] M. Ebell, H. Barry, K. Baduni and G. Grasso, "Clinically Important Benefits and Harms of Monoclonal Antibodies Targeting Amyloid for the Treatment of Alzheimer Disease: A Systematic Review and Meta-Analysis," *The Annals of Family Medicine,* vol. 22, no. 1, pp. 50-62, 2024.

[28] J. Cummings, "Meaningful benefit and minimal clinically important difference (MCID) in Alzheimer's disease: Open peer commentary," *Alzheimer's & Dementia: Translational Research & Clinical Interventions,* vol. 9, no. 3, p. e12411, 2023.

[29] N. Taylor and J. Shine, "A whole new world: embracing the systems-level to understand the indirect impact of pathology in neurodegenerative disorders," *Journal of Neurology,* vol. 270, no. 4, pp. 1969-1975, 2023.

[30] T. Golde, "Disease-modifying therapies for Alzheimer's disease: more questions than answers," *Neurotherapeutics,* vol. 19, no. 1, pp. 209-227, 2023.

[31] W. Heiss and K. Herholz, "Brain receptor imaging," *Journal of Nuclear Medicine,* vol. 47, no. 2, pp. 302-312, 2006.

[32] R. Kandimalla and P. H. Reddy, "Therapeutics of neurotransmitters in alzheimer's disease," *Journal of Alzheimer's Disease,* vol. 57, no. 4, pp. 1049-1069, 2017.

[33] Y. Iturria-Medina, F. Carbonell, R. Sotero, F. Chouinard-Decorte, A. Evans and A. D. N. Initiative, "Multifactorial causal model of brain (dis)organization and therapeutic intervention: Application to Alzheimer's disease," *Neuroimage,* vol. 152, pp. 60-77, 2017.

[34] H. Hippius and G. Neundörfer, "The discovery of Alzheimer's disease," *Dialogues in clinical neuroscience,* vol. 5, no. 1, pp. 101-108, 2003.

[35] J. Hardy and G. Higgins, "Alzheimer's disease: the amyloid cascade hypothesis," *Science,* vol. 256, no. 5054, pp. 184-185, 1992.

[36] R. O'Brien and P. Wong, "Amyloid precursor protein processing and Alzheimer's disease," *Annual review of neuroscience,* vol. 34, pp. 185-204, 2011.

[37] Y. Lian, Y. Jia, J. Wong, X. Zhou, W. Song, J. Guo, C. Masters and Y. Wang, "Clarity on the blazing trail: clearing the way for amyloid-removing therapies for Alzheimer's disease," *Molecular psychiatry,* pp. 1-9, 2023.

[38] D. Selkoe, "Normal and abnormal biology of the beta-amyloid precursor protein," *Annual review of neuroscience,* vol. 17, no. 1, pp. 489-517, 1994.

[39] M. Mattson, B. Cheng, D. Davis, K. Bryant, I. Lieberburg and R. Rydel, "beta-Amyloid peptides destabilize calcium homeostasis and render human cortical neurons vulnerable to excitotoxicity," *Journal of Neuroscience,* vol. 12, no. 2, pp. 376-389, 1992.

[40] D. Selkoe and J. Hardy, "The amyloid hypothesis of Alzheimer's disease at 25 years," *EMBO molecular medicine,* vol. 8, no. 6, pp. 595-608, 2016.

[41] M. Busche and B. Hyman, "Synergy between amyloid-β and tau in Alzheimer's disease," *Nature neuroscience,* vol. 23, no. 10, pp. 1183-1193, 2020.

[42] S. Nath, L. Agholme, F. Kurudenkandy, B. Granseth, J. Marcusson and M. Hallbeck, "Spreading of neurodegenerative pathology via neuron-to-neuron transmission of β-amyloid," *Journal of Neuroscience,* vol. 32, no. 26, pp. 8767-8777, 2012.

[43] X. Li, S. Ospitalieri, T. Robberechts, L. Hofmann, C. Schmid, A. Rijal Upadhaya, M. Koper, C. von Arnim, S. Kumar, M. Willem and K. Gnoth, "Seeding, maturation and propagation of amyloid β-peptide aggregates in Alzheimer's disease," *Brain,* vol. 145, no. 10, pp. 3558-3570, 2022.

[44] D. Thal, J. Attems and M. Ewers, "Spreading of amyloid, tau, and microvascular pathology in Alzheimer's disease: findings from neuropathological and neuroimaging studies," *Journal of Alzheimer's Disease,* vol. 42, no. s4, pp. S421-S429, 2014.

[45] J. Domert, S. Rao, L. Agholme, A. Brorsson, J. Marcusson, M. Hallbeck and S. Nath, "Spreading of amyloid-β peptides via neuritic cell-to-cell transfer is dependent on insufficient cellular clearance," *Neurobiology of disease,* vol. 65, pp. 82-92, 2014.

[46] K. Wildsmith, M. Holley, J. Savage, R. Skerrett and G. Landreth, "Evidence for impaired amyloid β clearance in Alzheimer's disease," *Alzheimer's research & therapy,* vol. 5, no. 4, pp. 1-6, 2013.

[47] K. Ezzat, A. Sturchio and A. Espay, "The shift to a proteinopenia paradigm in neurodegeneration," *Handbook of Clinical Neurology,* vol. 193, pp. 23-32, 2023.

[48] H. Hampel, J. Hardy, K. Blennow, C. Chen, G. Perry, S. Kim, V. Villemagne, P. Aisen, M. Vendruscolo, T. Iwatsubo and C. Masters, "The amyloid-β pathway in Alzheimer’s disease," *Molecular psychiatry,* vol. 26, no. 10, pp. 5481-5503, 2021.

[49] F. Kametani and M. Hasegawa, "Reconsideration of amyloid hypothesis and tau hypothesis in Alzheimer's disease," *Frontiers in neuroscience,* vol. 12, p. 25, 2018.

[50] E. Karran and B. De Strooper, "The amyloid hypothesis in Alzheimer disease: new insights from new therapeutics," *Nature Reviews Drug Discovery,* vol. 21, no. 4, pp. 306-318, 2022.

[51] C. Haass and D. Selkoe, "If amyloid drives Alzheimer disease, why have anti-amyloid therapies not yet slowed cognitive decline?," *PLoS biology,* vol. 20, no. 7, p. e3001694, 2022.

[52] W. Jagust, C. Teunissen and C. DeCarli, "The complex pathway between amyloid β and cognition: implications for therapy," *The Lancet Neurology,* vol. 22, no. 9, pp. 847-857, 2023.

[53] E. Hill, T. Karikari, K. Moffat, M. Richardson and M. Wall, "Introduction of tau oligomers into cortical neurons alters action potential dynamics and disrupts synaptic transmission and plasticity," *eneuro,* vol. 6, no. 5, pp. 1-20, 2019.

[54] C. Jack Jr, D. Knopman, W. Jagust, R. Petersen, M. Weiner, P. Aisen, L. Shaw, P. Vemuri, H. Wiste, S. Weigand and T. Lesnick, "Update on hypothetical

model of Alzheimer's disease biomarkers," *Lancet Neurology,* vol. 12, no. 2, p. 207, 2013.

[55] G. Bloom, "Amyloid-β and tau: the trigger and bullet in Alzheimer disease pathogenesis," *JAMA neurology,* vol. 71, no. 4, pp. 505-508, 2014.

[56] H. Braak and E. Braak, "Neuropathological stageing of Alzheimer-related changes," *Acta neuropathologica,* vol. 82, no. 4, pp. 239-259, 1991.

[57] R. van der Kant, L. Goldstein and R. Ossenkoppele, "Amyloid-β-independent regulators of tau pathology in Alzheimer disease," *Nature Reviews Neuroscience,* vol. 21, no. 1, pp. 21-35, 2020.

[58] Y. Zhang, K. Wu, L. Yang, Q. Dong and J. Yu, "Tauopathies: new perspectives and challenges," *Molecular Neurodegeneration,* vol. 17, no. 1, p. 28, 2022.

[59] J. Robinson, E. Lee, S. Xie, L. Rennert, E. Suh, C. Bredenberg, C. Caswell, V. Van Deerlin, N. Yan, A. Yousef and H. Hurtig, "Neurodegenerative disease concomitant proteinopathies are prevalent, age-related and APOE4-associated," *Brain,* vol. 141, no. 7, pp. 2181-2193, 2018.

[60] R. van der Kant, L. Goldstein and R. Ossenkoppele, "Amyloid-β-independent regulators of tau pathology in Alzheimer disease," *Nature Reviews Neuroscience,* vol. 21, no. 1, pp. 21-35, 2020.

[61] E. Coon and W. Singer, "Synucleinopathies," *Continuum (Minneapolis, Minn.),* vol. 26, no. 1, p. 72, 2020.

[62] H. McCann, C. Stevens, H. Cartwright and G. Halliday, "α-Synucleinopathy phenotypes," *Parkinsonism & related disorders,* vol. 20, pp. S62-S67, 2014.

[63] I. Brás and T. Outeiro, "Alpha-synuclein: mechanisms of release and pathology progression in synucleinopathies," *Cells,* vol. 10, no. 2, p. 375, 2021.

[64] S. Roshanbin, M. Xiong, G. Hultqvist, L. Söderberg, O. Zachrisson, S. Meier, S. Ekmark-Lewén, J. Bergström, M. Ingelsson, D. Sehlin and S. Syvänen, "In vivo imaging of alpha-synuclein with antibody-based PET," *Neuropharmacology,* vol. 208, p. 1089, 2022.

[65] T. Simuni, L. Chahine, K. Poston, M. Brumm, T. Buracchio, M. Campbell, S. Chowdhury, C. Coffey, L. Concha-Marambio, T. Dam and P. DiBiaso, "A biological definition of neuronal α-synuclein disease: towards an integrated staging system for research," *The Lancet Neurology,* vol. 23, no. 2, pp. 178-190, 2024.

[66] D. Twohig and H. Nielsen, "α-synuclein in the pathophysiology of Alzheimer's disease," *Molecular Neurodegeneration,* vol. 14, no. 1, pp. 1-19, 2019.

[67] H. Nakashima-Yasuda, K. Uryu, J. Robinson, S. Xie, H. Hurtig, J. Duda, S. Arnold, A. Siderowf, M. Grossman, J. Leverenz and R. Woltjer, "Co-morbidity of TDP-43 proteinopathy in Lewy body related diseases," *Acta neuropathologica,* vol. 114, pp. 221-229, 2007.

[68] H. Chen and J. Mitchell, "Mechanisms of TDP-43 proteinopathy onset and propagation," *International Journal of Molecular Sciences,* vol. 22, no. 11, p. 6004, 2021.

[69] A. Knight, C. Morrone, C. Varlow, W. Yu, P. McQuade and N. Vasdev, "Head-to-head comparison of tau-PET radioligands for imaging TDP-43 in post-mortem ALS brain," *Molecular Imaging and Biology,* vol. 25, no. 3, pp. 513-527, 2023.

[70] B. James, R. Wilson, P. Boyle, J. Trojanowski, D. Bennett and J. Schneider, "TDP-43 stage, mixed pathologies, and clinical Alzheimer's-type dementia," *Brain,* vol. 139, no. 11, pp. 2983-2993, 2016.

[71] J. Gao, L. Wang, M. Huntley, G. Perry and X. Wang, "Pathomechanisms of TDP-43 in neurodegeneration," *Journal of neurochemistry,* vol. 146, no. 1, pp. 7-20, 2018.

[72] P. Boyle, R. Wilson, L. Yu, A. Barr, W. Honer, J. Schneider and D. Bennett, "Much of late life cognitive decline is not due to common neurodegenerative pathologies," *Annals of neurology,* vol. 74, no. 3, pp. 478-489, 2013.

[73] A. Kouli, L. Spindler, T. Fryer, Y. Hong, M. Malpetti, F. Aigbirhio, S. White, M. Camacho, J. O'Brien and C. Williams-Gray, "Neuroinflammation is linked to dementia risk in Parkinson's disease," *Brain,* vol. 147, p. 923–935, 2024.

[74] F. Heppner, R. Ransohoff and B. Becher, "Immune attack: the role of inflammation in Alzheimer disease," *Nature Reviews Neuroscience,* vol. 16, no. 6, pp. 358-372, 2015.

[75] M. Tansey, R. Wallings, M. Houser, M. Herrick, C. Keating and V. Joers, "Inflammation and immune dysfunction in Parkinson disease," *Nature Reviews Immunology,* vol. 22, no. 11, pp. 657-673, 2022.

[76] E. Werry, F. Bright, O. Piguet, L. Ittner, G. Halliday, J. Hodges, M. Kiernan, C. Loy, J. Kril and M. Kassiou, "Recent developments in TSPO PET

imaging as a biomarker of neuroinflammation in neurodegenerative disorders," *International journal of molecular sciences,* vol. 20, no. 13, p. 3161, 2019.

[77] T. Bartels, S. De Schepper and S. Hong, "Microglia modulate neurodegeneration in Alzheimer's and Parkinson's diseases," *Science,* vol. 370, no. 6512, pp. 66-69, 2020.

[78] A. Tan, S. Lim and A. Lang, "The microbiome–gut–brain axis in Parkinson disease—from basic research to the clinic," *Nature Reviews Neurology,* vol. 18, no. 8, pp. 476-495, 2022.

[79] E. Haroon, A. Miller and G. Sanacora, "Inflammation, glutamate, and glia: a trio of trouble in mood disorders," *Neuropsychopharmacology,* vol. 42, no. 1, pp. 193-215, 2017.

[80] B. Bellaver, G. Povala, P. Ferreira, J. Ferrari-Souza, D. Leffa, F. Lussier, A. Benedet, N. Ashton, G. Triana-Baltzer, H. Kolb and C. Tissot, "Astrocyte reactivity influences amyloid-β effects on tau pathology in preclinical Alzheimer's disease," *Nature Medicine,* vol. 29, p. 1775–1781 , 2023.

[81] S. Sadigh-Eteghad, A. Majdi, J. Mahmoudi, S. Golzari and M. Talebi, "Astrocytic and microglial nicotinic acetylcholine receptors: an overlooked issue in Alzheimer's disease," *Journal of neural transmission,* vol. 123, pp. 1359-1367, 2016.

[82] M. Lee, "Neurotransmitters and microglial-mediated neuroinflammation," *Current Protein and Peptide Science,* vol. 14, no. 1, pp. 21-32, 2013.

[83] D. Feinstein, S. Kalinin and D. Braun, "Causes, consequences, and cures for neuroinflammation mediated via the locus coeruleus: noradrenergic signaling system," *Journal of neurochemistry,* vol. 139, pp. 154-178, 2016.

[84] J. Rivers-Auty, A. Mather, R. Peters, C. Lawrence and D. Brough, "Anti-inflammatories in Alzheimer's disease—potential therapy or spurious correlate?," *Brain communications,* vol. 2, no. 2, p. p.fcaa109, 2020.

[85] C. Xing, T. Tarumi, J. Liu, Y. Zhang, M. Turner, J. Riley, C. Tinajero, L. Yuan and R. Zhang, "Distribution of cardiac output to the brain across the adult lifespan," *Journal of Cerebral Blood Flow & Metabolism,* vol. 37, no. 8, pp. 2848-2856, 2017.

[86] Y. Iturria-Medina, R. C. Sotero, P. J. Toussaint, J. M. Mateos-Pérez, A. C. Evans and t. A. D. N. Initiative, "Early role of vascular dysregulation on late-onset Alzheimer's disease based on multifactorial data-driven analysis," *Nature Communications,* vol. 7, no. 1, pp. 1-14, 2016.

[87] J. De La Torre, "The vascular hypothesis of Alzheimer's disease: a key to preclinical prediction of dementia using neuroimaging," *Journal of Alzheimer's Disease,* vol. 63, no. 1, pp. 35-52, 2018.

[88] C. Finger, I. Moreno-Gonzalez, A. Gutierrez, J. Moruno-Manchon and L. McCullough, "Age-related immune alterations and cerebrovascular inflammation," *Molecular psychiatry,* vol. 27, no. 2, pp. 803-818, 2022.

[89] V. Hachinski, K. Einhäupl, D. Ganten, S. Alladi, C. Brayne, B. Stephan, M. Sweeney, B. Zlokovic, Y. Iturria-Medina, C. Iadecola and N. Nishimura, "Preventing dementia by preventing stroke: the Berlin Manifesto," *Alzheimer's & Dementia,* vol. 15, no. 7, pp. 961-984, 2019.

[90] K. Govindpani, L. McNamara, N. Smith, C. Vinnakota, H. Waldvogel, R. Faull and A. Kwakowsky, "Vascular dysfunction in Alzheimer's disease: a prelude to the pathological process or a consequence of it?," *Journal of clinical medicine,* vol. 8, no. 5, p. 651, 2019.

[91] D. Attwell, A. Buchan, S. Charpak, M. Lauritzen, B. MacVicar and E. Newman, "Glial and neuronal control of brain blood flow," *Nature,* vol. 468, no. 7321, pp. 232-243, 2010.

[92] J.-K. Choi, Y. I. Chen, E. Hamel and B. G. Jenkins, "Brain hemodynamic changes mediated by dopamine receptors: Role of the cerebral microvasculature in dopamine-mediated neurovascular coupling," *Neuroimage,* vol. 30, no. 3, pp. 700-712, 2006.

[93] N. Sibson, A. Dhankhar, G. Mason, D. Rothman, K. Behar and R. Shulman, "Stoichiometric coupling of brain glucose metabolism and glutamatergic neuronal activity," *Proceedings of the National Academy of Sciences,* vol. 95, no. 1, pp. 316-321, 1998.

[94] K. Jellinger, "Prevalence of cerebrovascular lesions in Parkinson's disease. A postmortem study," *Acta neuropathologica,* vol. 105, pp. 415-419, 2003.

[95] K. Jellinger and J. Attems, "Prevalence and impact of vascular and Alzheimer pathologies in Lewy body disease," *Acta neuropathologica,* vol. 115, pp. 427-436, 2008.

[96] A. Korczyn, "Vascular parkinsonism—characteristics, pathogenesis and treatment," *Nature Reviews Neurology,* vol. 11, no. 6, pp. 319-326., 2015.

[97] R. Terry, E. Masliah, D. Salmon, N. Butters, R. DeTeresa, R. Hill, L. Hansen and R. Katzman, "Physical basis of cognitive alterations in Alzheimer's disease: synapse loss is the major correlate of cognitive impairment," *Annals of*

Neurology: Official Journal of the American Neurological Association and the Child Neurology Society, vol. 30, no. 4, pp. 572-580, 1991.

[98] G. Aliev, H. Palacios, B. Walrafen, A. Lipsitt, M. Obrenovich and L. Morales, "Brain mitochondria as a primary target in the development of treatment strategies for Alzheimer disease," *The International Journal of Biochemistry & Cell Biology,* vol. 41, no. 10, pp. 1989-2004, 2009.

[99] H. Girouard and C. Iadecola, "Neurovascular coupling in the normal brain and in hypertension, stroke, and Alzheimer disease," *Journal of applied physiology,* vol. 100, no. 1, pp. 328-335, 2006.

[100] C. Iadecola, "Neurovascular regulation in the normal brain and in Alzheimer's disease," *Nature Reviews Neuroscience,* vol. 5, no. 5, pp. 347-360, 2004.

[101] W. Poewe, K. Seppi, C. Tanner, G. Halliday, P. Brundin, J. Volkmann, A. Schrag and A. Lang, "Parkinson disease," *Nature reviews Disease primers,* vol. 3, no. 1, pp. 1-21, 2017.

[102] J. W. Mink, R. J. Blumenschine and D. B. Adams, "Ratio of central nervous system to body metabolism in vertebrates: Its constancy and functional basis," *American Journal of Physiology-Regulatory, Integrative and Comparative Physiology,* vol. 231, no. 3, pp. R203-R212, 1981.

[103] J. J. Harris, R. Jolivet and D. Attwell, "Synaptic energy use and supply," *Neuron,* vol. 75, no. 5, pp. 762-777, 2012.

[104] L. Moroz, D. Romanova and A. Kohn, "Neural versus alternative integrative systems: molecular insights into origins of neurotransmitters," *Philosophical Transactions of the Royal Society B,* vol. 376, no. 1821, p. 20190762, 2021.

[105] C. M. McCann, J. Tapia, H. Kim, J. S. Coggan and J. Lichtman, "Rapid and modifiable neurotransmitter receptor dynamics at a neuronal synapse in vivo," *Nature neuroscience,* vol. 11, no. 7, p. 807, 2008.

[106] S. Davis, A. Cirincione, A. Jimenez-Torres and J. Zhu, "The Impact of Neurotransmitters on the Neurobiology of Neurodegenerative Diseases," *International Journal of Molecular Sciences,* vol. 24, no. 20, p. 15340, 2023.

[107] R. Teleanu, A. Niculescu, E. Roza, O. Vladâcenco, A. Grumezescu and D. Teleanu, "Neurotransmitters—Key Factors in Neurological and Neurodegenerative Disorders of the Central Nervous System," *International Journal of Molecular Sciences,* vol. 23, no. 11, p. 5954, 2022.

[108] M. Waxham, "Chapter 10 - Neurotransmitter receptors," in *From Molecules to Networks (Third Edition)*, Cambridge, Massachusetts, Academic Press, 2014, pp. 285-321.

[109] R. Webster, "Neurotransmitter systems and function," in *Neurotransmitters, drugs and brain function*, Hoboken, New Jersey, United States, John Wiley & Sons Ltd, 2001, pp. 1-32.

[110] D. Lovinger, Y. Mateo, K. Johnson, S. Engi, M. Antonazzo and J. Cheer, "Local modulation by presynaptic receptors controls neuronal communication and behaviour," *Nature Reviews Neuroscience,* vol. 23, no. 4, pp. 191-203, 2022.

[111] I. Wessler and C. Kirkpatrick, "Acetylcholine beyond neurons: the non-neuronal cholinergic system in humans," *British journal of pharmacology,* vol. 154, no. 8, pp. 1558-1571, 2008.

[112] M. Nedergaard, T. Takano and A. Hansen, "Beyond the role of glutamate as a neurotransmitter," *Nature Reviews Neuroscience,* vol. 3, no. 9, pp. 748-755, 2002.

[113] J. Pocock and H. Kettenmann, "Neurotransmitter receptors on microglia," *Trends in neurosciences,* vol. 30, no. 10, pp. 527-535, 2007.

[114] H. Liu, R. Leak and X. Hu, "Neurotransmitter receptors on microglia," *Stroke and vascular neurology,* vol. 1, p. e000012, 2016.

[115] M. Mattson, "Pathways towards and away from Alzheimer's disease," *Nature,* vol. 430, no. 7000, pp. 631-639, 2004.

[116] A. Martorana and G. Koch, "Is dopamine involved in Alzheimer's disease?," *Frontiers in aging neuroscience,* vol. 6, p. 252, 2014.

[117] S. Shang, H. Zhang, Y. Feng, J. Wu, W. Dou, Y. Chen and X. Yin, "Region-Specific neurovascular decoupling associated with cognitive decline in parkinson’s disease," *Frontiers in aging neuroscience,* vol. 13, p. 770528, 2021.

[118] A. Zarkali, P. McColgan, L. Leyland, A. Lees, G. Rees and R. Weil, "Organisational and neuromodulatory underpinnings of structural-functional connectivity decoupling in patients with Parkinson’s disease," *Communications biology,* vol. 4, no. 1, pp. 1-13, 2021.

[119] N. Bohnen, A. Yarnall, R. Weil, E. Moro, M. Moehle, P. Borghammer, M. Bedard and R. Albin, "Cholinergic system changes in Parkinson's disease: emerging therapeutic approaches," *The Lancet Neurology,* vol. 21, no. 4, pp. 381-392, 2022.

[120] M. Politis and F. Niccolini, "Serotonin in Parkinson's Disease," *Behavioural Brain Research,* vol. 277, pp. 136-145, 2015.

[121] Y. Grimbergen, J. Langston, R. Roos and B. Bloem, "Postural instability in Parkinson's disease: the adrenergic hypothesis and the locus coeruleus," *Expert review of neurotherapeutics,* vol. 9, no. 2, pp. 279-290, 2009.

[122] A. A. Kehagia, R. A. Barker and T. W. Robbins, "Cognitive impairment in Parkinson's disease: the dual syndrome hypothesis," *Neurodegenerative diseases,* vol. 11, no. 2, pp. 79-92, 2013.

[123] L. Brichta, P. Greengard and M. Flajolet, "Advances in the pharmacological treatment of Parkinson's disease: targeting neurotransmitter systems," *Trends in neurosciences,* vol. 36, no. 9, pp. 543-54, 2013.

[124] Y. Xu, J. Yan, P. Zhou, J. Li, H. Gao, Y. Xia and Q. Wang, "Neurotransmitter receptors and cognitive dysfunction in alzheimer's disease and parkinson's disease," *Progress in neurobiology,* vol. 97, no. 1, p. 1–13, 2012.

[125] A. Haake, K. Nguyen, L. Friedman, B. Chakkamparambil and G. Grossberg, "An update on the utility and safety of cholinesterase inhibitors for the treatment of Alzheimer's disease," *Expert opinion on drug safety,* vol. 19, no. 2, pp. 147-157, 2020.

[126] A. Espay, F. Morgante, A. Merola, A. Fasano, L. Marsili, S. Fox, E. Bezard, B. Picconi, P. Calabresi and A. Lang, "Levodopa-induced dyskinesia in Parkinson disease: current and evolving concepts," *Annals of Neurology,* vol. 84, no. 6, pp. 797-811, 2018.

[127] T. Ferreira-Vieira, I. Guimaraes, F. Silva and F. Ribeiro, "Alzheimer's disease: targeting the cholinergic system," *Current neuropharmacology,* vol. 14, no. 1, pp. 101-115, 2016.

[128] A. Contestabile, "The history of the cholinergic hypothesis," *Behavioural brain research,* vol. 221, no. 2, pp. 334-340, 2011.

[129] H. Hampel, M. Mesulam, A. Cuello, M. Farlow, E. Giacobini, G. Grossberg, A. Khachaturian, A. Vergallo, E. Cavedo, P. Snyder and Z. Khachaturian, "The cholinergic system in the pathophysiology and treatment of Alzheimer's disease," *Brain,* vol. 141, no. 7, pp. 1917-1933, 2018.

[130] P. Francis and E. Perry, "Cholinergic and Other Neurotransmitter Mechanisms in Parkinson's Disease, Parkinson's Disease Dementia, and Dementia with Lewy Bodies," *Movement Disorders,* vol. 22, no. S17, p. 351–357, 2007.

[131] J. Claassen and R. Jansen, "Cholinergically mediated augmentation of cerebral perfusion in alzheimer's disease and related cognitive disorders: the cholinergic–vascular hypothesis," *The Journals of Gerontology Series A: Biological Sciences and Medical Sciences,* vol. 61, no. 3, pp. 267-271, 2006.

[132] A. Sheldon and M. Robinson, "The role of glutamate transporters in neurodegenerative diseases and potential opportunities for intervention," *Neurochemistry international,* vol. 51, no. 6-7, pp. 333-355, 2007.

[133] I. Ip, A. Berrington, A. Hess, A. Parker, U. Emir and H. Bridge, "Combined fMRI-MRS acquires simultaneous glutamate and BOLD-fMRI signals in the human brain," *Neuroimage,* vol. 155, pp. 113-119, 2017.

[134] J. Watkins and D. Jane, "The glutamate story," *British journal of pharmacology,* vol. 147, no. S1, pp. S100-S108, 2006.

[135] C. Lüscher and R. Malenka, "NMDA receptor-dependent long-term potentiation and long-term depression (LTP/LTD)," *Cold Spring Harbor perspectives in biology,* vol. 4, no. 6, p. p.a005710, 2012.

[136] A. Todd and G. Hardingham, "The regulation of astrocytic glutamate transporters in health and neurodegenerative diseases," *International journal of molecular sciences,* vol. 21, no. 24, p. 9607, 2020.

[137] F. Hyder, A. Patel, A. Gjedde, D. Rothman, K. Behar and R. Shulman, "Neuronal–glial glucose oxidation and glutamatergic–GABAergic function," *Journal of Cerebral Blood Flow & Metabolism,* vol. 26, no. 7, pp. 865-877, 2006.

[138] M. Angulo, A. Kozlov, S. Charpak and E. Audinat, "Glutamate released from glial cells synchronizes neuronal activity in the hippocampus," *Journal of Neuroscience,* vol. 24, no. 31, pp. 6920-6927, 2004.

[139] J. Wang, F. Wang, D. Mai and S. Qu, "Molecular mechanisms of glutamate toxicity in Parkinson's disease," *Frontiers in Neuroscience,* vol. 14, p. 585584, 2020.

[140] D. Belov Kirdajova, J. Kriska, J. Tureckova and M. Anderova, "Ischemia-triggered glutamate excitotoxicity from the perspective of glial cells," *Frontiers in cellular neuroscience,* vol. 14, p. 51, 2020.

[141] S. Tekkök and M. Goldberg, "Ampa/kainate receptor activation mediates hypoxic oligodendrocyte death and axonal injury in cerebral white matter," *Journal of Neuroscience,* vol. 21, no. 12, pp. 4237-4248, 2001.

[142] J. Liu, L. Chang, Y. Song, H. Li and Y. Wu, "The role of NMDA receptors in Alzheimer's disease," *Frontiers in neuroscience,* vol. 13, p. 43, 2019.

[143] Z. Wang, J. Zhao and S. Li, "Dysregulation of synaptic and extrasynaptic N-methyl-D-aspartate receptors induced by amyloid-β," *Neuroscience Bulletin,* vol. 29, pp. 752-760, 2013.

[144] X. Sun, Q. Tuo, Z. Liuyang, A. Xie, X. Feng, X. Yan, M. Qiu, S. Li, X. Wang, F. Cao and X. Wang, "Extrasynaptic NMDA receptor-induced tau overexpression mediates neuronal death through suppressing survival signaling ERK phosphorylation," *Cell death & disease,* vol. 7, no. 11, pp. e2449-e2449, 2016.

[145] M. Armstrong and M. Okun, "Diagnosis and treatment of Parkinson disease: a review," *Jama,* vol. 323, no. 6, pp. 548-560, 2020.

[146] A. Martorana, F. Mori, Z. Esposito, H. Kusayanagi, F. Monteleone, C. Codeca, G. Sancesario, G. Bernardi and G. Koch, "Dopamine modulates cholinergic cortical excitability in Alzheimer's disease patients," *Neuropsychopharmacology,* vol. 34, no. 10, pp. 2323-2328, 2009.

[147] N. Kemppainen, M. Laine, M. Laakso, V. Kaasinen, K. Någren, T. Vahlberg, T. Kurki and J. Rinne, "Hippocampal dopamine D2 receptors correlate with memory functions in Alzheimer's disease," *European journal of neuroscience,* vol. 18, no. 1, pp. 149-154, 2003.

[148] K. Lee, B. Clennell, T. Steward, A. Gialeli, O. Cordero-Llana and D. Whitcomb, "Focused ultrasound stimulation as a neuromodulatory tool for Parkinson’s disease: a scoping review," *Brain Sciences,* vol. 12, no. 2, p. 289, 2022.

[149] K. Govindpani, B. Calvo-Flores Guzmán, C. Vinnakota, H. Waldvogel, R. Faull and A. Kwakowsky, "Towards a better understanding of GABAergic remodeling in Alzheimer’s disease," *International journal of molecular sciences,* vol. 18, no. 8, p. 1813, 2017.

[150] B. Calvo-Flores Guzmán, C. Vinnakota, K. Govindpani, H. Waldvogel, R. Faull and A. Kwakowsky, "The GABAergic system as a therapeutic target for Alzheimer's disease," *Journal of neurochemistry,* vol. 146, no. 6, pp. 649-669, 2018.

[151] R. Whittington, A. Bretteville, M. Dickler and E. Planel, "Anesthesia and tau pathology," *Progress in Neuro-Psychopharmacology and Biological Psychiatry,* vol. 47, pp. 147-155, 2013.

[152] Y. Li, H. Sun, Z. Chen, H. Xu, G. Bu and H. Zheng, "Implications of GABAergic neurotransmission in Alzheimer’s disease," *Frontiers in aging neuroscience,* vol. 8, p. 31, 2016.

[153] R. Bekdash, "The cholinergic system, the adrenergic system and the neuropathology of Alzheimer's disease," *International Journal of Molecular Sciences,* vol. 22, no. 3, p. 1273, 2021.

[154] M. Betts, E. Kirilina, M. Otaduy, D. Ivanov, J. Acosta-Cabronero, M. Callaghan, C. Lambert, A. Cardenas-Blanco, K. Pine, L. Passamonti and C. Loane, "Locus coeruleus imaging as a biomarker for noradrenergic dysfunction in neurodegenerative diseases," *Brain,* vol. 142, no. 9, pp. 2558-2571, 2019.

[155] B. Matchett, L. Grinberg, P. Theofilas and M. Murray, "The mechanistic link between selective vulnerability of the locus coeruleus and neurodegeneration in Alzheimer's disease," *Acta neuropathologica,* vol. 141, no. 5, pp. 631-650, 2021.

[156] H. Braak and K. Del Tredici, "Where, when, and in what form does sporadic Alzheimer's disease begin?," *Current opinion in neurology,* vol. 25, no. 6, pp. 708-714, 2012.

[157] M. Mesulam, "Cholinergic circuitry of the human nucleus basalis and its fate in Alzheimer's disease," *Journal of Comparative Neurology,* vol. 521, no. 18, pp. 4124-4144, 2013.

[158] K. Dyer-Reaves, A. Goodman, A. Nelson and L. McMahon, "Alpha1-adrenergic receptor mediated long-term depression at CA3-CA1 synapses can be induced via accumulation of endogenous norepinephrine and is preserved following noradrenergic denervation," *Frontiers in synaptic neuroscience,* vol. 11, p. 27, 2019.

[159] F. Zhang, M. Gannon, Y. Chen, S. Yan, S. Zhang, W. Feng, J. Tao, B. Sha, Z. Liu, T. Saito and T. Saido, "β-amyloid redirects norepinephrine signaling to activate the pathogenic GSK3β/tau cascade," *Science Translational Medicine,* vol. 12, no. 526, 2020.

[160] S. Song, L. Jiang, E. Oyarzabal, B. Wilson, Z. Li, Y. Shih, Q. Wang and J. Hong, "Loss of brain norepinephrine elicits neuroinflammation-mediated oxidative injury and selective caudo-rostral neurodegeneration," *Molecular neurobiology,* vol. 56, p. 2653–2669, 2019.

[161] R. Kalaria, A. Andorn and S. Harik, "Alterations in adrenergic receptors of frontal cortex and cerebral microvessels in Alzheimer's disease and aging," *Progress in clinical and biological research,* vol. 317, pp. 367-374, 1989.

[162] P. Karczewski, P. Hempel and M. Bimmler, "Role of alpha1-adrenergic receptor antibodies in Alzheimer's disease," *Front. Biosci,* vol. 23, pp. 2082-2089, 2018.

[163] L. Jones, E. Sun, A. Martin and D. Keating, "The ever-changing roles of serotonin," *The international journal of biochemistry & cell biology,* vol. 125, p. 105776, 2020.

[164] Y. Xie, P. Liu, Y. Lian, H. Liu and J. Kang, "The effect of selective serotonin reuptake inhibitors on cognitive function in patients with Alzheimer's disease and vascular dementia: focusing on fluoxetine with long follow-up periods," *Signal transduction and targeted therapy,* vol. 4, no. 1, p. 30, 2019.

[165] M. Husain, "Transdiagnostic neurology: neuropsychiatric symptoms in neurodegenerative diseases," *Brain,* vol. 140, no. 6, pp. 1535-1536, 2017.

[166] J. Cirrito, B. Disabato, J. Restivo, D. Verges, W. Goebel, A. Sathyan, D. Hayreh, G. D'Angelo, T. Benzinger, H. Yoon and J. Kim, "Serotonin signaling is associated with lower amyloid-β levels and plaques in transgenic mice and humans," *Proceedings of the National Academy of Sciences,* vol. 108, no. 36, pp. 14968-14973, 2011.

[167] G. Reynolds, L. Arnold, M. Rossor, L. Iversen, C. Mountjoy and M. Roth, "Reduced binding of [3H] ketanserin to cortical 5-HT2 receptors in senile dementia of the Alzheimer type," *Neuroscience letters,* vol. 44, no. 1, pp. 47-51, 1984.

[168] J. Blin, J. Baron, B. Dubois, C. Crouzel, M. Fiorelli, D. Attar-Lévy, B. Pillon, D. Fournier, M. Vidailhet and Y. Agid, "Loss of brain 5-HT2 receptors in Alzheimer's disease: in vivo assessment with positron emission tomography and (18) setoperone," *Brain,* vol. 116, no. 3, pp. 497-510, 1993.

[169] S. Claeysen, J. Bockaert and P. Giannoni, "Serotonin: a new hope in Alzheimer's disease?," *ACS chemical neuroscience,* vol. 6, no. 7, pp. 940-943, 2015.

[170] V. Kotagal, C. Spino, N. Bohnen, R. Koeppe and R. Albin, "Serotonin, β-amyloid, and cognition in Parkinson disease," *Annals of neurology,* vol. 83, no. 5, pp. 994-1002, 2018.

[171] R. Mittal, L. Debs, A. Patel, D. Nguyen, K. Patel, G. O'Connor, M. Grati, J. Mittal, D. Yan, A. Eshraghi and S. Deo, "Neurotransmitters: The critical modulators regulating gut–brain axis," *Journal of cellular physiology,* vol. 232, no. 9, pp. 2359-2372, 2017.

[172] K. McVey Neufeld, J. Bienenstock, A. Bharwani, K. Champagne-Jorgensen, Y. Mao, C. West, Y. Liu, M. Surette, W. Kunze and P. Forsythe, "Oral selective serotonin reuptake inhibitors activate vagus nerve dependent gut-brain signalling," *Scientific reports,* vol. 9, no. 1, p. 14290, 2019.

[173] G. Chételat, J. Arbizu, H. Barthel, V. Garibotto, I. Law, S. Morbelli, E. van de Giessen, F. Agosta, F. Barkhof, D. Brooks and M. Carrillo, "Amyloid-PET and 18F-FDG-PET in the diagnostic investigation of Alzheimer's disease and other dementias," *The Lancet Neurology,* vol. 19, no. 11, pp. 951-962, 2020.

[174] G. Frisoni, N. Fox, C. Jack Jr, P. Scheltens and P. Thompson, "The clinical use of structural MRI in Alzheimer disease," *Nature Reviews Neurology,* vol. 6, no. 2, pp. 67-77, 2010.

[175] L. Pini, M. Pievani, M. Bocchetta, D. Altomare, P. Bosco, E. Cavedo, S. Galluzzi, M. Marizzoni and G. Frisoni, "Brain atrophy in Alzheimer's disease and aging," *Ageing research reviews,* vol. 30, pp. 25-48, 2016.

[176] K. Poulakis, J. Pereira, P. Mecocci, B. Vellas, M. Tsolaki, I. Kłoszewska, H. Soininen, S. Lovestone, A. Simmons, L. Wahlund and E. Westman, "Heterogeneous patterns of brain atrophy in Alzheimer's disease," *Neurobiology of aging,* vol. 65, pp. 98-108, 2018.

[177] R. Ossenkoppele, C. Lyoo, C. Sudre, D. van Westen, H. Cho, Y. Ryu, J. Choi, R. Smith, O. Strandberg, S. Palmqvist and E. Westman, "Distinct tau PET patterns in atrophy-defined subtypes of Alzheimer's disease," *Alzheimer's & dementia,* vol. 16, no. 2, pp. 335-344, 2020.

[178] T. Ballarini, K. Mueller, F. Albrecht, F. Růžička, O. Bezdicek, E. Růžička, J. Roth, J. Vymazal, R. Jech and M. Schroeter, "Regional gray matter changes and age predict individual treatment response in Parkinson's disease," *NeuroImage: Clinical,* vol. 21, p. 101636, 2019.

[179] K. Rosenberg-Katz, T. Herman, Y. Jacob, N. Giladi, T. Hendler and J. Hausdorff, "Gray matter atrophy distinguishes between Parkinson disease motor subtypes," *Neurology,* vol. 80, no. 16, pp. 1476-1484, 2013.

[180] J. Filoteo, J. Reed, I. Litvan and D. Harrington, "Volumetric correlates of cognitive functioning in nondemented patients with Parkinson's disease," *Movement Disorders,* vol. 29, no. 3, pp. 360-367, 2014.

[181] M. Glasser, M. Goyal, T. Preuss, M. Raichle and D. Van Essen, "Trends and properties of human cerebral cortex: correlations with cortical myelin content," *Neuroimage,* vol. 93, pp. 165-175, 2014.

[182] M. Uddin, T. Figley, K. Solar, A. Shatil and C. Figley, "Comparisons between multi-component myelin water fraction, T1w/T2w ratio, and diffusion tensor imaging measures in healthy human brain structures," *Scientific reports,* vol. 9, no. 1, p. 2500, 2019.

[183] D. Pareto, A. Garcia-Vidal, M. Alberich, C. Auger, X. Montalban, M. Tintoré, J. Sastre-Garriga and À. Rovira, "Ratio of T1-weighted to T2-weighted

signal intensity as a measure of tissue integrity: comparison with magnetization transfer ratio in patients with multiple sclerosis," *American Journal of Neuroradiology,* vol. 41, no. 3, pp. 461-463, 2020.

[184] M. Mühlau, "T1/T2-weighted ratio is a surrogate marker of demyelination in multiple sclerosis: No," *Multiple Sclerosis Journal,* vol. 28, no. 3, pp. 355-356, 2022.

[185] R. Righart, V. Biberacher, L. Jonkman, R. Klaver, P. Schmidt, D. Buck, A. Berthele, J. Kirschke, C. Zimmer, B. Hemmer, J. Geurts and M. Mühlau, "Cortical pathology in multiple sclerosis detected by the T 1/T 2-weighted ratio from routine magnetic resonance imaging," *Annals of neurology,* vol. 82, no. 4, pp. 519-529., 2017.

[186] C. Beaulieu, "The basis of anisotropic water diffusion in the nervous system–a technical review," *NMR in Biomedicine: An International Journal Devoted to the Development and Application of Magnetic Resonance In Vivo,* vol. 15, no. 7-8, pp. 435-455, 2002.

[187] D. Alexander, T. Dyrby, M. Nilsson and H. Zhang, "Imaging brain microstructure with diffusion MRI: practicality and applications," *NMR in Biomedicine,* vol. 32, no. 4, p. e3841, 2019.

[188] Y. Iturria-Medina, E. Canales-Rodríguez, L. Melie-García, P. Valdés-Hernández, E. Martínez-Montes, Y. Alemán-Gómez and J. Sánchez-Bornot, "Characterizing brain anatomical connections using diffusion weighted MRI and graph theory.," *Neuroimage,* vol. 36, no. 3, pp. 645-660, 2007.

[189] P. Nucifora, R. Verma, S. Lee and E. Melhem, "Diffusion-tensor MR imaging and tractography: exploring brain microstructure and connectivity," *Radiology,* vol. 245, no. 2, pp. 367-384, 2007.

[190] P. Basser, J. Mattiello and D. LeBihan, "MR diffusion tensor spectroscopy and imaging," *Biophysical journal,* vol. 66, no. 1, pp. 259-267, 1994.

[191] H. Torrey, "Bloch equations with diffusion terms," *Physical review,* vol. 104, no. 3, p. 563, 1956.

[192] M. Afzali, T. Pieciak, S. Newman, E. Garyfallidis, E. Özarslan, H. Cheng and D. Jones, "The sensitivity of diffusion MRI to microstructural properties and experimental factors," *Journal of Neuroscience Methods,* vol. 347, p. 108951, 2021.

[193] C. Figley, M. Uddin, K. Wong, J. Kornelsen, J. Puig and T. Figley, "Potential pitfalls of using fractional anisotropy, axial diffusivity, and radial

diffusivity as biomarkers of cerebral white matter microstructure," *Frontiers in Neuroscience,* vol. 15, p. 799576, 2022.

[194] J. Scholz, V. Tomassini and H. Johansen-Berg, "Individual differences in white matter microstructure in the healthy brain," in *Diffusion mri*, Academic Press, 2014, pp. 301-316.

[195] P. Winklewski, A. Sabisz, E. Szurowska and A. Szarmach, "Understanding the physiopathology behind axial and radial diffusivity changes—what do we know?," *Frontiers in neurology,* vol. 9, p. 336887, 2018.

[196] M. Budde, J. Kim, H. Liang, R. Schmidt, J. Russell, A. Cross and S. Song, "Toward accurate diagnosis of white matter pathology using diffusion tensor imaging," *Magnetic Resonance in Medicine: An Official Journal of the International Society for Magnetic Resonance in Medicine,* vol. 57, no. 4, pp. 688-695, 2007.

[197] E. Chang, M. Argyelan, M. Aggarwal, T. Chandon, K. Karlsgodt, S. Mori and A. Malhotra, "The role of myelination in measures of white matter integrity: combination of diffusion tensor imaging and two-photon microscopy of CLARITY intact brains," *Neuroimage,* vol. 147, pp. 253-261, 2017.

[198] E. Panagiotaki, T. Schneider, B. Siow, M. Hall, M. Lythgoe and D. Alexander, "Compartment models of the diffusion MR signal in brain white matter: a taxonomy and comparison," *Neuroimage,* vol. 59, no. 3, pp. 2241-2254, 2012.

[199] Y. Zhang, N. Schuff, A. Du, H. Rosen, J. Kramer, M. Gorno-Tempini, B. Miller and M. Weiner, "White matter damage in frontotemporal dementia and Alzheimer's disease measured by diffusion MRI," *Brain,* vol. 132, no. 9, pp. 2579-2592, 2009.

[200] M. Bergamino, E. Keeling, V. Mishra, A. Stokes and R. Walsh, "Assessing white matter pathology in early-stage Parkinson disease using diffusion MRI: a systematic review," *Frontiers in neurology,* vol. 11, p. 314, 2020.

[201] H. Kim, S. Kim, H. Kim, C. Choi, N. Kim, S. Han, E. Jang, S. Chung and C. Lee, "Alterations of mean diffusivity in brain white matter and deep gray matter in Parkinson's disease," *Neuroscience letters,* vol. 550, pp. 64-68, 2013.

[202] N. Spotorno, O. Strandberg, E. Stomrud, S. Janelidze, K. Blennow, M. Nilsson, D. van Westen and O. Hansson, "Diffusion MRI tracks cortical microstructural changes during the early stages of Alzheimer’s disease," *Brain,* vol. 147, no. 3, p. 961–969, 2023.

[203] B. Jeurissen, M. Descoteaux, S. Mori and A. Leemans, "Diffusion MRI fiber tractography of the brain," *NMR in Biomedicine,* vol. 32, no. 4, p. e3785, 2019.

[204] T. Sarwar, K. Ramamohanarao and A. Zalesky, "Mapping connectomes with diffusion MRI: deterministic or probabilistic tractography?," *Magnetic resonance in medicine,* vol. 81, no. 2, pp. 1368-1384, 2019.

[205] S. Jbabdi and H. Johansen-Berg, "Tractography: where do we go from here?," *Brain connectivity,* vol. 1, no. 3, pp. 169-183, 2011.

[206] M. Yu, O. Sporns and A. Saykin, "The human connectome in Alzheimer disease—relationship to biomarkers and genetics," *Nature Reviews Neurology,* vol. 17, no. 9, pp. 545-563., 2021.

[207] F. Carbonell, Y. Iturria-Medina and A. Evans, "Mathematical modeling of protein misfolding mechanisms in neurological diseases: a historical overview," *Frontiers in Neurology,* vol. 9, p. 37, 2018.

[208] J. Torok, C. Anand, P. Verma and A. Raj, "Connectome-based biophysics models of Alzheimer's disease diagnosis and prognosis," *Translational Research,* vol. 254, pp. 13-23, 2023.

[209] J. Vogel, N. Corriveau-Lecavalier, N. Franzmeier, J. Pereira, J. Brown, A. Maass, H. Botha, W. Seeley, D. Bassett, D. Jones and M. Ewers, "Connectome-based modelling of neurodegenerative diseases: towards precision medicine and mechanistic insight," *Nature Reviews Neuroscience,* pp. 1-20, 2023.

[210] A. Raj, "Graph models of pathology spread in Alzheimer's disease: an alternative to conventional graph theoretic analysis," *Brain connectivity,* vol. 11, no. 10, pp. 799-814, 2021.

[211] P. Bandettini, "Twenty years of functional MRI: the science and the stories," *Neuroimage,* vol. 62, no. 2, pp. 575-588, 2012.

[212] S. Ogawa, T. Lee, A. Nayak and P. Glynn, "Oxygenation-sensitive contrast in magnetic resonance image of rodent brain at high magnetic fields," *Magnetic resonance in medicine,* vol. 14, no. 1, pp. 68-78, 1990.

[213] N. Logothetis and B. Wandell, "Interpreting the BOLD signal," *Annu. Rev. Physiol.,* no. 66, pp. 735-769, 2004.

[214] P. Fox, "The coupling controversy," *Neuroimage,* vol. 62, no. 2, pp. 594-601, 2012.

[215] N. Logothetis, "What we can do and what we cannot do with fMRI," *Nature,* vol. 453, no. 7197, pp. 869-878, 2008.

[216] P. Vemuri, D. Jones and C. Jack, "Resting state functional MRI in Alzheimer's Disease," *Alzheimer's research & therapy,* vol. 4, pp. 1-9, 2012.

[217] L. Ferreira and G. Busatto, "Resting-state functional connectivity in normal brain aging," *Neuroscience & Biobehavioral Reviews,* vol. 37, no. 3, pp. 384-400, 2013.

[218] L. Yang, Y. Yan, Y. Wang, X. Hu, J. Lu, P. Chan, T. Yan and Y. Han, "Gradual disturbances of the amplitude of low-frequency fluctuations (ALFF) and fractional ALFF in Alzheimer spectrum," *Frontiers in neuroscience,* vol. 12, p. 423937, 2018.

[219] F. de Vos, M. Koini, T. Schouten, S. Seiler, J. van der Grond, A. Lechner, R. Schmidt, M. de Rooij and S. Rombouts, "A comprehensive analysis of resting state fMRI measures to classify individual patients with Alzheimer's disease.," *Neuroimage,* vol. 15, no. 167, pp. 62-72, 15 February 2018.

[220] Y. Tang, L. Meng, C. Wan, Z. Liu, W. Liao, X. Yan, X. Wang, B. Tang and J. Guo, "Identifying the presence of Parkinson's disease using low-frequency fluctuations in BOLD signals," *Neuroscience letters,* vol. 645, pp. 1-6, 2017.

[221] A. Koretsky, "Is there a path beyond BOLD? Molecular imaging of brain function," *Neuroimage,* vol. 62, no. 2, pp. 1208-1215, 2012.

[222] M. Wintermark, M. Sesay, E. Barbier, K. Borbély, W. Dillon, J. Eastwood, T. Glenn, C. Grandin, S. Pedraza, J. Soustiel and T. Nariai, "Comparative overview of brain perfusion imaging techniques," *Stroke,* vol. 36, no. 9, pp. e83-e99, 2005.

[223] X. Golay, J. Hendrikse and T. Lim, "Perfusion imaging using arterial spin labeling," *Topics in Magnetic Resonance Imaging,* vol. 15, no. 1, pp. 10-27, 2004.

[224] Y. Chen, D. Wolk, J. Reddin, M. Korczykowski, P. Martinez, E. Musiek, A. Newberg, P. Julin, S. Arnold, J. Greenberg and J. Detre, "Voxel-level comparison of arterial spin-labeled perfusion MRI and FDG-PET in Alzheimer disease," *Neurology,* vol. 77, no. 22, pp. 1977-1985, 2011.

[225] L. Zhu, K. Ploessl and H. Kung, "PET/SPECT imaging agents for neurodegenerative diseases," *Chemical Society Reviews,* vol. 43, no. 19, pp. 6683-6691, 2014.

[226] N. Gharibkandi and S. Hosseinimehr, "Radiotracers for imaging of Parkinson's disease," *European journal of medicinal chemistry,* vol. 166, pp. 75-89, 2019.

[227] W. Moses, "Fundamental limits of spatial resolution in PET," *Nuclear Instruments and Methods in Physics Research Section A: Accelerators, Spectrometers, Detectors and Associated Equipment,* vol. 648, pp. S236-S240, 2011.

[228] A. Rahmim and H. Zaidi, "PET versus SPECT: strengths, limitations and challenges," *Nuclear medicine communications,* vol. 29, no. 3, pp. 193-207, 2008.

[229] R. Gunn, M. Slifstein, G. Searle and J. Price, "Quantitative imaging of protein targets in the human brain with PET," *Physics in Medicine & Biology,* vol. 60, no. 22, p. R363, 2015.

[230] W. Pardridge, "Drug transport across the blood–brain barrier," *Journal of cerebral blood flow & metabolism,* vol. 32, no. 11, pp. 1959-1972, 2012.

[231] R. Laforce Jr, J. Soucy, L. Sellami, C. Dallaire-Théroux, F. Brunet, D. Bergeron, B. Miller and R. Ossenkoppele, "Molecular imaging in dementia: Past, present, and future.," *Alzheimer's & Dementia,* vol. 14, no. 11, pp. 1522-1552, 2018.

[232] W. Kreisl, M. Kim, J. Coughlin, I. Henter, D. Owen and R. Innis, "PET imaging of neuroinflammation in neurological disorders," *The Lancet Neurology,* vol. 19, no. 11, pp. 940-950, 2020.

[233] T. Pascoal, A. Benedet, N. Ashton, M. Kang, J. Therriault, M. Chamoun, M. Savard, F. Lussier, C. Tissot, T. Karikari and J. Ottoy, "Microglial activation and tau propagate jointly across Braak stages," *Nature medicine,* vol. 27, no. 9, pp. 1592-1599, 2021.

[234] C. van der Weijden, E. Biondetti, I. Gutmann, H. Dijkstra, R. McKerchar, D. de Paula Faria, E. de Vries, J. Meilof, R. Dierckx, V. Prevost and A. Rauscher, "Quantitative myelin imaging with MRI and PET: an overview of techniques and their validation status," *Brain,* vol. 146, no. 4, pp. 1243-1266, 2023.

[235] W. Weber, J. Czernin, C. Anderson, R. Badawi, H. Barthel, F. Bengel, L. Bodei, I. Buvat, M. DiCarli, M. Graham and J. Grimm, "The future of nuclear medicine, molecular imaging, and theranostics," *Journal of Nuclear Medicine,* vol. 61, no. Supplement 2, pp. 263S-272S, 2020.

[236] C. Jack Jr, D. Bennett, K. Blennow, M. Carrillo, B. Dunn, S. Haeberlein, D. Holtzman, W. Jagust, F. Jessen, J. Karlawish and E. Liu, "NIA-AA research

framework: toward a biological definition of Alzheimer's disease," *Alzheimer's & Dementia,* vol. 14, no. 4, pp. 535-562, 2018.

[237] D. Perani, "FDG PET and cognitive symptoms of dementia," *Clinical and Translational Imaging,* vol. 1, pp. 247-260, 2013.

[238] J. Brettschneider, K. Tredici, V. Lee and J. Trojanowski, "Spreading of pathology in neurodegenerative diseases: a focus on human studies," *Nature Reviews Neuroscience,* vol. 16, no. 2, pp. 109-120, 2015.

[239] R. Ossenkoppele, W. Jansen, G. Rabinovici, D. Knol, W. van der Flier, B. van Berckel, P. Scheltens, P. Visser, S. Verfaillie, M. Zwan and S. Adriaanse, "Prevalence of amyloid PET positivity in dementia syndromes: a meta-analysis," *JAMA,* vol. 313, no. 19, pp. 1939-1950, 2015.

[240] A. Macedo, C. Tissot, J. Therriault, S. Servaes, Y. Wang, J. Fernandez-Arias, N. Rahmouni, F. Lussier, M. Vermeiren, G. Bezgin and P. Vitali, "The Use of Tau PET to Stage Alzheimer Disease According to the Braak Staging Framework," *Journal of Nuclear Medicine,* vol. 64, no. 8, pp. 1171-1178, 2023.

[241] J. Vogel, Y. Iturria-Medina, O. Strandberg, R. Smith, E. Levitis, A. Evans and O. Hansson, "Spread of pathological tau proteins through communicating neurons in human Alzheimer's disease," *Nature communications,* vol. 11, no. 1, p. 2612, 2020.

[242] J. Vogel, A. Young, N. Oxtoby, R. Smith, R. Ossenkoppele, O. Strandberg, R. La Joie, L. Aksman, M. Grothe and Y. Iturria-Medina, "Four distinct trajectories of tau deposition identified in Alzheimer's disease," *Nature medicine,* vol. 27, no. 5, pp. 871-881, 2021.

[243] D. Berron, J. Vogel, P. Insel, J. Pereira, L. Xie, L. Wisse, P. Yushkevich, S. Palmqvist, N. Mattsson-Carlgren, E. Stomrud and R. Smith, "Early stages of tau pathology and its associations with functional connectivity, atrophy and memory," *Brain,* vol. 144, no. 9, pp. 2771-2783, 2021.

[244] C. Groot, S. Villeneuve, R. Smith, O. Hansson and R. Ossenkoppele, "Tau PET imaging in neurodegenerative disorders," *Journal of Nuclear Medicine,* vol. 63, no. (Supplement 1), pp. 20S-26S, 2022.

[245] M. Bucci, K. Chiotis, A. Nordberg and A. D. N. Initiative, "Alzheimer's disease profiled by fluid and imaging markers: tau PET best predicts cognitive decline," *Molecular Psychiatry,* vol. 26, no. 10, pp. 5888-5898, 2021.

[246] A. Aschenbrenner, B. Gordon, T. Benzinger, J. Morris and J. Hassenstab, "Influence of tau PET, amyloid PET, and hippocampal volume on cognition in Alzheimer disease," *Neurology,* vol. 91, no. 9, pp. e859-e866, 2018.

[247] W. Frankle and M. Laruelle, "Neuroreceptor imaging in psychiatric disorders," *Annals of nuclear medicine,* vol. 16, pp. 437-446, 2002.

[248] A. Lammertsma, "Forward to the past: the case for quantitative PET imaging," *Journal of Nuclear Medicine,* vol. 58, no. 7, pp. 1019-1024, 2017.

[249] A. Takano, A. Varrone, B. Gulyás, P. Salvadori, A. Gee, A. Windhorst, J. Vercouillie, G. Bormans, A. Lammertsma and C. Halldin, "Guidelines to PET measurements of the target occupancy in the brain for drug development," *European journal of nuclear medicine and molecular imaging,* vol. 43, pp. 2255-2262, 2016.

[250] E. Novotny Jr, R. Fulbright, P. Pearl, K. Gibson and D. Rothman, "Magnetic resonance spectroscopy of neurotransmitters in human brain," *Annals of Neurology: Official Journal of the American Neurological Association and the Child Neurology Society,* vol. 54, no. S6, pp. S25-S31, 2003.

[251] Y. Koush, D. Rothman, K. Behar, R. de Graaf and F. Hyder, "Human brain functional MRS reveals interplay of metabolites implicated in neurotransmission and neuroenergetics," *Journal of Cerebral Blood Flow & Metabolism,* vol. 42, no. 6, pp. 911-934, 2022.

[252] C. Pilgrim and W. Stumpf, "Applications of autoradiography in neurobiological research," *Journal of Histochemistry & Cytochemistry,* vol. 35, no. 8, pp. 917-928, 1987.

[253] K. Zilles and N. and Palomero-Gallagher, "Multiple transmitter receptors in regions and layers of the human cerebral cortex," *Frontiers in neuroanatomy,* vol. 11, p. 78, 2017.

[254] C. Olanow, K. Kieburtz and A. Schapira, "Why have we failed to achieve neuroprotection in Parkinson's disease?," *Annals of Neurology: Official Journal of the American Neurological Association and the Child Neurology Society,* vol. 64, no. S2, pp. S101-S110, 2008.

[255] J. Sims, J. Zimmer, C. Evans, M. Lu, P. Ardayfio, J. Sparks, A. Wessels, S. Shcherbinin, H. Wang, E. Nery and E. Collins, "Donanemab in early symptomatic Alzheimer disease: the TRAILBLAZER-ALZ 2 randomized clinical trial," *Jama,* vol. 330, no. 6, pp. 512-527, 2023.

[256] C. Van Dyck, C. Swanson, P. Aisen, R. Bateman, C. Chen, M. Gee, M. Kanekiyo, D. Li, L. Reyderman, S. Cohen and L. Froelich, "Lecanemab in early Alzheimer's disease," *New England Journal of Medicine,* vol. 388, no. 1, pp. 9-21, 2023.

[257] M. Mortberg, S. Vallabh and E. Minikel, "Disease stages and therapeutic hypotheses in two decades of neurodegenerative disease clinical trials," *Scientific Reports,* vol. 12, no. 1, p. 17708, 2022.

[258] N. Berchtold and C. Cotman, "Neurobiology of aging," *Evolution in the conceptualization of dementia and Alzheimer's disease: Greco-Roman period to the 1960s,* vol. 19, no. 3, pp. 173-189, 1998.

[259] C. G. Goetz, "The history of Parkinson's disease: early clinical descriptions and neurological therapies," *Cold Spring Harbor Perspectives in Medicine,* vol. 1, no. 1, p. a008862, 2011.

[260] D. Knopman, R. Petersen and C. Jack, "A brief history of "Alzheimer disease": Multiple meanings separated by a common name," *Neurology,* vol. 92, no. 22, pp. 1053-1059, 2019.

[261] S. Das, Z. Zhang and L. Ang, "Clinicopathological overlap of neurodegenerative diseases: A comprehensive review," *Journal of Clinical Neuroscience,* vol. 78, pp. 30-33, 2020.

[262] G. Rizzo, M. Copetti, S. Arcuti, D. Martino, A. Fontana and G. Logroscino, "Accuracy of clinical diagnosis of Parkinson disease: a systematic review and meta-analysis," *Neurology,* vol. 86, no. 6, pp. 566-576, 2016.

[263] J. Gaugler, H. Ascher-Svanum, D. Roth, T. Fafowora, A. Siderowf and T. Beach, "Characteristics of patients misdiagnosed with Alzheimer's disease and their medication use: an analysis of the NACC-UDS database," *BMC geriatrics,* vol. 13, no. 1, pp. 1-10, 2013.

[264] R. Postuma, D. Berg, M. Stern, W. Poewe, C. Olanow, W. Oertel, J. Obeso, K. Marek, I. Litvan, A. Lang and G. Halliday, "MDS clinical diagnostic criteria for Parkinson's disease," *Movement disorders,* vol. 30, no. 12, pp. 1591-1601, 2015.

[265] D. Berg, R. Postuma, C. Adler, B. Bloem, P. Chan, B. Dubois, T. Gasser, C. Goetz, G. Halliday, L. Joseph and A. Lang, "MDS research criteria for prodromal Parkinson's disease," *Movement Disorders,* vol. 30, no. 12, pp. 1600-1611, 2015.

[266] W. Weiner, "There is no Parkinson disease," *Archives of neurology,* vol. 65, no. 6, pp. 705-708, 2008.

[267] A. Bayón, "Degenerative dementias: A question of syndrome or disease?," *Neurología (English Edition),* vol. 37, no. 6, pp. 480-491, 2022.

[268] A. Buchman, L. Yu, S. Oveisgharan, J. Farfel, J. Schneider and D. Bennett, "Person-specific contributions of brain pathologies to progressive parkinsonism in

older adults," *The Journals of Gerontology: Series A,* vol. 76, no. 4, pp. 615-621, 2021.

[269] Y. Chu, W. Hirst and J. Kordower, "Chapter 4 - Mixed pathology as a rule, not exception: Time to reconsider disease nosology," in *Handbook of Clinical Neurology*, Elsevier, 2023, pp. 57-71.

[270] M. DeTure and D. Dickson, "The neuropathological diagnosis of Alzheimer's disease," *Molecular Neurodegeneration,* vol. 14, no. 1, pp. 1-18, 2019.

[271] K. Jellinger, "Recent update on the heterogeneity of the Alzheimer's disease spectrum," *Journal of Neural Transmission,* vol. 129, no. 1, pp. 1-24, 2022.

[272] D. Thomas, S. Bajaj, K. McRae-McKee, C. Hadjichrysanthou, R. Anderson and J. Collinge, "Association of TDP-43 proteinopathy, cerebral amyloid angiopathy, and Lewy bodies with cognitive impairment in individuals with or without Alzheimer's disease neuropathology," *Scientific reports,* vol. 10, no. 1, p. 14579, 2020.

[273] M. Azarpazhooh, A. Avan, L. Cipriano, D. Munoz, L. Sposato and V. Hachinski, "Concomitant vascular and neurodegenerative pathologies double the risk of dementia," *Alzheimer's & Dementia,* vol. 14, no. 2, pp. 148-156, 2018.

[274] J. Schneider, Z. Arvanitakis, W. Bang and D. Bennett, "Mixed brain pathologies account for most dementia cases in community-dwelling older persons," *Neurology,* vol. 69, no. 24, pp. 2197-2204, 2007.

[275] J. Robinson, S. Xie, D. Baer, E. Suh, V. Van Deerlin, N. Loh, D. Irwin, C. McMillan, D. Wolk, A. Chen-Plotkin and D. Weintraub, "Pathological combinations in neurodegenerative disease are heterogeneous and disease-associated," *Brain,* vol. 146, no. 6, pp. 2557-2569, 2023.

[276] C. Greaves and J. Rohrer, "An update on genetic frontotemporal dementia," *Journal of neurology,* vol. 266, no. 8, pp. 2075-2086, 2019.

[277] Y. Abramzon, P. Fratta, B. Traynor and R. Chia, "The overlapping genetics of amyotrophic lateral sclerosis and frontotemporal dementia," *Frontiers in neuroscience,* vol. 14, p. 42, 2020.

[278] A. Murley, I. Coyle-Gilchrist, M. Rouse, P. Jones, W. Li, J. Wiggins, C. Lansdall, P. Rodríguez, A. Wilcox, K. Tsvetanov and K. Patterson, "Redefining the multidimensional clinical phenotypes of frontotemporal lobar degeneration syndromes," *Brain,* vol. 143, no. 5, pp. 1555-1571, 2020.

[279] P. Calabresi, A. Mechelli, G. Natale, L. Volpicelli-Daley, G. Di Lazzaro and V. Ghiglieri, "Alpha-synuclein in Parkinson's disease and other synucleinopathies: from overt neurodegeneration back to early synaptic dysfunction," *Cell death & disease,* vol. 14, no. 3, p. 176, 2023.

[280] E. Klann, U. Dissanayake, A. Gurrala, M. Farrer, A. Shukla, A. Ramirez-Zamora, V. Mai and V. Vedam-Mai, "The gut–brain axis and its relation to parkinson's disease: a review," *Frontiers in Aging Neuroscience,* vol. 13, p. 782082, 2022.

[281] D. Tosun, O. Yardibi, T. Benzinger, W. Kukull, C. Masters, R. Perrin, M. Weiner, A. Simen, A. Schwarz and A. D. N. Initiative, "Identifying individuals with non-Alzheimer's disease co-pathologies: A precision medicine approach to clinical trials in sporadic Alzheimer's disease," *Alzheimer's & Dementia,* vol. 20, pp. 421-436, 2023.

[282] A. Perna, K. Montine, L. White, T. Montine and B. Cholerton, "Paradigm Shift: Multiple Potential Pathways to Neurodegenerative Dementia," *Neurotherapeutics,* vol. 20, no. 6, pp. 1641-1652, 2023.

[283] R. McMackin, P. Bede, N. Pender, O. Hardiman and B. Nasseroleslami, "Neurophysiological markers of network dysfunction in neurodegenerative diseases," *NeuroImage: Clinical,* vol. 22, p. 101706, 2019.

[284] M. Murdock and L. Tsai, "Insights into Alzheimer's disease from single-cell genomic approaches," *Nature Neuroscience,* vol. 26, no. 2, pp. 181-195, 2023.

[285] T. Kamath, A. Abdulraouf, S. Burris, J. Langlieb, V. Gazestani, N. Nadaf, K. Balderrama, C. Vanderburg and E. Macosko, "Single-cell genomic profiling of human dopamine neurons identifies a population that selectively degenerates in Parkinson's disease," *Nature Neuroscience,* vol. 25, no. 5, pp. 588-595, 2022.

[286] O. Hansson, "Biomarkers for neurodegenerative diseases," *Nature Medicine,* vol. 27, no. 6, pp. 954-963, 2021.

[287] A. Espay, M. Schwarzschild, C. Tanner, H. Fernandez, D. Simon, J. Leverenz, A. Merola, A. Chen-Plotkin, P. Brundin, M. Kauffman and R. Erro, "Biomarker-driven phenotyping in Parkinson's disease: a translational missing link in disease-modifying clinical trials," *Movement Disorders,* vol. 32, no. 3, pp. 319-324, 2017.

[288] A. Lloret, D. Esteve, M. Lloret, A. Cervera-Ferri, B. Lopez, M. Nepomuceno and P. Monllor, "When does Alzheimer′s disease really start? The role of biomarkers," *International journal of molecular sciences,* vol. 20, no. 22, p. 5536, 2019.

[289] C. Jack, D. Bennett, K. Blennow, M. Carrillo, H. Feldman, G. Frisoni, H. Hampel, W. Jagust, K. Johnson, D. Knopman and R. Petersen, "A/T/N: An unbiased descriptive classification scheme for Alzheimer disease biomarkers," *Neurology,* vol. 87, no. 5, pp. 539-547, 2016.

[290] B. Dubois, H. Feldman, C. Jacova, J. Cummings, S. DeKosky, P. Barberger-Gateau, A. Delacourte, G. Frisoni, N. Fox, D. Galasko and S. Gauthier, "Revising the definition of Alzheimer's disease: a new lexicon," *The Lancet Neurology,* vol. 9, no. 11, pp. 1118-1127, 2010.

[291] S. Tabrizi, S. Schobel, E. Gantman, A. Mansbach, B. Borowsky, P. Konstantinova, T. Mestre, J. Panagoulias, C. Ross, M. Zauderer and A. Mullin, "A biological classification of Huntington's disease: the Integrated Staging System," *The Lancet Neurology,* vol. 21, no. 7, pp. 632-644, 2022.

[292] N. Mattsson-Carlgren, A. Leuzy, S. Janelidze, S. Palmqvist, E. Stomrud, O. Strandberg, R. Smith and O. Hansson, "The implications of different approaches to define AT (N) in Alzheimer disease," *Neurology,* vol. 94, no. 21, pp. e2233-e2244, 2020.

[293] L. Concha-Marambio, S. Pritzkow, M. Shahnawaz, C. Farris and C. Soto, "Seed amplification assay for the detection of pathologic alpha-synuclein aggregates in cerebrospinal fluid," *Nature Protocols,* vol. 18, no. 4, pp. 1179-1196, 2023.

[294] G. Höglinger, C. Adler, D. Berg, C. Klein, T. Outeiro, W. Poewe, R. Postuma, A. Stoessl and A. Lang, "A biological classification of Parkinson's disease: the SynNeurGe research diagnostic criteria," *The Lancet Neurology,* vol. 23, no. 2, pp. 191-204, 2024.

[295] L. Parkkinen, T. Pirttilä and I. Alafuzoff, "Applicability of current staging/categorization of α-synuclein pathology and their clinical relevance," *Acta neuropathologica,* vol. 115, pp. 399-407, 2008.

[296] M. Menéndez-González, "Toward a new nosology of neurodegenerative diseases," *Alzheimer's & Dementia,* vol. 19, no. 8, pp. 3731-3737, 2023.

[297] A. Korczyn, "Is Alzheimer’s disease a homogeneous disease entity?," *Journal of Neural Transmission,* vol. 120, pp. 1475-1477, 2013.

[298] A. Espay and A. Lees, "Are we entering the ‘Tau-lemaic’era of Parkinson’s disease?," *Brain,* p. p.awae002, 2024.

[299] C. Hawkes, K. Del Tredici and H. Braak, "A timeline for Parkinson's disease," *Parkinsonism & related disorders,* vol. 16, no. 2, pp. 79-84, 2010.

[300] H. Amieva, M. Le Goff, X. Millet, J. Orgogozo, K. Pérès, P. Barberger-Gateau, H. Jacqmin-Gadda and J. Dartigues, "Prodromal Alzheimer's disease: successive emergence of the clinical symptoms," *Annals of Neurology: Official Journal of the American Neurological Association and the Child Neurology Society,* vol. 64, no. 5, pp. 492-498, 2008.

[301] J. Brettschneider, K. Tredici, V. Lee and J. Trojanowski, "Spreading of pathology in neurodegenerative diseases: a focus on human studies," *Nature Reviews Neuroscience,* vol. 16, no. 2, pp. 109-120, 2015.

[302] H. Braak and E. Braak, "Neuropathological stageing of Alzheimer-related changes," *Acta neuropathologica,* vol. 82, no. 4, pp. 239-259, 1991.

[303] D. Thal, U. Rüb, M. Orantes and H. Braak, "Phases of Aβ-deposition in the human brain and its relevance for the development of AD," *Neurology,* vol. 58, no. 12, pp. 1791-1800, 2002.

[304] H. Braak and K. Del Tredici, "Neuropathological staging of brain pathology in sporadic Parkinson's disease: separating the wheat from the chaff," *Journal of Parkinson's disease,* vol. 7, no. s1, pp. S71-S85, 2017.

[305] D. Selkoe and J. Hardy, "The amyloid hypothesis of Alzheimer's disease at 25 years," *EMBO molecular medicine,* vol. 8, no. 6, pp. 595-608, 2016.

[306] K. Marek, D. Jennings, S. Lasch, A. Siderowf, C. Tanner, T. Simuni, C. Coffey, K. Kieburtz, E. Flagg, S. Chowdhury and W. Poewe, "The Parkinson progression marker initiative (PPMI)," *Progress in neurobiology,* vol. 95, no. 4, pp. 629-635, 2011.

[307] K. Moulder, B. Snider, S. Mills, V. Buckles, A. Santacruz, R. Bateman and J. Morris, "Dominantly Inherited Alzheimer Network: facilitating research and clinical trials," *Alzheimer's research & therapy,* vol. 5, pp. 1-7, 2013.

[308] S. Mueller, M. Weiner, L. Thal, R. Petersen, C. Jack, W. Jagust, J. Trojanowski, A. Toga and L. Beckett, "The Alzheimer's disease neuroimaging initiative," *Neuroimaging Clinics of North America,* vol. 15, no. 4, pp. 869-877, 2005.

[309] M. Donohue, H. Jacqmin-Gadda, M. Le Goff, R. Thomas, R. Raman, A. Gamst, L. Beckett, C. Jack Jr, M. Weiner, J. Dartigues and P. Aisen, "Estimating long-term multivariate progression from short-term data," *Alzheimer's & Dementia,* vol. 10, pp. S400-S410, 2014.

[310] D. Li, S. Iddi, W. Thompson, M. Donohue and A. D. N. Initiative, "Bayesian latent time joint mixed effect models for multicohort longitudinal data," *Statistical methods in medical research,* vol. 28, no. 3, pp. 835-845, 2019.

[311] R. Bateman, P. Aisen, B. De Strooper, N. Fox, C. Lemere, J. Ringman, S. Salloway, R. Sperling, M. Windisch and C. Xiong, "Autosomal-dominant Alzheimer's disease: a review and proposal for the prevention of Alzheimer's disease," *Alzheimer's research & therapy,* vol. 3, pp. 1-13, 2011.

[312] E. Gómez-Tortosa, M. Barquero, M. Barón, M. Sainz, S. Manzano, M. Payno, R. Ros, C. Almaraz, P. Gómez-Garré and A. Jiménez-Escrig, "Variability of age at onset in siblings with familial Alzheimer disease," *Archives of neurology,* vol. 64, no. 12, pp. 1743-1748, 2007.

[313] D. Ryman, N. Acosta-Baena, P. Aisen, T. Bird, A. Danek, N. Fox, A. Goate, P. Frommelt, B. Ghetti, J. Langbaum and F. Lopera, "Symptom onset in autosomal dominant Alzheimer disease: a systematic review and meta-analysis," *Neurology,* vol. 83, no. 3, pp. 253-260, 2014.

[314] I. Woollacott and J. Rohrer, "The clinical spectrum of sporadic and familial forms of frontotemporal dementia," *Journal of neurochemistry,* vol. 138, pp. 6-31, 2016.

[315] M. Barbier, A. Camuzat, M. Houot, F. Clot, P. Caroppo, C. Fournier, D. Rinaldi, F. Pasquier, D. Hannequin, J. Pariente and K. Larcher, "Factors influencing the age at onset in familial frontotemporal lobar dementia: Important weight of genetics," *Neurology: Genetics,* vol. 3, no. 6, p. e203, 2017.

[316] A. Staffaroni, S. Goh, Y. Cobigo, E. Ong, S. Lee, K. Casaletto, A. Wolf, L. Forsberg, N. Ghoshal, N. Graff-Radford and M. Grossman, "Rates of brain atrophy across disease stages in familial frontotemporal dementia associated with MAPT, GRN, and C9orf72 pathogenic variants," *JAMA network open,* vol. 3, no. 10, pp. e2022847-e2022847, 2020.

[317] O. Almkvist, E. Rodriguez-Vieitez, S. Thordardottir, K. Amberla, K. Axelman, H. Basun, A. Kinhult-Ståhlbom, L. Lilius, A. Remes, L. Wahlund and M. Viitanen, "Predicting cognitive decline across four decades in mutation carriers and non-carriers in autosomal-dominant Alzheimer's disease," *Journal of the International Neuropsychological Society,* vol. 23, no. 3, pp. 195-203, 2017.

[318] O. Almkvist and A. Nordberg, "A biomarker-validated time scale in years of disease progression has identified early-and late-onset subgroups in sporadic Alzheimer's disease," *Alzheimer's Research & Therapy,* vol. 15, no. 1, p. 89, 2023.

[319] D. Knopman, "Is dominantly inherited Alzheimer disease a clone of sporadic Alzheimer disease?," *Neurology,* vol. 85, no. 9, pp. 750-751, 2015.

[320] J. Llibre-Guerra, L. Iaccarino, D. Coble, L. Edwards, Y. Li, E. McDade, A. Strom, B. Gordon, N. Mundada, S. Schindler and E. Tsoy, "Longitudinal clinical, cognitive and biomarker profiles in dominantly inherited versus sporadic early-

onset Alzheimer’s disease," *Brain Communications,* vol. 5, no. 6, p. fcad280, 2023.

[321] H. Wang, X. Shen, J. Li, J. Suckling, C. Tan, Y. Wang, L. Feng, C. Zhang, L. Tan, Q. Dong and J. Touchon, "Clinical and biomarker trajectories in sporadic Alzheimer's disease: A longitudinal study," *Alzheimer's & Dementia: Diagnosis, Assessment & Disease Monitoring,* vol. 12, no. 1, p. e12095, 2020.

[322] K. Ito, B. Corrigan, Q. Zhao, J. French, R. Miller, H. Soares, E. Katz, T. Nicholas, B. Billing, R. Anziano and T. Fullerton, "Disease progression model for cognitive deterioration from Alzheimer's Disease Neuroimaging Initiative database," *Alzheimer's & Dementia,* vol. 7, no. 2, pp. 151-160, 2011.

[323] I. Delor, J. Charoin, R. Gieschke, S. Retout, P. Jacqmin and A. D. N. Initiative, "Modeling Alzheimer's disease progression using disease onset time and disease trajectory concepts applied to CDR-SOB scores from ADNI," *CPT: pharmacometrics & systems pharmacology,* vol. 2, no. 10, pp. 1-10, 2013.

[324] E. Yang, M. Farnum, V. Lobanov, T. Schultz, N. Raghavan, M. Samtani, G. Novak, V. Narayan, A. DiBernardo and A. D. N. Initiative, "Quantifying the pathophysiological timeline of Alzheimer's disease," *Journal of Alzheimer's Disease,* vol. 26, no. 4, pp. 745-753, 2011.

[325] H. Dodge, J. Zhu, D. Harvey, N. Saito, L. Silbert, J. Kaye, R. Koeppe, R. Albin and A. D. N. Initiative, "Biomarker progressions explain higher variability in stage-specific cognitive decline than baseline values in Alzheimer disease," *Alzheimer's & Dementia,* vol. 10, no. 6, pp. 690-703, 2014.

[326] B. Jedynak, A. Lang, B. Liu, E. Katz, Y. Zhang, B. Wyman, D. Raunig, C. Jedynak, B. Caffo, J. Prince and A. D. N. Initiative, "A computational neurodegenerative disease progression score: method and results with the Alzheimer's disease neuroimaging initiative cohort," *Neuroimage,* vol. 63, no. 3, pp. 1478-1486, 2012.

[327] T. Ishida, K. Tokuda, A. Hisaka, M. Honma, S. Kijima, H. Takatoku, T. Iwatsubo, T. Moritoyo, H. Suzuki and A. D. N. Initiative, "A novel method to estimate long-term chronological changes from fragmented observations in disease progression," *Clinical Pharmacology & Therapeutics,* vol. 105, no. 2, pp. 436-447, 2019.

[328] M. Bilgel and B. Jedynak, "Predicting time to dementia using a quantitative template of disease progression," *Alzheimer's & Dementia: Diagnosis, Assessment & Disease Monitoring,* vol. 11, no. 1, pp. 205-215, 2019.

[329] M. Lorenzi, M. Filippone, G. Frisoni, D. Alexander, S. Ourselin and A. D. N. Initiative, "Probabilistic disease progression modeling to characterize

diagnostic uncertainty: application to staging and prediction in Alzheimer's disease," *NeuroImage,* vol. 190, pp. 56-68, 2019.

[330] S. Garbarino, M. Lorenzi, N. Oxtoby, E. Vinke, R. Marinescu, A. Eshaghi, M. Ikram, W. Niessen, O. Ciccarelli, F. Barkhof and J. Schott, "Differences in topological progression profile among neurodegenerative diseases from imaging data," *Elife,* vol. 8, p. e49298, 2019.

[331] S. Siddiqi, K. Kording, J. Parvizi and M. Fox, "Causal mapping of human brain function," *Nature reviews neuroscience,* vol. 23, no. 6, pp. 361-375, 2022.

[332] J. Crary, J. Trojanowski, J. Schneider, J. Abisambra, E. Abner, I. Alafuzoff, S. Arnold, J. Attems, T. Beach, E. Bigio and N. Cairns, "Primary age-related tauopathy (PART): a common pathology associated with human aging," *Acta neuropathologica,* vol. 128, pp. 755-766, 2014.

[333] M. Busche and B. Hyman, "Synergy between amyloid-β and tau in Alzheimer's disease," *Nature neuroscience,* vol. 23, no. 10, pp. 1183-1193, 2020.

[334] T. Therneau, D. Knopman, V. Lowe, H. Botha, J. Graff-Radford, D. Jones, P. Vemuri, M. Mielke, C. Schwarz, M. Senjem and J. Gunter, "Relationships between β-amyloid and tau in an elderly population: An accelerated failure time model," *Neuroimage,* vol. 242, p. 118440, 2021.

[335] P. Cogswell, E. Lundt, T. Therneau, C. Mester, H. Wiste, J. Graff-Radford, C. Schwarz, M. Senjem, J. Gunter, R. Reid and S. Przybelski, "Evidence against a temporal association between cerebrovascular disease and Alzheimer's disease imaging biomarkers," *Nature communications,* vol. 14, no. 1, p. 3097, 2023.

[336] X. Golay, J. Hendrikse and T. Lim, "Perfusion imaging using arterial spin labeling," *Topics in Magnetic Resonance Imaging,* vol. 15, no. 1, pp. 10-27, 2004.

[337] Y. Iturria-Medina, R. Sotero, P. Toussaint, J. Mateos-Pérez and A. Evans, "Early role of vascular dysregulation on late-onset Alzheimer's disease based on multifactorial data-driven analysis," *Nature Communications,* vol. 7, no. 1, p. 11934, 21 June 2016.

[338] H. Kim, K. Yoo, D. Na, S. Seo, J. Jeong and Y. Jeong, "Non-monotonic reorganization of brain networks with Alzheimer's disease progression," *Frontiers in aging neuroscience,* vol. 7, p. 111, 2015.

[339] R. Guerrero, R. Wolz, A. Rao, D. Rueckert and A. D. N. I. (ADNI), "Manifold population modeling as a neuro-imaging biomarker: application to ADNI and ADNI-GO," *NeuroImage,* vol. 94, pp. 275-286, 2014.

[340] A. Schmidt-Richberg, C. Ledig, R. Guerrero, H. Molina-Abril, A. Frangi, D. Rueckert and A. D. N. Initiative, "Learning biomarker models for progression estimation of Alzheimer's disease," *PloS one,* vol. 11, no. 4, p. e0153040, 2016.

[341] R. Guerrero, A. Schmidt-Richberg, C. Ledig, T. Tong, R. Wolz, D. Rueckert and A. D. N. I. (ADNI), "Instantiated mixed effects modeling of Alzheimer's disease markers," *NeuroImage,* vol. 142, pp. 113-125, 2016.

[342] J. Schiratti, S. Allassonniere, O. Colliot and S. Durrleman, "Learning spatiotemporal trajectories from manifold-valued longitudinal data," *Advances in neural information processing systems,* vol. 28, 2015.

[343] I. Koval, J. Schiratti, A. Routier, M. Bacci, O. Colliot, S. Allassonniere and S. Durrleman, "Spatiotemporal propagation of the cortical atrophy: Population and individual patterns," *Frontiers in neurology,* p. 235, 2018.

[344] M. Bilgel, J. Prince, D. Wong, S. Resnick and B. Jedynak, "A multivariate nonlinear mixed effects model for longitudinal image analysis: Application to amyloid imaging," *Neuroimage,* vol. 134, pp. 658-670, 2016.

[345] S. Garbarino, M. Lorenzi and A. D. N. Initiative, "Investigating hypotheses of neurodegeneration by learning dynamical systems of protein propagation in the brain," *Neuroimage,* vol. 235, p. 117980, 2021.

[346] R. Marinescu, A. Eshaghi, M. Lorenzi, A. Young, N. Oxtoby, S. Garbarino, S. Crutch, D. Alexander and A. D. N. Initiative, "DIVE: A spatiotemporal progression model of brain pathology in neurodegenerative disorders," *NeuroImage,* vol. 192, pp. 166-177, 2019.

[347] W. Saelens, R. Cannoodt, H. Todorov and Y. Saeys, "A comparison of single-cell trajectory inference methods," *Nature biotechnology,* vol. 37, no. 5, pp. 547-554, 2019.

[348] Y. Iturria-Medina, A. Khan, Q. Adewale, A. Shirazi and A. D. N. Initiative, "Blood and brain gene expression trajectories mirror neuropathology and clinical deterioration in neurodegeneration," *Brain,* vol. 143, no. 2, pp. 661-673, 2020.

[349] S. Mukherjee, L. Heath, C. Preuss, S. Jayadev, G. Garden, A. Greenwood, S. Sieberts, P. De Jager, N. Ertekin-Taner, G. Carter and L. Mangravite, "Molecular estimation of neurodegeneration pseudotime in older brains," *Nature communications,* vol. 11, no. 1, p. 5781, 2020.

[350] A. Chervov, J. Bac and A. Zinovyev, "Minimum spanning vs. principal trees for structured approximations of multi-dimensional datasets," *Entropy,* vol. 22, no. 11, p. 1274, 2020.

[351] J. Hong, S. Kang, I. Alberts, J. Lu, R. Sznitman, J. Lee, A. Rominger, H. Choi, K. Shi and A. D. N. Initiative, "Image-level trajectory inference of tau pathology using variational autoencoder for Flortaucipir PET," *European journal of nuclear medicine and molecular imaging,* vol. 49, no. 9, pp. 3061-3072, 2022.

[352] P. Chen, S. Zhang, K. Zhao, X. Kang, T. Rittman and Y. Liu, "Robustly uncovering the heterogeneity of neurodegenerative disease by using data-driven subtyping in neuroimaging: A review," *Brain Research,* p. 148675, 2023.

[353] K. Poulakis and E. Westman, "Clustering and disease subtyping in Neuroscience, towards better methodological adaptations," *Frontiers in Computational Neuroscience,* vol. 17, p. 1243092, 2023.

[354] B. Avelar-Pereira, M. Belloy, R. O'Hara, S. Hosseini and A. D. N. Initiative, "Decoding the heterogeneity of Alzheimer's disease diagnosis and progression using multilayer networks," *Molecular Psychiatry,* vol. 28, no. 6, pp. 2423-2432, 2023.

[355] Z. Yang, I. Nasrallah, H. Shou, J. Wen, J. Doshi, M. Habes, G. Erus, A. Abdulkadir, S. Resnick, M. Albert and P. Maruff, "A deep learning framework identifies dimensional representations of Alzheimer's Disease from brain structure," *Nature communications,* vol. 12, no. 1, p. 7065, 2021.

[356] K. Poulakis, J. Pereira, J. Muehlboeck, L. Wahlund, Ö. Smedby, G. Volpe, C. Masters, D. Ames, Y. Niimi, T. Iwatsubo and D. Ferreira, "Multi-cohort and longitudinal Bayesian clustering study of stage and subtype in Alzheimer's disease," *Nature communications,* vol. 13, no. 1, p. 4566, 2022.

[357] M. Murray, N. Graff-Radford, O. Ross, R. Petersen, R. Duara and D. Dickson, "Neuropathologically defined subtypes of Alzheimer's disease with distinct clinical characteristics: a retrospective study," *The Lancet Neurology,* vol. 10, no. 9, pp. 785-796, 2011.

[358] B. Tijms, E. Vromen, O. Mjaavatten, H. Holstege, L. Reus, S. van der Lee, K. Wesenhagen, L. Lorenzini, L. Vermunt, V. Venkatraghavan and N. Tesi, "Cerebrospinal fluid proteomics in patients with Alzheimer's disease reveals five molecular subtypes with distinct genetic risk profiles," *Nature Aging,* vol. 4, pp. 33-47, 2024.

[359] R. Erro, M. Picillo, S. Scannapieco, S. Cuoco, M. Pellecchia and P. Barone, "The role of disease duration and severity on novel clinical subtypes of Parkinson disease," *Parkinsonism & related disorders,* vol. 73, pp. 31-34, 2020.

[360] Y. Iturria-Medina, Q. Adewale, A. Khan, S. Ducharme, P. Rosa-Neto, K. O'Donnell, V. Petyuk, S. Gauthier, P. De Jager, J. Breitner and D. Bennett, "Unified epigenomic, transcriptomic, proteomic, and metabolomic taxonomy of

Alzheimer’s disease progression and heterogeneity," *Science Advances,* vol. 8, no. 46, p. eabo6764, 2022.

[361] H. Fonteijn, M. Modat, M. Clarkson, J. Barnes, M. Lehmann, N. Hobbs, R. Scahill, S. Tabrizi, S. Ourselin, N. Fox and D. Alexander, "An event-based model for disease progression and its application in familial Alzheimer's disease and Huntington's disease," *NeuroImage,* vol. 60, no. 3, pp. 1880-1889, 2012.

[362] A. Young, N. Oxtoby, P. Daga, D. Cash, N. Fox, S. Ourselin, J. Schott and D. Alexander, "A data-driven model of biomarker changes in sporadic Alzheimer's disease," *Brain,* vol. 137, no. 9, pp. 2564-2577, 2014.

[363] N. Oxtoby, S. Garbarino, N. Firth, J. Warren, J. Schott, D. Alexander and A. D. N. Initiative, "Data-driven sequence of changes to anatomical brain connectivity in sporadic Alzheimer’s disease," *Frontiers in neurology,* vol. 8, p. 580, 2017.

[364] N. Oxtoby, A. Young, D. Cash, T. Benzinger, A. Fagan, J. Morris, R. Bateman, N. Fox, J. Schott and D. Alexander, "Data-driven models of dominantly-inherited Alzheimer’s disease progression," *Brain,* vol. 141, no. 5, pp. 1529-1544, 2018.

[365] A. Eshaghi, R. Marinescu, A. Young, N. Firth, F. Prados, M. Jorge Cardoso, C. Tur, F. De Angelis, N. Cawley, W. Brownlee and N. De Stefano, "Progression of regional grey matter atrophy in multiple sclerosis," *Brain,* vol. 141, no. 6, pp. 1665-1677, 2018.

[366] P. Wijeratne, A. Eshaghi, W. Scotton, M. Kohli, L. Aksman, N. Oxtoby, D. Pustina, J. Warner, J. Paulsen, R. Scahill and C. Sampaio, "The temporal event-based model: Learning event timelines in progressive diseases," *Imaging Neuroscience,* vol. 1, pp. 1-19, 2023.

[367] V. Venkatraghavan, E. Bron, W. Niessen, S. Klein and A. D. N. Initiative, "Disease progression timeline estimation for Alzheimer's disease using discriminative event based modeling," *NeuroImage,* vol. 186, pp. 518-532, 2019.

[368] J. Huang and D. Alexander, "Probabilistic event cascades for Alzheimer's disease," *Advances in neural information processing systems,* vol. 25, 2012.

[369] A. Young, R. Marinescu, N. Oxtoby, M. Bocchetta, K. Yong, N. Firth, D. Cash, D. Thomas, K. Dick, J. Cardoso and J. van Swieten, "Uncovering the heterogeneity and temporal complexity of neurodegenerative diseases with Subtype and Stage Inference," *Nature communications,* vol. 9, no. 1, p. 4273, 2018.

[370] J. Whitwell, D. Dickson, M. Murray, S. Weigand, N. Tosakulwong, M. Senjem, D. Knopman, B. Boeve, J. Parisi, R. Petersen and C. Jack, "Neuroimaging

correlates of pathologically defined subtypes of Alzheimer's disease: a case-control study," *The Lancet Neurology,* vol. 11, no. 10, pp. 868-877, 2012.

[371] Y. Sun, Y. Zhao, K. Hu, M. Wang, Y. Liu, B. Liu and A. D. N. Initiative, "Distinct spatiotemporal subtypes of amyloid deposition are associated with diverging disease profiles in cognitively normal and mild cognitive impairment individuals," *Translational Psychiatry,* vol. 13, no. 1, p. 35, 2023.

[372] L. Collij, G. Salvadó, V. Wottschel, S. Mastenbroek, P. Schoenmakers, F. Heeman, L. Aksman, A. Wink, B. Berckel, W. van de Flier and P. Scheltens, "Spatial-temporal patterns of β-amyloid accumulation: a subtype and stage inference model analysis," *Neurology,* vol. 98, no. 17, pp. e1692-e1703, 2022.

[373] L. Aksman, N. Oxtoby, M. Scelsi, P. Wijeratne, A. Young, I. Alves, L. Collij, J. Vogel, F. Barkhof, D. Alexander and A. Altmann, "A data-driven study of Alzheimer's disease related amyloid and tau pathology progression," *Brain,* vol. 146, no. 12, pp. 4935-4948, 2023.

[374] P. Nelson, D. Dickson, J. Trojanowski, C. Jack, P. Boyle, K. Arfanakis, R. Rademakers, I. Alafuzoff, J. Attems, C. Brayne and I. Coyle-Gilchrist, "Limbic-predominant age-related TDP-43 encephalopathy (LATE): consensus working group report," *Brain,* vol. 142, no. 6, pp. 1503-1527, 2019.

[375] A. Young, J. Vogel, J. Robinson, C. McMillan, R. Ossenkoppele, D. Wolk, D. Irwin, L. Elman, M. Grossman, V. Lee and E. Lee, "Data-driven neuropathological staging and subtyping of TDP-43 proteinopathies," *Brain,* vol. 146, no. 7, pp. 2975-2988, 2023.

[376] T. Shen, J. Vogel, J. Duda, J. Phillips, P. Cook, J. Gee, L. Elman, C. Quinn, D. Amado, M. Baer and L. Massimo, "Novel data-driven subtypes and stages of brain atrophy in the ALS-FTD spectrum," 2023.

[377] C. Zhou, L. Wang, W. Cheng, J. Lv, X. Guan, T. Guo, J. Wu, W. Zhang, T. Gao, X. Liu and X. Bai, "Two distinct trajectories of clinical and neurodegeneration events in Parkinson's disease," *npj Parkinson's Disease,* vol. 9, no. 1, p. 111, 2023.

[378] A. Eshaghi, A. Young, P. Wijeratne, F. Prados, D. Arnold, S. Narayanan, C. Guttmann, F. Barkhof, D. Alexander, A. Thompson and D. Chard, "Identifying multiple sclerosis subtypes using unsupervised machine learning and MRI data," *Nature communications,* vol. 12, no. 1, p. 2078, 2021.

[379] R. Armstrong, "On the 'classification' of neurodegenerative disorders: discrete entities, overlap or continuum?," *Folia neuropathologica,* vol. 50, no. 3, pp. 201-218, 2012.

[380] A. Macedo, C. Tissot, J. Therriault, S. Servaes, Y. Wang, J. Fernandez-Arias, N. Rahmouni, F. Lussier, M. Vermeiren, G. Bezgin and P. Vitali, "The use of tau PET to stage Alzheimer disease according to the Braak staging framework," *Journal of Nuclear Medicine,* vol. 64, no. 8, pp. 1171-1178, 2023.

[381] A. Tan, S. Lim and A. Lang, "The microbiome–gut–brain axis in Parkinson disease—from basic research to the clinic," *Nature Reviews Neurology,* vol. 18, no. 8, pp. 476-495, 2022.

[382] J. de Magalhães, "Distinguishing between driver and passenger mechanisms of aging," *Nature Genetics,* pp. 1-8, 2024.

[383] S. Gauthier, J. Alam, H. Fillit, T. Iwatsubo, H. Liu-Seifert, M. Sabbagh, S. Salloway, C. Sampaio, J. Sims, B. Sperling and R. Sperling, "Combination therapy for Alzheimer's disease: Perspectives of the EU/US CTAD Task Force," *The journal of prevention of Alzheimer's disease,* vol. 6, pp. 164-168, 2019.

[384] P. Modrego and A. Lobo, "A good marker does not mean a good target for clinical trials in Alzheimer's disease: the amyloid hypothesis questioned," *Neurodegenerative disease management,* vol. 9, no. 3, pp. 119-121, 2019.

[385] H. Fillit, L. Nisenbaum and A. Burstein, "Future of Alzheimer's Disease Treatment: Combination Therapy and Precision Medicine," *The Journal of Prevention of Alzheimer's Disease,* vol. 10, no. 4, pp. 743-745, 2023.

[386] A. Vinayagam, T. Gibson, H. Lee, B. Yilmazel, C. Roesel, Y. Hu, Y. Kwon, A. Sharma, Y. Liu, N. Perrimon and A. Barabási, "Controllability analysis of the directed human protein interaction network identifies disease genes and drug targets," *Proceedings of the National Academy of Sciences,* vol. 113, no. 18, pp. 4976-4981, 2016.

[387] L. Sanchez-Rodriguez, Y. Iturria-Medina, E. Baines, S. Mallo, M. Dousty, R. Sotero and A. D. N. Initiative, "Design of optimal nonlinear network controllers for Alzheimer's disease," *PLoS computational biology,* vol. 14, no. 5, p. e1006136, 2018.

[388] H. Zheng, J. Petrella, P. Doraiswamy, G. Lin, W. Hao and A. D. N. Initiative, "Data-driven causal model discovery and personalized prediction in Alzheimer's disease," *npj Digital Medicine,* vol. 5, no. 1, p. 137, 2022.

[389] Y. Iturria-Medina, F. Carbonell, A. Evans and A. D. N. Initiative, "Multimodal imaging-based therapeutic fingerprints for optimizing personalized interventions: Application to neurodegeneration," *Neuroimage,* vol. 179, pp. 40-50, 2018.

[390] C. Peng, J. Trojanowski and V. Lee, "Protein transmission in neurodegenerative disease," *Nature Reviews Neurology,* vol. 16, no. 4, pp. 199-212, 2020.

[391] W. Seeley, R. Crawford, J. Zhou, B. Miller and M. Greicius, "Neurodegenerative diseases target large-scale human brain networks," *Neuron,* vol. 62, no. 1, pp. 42-52, 2009.

[392] J. Zhou, E. Gennatas, J. Kramer, B. Miller and W. Seeley, "Predicting regional neurodegeneration from the healthy brain functional connectome," *Neuron,* vol. 73, no. 6, pp. 1216-1227, 2012.

[393] A. Drzezga, "The network degeneration hypothesis: Spread of neurodegenerative patterns along neuronal brain networks," *Journal of Nuclear Medicine,* vol. 59, no. 11, pp. 1645-1648, 2018.

[394] N. Franzmeier, M. Brendel, L. Beyer, L. Slemann, G. Kovacs, T. Arzberger, C. Kurz, G. Respondek, M. Lukic, D. Biel and A. Rubinski, "Tau deposition patterns are associated with functional connectivity in primary tauopathies," *Nature Communications,* vol. 13, no. 1, p. 1362, 2022.

[395] A. Raj and F. Powell, "Models of network spread and network degeneration in brain disorders," *Biological Psychiatry: Cognitive Neuroscience and Neuroimaging,* vol. 3, no. 9, pp. 788-797, 2018.

[396] J. Palop, J. Chin and L. Mucke, "A network dysfunction perspective on neurodegenerative diseases," *Nature,* vol. 443, no. 7113, pp. 768-773, 2006.

[397] D. Bassett and O. Sporns, "Network neuroscience," *Nature neuroscience,* vol. 20, no. 3, pp. 353-364, 2017.

[398] A. Luppi, J. Cabral, R. Cofre, P. Mediano, F. Rosas, A. Qureshi, A. Kuceyeski, E. Tagliazucchi, F. Raimondo, G. Deco and J. Shine, "Computational modelling in disorders of consciousness: closing the gap towards personalised models for restoring consciousness," *NeuroImage,* vol. 275, p. 120162, 2023.

[399] A. Raj, A. Kuceyeski and M. Weiner, "A network diffusion model of disease progression in dementia," *Neuron,* vol. 73, no. 6, pp. 1204-1215, 2012.

[400] A. Raj, E. LoCastro, A. Kuceyeski, D. Tosun, N. Relkin and M. Weiner, "Network diffusion model of progression predicts longitudinal patterns of atrophy and metabolism in Alzheimer's disease," *Cell reports,* vol. 10, no. 3, pp. 359-369, 2015.

[401] S. Pandya, C. Mezias and A. Raj, "Predictive model of spread of progressive supranuclear palsy using directional network diffusion," *Frontiers in neurology,* vol. 8, p. 692, 2017.

[402] J. Torok, P. Maia, F. Powell, S. Pandya and A. Raj, "A method for inferring regional origins of neurodegeneration," *Brain,* vol. 141, no. 3, pp. 863-876, 2018.

[403] J. Weickenmeier, E. Kuhl and A. Goriely, "Multiphysics of prionlike diseases: Progression and atrophy," *Physical review letters,* vol. 121, no. 15, p. 158101, 2018.

[404] Y. Iturria-Medina, R. Sotero, P. Toussaint, A. Evans and A. D. N. Initiative, "Epidemic spreading model to characterize misfolded proteins propagation in aging and associated neurodegenerative disorders," *PLoS computational biology,* vol. 10, no. 11, p. e1003956, 2014.

[405] D. Schoonhoven, E. Coomans, A. Millán, A. van Nifterick, D. Visser, R. Ossenkoppele, H. Tuncel, W. van der Flier, S. Golla, P. Scheltens and A. Hillebrand, "Tau protein spreads through functionally connected neurons in Alzheimer's disease: a combined MEG/PET study," *Brain,* vol. 146, no. 10, p. 4040–4054, 2023.

[406] W. Zhu, A. Neuhaus, D. Beard, B. Sutherland and G. DeLuca, "Neurovascular coupling mechanisms in health and neurovascular uncoupling in Alzheimer's disease," *Brain,* vol. 145, no. 7, pp. 2276-2292, 2022.

[407] M. Bilgel, D. Wong, A. Moghekar, L. Ferrucci, S. Resnick and A. D. N. Initiative, "Causal links among amyloid, tau, and neurodegeneration," *Brain Communications,* vol. 4, no. 4, p. fcac193, 2022.

[408] T. Thompson, G. Meisl, T. Knowles and A. Goriely, "The role of clearance mechanisms in the kinetics of pathological protein aggregation involved in neurodegenerative diseases," *The Journal of chemical physics,* vol. 154, no. 12, 2021.

[409] T. Thompson, P. Chaggar, E. Kuhl, A. Goriely and A. D. N. Initiative, "Protein-protein interactions in neurodegenerative diseases: A conspiracy theory," *PLoS computational biology,* vol. 16, no. 10, p. e1008267, 2020.

[410] Y. Zheng, Y. Zhang, Y. Yau, Y. Zeighami, K. Larcher, B. Misic and A. Dagher, "Local vulnerability and global connectivity jointly shape neurodegenerative disease propagation," *PLoS biology,* vol. 17, no. 11, p. e3000495, 2019.

[411] A. Schäfer, E. Mormino and E. Kuhl, "Network diffusion modeling explains longitudinal tau PET data," *Frontiers in Neuroscience,* vol. 14, p. 566876, 2020.

[412] A. Schäfer, M. Peirlinck, K. Linka, E. Kuhl and A. D. N. I. (ADNI), "Bayesian physics-based modeling of tau propagation in Alzheimer's disease," *Frontiers in physiology,* vol. 12, p. 702975, 2021.

[413] A. Schäfer, P. Chaggar, A. Goriely, E. Kuhl and A. D. N. Initiative, "Correlating tau pathology to brain atrophy using a physics-based Bayesian model," *Engineering with Computers,* vol. 38, no. 5, pp. 3867-3877, 2022.

[414] P. Chaggar, J. Vogel, A. Pichet-Binette, T. Thompson, O. Strandberg, E. Stomrud, N. Mattsson-Carlgren, L. Karlsson, S. Jbabdi, S. Magon and G. Klein, "Personalised Regional Modelling Predicts Tau Progression in the Human Brain," *bioRxiv,* pp. 2023-09, 2023.

[415] J. Phillips, F. Nitchie IV, F. Da Re, C. Olm, P. Cook, C. McMillan, D. Irwin, J. Gee, J. Dubroff, M. Grossman and I. Nasrallah, "Rates of longitudinal change in 18F-flortaucipir PET vary by brain region, cognitive impairment, and age in atypical Alzheimer's disease," *Alzheimer's & Dementia,* vol. 18, no. 6, pp. 1235-1247, 2022.

[416] D. Walsh and D. Selkoe, "A critical appraisal of the pathogenic protein spread hypothesis of neurodegeneration," *Nature Reviews Neuroscience,* vol. 17, no. 4, pp. 251-260, 2016.

[417] S. Singleton, A. Luppi, R. Carhart-Harris, J. Cruzat, L. Roseman, D. Nutt, G. Deco, M. Kringelbach, E. Stamatakis and A. Kuceyeski, "Receptor-informed network control theory links LSD and psilocybin to a flattening of the brain's control energy landscape," *Nature communications,* vol. 13, no. 1, p. 5812, 2022.

[418] D. Zachlod, S. Bludau, S. Cichon, N. Palomero-Gallagher and K. Amunts, "Combined analysis of cytoarchitectonic, molecular and transcriptomic patterns reveal differences in brain organization across human functional brain systems," *Neuroimage,* vol. 257, p. 119286, 2022.

[419] K. Siletti, R. Hodge, A. Mossi Albiach, K. Lee, S. Ding, L. Hu, P. Lönnerberg, T. Bakken, T. Casper, M. Clark and N. Dee, "Transcriptomic diversity of cell types across the adult human brain," *Science,* vol. 382, no. 6667, p. p.eadd7046, 2023.

[420] C. Figley, M. Uddin, K. Wong, J. Kornelsen and J. Puig, "Potential pitfalls of using fractional anisotropy, axial diffusivity, and radial diffusivity as biomarkers of cerebral white matter microstructure," *Frontiers in Neuroscience,* vol. 15, p. 799, 2022.

[421] M. Hawrylycz, E. Lein, A. Guillozet-Bongaarts, E. Shen, L. Ng, J. Miller, L. Van De Lagemaat, K. Smith, A. Ebbert, Z. Riley and C. Abajian, "An anatomically comprehensive atlas of the adult human brain transcriptome," *Nature,* vol. 489, no. 7416, pp. 391-399, 2012.

[422] M. Hawrylycz, J. Miller, V. Menon, D. Feng, T. Dolbeare, A. Guillozet-Bongaarts, A. Jegga, B. Aronow, C. Lee, A. Bernard and M. Glasser, "Canonical genetic signatures of the adult human brain," *Nature neuroscience,* vol. 18, no. 12, pp. 1832-1844, 2015.

[423] K. Zilles and N. Palomero-Gallagher, "Multiple transmitter receptors in regions and layers of the human cerebral cortex," *Frontiers in neuroanatomy,* vol. 11, p. 78, 2017.

[424] N. Palomero-Gallagher and K. Zilles, "Cortical layers: Cyto-, myelo-, receptor-and synaptic architecture in human cortical areas," *Neuroimage,* vol. 197, pp. 716-741, 2019.

[425] M. Savli, A. Bauer, M. Mitterhauser, Y. Ding, A. Hahn, T. Kroll, A. Neumeister, D. Haeusler, J. Ungersboeck, S. Henry and S. Isfahani, "Normative database of the serotonergic system in healthy subjects using multi-tracer PET," *Neuroimage,* vol. 63, no. 1, pp. 447-459, 2012.

[426] J. Warren, J. Rohrer, J. Schott, N. Fox, J. Hardy and M. Rossor, "Molecular nexopathies: a new paradigm of neurodegenerative disease," *Trends in neurosciences,* vol. 36, no. 10, pp. 561-569, 2013.

[427] D. Martins, A. Giacomel, S. Williams, F. Turkheimer, O. Dipasquale and M. Veronese, "Imaging transcriptomics: Convergent cellular, transcriptomic, and molecular neuroimaging signatures in the healthy adult human brain," *Cell Reports,* vol. 37, no. 13, p. 110173, 2021.

[428] A. Arnatkeviciute, B. Fulcher, M. Bellgrove and A. Fornito, "Imaging transcriptomics of brain disorders," *Biological Psychiatry Global Open Science,* vol. 2, no. 4, pp. 319-331, 2022.

[429] T. Lawn, M. Howard, F. Turkheimer, B. Misic, G. Deco, D. Martins and O. Dipasquale, "From neurotransmitters to networks: Transcending organisational hierarchies with molecular-informed functional imaging," *Neuroscience & Biobehavioral Reviews,* p. 105193, 2023.

[430] J. Woolley, B. Khan, N. Murthy, B. Miller and K. Rankin, "The diagnostic challenge of psychiatric symptoms in neurodegenerative disease: rates of and risk factors for prior psychiatric diagnosis in patients with early neurodegenerative disease," *The Journal of clinical psychiatry,* vol. 72, no. 2, p. 4437, 2011.

[431] W. Heiss and K. Herholz, "Brain receptor imaging," *Journal of Nuclear Medicine,* vol. 47, no. 2, pp. 302-312, 2006.

[432] J. Dukart, Š. Holiga, C. Chatham, P. Hawkins, A. Forsyth, R. McMillan, J. Myers, A. Lingford-Hughes, D. Nutt, E. Merlo-Pich and C. Risterucci, "Cerebral blood flow predicts differential neurotransmitter activity," *Scientific reports,* vol. 8, no. 1, p. 4074, 2018.

[433] P. Selvaggi, P. Hawkins, O. Dipasquale, G. Rizzo, A. Bertolino, J. Dukart, F. Sambataro, G. Pergola, S. Williams, F. Turkheimer and F. Zelaya, "Increased cerebral blood flow after single dose of antipsychotics in healthy volunteers depends on dopamine D2 receptor density profiles," *NeuroImage,* vol. 188, pp. 774-784, 2019.

[434] A. Luppi, J. Hansen, R. Adapa, R. Carhart-Harris, L. Roseman, C. Timmermann, D. Golkowski, A. Ranft, R. Ilg, D. Jordan and V. Bonhomme, "In vivo mapping of pharmacologically induced functional reorganization onto the human brain's neurotransmitter landscape," *Science Advances,* vol. 9, no. 24, p. eadf8332, 2023.

[435] K. Sakreida, W. Chiu, J. Dukart, S. Eickhoff, T. Frodl, C. Gaser, M. Landgrebe, B. Langguth, D. Mirlach, I. Rautu and M. Wittmann, "Disentangling dyskinesia from parkinsonism in motor structures of patients with schizophrenia," *Brain communications,* vol. 4, no. 4, p. fcac190, 2022.

[436] M. Vignando, D. Ffytche, S. Lewis, P. Lee, S. Chung, R. Weil, M. Hu, C. Mackay, L. Griffanti, D. Pins and K. Dujardin, "Mapping brain structural differences and neuroreceptor correlates in Parkinson's disease visual hallucinations," *Nature communications,* vol. 13, no. 1, p. 519, 2022.

[437] G. Ji, J. Sun, Q. Hua, L. Zhang, T. Zhang, T. Bai, L. Wei, X. Wang, B. Qiu, A. Wang and H. Sun, "White matter dysfunction in psychiatric disorders is associated with neurotransmitter and genetic profiles," *Nature Mental Health,* pp. 1-12, 2023.

[438] L. Hahn, S. Eickhoff, K. Mueller, L. Schilbach, H. Barthel, K. Fassbender, K. Fliessbach, J. Kornhuber, J. Prudlo, M. Synofzik and J. Wiltfang, "Resting-state alterations in behavioral variant frontotemporal dementia are related to the distribution of monoamine and GABA neurotransmitter systems," *medRxiv,* 2022.

[439] J. Dukart, S. Holiga, M. Rullmann, R. Lanzenberger, P. Hawkins, M. Mehta, S. Hesse, H. Barthel, O. Sabri, R. Jech and S. Eickhoff, "JuSpace: A tool for spatial correlation analyses of magnetic resonance imaging data with nuclear imaging derived neurotransmitter maps," *Human Brain Mapping,* vol. 42, no. 3, pp. 555-566, 2021.

[440] E. Premi, J. Dukart, I. Mattioli, I. Libri, M. Pengo, Y. Gadola, M. Cotelli, R. Manenti, G. Binetti, S. Gazzina and A. Alberici, "Unravelling neurotransmitters impairment in primary progressive aphasias," *Human Brain Mapping,* vol. 44, no. 6, pp. 2245-2253, 2023.

[441] E. Premi, M. Pengo, I. Mattioli, V. Cantoni, J. Dukart, R. Gasparotti, E. Buratti, A. Padovani, M. Bocchetta, E. Todd and A. Bouzigues, "Early neurotransmitters changes in prodromal frontotemporal dementia: A GENFI study," *Neurobiology of disease,* vol. 179, p. 106068, 2023.

[442] B. Bernhardt, J. Smallwood, S. Keilholz and D. Margulies, "Gradients in brain organization," *NeuroImage,* vol. 251, p. 118987, 2022.

[443] S. Morgan, J. Seidlitz, K. Whitaker, R. Romero-Garcia, N. Clifton, C. Scarpazza, T. Van Amelsvoort, M. Marcelis, J. Van Os, G. Donohoe and D. Mothersill, "Cortical patterning of abnormal morphometric similarity in psychosis is associated with brain expression of schizophrenia-related genes," *Proceedings of the National Academy of Sciences,* vol. 116, no. 19, pp. 9604-9609, 2019.

[444] J. Li, G. Wu, B. Li, F. Fan, X. Zhao, Y. Meng, P. Zhong, S. Yang, B. Biswal, H. Chen and W. Liao, "Transcriptomic and macroscopic architectures of intersubject functional variability in human brain white-matter," *Communications Biology,* vol. 4, no. 1, p. 1417, 2021.

[445] M. Grothe, J. Sepulcre, G. Gonzalez-Escamilla, I. Jelistratova, M. Schöll, O. Hansson, S. Teipel and A. D. N. Initiative, "Molecular properties underlying regional vulnerability to Alzheimer's disease pathology," *Brain,* vol. 141, no. 9, pp. 2755-2771, 2018.

[446] A. Altmann, D. Cash, M. Bocchetta, C. Heller, R. Reynolds, K. Moore, R. Convery, D. Thomas, J. van Swieten, F. Moreno and R. Sanchez-Valle, "Analysis of brain atrophy and local gene expression in genetic frontotemporal dementia," *Brain communications,* vol. 2, no. 2, p. fcaa122, 2020.

[447] S. Pandya, P. Maia, B. Freeze, R. Menke, K. Talbot, M. Turner and A. Raj, "Modeling seeding and neuroanatomic spread of pathology in amyotrophic lateral sclerosis," *NeuroImage,* vol. 251, p. 118968, 2022.

[448] H. Fu, J. Hardy and K. Duff, "Selective vulnerability in neurodegenerative diseases," *Nature neuroscience,* vol. 21, no. 10, pp. 1350-1358, 2018.

[449] N. Sun, M. Victor, Y. Park, X. Xiong, A. Scannail, N. Leary, S. Prosper, S. Viswanathan, X. Luna, C. Boix and B. James, "Human microglial state dynamics in Alzheimer's disease progression," *Cell,* vol. 186, no. 20, pp. 4386-4403, 2023.

[450] B. Vahsen, E. Gray, A. Thompson, O. Ansorge, D. Anthony, S. Cowley, K. Talbot and M. Turner, "Non-neuronal cells in amyotrophic lateral sclerosis—

from pathogenesis to biomarkers," *Nature Reviews Neurology,* vol. 17, no. 6, pp. 333-348, 2021.

[451] J. Blumenfeld, O. Yip, M. Kim and Y. Huang, "Cell type-specific roles of APOE4 in Alzheimer disease," *Nature Reviews Neuroscience,* pp. 1-20, 2024.

[452] A. Cain, M. Taga, C. McCabe, G. Green, I. Hekselman, C. White, D. Lee, P. Gaur, O. Rozenblatt-Rosen, F. Zhang and E. Yeger-Lotem, "Multicellular communities are perturbed in the aging human brain and Alzheimer's disease," *Nature Neuroscience,* pp. 1-14, 2023.

[453] I. Kerrebijn, M. Wainberg, P. Zhukovsky, Y. Chen, M. Davie, D. Felsky and S. Tripathy, "Case-control virtual histology elucidates cell types associated with cortical thickness differences in Alzheimer's disease," *NeuroImage,* vol. 276, p. 120177, 2023.

[454] V. Pak, Q. Adewale, D. Bzdok, M. Dadar, Y. Zeighami and Y. Iturria Medina, "Distinctive Whole-brain Cell-Types Strongly Predict Tissue Damage Patterns in Eleven Neurodegenerative Disorders," *eLife,* vol. 12, p. RP89368, 2023.

[455] H. Mathys, J. Davila-Velderrain, Z. Peng, F. Gao, S. Mohammadi, J. Young, M. Menon, L. He, F. Abdurrob, X. Jiang and A. Martorell, "Single-cell transcriptomic analysis of Alzheimer's disease," *Nature,* vol. 570, no. 7761, pp. 332-337, 2019.

[456] X. Xiong, B. James, C. Boix, Y. Park, K. Galani, M. Victor, N. Sun, L. Hou, L. Ho, J. Mantero and A. Scannail, "Epigenomic dissection of Alzheimer's disease pinpoints causal variants and reveals epigenome erosion," *Cell,* vol. 186, no. 20, pp. 4422-4437, 2023.

[457] J. Miller, M. Hawrylycz, M. Aitken, J. Ariza, R. Chakrabarty, S. Ding, Y. Ding, R. Ferrer, J. Goldy, S. Gratiy and N. Guilford, "SEA-AD: Scientific analysis and open access resources targeting early changes in Alzheimer's disease," *Alzheimer's & Dementia, , p..,* vol. 19, p. e063478, 2023.

[458] N. Johansen, S. Somasundaram, K. Travaglini, A. Yanny, M. Shumyatcher, T. Casper, C. Cobbs, N. Dee, R. Ellenbogen, M. Ferreira and J. Goldy, "Interindividual variation in human cortical cell type abundance and expression," *Science,* vol. 382, no. 6667, p. p.eadf2359, 2023.

[459] M. Piwecka, N. Rajewsky and A. Rybak-Wolf, "Single-cell and spatial transcriptomics: deciphering brain complexity in health and disease," *Nature Reviews Neurology,* pp. 1-17, 2023.

[460] Y. Zeighami, T. Bakken, T. Nickl-Jockschat, Z. Peterson, A. Jegga, J. Miller, J. Schulkin, A. Evans, E. Lein and M. Hawrylycz, "A comparison of

anatomic and cellular transcriptome structures across 40 human brain diseases," *Plos Biology,* vol. 21, no. 4, p. e3002058, 2023.

[461] Q. Adewale, A. Khan, F. Carbonell, Y. Iturria-Medina and A. D. N. Initiative, "Integrated transcriptomic and neuroimaging brain model decodes biological mechanisms in aging and Alzheimer's disease," *Elife,* vol. 10, p. e62589, 2021.

[462] A. Khan, Q. Adewale, T. Baumeister, F. Carbonell, K. Zilles, N. Palomero-Gallagher, Y. Iturria-Medina and A. D. N. Initiative, "Personalized brain models identify neurotransmitter receptor changes in Alzheimer's disease," *Brain,* vol. 145, no. 5, pp. 1785-1804, 2022.

[463] A. Kehagia, R. Barker and T. Robbins, "Cognitive impairment in Parkinson's disease: the dual syndrome hypothesis," *Neurodegenerative diseases,* vol. 11, no. 2, pp. 79-92, 2012.

[464] A. Khan, Q. Adewale, S. Lin, T. Baumeister, Y. Zeighami, F. Carbonell, N. Palomero-Gallagher and Y. Iturria-Medina, "Patient-specific models link neurotransmitter receptor mechanisms with motor and visuospatial axes of Parkinson's disease," *Nature Communications,* vol. 14, p. 6009, 2023.

[465] J. Sepulcre, M. Grothe, F. d'Oleire Uquillas, L. Ortiz-Terán, I. Diez, H. Yang, H. Jacobs, B. Hanseeuw, Q. Li, G. El-Fakhri and R. Sperling, "Neurogenetic contributions to amyloid beta and tau spreading in the human cortex," *Nature medicine,* vol. 24, no. 12, pp. 1910-1918, 2018.

[466] V. Montal, I. Diez, C. Kim, W. Orwig, E. Bueichekú, R. Gutiérrez-Zúñiga, A. Bejanin, J. Pegueroles, O. Dols-Icardo, P. Vannini and G. El-Fakhri, "Network Tau spreading is vulnerable to the expression gradients of APOE and glutamatergic-related genes," *Science translational medicine,* vol. 14, no. 655, p. eabn7273, 2022.

[467] D. Acosta, F. Powell, Y. Zhao and A. Raj, "Regional vulnerability in Alzheimer's disease: The role of cell-autonomous and transneuronal processes," *Alzheimer's & Dementia,* vol. 14, no. 6, pp. 797-810, 2018.

[468] S. Rahayel, C. Tremblay, A. Vo, Y. Zheng, S. Lehéricy, I. Arnulf, M. Vidailhet, J. Corvol, J. Gagnon and R. Postuma, "Brain atrophy in prodromal synucleinopathy is shaped by structural connectivity and gene expression," *Brain,* vol. 145, no. 9, pp. 3162-3178, 2022.

[469] M. Henderson, E. Cornblath, A. Darwich, B. Zhang, H. Brown, R. Gathagan, R. Sandler, D. Bassett, J. Trojanowski and V. Lee, "Spread of α-synuclein pathology through the brain connectome is modulated by selective

vulnerability and predicted by network analysis," *Nature neuroscience,* vol. 22, no. 8, pp. 1248-1257, 2019.

[470] G. Shafiei, V. Bazinet, M. Dadar, A. Manera, D. Collins, A. Dagher, B. Borroni, R. Sanchez-Valle, F. Moreno, R. Laforce Jr and C. Graff, "Network structure and transcriptomic vulnerability shape atrophy in frontotemporal dementia," *Brain,* vol. 146, no. 1, pp. 321-336, 2023.

[471] C. Lenglos, S. Lin, Y. Zeighami, T. Baumeister, F. Carbonell and Y. Iturria-Medina, "Multivariate genomic and transcriptomic determinants of imaging-derived personalized therapeutic needs in Parkinson's disease," *Scientific Reports,* vol. 12, no. 1, p. 5483, 2022.

[472] A. Mandal, M. Gandal, J. Seidlitz and A. Alexander-Bloch, "A Critical Appraisal of Imaging Transcriptomics," *Biological Psychiatry: Global Open Science,* vol. 2, no. 4, pp. 311-313, 2022.

[473] G. Rizzo, M. Veronese, P. Expert, F. Turkheimer and A. Bertoldo, "MENGA: a new comprehensive tool for the integration of neuroimaging data and the Allen human brain transcriptome atlas," *PloS one,* vol. 11, no. 2, p. e0148744, 2016.

[474] P. Selvaggi, G. Rizzo, M. Mehta, F. Turkheimer and M. Veronese, "Integration of human whole-brain transcriptome and neuroimaging data: Practical considerations of current available methods," *Journal of neuroscience methods,* vol. 355, p. 109128, 2021.

[475] A. Arnatkevičiūtė, B. Fulcher and A. Fornito, "A practical guide to linking brain-wide gene expression and neuroimaging data," *Neuroimage,* vol. 189, pp. 353-367, 2019.

[476] R. Markello, A. Arnatkeviciute, J. Poline, B. Fulcher, A. Fornito and B. Misic, "Standardizing workflows in imaging transcriptomics with the abagen toolbox," *elife,* vol. 10, p. e72129, 2021.

[477] H. Zeng, "Mesoscale connectomics," *Current opinion in neurobiology,* vol. 50, pp. 154-162, 2018.

[478] J. Murray, M. Demirtaş and A. Anticevic, "Biophysical modeling of large-scale brain dynamics and applications for computational psychiatry," *Biological Psychiatry: Cognitive Neuroscience and Neuroimaging,* vol. 3, no. 9, pp. 777-787, 2018.

[479] D. Kurtin, V. Giunchiglia, J. Vohryzek, J. Cabral, A. Skeldon and I. Violante, "Moving from phenomenological to predictive modelling: Progress and

pitfalls of modelling brain stimulation in-silico," *Neuroimage,* vol. 272, p. 120042, 2023.

[480] G. Deco and M. Kringelbach, "Great expectations: using whole-brain computational connectomics for understanding neuropsychiatric disorders," *Neuron,* vol. 84, no. 5, pp. 892-905, 2014.

[481] K. Stephan and C. Mathys, "Computational approaches to psychiatry," *Current opinion in neurobiology,* vol. 25, pp. 85-92, 2014.

[482] K. Friston, K. Preller, C. Mathys, H. Cagnan, J. Heinzle, A. Razi and P. Zeidman, "Dynamic causal modelling revisited," *Neuroimage,, pp..,* vol. 199, pp. 730-744, 2019.

[483] W. Penny, K. Stephan, J. Daunizeau, M. Rosa, K. Friston, T. Schofield and A. Leff, "Comparing families of dynamic causal models," *PLoS computational biology,* vol. 6, no. 3, p. e1000709, 2010.

[484] K. Stephan and K. Friston, "Analyzing effective connectivity with functional magnetic resonance imaging," *Wiley Interdisciplinary Reviews: Cognitive Science,* vol. 1, no. 3, pp. 446-459, 2010.

[485] E. Scheller, A. Abdulkadir, J. Peter, S. Tabrizi, R. Frackowiak and S. Klöppel, "Interregional compensatory mechanisms of motor functioning in progressing preclinical neurodegeneration," *Neuroimage,* vol. 75, pp. 146-154, 2013.

[486] M. Kringelbach, J. Cruzat, J. Cabral, G. Knudsen, R. Carhart-Harris, P. Whybrow, N. Logothetis and G. Deco, "Dynamic coupling of whole-brain neuronal and neurotransmitter systems," *Proceedings of the National Academy of Sciences,* vol. 117, no. 17, pp. 9566-9576, 2020.

[487] G. Deco, J. Cruzat, J. Cabral, G. Knudsen, R. Carhart-Harris, P. Whybrow, N. Logothetis and M. Kringelbach, "Whole-brain multimodal neuroimaging model using serotonin receptor maps explains non-linear functional effects of LSD," *Current biology,* vol. 28, no. 19, pp. 3065-3074, 2018.

[488] M. Schartner, R. Carhart-Harris, A. Barrett, A. Seth and S. Muthukumaraswamy, "Increased spontaneous MEG signal diversity for psychoactive doses of ketamine, LSD and psilocybin," *Scientific reports,* vol. 7, no. 1, p. 46421, 2017.

[489] R. Herzog, P. Mediano, F. Rosas, P. Lodder, R. Carhart-Harris, Y. Perl, E. Tagliazucchi and R. Cofre, "A whole-brain model of the neural entropy increase elicited by psychedelic drugs," *Scientific Reports,* vol. 13, no. 1, p. 6244, 2023.

[490] S. Singleton, C. Timmermann, A. Luppi, E. Eckernäs, L. Roseman, R. Carhart-Harris and A. Kuceyeski, "Time-resolved network control analysis links reduced control energy under DMT with the serotonin 2a receptor, signal diversity, and subjective experience," *bioRxiv,* 2023.

[491] M. Girn, L. Roseman, B. Bernhardt, J. Smallwood, R. Carhart-Harris and R. Spreng, "Serotonergic psychedelic drugs LSD and psilocybin reduce the hierarchical differentiation of unimodal and transmodal cortex," *NeuroImage,* vol. 256, p. 119220, 2022.

[492] C. Coronel-Oliveros, C. Gießing, V. Medel, R. Cofré and P. Orio, "Whole-brain modeling explains the context-dependent effects of cholinergic neuromodulation," *NeuroImage,* vol. 265, p. 119782, 2023.

[493] A. Naskar, A. Vattikonda, G. Deco, D. Roy and A. Banerjee, "Multiscale dynamic mean field (MDMF) model relates resting-state brain dynamics with local cortical excitatory–inhibitory neurotransmitter homeostasis," *Network Neuroscience,* vol. 5, no. 3, pp. 757-782, 2021.

[494] A. Jafarian, L. Hughes, N. Adams, J. Lanskey, M. Naessens, M. Rouse, A. Murley, K. Friston and J. Rowe, "Neurochemistry-enriched dynamic causal models of magnetoencephalography, using magnetic resonance spectroscopy," *NeuroImage,* vol. 276, p. 120193, 2023.

[495] A. Horvath, A. Szucs, G. Csukly, A. Sakovics, G. Stefanics and A. Kamondi, "EEG and ERP biomarkers of Alzheimer's disease: a critical review," *Frontiers in bioscience (Landmark edition),* no. 23, pp. 183-220, 2018.

[496] W. De Haan, K. Mott, E. Van Straaten, P. Scheltens and C. Stam, "Activity dependent degeneration explains hub vulnerability in Alzheimer's disease," *PLOS Computational Biology,* vol. 8, no. 8, p. e1002582, 2012.

[497] W. de Haan, E. van Straaten, A. Gouw and C. Stam, "Altering neuronal excitability to preserve network connectivity in a computational model of Alzheimer's disease," *PLoS computational biology,* vol. 13, no. 9, p. e1005707, 2017.

[498] A. van Nifterick, A. Gouw, R. van Kesteren, P. Scheltens, C. Stam and W. de Haan, "A multiscale brain network model links Alzheimer’s disease-mediated neuronal hyperactivity to large-scale oscillatory slowing," *Alzheimer's Research & Therapy,* vol. 14, no. 1, pp. 1-20, 2022.

[499] A. van Nifterick, E. Scheijbeler, A. Gouw, W. de Haan and C. Stam, "Local signal variability and functional connectivity: Sensitive measures of the excitation-inhibition ratio?," *Cognitive Neurodynamics,* pp. 1-19, 2023.

[500] C. Alexandersen, W. de Haan, C. Bick and A. Goriely, "A multi-scale model explains oscillatory slowing and neuronal hyperactivity in Alzheimer's disease," *Journal of the Royal Society Interface,* vol. 20, no. 198, p. 20220607, 2023.

[501] L. Sanchez-Rodriguez, G. Bezgin, F. Carbonell, J. Therriault, J. Fernandez-Arias, S. Servaes, N. Rahmouni, C. Tissot, J. Stevenson, T. Karikari and N. Ashton, "Revealing the combined roles of Aβ and tau in Alzheimer's disease via a pathophysiological activity decoder," *bioRxiv,* 2023.

[502] P. Sanz Leon, S. Knock, M. Woodman, L. Domide, J. Mersmann, A. McIntosh and V. Jirsa, "The Virtual Brain: a simulator of primate brain network dynamics," *Frontiers in neuroinformatics,* vol. 7, p. 10, 2013.

[503] P. Ritter, M. Schirner, A. McIntosh and V. Jirsa, "The virtual brain integrates computational modeling and multimodal neuroimaging," *Brain connectivity,* vol. 3, no. 2, pp. 121-145, 2013.

[504] M. Schirner, A. McIntosh, V. Jirsa, G. Deco and P. Ritter, "Inferring multi-scale neural mechanisms with brain network modelling," *elife,* vol. 7, p. e28927, 2018.

[505] J. Meier, D. Perdikis, A. Blickensdörfer, L. Stefanovski, Q. Liu, O. Maith, H. Dinkelbach, J. Baladron, F. Hamker and P. Ritter, "Virtual deep brain stimulation: Multiscale co-simulation of a spiking basal ganglia model and a whole-brain mean-field model with The Virtual Brain," *Experimental Neurology,* vol. 354, p. 114111, 2022.

[506] H. Aerts, M. Schirner, T. Dhollander, B. Jeurissen, E. Achten, D. Van Roost, P. Ritter and D. Marinazzo, "Modeling brain dynamics after tumor resection using The Virtual Brain," *NeuroImage,* vol. 213, p. 116738, 2020.

[507] V. Jirsa, H. Wang, P. Triebkorn, M. Hashemi, J. Jha, J. Gonzalez-Martinez, M. Guye, J. Makhalova and F. Bartolomei, "Personalised virtual brain models in epilepsy," *The Lancet Neurology,* vol. 22, no. 5, pp. 443-454, 2023.

[508] L. Stefanovski, P. Triebkorn, A. Spiegler, M. Diaz-Cortes, A. Solodkin, V. Jirsa, A. McIntosh, P. Ritter and A. D. N. Initiative, "Linking molecular pathways and large-scale computational modeling to assess candidate disease mechanisms and pharmacodynamics in Alzheimer's disease," *Frontiers in computational neuroscience,* vol. 13, p. 54, 2019.

[509] J. Zimmermann, A. Perry, M. Breakspear, M. Schirner, P. Sachdev, W. Wen, N. Kochan, M. Mapstone, P. Ritter, A. McIntosh and A. Solodkin, "Differentiation of Alzheimer's disease based on local and global parameters in

personalized Virtual Brain models," *NeuroImage: Clinical,* vol. 19, pp. 240-251, 2018.

[510] A. Monteverdi, F. Palesi, M. Schirner, F. Argentino, M. Merante, A. Redolfi, F. Conca, L. Mazzocchi, S. Cappa, M. Ramusino and A. Costa, "Virtual brain simulations reveal network-specific parameters in neurodegenerative dementias," *Frontiers in Aging Neuroscience,* vol. 15, p. 1204134, 2023.

[511] Y. Perl, H. Bocaccio, I. Pérez-Ipiña, F. Zamberlán, J. Piccinini, H. Laufs, M. Kringelbach, G. Deco and E. Tagliazucchi, "Generative embeddings of brain collective dynamics using variational autoencoders," *Physical review letters,* vol. 125, no. 23, p. 238101, 2020.

[512] Y. Perl, S. Fittipaldi, C. Campo, S. Moguilner, J. Cruzat, M. Fraile-Vazquez, R. Herzog, M. Kringelbach, G. Deco, P. Prado and A. Ibanez, "Model-based whole-brain perturbational landscape of neurodegenerative diseases," *eLife,* vol. 12, p. e83970, 2023.

[513] B. Khanal, M. Lorenzi, N. Ayache and X. Pennec, "A biophysical model of brain deformation to simulate and analyze longitudinal MRIs of patients with Alzheimer's disease," *NeuroImage,* vol. 134, pp. 35-52, 2016.

[514] J. Rollo, J. Crawford and J. Hardy, "A dynamical systems approach for multiscale synthesis of Alzheimer's pathogenesis," *Neuron,* vol. 111, no. 14, pp. 2126-2139, 2023.

[515] N. Oxtoby, L. Leyland, L. Aksman, G. Thomas, E. Bunting, P. Wijeratne, A. Young, A. Zarkali, M. Tan, F. Bremner and P. Keane, "Sequence of clinical and neurodegeneration events in Parkinson's disease progression," *Brain,* vol. 144, no. 3, pp. 975-988, 2021.

[516] N. Firth, S. Primativo, R. Marinescu, T. Shakespeare, A. Suarez-Gonzalez, M. Lehmann, A. Carton, D. Ocal, I. Pavisic, R. Paterson and C. Slattery, "Longitudinal neuroanatomical and cognitive progression of posterior cortical atrophy," *Brain,* vol. 142, no. 7, pp. 2082-2095, 2019.

[517] L. Sanchez-Rodriguez, A. Khan, Q. Adewale, G. Bezgin, J. Therriault, J. Fernandez-Arias, S. Servaes, N. Rahmouni, C. Tissot, J. Stevenson and H. Jiang, "Transcriptomic signatures of Abeta-and tau-induced neuronal dysfunction reveal inflammatory processes at the core of Alzheimer's disease pathophysiology," *bioRxiv,* pp. 2023-09., 2023.

[518] E. Dadgar-Kiani, G. Bieri, R. Melki, A. Gitler and J. Lee, "Mesoscale connections and gene expression empower whole-brain modeling of α-synuclein spread, aggregation, and decay dynamics," *Cell Reports,* vol. 41, no. 6, p. 111631, 2022.

[519] A. Etkin, "A reckoning and research agenda for neuroimaging in psychiatry," *American Journal of Psychiatry,* vol. 176, no. 7, pp. 507-511, 2019.

[520] S. Ducharme, "Brain MRI research in neurodegenerative dementia: time to deliver on promises," *Brain,* p. awad320, 2023.

[521] J. Bayer, P. Thompson, C. Ching, M. Liu, A. Chen, A. Panzenhagen, N. Jahanshad, A. Marquand, L. Schmaal and P. Sämann, "Site effects how-to and when: An overview of retrospective techniques to accommodate site effects in multi-site neuroimaging analyses," *Frontiers in Neurology,* no. 13, p. 923988, 2022.

[522] M. Hernán and J. Robins, "Using big data to emulate a target trial when a randomized trial is not available," *American journal of epidemiology,* vol. 183, no. 8, pp. 758-764, 2016.

[523] I. Marinescu, P. Lawlor and K. Kording, "Quasi-experimental causality in neuroscience and behavioural research," *Nature human behaviour,* vol. 2, no. 12, pp. 891-898, 2018.

[524] L. Ross and D. Bassett, "Causation in neuroscience: keeping mechanism meaningful," *Nature Reviews Neuroscience,* vol. 25, pp. 81-90, 2024.

[525] P. Rosenbaum, "Design of observational studies," in *Springer Series in Statistics*, New York, Springer, 2010, pp. 978-1.

[526] A. Ehrenberg, A. Khatun, E. Coomans, M. Betts, F. Capraro, E. Thijssen, K. Senkevich, T. Bharucha, M. Jafarpour, P. Young and W. Jagust, "Relevance of biomarkers across different neurodegenerative diseases," *Alzheimer's research & therapy,* no. 12, pp. 1-11, 2020.

[527] A. Etkin, "Addressing the causality gap in human psychiatric neuroscience," *JAMA psychiatry,* vol. 75, no. 1, pp. 3-4, 2018.

[528] S. Siddiqi, S. Khosravani, J. Rolston and M. Fox, "The future of brain circuit-targeted therapeutics," *Neuropsychopharmacology,* pp. 1-10, 2023.

[529] D. Bennett, A. Buchman, P. Boyle, L. Barnes, R. Wilson and J. Schneider, "Religious orders study and rush memory and aging project," *Journal of Alzheimer's disease,* vol. 64, no. s1, pp. S161-S189, 2018.

[530] S. Benoit, H. Xu, S. Schmid, R. Alexandrova, G. Kaur, B. Thiruvahindrapuram, S. Pereira, M. Jog and M. Hebb, "Expanding the search for genetic biomarkers of Parkinson's disease into the living brain," *Neurobiology of Disease,* vol. 140, p. 104, 2020.

[531] S. Lin, R. Rodriguez-Rojas, T. Baumeister, C. Lenglos, J. Pineda-Pardo, J. Máñez-Miró, M. Del Alamo, R. Martinez-Fernandez, J. Obeso and Y. Iturria-Medina, "Neuroimaging signatures predicting motor improvement to focused ultrasound subthalamotomy in Parkinson's disease," *npj Parkinson's Disease,* vol. 8, no. 1, p. 70, 2022.

[532] A. Fornito, E. Bullmore and A. Zalesky, "Opportunities and challenges for psychiatry in the connectomic era," *Biological Psychiatry: Cognitive Neuroscience and Neuroimaging,* vol. 2, no. 1, pp. 9-19, 2017.

[533] N. Sinha, J. Dauwels, M. Kaiser, S. Cash, M. Brandon Westover, Y. Wang and P. Taylor, "Predicting neurosurgical outcomes in focal epilepsy patients using computational modelling," *Brain,* vol. 140, no. 2, pp. 319-332, 2017.

[534] K. Bansal, J. Nakuci and S. Muldoon, "Personalized brain network models for assessing structure–function relationships," *Current Opinion in Neurobiology,* vol. 52, pp. 42-47, 2018.

[535] C. Tu, R. Rocha, M. Corbetta, S. Zampieri, M. Zorzi and S. Suweis, "Warnings and caveats in brain controllability," *NeuroImage,* vol. 176, pp. 83-91, 2018.

[536] A. Sala, A. Lizarraga, S. Caminiti, V. Calhoun, S. Eickhoff, C. Habeck, S. Jamadar, D. Perani, J. Pereira, M. Veronese and I. Yakushev, "Brain connectomics: time for a molecular imaging perspective?," *Trends in Cognitive Sciences,* vol. 27, no. 4, pp. 353-366, 2023.

[537] G. Bischof, M. Ewers, N. Franzmeier, M. Grothe, M. Hoenig, E. Kocagoncu, J. Neitzel, J. Rowe, A. Strafella, A. Drzezga and T. van Eimeren, "Connectomics and molecular imaging in neurodegeneration," *European journal of nuclear medicine and molecular imaging,* vol. 46, pp. 2819-2830, 2019.

[538] T. Dawson, T. Golde and C. Lagier-Tourenne, "Animal models of neurodegenerative diseases," *Nature neuroscience,* vol. 21, no. 10, pp. 1370-1379, 2018.

[539] J. Brynildsen, K. Rajan, M. Henderson and D. Bassett, "Network models to enhance the translational impact of cross-species studies," *Nature Reviews Neuroscience,* pp. 1-14, 2023.

[540] S. Sun, J. Torok, C. Mezias, D. Ma and A. Raj, "Spatial cell-type enrichment predicts mouse brain connectivity," *Cell Reports,* vol. 42, no. 10, p. 113258, 2023.

[541] C. Anand, P. Maia, J. Torok, C. Mezias and A. Raj, "The effects of microglia on tauopathy progression can be quantified using Nexopathy in silico (Nexis) models," *Scientific Reports,* vol. 12, no. 1, p. 21170, 2022.

[542] D. Norris and J. Polimeni, "Laminar (f) MRI: A short history and future prospects," *Neuroimage,* vol. 197, pp. 643-649, 2019.

[543] J. Manuello, J. Min, P. McCarthy, F. Alfaro-Almagro, S. Lee, S. Smith, L. Elliott, A. Winkler and G. Douaud, "The effects of genetic and modifiable risk factors on brain regions vulnerable to ageing and disease," *Nature Communications,* vol. 15, no. 1, p. 2576, 2024.

[544] F. Márquez and M. Yassa, "Neuroimaging biomarkers for Alzheimer's disease," *Molecular neurodegeneration,* vol. 14, pp. 1-14, 2019.

[545] J. Whitwell, "FTD spectrum: Neuroimaging across the FTD spectrum," *Progress in molecular biology and translational science,* vol. 165, pp. 187-223, 2019.

[546] T. Mitchell, S. Lehéricy, S. Chiu, S. A.P., A. Stoessl and D. Vaillancourt, "Emerging neuroimaging biomarkers across disease stage in Parkinson disease: a review," *JAMA neurology,* vol. 78, no. 10, pp. 1262-1272, 2021.

[547] T. Beach, "A review of biomarkers for neurodegenerative disease: will they swing us across the valley?," *Neurology and therapy,* vol. 6, pp. 5-13, 2017.

[548] G. Frisoni, M. Boccardi, F. Barkhof, K. Blennow, S. Cappa, K. Chiotis, J. Démonet, V. Garibotto, P. Giannakopoulos, A. Gietl and O. Hansson, "Strategic roadmap for an early diagnosis of Alzheimer's disease based on biomarkers," *The Lancet Neurology,* vol. 16, no. 8, pp. 661-676, 2017.

[549] N. Logothetis, "The underpinnings of the BOLD functional magnetic resonance imaging signal," *Journal of Neuroscience,* vol. 23, no. 10, pp. 3963-3971, 2003.

[550] N. Oxtoby and D. Alexander, "Imaging plus X: multimodal models of neurodegenerative disease," *Current opinion in neurology,* vol. 30, no. 4, pp. 371-379, 2017.

[551] C. Nogales, Z. Mamdouh, M. List, C. Kiel, A. Casas and H. Schmidt, "Network pharmacology: curing causal mechanisms instead of treating symptoms," *Trends in Pharmacological Sciences,* vol. 43, no. 2, pp. 136-150, 2022.

[552] J. Scannell, A. Blanckley, H. Boldon and B. Warrington, "Diagnosing the decline in pharmaceutical R&D efficiency," *Nature reviews Drug discovery,* vol. 11, no. 3, pp. 191-200, 2012.

[553] M. Ringel, J. Scannell, M. Baedeker and U. Schulze, "Breaking Eroom's law," *Nat Rev Drug Discov,* vol. 19, no. 12, pp. 833-834, 2020.

[554] A. Espay and K. McFarthing, "Alpha-synuclein and the Parkinson's disease drug pipeline," *Parkinsonism & Related Disorders,* vol. 111, p. 105432, 2023.

[555] W. Self and D. Holtzman, "Emerging diagnostics and therapeutics for Alzheimer disease," *Nature medicine,* vol. 29, no. 9, pp. 2187-2199, 2023.

[556] L. Hayes and P. Kalab, "Emerging therapies and novel targets for TDP-43 proteinopathy in ALS/FTD," *Neurotherapeutics,* vol. 19, no. 4, pp. 1061-1084, 2022.

[557] A. Badhwar, G. McFall, S. Sapkota, S. Black, H. Chertkow, S. Duchesne, M. Masellis, L. Li, R. Dixon and P. Bellec, "A multiomics approach to heterogeneity in Alzheimer's disease: focused review and roadmap," *Brain,* vol. 143, no. 5, pp. 1315-1331, 2020.

[558] E. Cornblath, J. Robinson, D. Irwin, E. Lee, V. Lee, J. Trojanowski and D. Bassett, "Defining and predicting transdiagnostic categories of neurodegenerative disease," *Nature biomedical engineering,* vol. 4, no. 8, pp. 787-800, 2020.

[559] C. R. Jack Jr, D. S. Knopman, W. J. Jagust, L. M. Shaw, P. S. Aisen, M. W. Weiner, R. C. Petersen and J. Q. Trojanowski, "Hypothetical model of dynamic biomarkers of the alzheimer's pathological cascade," *The Lancet Neurology,* vol. 9, no. 1, p. 119–128, 2010.

[560] B. Lam, M. Masellis, M. Freedman, D. T. Stuss and S. E. Black, "Clinical, imaging, and pathological heterogeneity of the alzheimer's disease syndrome," *Alzheimer's research & therapy,* vol. 5, no. 1, p. 1, 2013.

[561] Y. Iturria-Medina, F. M. Carbonell and A. C. Evans, "Multimodal imaging-based therapeutic fingerprints for optimizing personalized interventions: Application to neurodegeneration," *NeuroImage,* vol. 179, pp. 40-50, 2018.

[562] K. Kosik, "Personalized medicine for effective alzheimer disease treatment," *JAMA Neurology,* vol. 72, no. 5, pp. 497-498, 2015.

[563] N. J. Schork, "Personalized medicine: Time for one-person trials," *Nature,* vol. 520, no. 7549, pp. 609-611, 2015.

[564] A. Prakash, J. Kalra, V. Mani, K. Ramasamy and A. B. A. Majeed, "Pharmacological approaches for alzheimer's disease: Neurotransmitter as drug targets," *Expert review of neurotherapeutics,* vol. 15, no. 1, pp. 53-71, 2015.

[565] K. Roy, Computational modeling of drugs against Alzheimer's disease, Springer, 2018.

[566] C. R. Jack Jr., D. S. Knopman, W. J. Jagust, R. C. Petersen, M. W. Weiner, P. S. Aisen, L. M. Shaw, P. Vemuri, H. J. Wiste, S. D. Weigand, T. G. Lesnick, V. S. Pankratz, M. C. Donohue and J. Q. Trojanowski, "Tracking pathophysiological processes in Alzheimer's disease: an updated hypothetical model of dynamic biomarkers," *The Lancet Neurology,* vol. 12, no. 2, pp. 207-216, 2013.

[567] Y. Iturria-Medina, F. M.Carbonell, R. C. Sotero, F. Chouinard-Decorte and A. C.Evans, "Multifactorial causal model of brain (dis)organization and therapeutic intervention: Application to Alzheimer's disease," *NeuroImage,* vol. 152, pp. 60-77, 2017.

[568] F. Mora, G. Segovia and A. del Arco, "Aging, plasticity and environmental enrichment: structural changes and neurotransmitter dynamics in several areas of the brain," *Brain research reviews,* vol. 55, no. 1, pp. 78-88, 2007.

[569] A. Bejanin, D. Schonhaut, R. La Joie, J. Kramer, S. Baker, N. Sosa, N. Ayakta, A. Cantwell, M. Janabi, M. Lauriola and J. O'Neil, "Tau pathology and neurodegeneration contribute to cognitive impairment in Alzheimer's disease," *Brain,* vol. 140, no. 12, pp. 3286-3300, 2017.

[570] M. Busche, S. Wegmann, S. Dujardin, C. Commins, J. Schiantarelli, N. Klickstein, T. Kamath, G. Carlson, I. Nelken and B. Hyman, "Tau impairs neural circuits, dominating amyloid-β effects, in Alzheimer models in vivo," *Nature neuroscience,* vol. 22, no. 1, pp. 57-64, 2019.

[571] J. G. Sled, A. P. Zijdenbos and A. C. Evans, "A nonparametric method for automatic correction of intensity nonuniformity in MRI data," *IEEE transactions on medical imaging,* vol. 17, no. 1, p. 87–97, 1998.

[572] A. C. Evans, M. Kamber, D. Collins and D. MacDonald, "An MRI-based probabilistic atlas of neuroanatomy," *Magnetic resonance scanning and epilepsy,* pp. 263-274, 1994.

[573] J. Ashburner, "A fast diffeomorphic image registration algorithm," *NeuroImage,* vol. 38, no. 1, pp. 95-113, 2007.

[574] W. Jagust, D. Bandy, K. Chen, N. Foster, S. Landau, C. Mathis, J. Price, E. Reiman, D. Skovronsky, R. Koeppe and ADNI, "The Alzheimer's Disease

Neuroimaging Initiative positron emission tomography core," *Alzheimer's & Dementia,* vol. 6, no. 3, pp. 221-229, 2010.

[575] C. Yan and Y. Zang, "DPARSF: A matlab toolbox for “pipeline" data analysis of resting-state fMRI," *Frontiers in systems neuroscience,* vol. 4, p. 13, 2010.

[576] M. Aiello, E. Salvatore, A. Cachia, S. Pappatà, C. Cavaliere, A. Prinster, E. Nicolai, M. Salvatore, J. Baron and M. Quarantelli, "Relationship between simultaneously acquired resting-state regional cerebral glucose metabolism and functional MRI: a PET/MR hybrid scanner study," *Neuroimage,* no. 113, pp. 111-121, 1 June 2015.

[577] L. Yang, Y. Yan, Y. Wang, X. Hu, J. Lu, P. Chan, T. Yan and Y. Han, "Gradual disturbances of the amplitude of low-frequency fluctuations (ALFF) and fractional ALFF in Alzheimer spectrum," *Frontiers in neuroscience,* vol. 12, p. 975, 2018.

[578] Q.-H. Zou, C.-Z. Zhu, Y. Yang, X.-N. Zuo, X.-Y. Long, Q.-J. Cao, Y.-F. Wang and Y.-F. Zang, "An improved approach to detection of amplitude of low-frequency fluctuation (ALFF) for resting-state fMRI: Fractional ALFF," *Journal of neuroscience methods,* vol. 172, no. 1, pp. 137-141, 2008.

[579] N. Palomero-Gallagher and K. Zilles, "Cyto-and receptor architectonic mapping of the human brain," *Handbook of clinical neurology,* vol. 150, pp. 355-387, 2018.

[580] B. Merker, "Silver staining of cell bodies by means of physical development," *Journal of neuroscience methods,* vol. 9, no. 3, pp. 235-241, 1983.

[581] S. Eickhoff, T. Paus, S. Caspers, M. Grosbras, A. Evans, K. Zilles and K. Amunts, "Assignment of functional activations to probabilistic cytoarchitectonic areas revisited," *NeuroImage,* vol. 36, no. 3, pp. 511-521, 2007.

[582] K. Brodmann, Vergleichende Lokalisationslehre der Grosshirnrinde in ihren Prinzipien dargestellt auf Grund des Zellenbaues, Leipzig: Barth JA, 1909.

[583] M. Jenkinson, C. Beckmann, T. Behrens, M. Woolrich and S. Smith, "FSL," vol. 62, pp. 782-90, 2012.

[584] F. Yeh, S. Panesar, D. Fernandes, A. Meola, M. Yoshino, J. Fernandez-Miranda, J. Vettel and T. Verstynen, "Population-averaged atlas of the macroscale human structural connectome and its network topology," *NeuroImage,* vol. 178, pp. 57-68, 2018.

[585] F. Yeh and W. I. Tseng, "NTU-90: A high angular resolution brain atlas constructed by q-space diffeomorphic reconstruction," *NeuroImage,* vol. 58, no. 1, pp. 91-99, 2011.

[586] F. Yeh, V. J. Wedeen and W.-Y. I. Tseng, "Generalized q-sampling imaging," *IEEE transactions on medical imaging,* vol. 29, no. 9, pp. 1626-1635, 2010.

[587] F. Yeh, L. Liu, T. K. Hitchens and Y. L. Wu, "Mapping immune cell infiltration using restricted diffusion MRI," *Magnetic resonance in medicine,* vol. 77, no. 2, pp. 603-612, 2017.

[588] F. Yeh, T. D. Verstynen, Y. Wang, J. C. Fernández-Miranda and W. I. Tseng, "Deterministic diffusion fiber tracking improved by quantitative anisotropy," *PloS One,* pp. vol. 8, no. 11, 2013.

[589] A. Folch-Fortuny, F. Arteaga and A. Ferrer, "Missing data imputation toolbox for MATLAB," *Chemometrics and Intelligent Laboratory Systems,* vol. 154, pp. 93-100, 2016.

[590] L. Gibbons, A. Carle, R. Scott-Mackin, D. Harvey, S. Mukherjee, P. Insel, S. Curtis, A. Gross, R. Jones, D. Mungas, M. Weiner, P. Crane and ADNI, "Composite measures of executive function and memory: ADNI_EF and ADNI_Mem," 23 October 2015. [Online]. [Accessed May 2021].

[591] S. Choi, S. Mukherjee, L. Gibbons, R. Sanders, R. Jones, D. Tommet, J. Mez, E. Trittschuh, A. Saykin, M. Lamar and L. Rabin, "Development and validation of language and visuospatial composite scores in ADNI," *Alzheimer's & Dementia: Translational Research & Clinical Interventions,* vol. 6, no. 1, p. e12072, 2020.

[592] Alzheimer's Disease Neuroimaging Initiative, "ADNI2 Procedures Manual," July 2008. [Online]. Available: https://adni.loni.usc.edu/wp-content/uploads/2008/07/adni2-procedures-manual.pdf. [Accessed May 2021].

[593] Y. Iturria-Medina, F. Carbonell, A. Assadi, Q. Adewale, A. Khan, R. Baumeister and L. Sanchez-Rodriguez, "NeuroPM toolbox: integrating Molecular, Neuroimaging and Clinical data for Characterizing Neuropathological Progression and Individual Therapeutic Needs," *medRvix DOI: 10.1101/2020.09.24.20200964 ,* 2020.

[594] C. Honey, O. Sporns, L. Cammoun, X. Gigandet, J. Thiran, R. Meuli and P. Hagmann, "Predicting human resting-state functional connectivity from structural connectivity," *Proceedings of the National Academy of Sciences,* vol. 106, no. 6, pp. 2035-2040, 2009.

[595] R. Desikan, C. Fan, Y. Wang, A. Schork, H. Cabral, L. Cupples, W. Thompson, L. Besser, W. Kukull and D. C. C. Holland, "Genetic assessment of age-associated Alzheimer disease risk: Development and validation of a polygenic hazard score," *PLoS medicine,* vol. 14, no. 3, p. e1002258, 21 March 2017.

[596] J. Wu, S. Hussaini, I. Bastille, G. Rodriguez, A. Mrejeru, K. Rilett, D. Sanders, C. Cook, H. Fu, R. Boonen and M. Herman, "Neuronal activity enhances tau propagation and tau pathology in vivo," *Nature neuroscience,* vol. 19, no. 8, pp. 1085-10, 2016.

[597] Y. Wang, Q. Ren, W. Gong, D. Wu, X. Tang, X. Li, F. Wu, F. Bai, L. Xu and Z. Zhang, "Escitalopram attenuates β-amyloid-induced tau hyperphosphorylation in primary hippocampal neurons through the 5-HT1A receptor mediated Akt/GSK-3β pathway," *Oncotarget,* vol. 7, no. 12, p. 13328, 2016.

[598] R. Wang and P. H. Reddy, "Role of glutamate and nmda receptors in Alzheimer's disease," *Journal of Alzheimer's Disease,* vol. 57, no. 4, pp. 1041-1048, 2017.

[599] M. R. Hynd, H. L. Scott and P. R. Dodd, "Glutamate-mediated excitotoxicity and neurodegeneration in Alzheimer's disease," *Neurochemistry international,* vol. 45, no. 5, pp. 583-595, 2004.

[600] D. Butterfield and C. Pocernich, "The glutamatergic system and Alzheimer's disease," *CNS drugs,* vol. 17, no. 9, pp. 641-652, 2003.

[601] C. Lau and R. Zukin, "NMDA receptor trafficking in synaptic plasticity and neuropsychiatric disorders," *Nature Reviews Neuroscience,* vol. 8, no. 6, pp. 413-426, 2007.

[602] E. Chang, M. Savage, D. Flood, J. Thomas, R. Levy, V. Mahadomrongkul, T. Shirao, C. Aoki and P. Huerta, "AMPA receptor downscaling at the onset of Alzheimer's disease pathology in double knockin mice," *Proceedings of the National Academy of Sciences,* vol. 103, no. 9, pp. 3410-3415, 2006.

[603] R. Yasuda, M. Ikonomovic, R. Sheffield, R. Rubin, B. Wolfe and D. Armstrong, "Reduction of AMPA-selective glutamate receptor subunits in the entorhinal cortex of patients with Alzheimer's disease pathology: a biochemical study," *Brain research,* vol. 678, no. 1-2, pp. 161-167, 1995.

[604] T. Carter, R. Rissman, A. Mishizen-Eberz, B. Wolfe, R. Hamilton, S. Gandy and D. Armstrong, "Differential preservation of AMPA receptor subunits in the hippocampi of Alzheimer's disease patients according to Braak stage," *Experimental neurology,* vol. 187, no. 2, pp. 299-309, 2004.

[605] E. Miller, P. Teravskis, B. Dummer, X. Zhao, R. Huganir and D. Liao, "Tau phosphorylation and tau mislocalization mediate soluble Aβ oligomer-induced AMPA glutamate receptor signaling deficits," *European Journal of Neuroscience,* vol. 39, no. 7, pp. 1214-1224, 2014.

[606] C. Iadecola, "Neurovascular regulation in the normal brain and in Alzheimer's disease," *Nature Reviews Neuroscience,* vol. 5, no. 5, pp. 347-360, 2004.

[607] K. Bangen, A. Clark, E. Edmonds, N. Evangelista, M. Werhane, K. Thomas, L. Locano, M. Tran, Z. Zlatar, D. Nation and M. Bondi, "Cerebral Blood Flow and Amyloid-β Interact to Affect Memory Performance in Cognitively Normal Older Adults," *Frontiers in Aging Neuroscience,* vol. 9, p. 181, 2017.

[608] A. Bryant, M. Hu, B. Carlyle, S. Arnold, M. Frosch, S. Das, B. Hyman and R. Bennett, "Cerebrovascular Senescence Is Associated With Tau Pathology in Alzheimer's Disease," *Frontiers in neurology,* vol. 11, p. 1058, 2020.

[609] L. M. Ittner and J. Götz, "Amyloid-β and tau—a toxic pas de deux in alzheimer's disease," *Nature Reviews Neuroscience,* vol. 12, no. 2, p. 67–72, 2011.

[610] G. Bischof, F. Jessen, Fliessbach, D. J. K., J. Hammes, B. Neumaier, O. Onur, G. Fink, J. Kukolja, A. Drzezga and T. van Eimeren, "Impact of tau and amyloid burden on glucose metabolism in Alzheimer's disease," *Annals of clinical and translational neurology,* vol. 3, no. 12, pp. 934-939, 2016.

[611] E. Planel, T. Miyasaka, T. Launey, D. Chui, K. Tanemura, S. Sato, O. Murayama, K. Ishiguro, Y. Tatebayashi and A. Takashima, "Alterations in glucose metabolism induce hypothermia leading to tau hyperphosphorylation through differential inhibition of kinase and phosphatase activities: implications for Alzheimer's disease," *Journal of Neuroscience,* vol. 24, no. 10, pp. 2401-2411, 2004.

[612] N. Menkes-Caspi, H. Yamin, V. Kellner, T. Spires-Jones, D. Cohen and E. Stern, "Pathological tau disrupts ongoing network activity," *Neuron,* vol. 85, no. 5, pp. 959-966, 2015.

[613] S. Verma, A. Kumar, T. Tripathi and A. Kumar, "Muscarinic and nicotinic acetylcholine receptor agonists: current scenario in Alzheimer's disease therapy," *Journal of Pharmacy and Pharmacology,* vol. 70, no. 8, pp. 985-993, 2018..

[614] H. Hampel, M.-M. M. A. C. Cuello, A. S. Khachaturian, A. Vergallo, M. R. Farlow, P. J. Snyder, E. Giacobini and Z. S. Khachaturian, "Revisiting the cholinergic hypothesis in alzheimer's disease: Emerging evidence from

translational and clinical research," *Alzheimer's Dementia,* vol. 6, no. 1, pp. 2-15, 2017.

[615] M. Grothe, L. Zaborszky, M. Atienza, E. Gil-Neciga, R. Rodriguez-Romero, S. Teipel, K. Amunts, A. Suarez-Gonzalez and J. Cantero, "Reduction of basal forebrain cholinergic system parallels cognitive impairment in patients at high risk of developing Alzheimer's disease," *Cerebral Cortex,* vol. 20, no. 7, pp. 1685-1695, 2010.

[616] J. Levenga, P. Krishnamurthy, H. Rajamohamedsait, H. Wong, T. Franke, P. Cain, E. Sigurdsson and C. Hoeffer, "Tau pathology induces loss of GABAergic interneurons leading to altered synaptic plasticity and behavioral impairments," *Acta neuropathologica communiucations,* vol. 1, no. 1, p. 34, 2013.

[617] A. Limon, J. Reyes-Ruiz and R. Miledi, "Loss of functional GABAA receptors in the Alzheimer diseased brain," *Proceedings of the National Academy of Sciences,* vol. 109, no. 25, pp. 10071-10076, 2012.

[618] R. Whittington, L. Virág, M. Gratuze, H. Lewkowitz-Shpuntoff, M. Cheheltanan, F. Petry, I. Poitras, F. Morin and E. Planel, "Administration of the benzodiazepine midazolam increases tau phosphorylation in the mouse brain," *Neurobiology of aging,* vol. 75, pp. 11-24, 2019.

[619] M. Küblböck, M. Woletz, A. Höflich, R. Sladky, G. Kranz, A. Hoffmann, R. Lanzenberger and C. Windischberger, "Stability of low-frequency fluctuation amplitudes in prolonged resting-state fMRI," *Neuroimage,* vol. 1, no. 103, pp. 249-257, 1 December 2014.

[620] X. Zuo and X. Xing, "Test-retest reliabilities of resting-state FMRI measurements in human brain functional connectomics: a systems neuroscience perspective," *Neuroscience & Biobehavioral Reviews,* vol. 45, pp. 100-118, 1 September 2014.

[621] Y. Zang, T. Jiang, Y. Lu, Y. He and L. Tian, "Regional homogeneity approach to fMRI data," *NeuroImage,* vol. 22, no. 1, pp. 394-400, 2004.

[622] M. V. D. Heuvel and H. Pol, "Exploring the brain network: a review on resting-state fMRI functional connectivity," *European neuropsychopharmacology,* vol. 20, no. 8, pp. 519-534, 2010.

[623] H. Lu, S. Jaime and Y. Yang, "Origins of the resting-state functional MRI signal: potential limitations of the “neurocentric” model," *Frontiers in neuroscience,* vol. 13, p. 1136, 23 October 2019.

[624] V. Riedl, L. Utz, G. Castrillon, T. Grimmer, J. Rauschecker, M. Ploner, K. Friston, A. Drzezga and C. Sorg, "Metabolic connectivity mapping reveals

effective connectivity in the resting human brain," *Proceedings of the National Academy of Sciences,* vol. 113, no. 2, pp. 428-433, 2016.

[625] G. Deco, A. Ponce-Alvarez, D. Mantini, G. Romani, P. Hagmann and M. Corbetta, "Resting-state functional connectivity emerges from structurally and dynamically shaped slow linear fluctuations," *Journal of Neuroscience,* vol. 33, no. 27, pp. 11239-11252, 2013.

[626] M. Bright, J. Whittaker, I. Driver and K. Murphy, "Vascular physiology drives functional brain networks," *NeuroImage,* vol. 217, p. 116907, 2020.

[627] T. Aso, G. Sugihara, T. Murai, S. Ubukata, S. Urayama, T. Ueno, G. Fujimoto, D. Thuy, H. Fukuyama and K. Ueda, "A venous mechanism of ventriculomegaly shared between traumatic brain injury and normal ageing," *Brain,* vol. 143, no. 6, pp. 1843-1856, June 2020.

[628] S. Kaur, G. DasGupta and S. Singh, "Altered Neurochemistry in Alzheimer's Disease: Targeting Neurotransmitter Receptor Mechanisms and Therapeutic Strategy," *Neurophysiology,* pp. 1-17, 2019.

[629] P. Whitehouse and K.-S. Au, "Neurotransmitter receptor alterations in Alzheimer's disease," *Senile Dementia of the Alzheimer Type,* pp. 175-182, 1985.

[630] G. Alexander, "Biology of Parkinson's disease: pathogenesis and pathophysiology of a multisystem neurodegenerative disorder," *Dialogues in clinical neuroscience,* vol. 6, no. 3, pp. 259-280, 2004.

[631] J. Han, Y. Ahn, W. Kim, C. Shin, S. Jeong, Y. Song, Y. Bae and J. Kim, "Psychiatric manifestation in patients with Parkinson's disease," *Journal of Korean medical science,* vol. 33, no. 47, p. e300, 2018.

[632] K. Jellinger, "Neuropathology of sporadic Parkinson's disease: evaluation and changes of concepts," *Movement disorders,* vol. 27, no. 1, 2012.

[633] A. Sauerbier, M. Qamar, T. Rajah and K. Chaudhuri, "New concepts in the pathogenesis and presentation of Parkinson's disease," *Clinical Medicine,* vol. 16, no. 4, p. 365, 2016.

[634] R. von Coelln and L. Shulman, "Clinical subtypes and genetic heterogeneity: of lumping and splitting in Parkinson disease," *Current opinion in neurology,* vol. 29, no. 6, pp. 727-734, 2016.

[635] O. W. and J. Schulz, "Current and experimental treatments of Parkinson disease: A guide for neuroscientists," *Journal of neurochemistry,* vol. 139, pp. 325-337, 2016.

[636] C. Adler, T. Beach, J. Hentz, H. Shill, J. Caviness, E. Driver-Dunckley, M. Sabbagh, L. Sue, S. Jacobson and C. D. B. Belden, "Low clinical diagnostic accuracy of early vs. advance Parkinson disease (Clinicopathologic study)," *Neurology,* vol. 83, p. 406–412, 2014.

[637] G. Pagano, F. Niccolini and M. Politis, "Imaging in Parkinson's disease," *Clinical Medicine,* vol. 16, no. 4, p. 371, 2016.

[638] J. Ellis and M. Fell, "Current approaches to the treatment of Parkinson's Disease," *Bioorganic & Medicinal Chemistry Letters,* vol. 27, no. 18, pp. 4247-55, 2017.

[639] P. A. LeWitt and K. Chaudhuri, "Unmet needs in Parkinson disease: Motor and non-motor," *Parkinsonism & Related Disorders,* vol. 80, pp. S7-S12, 2020.

[640] G. M. Halliday, J. B. Leverenz, J. S. Schneider and C. H. Adler, "The neurobiological basis of cognitive impairment in Parkinson's disease," *Movement Disorders,* vol. 29, no. 5, pp. 634-650, 2014.

[641] C. Weingarten, M. Sundman, P. Hickey and N. Chen, "Neuroimaging of Parkinson's disease: Expanding views," *Neuroscience & Biobehavioral Reviews,* vol. 59, pp. 16-52, 2015.

[642] N. Bidesi, I. Vang Andersen, A. Windhorst, V. Shalgunov and M. Herth, "The role of neuroimaging in Parkinson's disease," *Journal of Neurochemistry,* vol. 159, no. 4, pp. 660-89, 2021.

[643] C. Atkinson-Clement, S. Pinto, E. A. and O. Coulon, "Diffusion tensor imaging in Parkinson's disease: review and meta-analysis," *NeuroImage: Clinical,* vol. 16, pp. 98-110, 2017.

[644] S. Lin, R. Rodriguez-Rojas, T. Baumeister, C. Lenglos, J. Pineda-Pardo, J. Máñez-Miró, M. Del Alamo, R. Martinez-Fernandez, J. Obeso and Y. Iturria-Medina, "Neuroimaging signatures predicting motor improvement to focused ultrasound subthalamotomy in Parkinson's disease," *npj Parkinson's Disease,* vol. 8, no. 1, p. 70, 2022.

[645] C. Lenglos, S. Lin, Y. Zeighami, T. Baumeister, F. Carbonell and Y. Iturria-Medina, "Multivariate genomic and transcriptomic determinants of imaging-derived personalized therapeutic needs in Parkinson's disease," *Scientific Reports,* vol. 12, no. 1, p. 5483, 2022.

[646] A. Khan, Q. Adewale, T. Baumeister, F. Carbonell, K. Zilles, N. Palomero-Gallagher and Y. Iturria-Medina, "Personalized brain models identify neurotransmitter receptor changes in Alzheimer's disease," *Brain,* vol. 145, no. 5, pp. 1785-1804, 2022.

[647] K. Kiely, P. Butterworth, N. Watson and M. Wooden, "The Symbol Digit Modalities Test: Normative data from a large nationally representative sample of Australian," *Archives of Clinical Neuropsychology,* vol. 29, no. 8, pp. 767-775, 2014.

[648] G. Pagano, F. Niccolini and M. Politis, "Imaging in Parkinson's disease," *Clinical Medicine,* vol. 16, no. 4, p. 371, 2016.

[649] N. I. Bohnen, S. Roytman, P. Kanel, M. L. Müller, P. J. Scott, K. A. Frey, R. Albin and R. A. Koeppe, "Progression of regional cortical cholinergic denervation in Parkinson's disease," *Brain Communications,* vol. 4, no. 6, p. fcac320, 2022.

[650] W. Chiu, L. Donker Kaat, A. Boon, W. Kamphorst, A. Schleicher, K. Zilles, J. Van Swieten and N. Palomero-Gallagher, "Multireceptor fingerprints in progressive supranuclear palsy," *Alzheimer's research & therapy,* vol. 9, no. 1, pp. 1-13, 2017.

[651] J. Zimmermann, A. Perry, M. Breakspear, M. Schirner, P. Sachdev, W. Wen, N. Kochan, M. Mapstone, P. Ritter, A. McIntosh and A. Solodkin, "Differentiation of Alzheimer's disease based on local and global parameters in personalized Virtual Brain models," *NeuroImage: Clinical,* vol. 19, pp. 240-251, 2018.

[652] Q. Adewale, A. Khan, F. Carbonell and Y. Iturria-Medina, "Integrated transcriptomic and neuroimaging brain model decodes biological mechanisms in aging and Alzheimer's disease," *Elife,* vol. 10, p. e62589, 2021.

[653] G. Ballentine, S. Friedman and D. Bzdok, "Trips and neurotransmitters: Discovering principled patterns across 6850 hallucinogenic experiences," *Science Advances,* vol. 8, no. 11, 16 March 2022.

[654] D. Zachlod, S. Bludau, S. Cichon, N. Palomero-Gallagher and K. Amunts, "Combined analysis of cytoarchitectonic, molecular and transcriptomic patterns reveal differences in brain organization across human functional brain systems," *NeuroImage,* p. 119286, 2022.

[655] J. Hansen, R. Markello, L. Tuominen, M. Nørgaard, E. Kuzmin, N. Palomero-Gallagher, A. Dagher and B. Misic, "Correspondence between gene expression and neurotransmitter receptor and transporter density in the human brain," *NeuroImage,* vol. 264, p. 119671, 2022.

[656] K. Pak, S. Seo, M. Lee, H. Im, K. Kim and I. Kim, "Limited power of dopamine transporter mRNA mapping for predicting dopamine transporter availability," *Synapse,* vol. 76, no. 5-6, p. e22226, 2022.

[657] J. Dukart, S. Holiga, M. Rullmann, R. Lanzenberger, P. Hawkins, M. Mehta, S. Hesse, H. Barthel, O. Sabri, R. Jech and S. Eickhoff, "JuSpace: A tool for spatial correlation analyses of magnetic resonance imaging data with nuclear imaging derived neurotransmitter maps," *Human Brain Mapping,* vol. 42, no. 3, pp. 555-566, 2020.

[658] K. Sakreida, W. Chiu, J. Dukart, S. Eickhoff, T. Frodl, C. Gaser, M. Landgrebe, B. Langguth, D. Mirlach, I. Rautu and M. Wittmann, "Disentangling dyskinesia from parkinsonism in motor structures of patients with schizophrenia," *Brain Communications,* vol. 4, no. 4, p. fcac190, 2022.

[659] E. Premi, M. Pengo, I. Mattioli, V. Cantoni, J. Dukart, R. Gasparotti, E. Buratti, A. Padovani, M. Bocchetta, E. Todd and A. Bouzigues, "Early neurotransmitters changes in prodromal frontotemporal dementia: A GENFI study," *Neurobiology of disease,* vol. 179, p. 106068, 2023.

[660] L. Hahn, S. Eickhoff, K. Mueller, L. Schilbach, H. Barthel, K. Fassbender, K. Fliessbach, J. Kornhuber, J. Prudlo, M. Synofzik and J. Wiltfang, "Resting-state alterations in behavioral variant frontotemporal dementia are related to the distribution of monoamine and GABA neurotransmitter systems," *medRxiv,* 2022.

[661] J. Dukart, Š. Holiga, C. Chatham, P. Hawkins, A. Forsyth, R. McMillan, J. Myers, A. Lingford-Hughes, D. Nutt, E. Merlo-Pich and C. Risterucci, "Cerebral blood flow predicts differential neurotransmitter activity," *Scientific reports,* vol. 8, no. 1, pp. 1-11, 2018.

[662] W. Moses, "Fundamental limits of spatial resolution in PET.," *Nuclear Instruments and Methods in Physics Research Section A: Accelerators, Spectrometers, Detectors and Associated Equipment,* vol. 648, pp. S236-S240, 2011.

[663] E. Mak, L. Su, G. Williams and J. O'Brien, "Neuroimaging correlates of cognitive impairment and dementia in Parkinson's disease," *Parkinsonism & related disorders,* vol. 21, no. 8, pp. 862-870, 2015.

[664] W. Zhan, G. Kang, G. Glass, Y. Zhang, C. Shirley, R. Millin, K. Possin, M. Nezamzadeh, M. Weiner, W. Marks Jr and N. Schuff, "Regional alterations of brain microstructure in Parkinson's disease using diffusion tensor imaging," *Movement disorders,* vol. 27, no. 1, pp. 90-97, 2012.

[665] K. Nguyen, V. Raval, A. Treacher, C. Mellema, F. Yu, M. Pinho, R. Subramaniam, D. J. R.B. and A. Montillo, "Predicting Parkinson's disease trajectory using clinical and neuroimaging baseline measures," *Parkinsonism & related disorders,* vol. 85, pp. 44-51, 2021.

[666] R. Markello and B. Misic, "Comparing spatial null models for brain maps," *NeuroImage,* vol. 236, p. 118052, 2021.

[667] Y. Assaf, "Imaging laminar structures in the gray matter with diffusion MRI," *Neuroimage,* vol. 197, pp. 677-688, 2019.

[668] P. Weston, I. Simpson, N. Ryan, S. Ourselin and N. Fox, "Diffusion imaging changes in grey matter in Alzheimer's disease: a potential marker of early neurodegeneration," *Alzheimer's research & therapy,* vol. 7, no. 1, pp. 1-8, 2015.

[669] M. Cercignani, M. Inglese, E. Pagani, G. Comi and M. Filippi, "Mean diffusivity and fractional anisotropy histograms of patients with multiple sclerosis," *American Journal of Neuroradiology,* vol. 22, no. 5, pp. 952-958, 2001.

[670] N. Volkow, G. Wang, J. Fowler, J. Logan, R. Hitzemann, Y. Ding, N. Pappas, C. Shea and K. Piscani, "Decreases in dopamine receptors but not in dopamine transporters in alcoholics," *Alcoholism: Clinical and Experimental Research,* vol. 20, no. 9, pp. 1594-1598, 1996.

[671] S. Thobois, S. Prange, C. Scheiber and E. Broussolle, "What a neurologist should know about PET and SPECT functional imaging for parkinsonism: A practical perspective," *Parkinsonism & related disorders,* vol. 59, pp. 93-100, 2019.

[672] M. Bu, M. Farrer and H. Khoshbouei, "Dynamic control of the dopamine transporter in neurotransmission and homeostasis," *NPJ Parkinson's disease,* vol. 7, no. 1, pp. 1-11, 2021.

[673] V. Kerstens and A. Varrone, "Dopamine transporter imaging in neurodegenerative movement disorders: PET vs. SPECT," *Clinical and Translational Imaging,* vol. 8, pp. 349-356, 2020.

[674] Y. Zeighami, M. Ulla, Y. Iturria-Medina, M. Dadar, Y. Zhang, K. Larcher, V. Fonov, A. Evans, D. Collins and A. Dagher, "Network structure of brain atrophy in de novo Parkinson's disease," *eLife,* vol. 4, p. e08440, 7 Sep 2015.

[675] M. Ruppert, A. Greuel, M. Tahmasian, F. Schwartz, S. Stürmer, F. Maier, J. Hammes, M. Tittgemeyer, L. Timmermann, T. Van Eimeren and A. Drzezga, "Network degeneration in Parkinson's disease: multimodal imaging of nigro-striato-cortical dysfunction," *Brain,* vol. 143, no. 3, pp. 944-959, 1 Mar 2020.

[676] W. Caudle and J. Zhang, "Glutamate, excitotoxicity, and programmed cell death in Parkinson disease," *Experimental neurology,* vol. 220, no. 2, pp. 230-233, 2009.

[677] Z. Zhang, S. Zhang, P. Fu, Z. Zhang, K. Lin, J. Ko and K. Yung, "Roles of glutamate receptors in Parkinson's disease," *International journal of molecular sciences,* vol. 20, no. 18, p. 4391, 2019.

[678] M. Firbank, J. Parikh, N. Murphy, A. Killen, C. Allan, D. Collerton, A. Blamire and J. Taylor, "Reduced occipital GABA in Parkinson disease with visual hallucinations," *Neurology,* vol. 91, no. 7, pp. e675-e685, 2018.

[679] P. Calabresi, B. Picconi, L. Parnetti and M. Di Filippo, "A convergent model for cognitive dysfunctions in Parkinson's disease: the critical dopamine–acetylcholine synaptic balance," *The Lancet Neurology,* vol. 5, no. 11, pp. 974-983, 2006.

[680] S. Vegas-Suarez, E. Paredes-Rodriguez, A. Aristieta, J. Lafuente, C. Miguelez and L. Ugedo, "Dysfunction of serotonergic neurons in Parkinson's disease and dyskinesia," *International Review of Neurobiology,* vol. 146, pp. 259-279, 2019.

[681] B. Ballanger, A. Strafella, T. van Eimeren, M. Zurowski, P. Rusjan, S. Houle and S. Fox, "Serotonin 2A receptors and visual hallucinations in Parkinson disease," *Archives of neurology,* vol. 67, no. 4, pp. 416-421, 2010.

[682] A. Nelson, T. Hoque, C. Gunraj and R. Chen, "Altered somatosensory processing in Parkinson's disease and modulation by dopaminergic medications," *Parkinsonism & Related Disorders,* vol. 53, pp. 76-81, 2018.

[683] M. Müller and N. Bohnen, "Cholinergic dysfunction in Parkinson's disease," *Current neurology and neuroscience reports,* vol. 13, no. 9, pp. 1-9, 2013.

[684] M. Quik and J. Kulak, "Nicotine and nicotinic receptors; relevance to Parkinson's disease," *Neurotoxicology,* vol. 23, no. 4-5, pp. 581-594, 2002.

[685] M. Fujita, M. Ichise, S. Zoghbi, J. Liow, S. Ghose, D. Vines, J. Sangare, J. Lu, V. Cropley, H. Iida and K. Kim, "Widespread decrease of nicotinic acetylcholine receptors in Parkinson's disease," *Annals of neurology,* vol. 59, no. 1, pp. 174-177, 2006.

[686] D. Lester, T. Rogers and C. Blaha, "Acetylcholine–dopamine interactions in the pathophysiology and treatment of CNS disorders," *CNS neuroscience & therapeutics,* vol. 16, no. 3, pp. 137-162, 2010.

[687] E. Schlicker and T. Feuerstein, "Human presynaptic receptors," *Pharmacology & Therapeutics,* vol. 172, pp. 1-21, 2017.

[688] R. de la Fuente-Fernández, M. Schulzer, E. Mak, D. Calne and A. Stoessl, "Presynaptic mechanisms of motor fluctuations in Parkinson's disease: a probabilistic model," *Brain,* vol. 127, no. 4, pp. 888-899, 2004.

[689] J. Chu, A. Wagle-Shukla, C. Gunraj, A. Lang and R. Chen, "Impaired presynaptic inhibition in the motor cortex in Parkinson disease," *Neurology,* vol. 72, no. 9, pp. 842-849, 2009.

[690] N. Sterling, M. Wang, L. Zhang, E. Lee, G. Du, M. Lewis, M. Styner and X. Huang, "Stage-dependent loss of cortical gyrification as Parkinson disease "unfolds"," *Neurology,* vol. 86, no. 12, pp. 1143-1151, 2016.

[691] Y. Zhang, J. Zhang, J. Xu, X. Wu, Y. Zhang, H. Feng, J. Wang and T. Jiang, "Cortical gyrification reductions and subcortical atrophy in Parkinson's disease," *Movement Disorders,* vol. 29, no. 1, pp. 122-126, 2014.

[692] K. Jamebozorgi, E. Taghizadeh, D. Rostami, H. Pormasoumi, G. Barreto, S. Hayat and A. Sahebkar, "Cellular and molecular aspects of Parkinson treatment: future therapeutic perspectives," *Molecular Neurobiology,* pp. 4799-4811, 2019.

[693] L. Brichta, P. Greengard and M. Flajolet, "Advances in the pharmacological treatment of Parkinson's disease: targeting neurotransmitter systems," *Trends in neurosciences,* vol. 36, no. 9, pp. 543-554, 2013.

[694] S. E. C. A. P. S. C. C. Aiello M, A. Prinster, E. Nicolai, M. Salvatore, J. Baron and M. Quarantelli, "Relationship between simultaneously acquired resting-state regional cerebral glucose metabolism and functional MRI: a PET/MR hybrid scanner study," *Neuroimage,* no. 113, pp. 111-121, 1 June 2015.

[695] G. Rohde, A. Barnett, P. Basser, S. Marenco and C. Pierpaoli, "Rohde, G.K., Barnett, A.S., Basser, P.J., Marenco, S. and Pierpaoli, C., 2004. Comprehensive approach for correction of motion and distortion in diffusion-weighted MRI. Magnetic Resonance in Medicine:," *Magnetic Resonance in Medicine: An Official Journal of the International Society for Magnetic Resonance in Medicine,* vol. 51, no. 1, pp. 103-114, 2004.

[696] E. Rolls, C. Huang, C. Lin, J. Feng and M. Joliot, "Automated anatomical labelling atlas 3," *Neuroimage,* vol. 206, p. 116189, 1 February 2020.

[697] S. Ewert, P. Plettig, N. Li, M. Chakravarty, D. Collins, T. Herrington, A. Kühn and A. Horn, "Toward defining deep brain stimulation targets in MNI space: a subcortical atlas based on multimodal MRI, histology and structural connectivity," *Neuroimage,* vol. 170, pp. 271-282, 15 April 2018.

[698] M. Jenkinson, C. Beckmann, T. Behrens, M. Woolrich and S. Smith, "FSL," *NeuroImage,* vol. 62, pp. 782-90, 2012.

[699] J. P. D. T. B. W. T. E. M. R. K. R. D. Fortin, T. Satterthwaite, R. Gur, R. Gur and R. Schultz, "Harmonization of multi-site diffusion tensor imaging data," *Neuroimage,* vol. 161, pp. 149-170, 2017.

[700] C. Qualls, N. Bliwise and A. Stringer, "Short forms of the Benton judgment of line orientation test: Development and psychometric properties," *Archives of Clinical Neuropsychology,* vol. 15, no. 2, pp. 159-163, 2000.

[701] J. Yesavage, "Geriatric depression scale," *Psychopharmacol Bull,* vol. 24, no. 4, pp. 709-711, 1988.

[702] J. Brandt, "The Hopkins Verbal Learning Test: Development of a new memory test with six equivalent forms," *The clinical neuropsychologist,* vol. 5, no. 2, pp. 125-142, 1991.

[703] D. Wechsler, "Wechsler adult intelligence scale," *Archives of Clinical Neuropsychology,* 1955.

[704] C. Goetz, B. Tilley, S. Shaftman, G. Stebbins, S. Fahn, P. Martinez-Martin, W. Poewe, C. Sampaio, M. Stern, R. Dodel and B. Dubois, "Movement Disorder Society-sponsored revision of the Unified Parkinson's Disease Rating Scale (MDS-UPDRS): scale presentation and clinimetric testing results," *Movement disorders: official journal of the Movement Disorder Society,* vol. 23, no. 15, pp. 2129-2170, 2008.

[705] Z. Nasreddine, N. Phillips, V. Bédirian, S. Charbonneau, V. Whitehead, I. Collin, J. Cummings and H. Chertkow, "The Montreal Cognitive Assessment, MoCA: a brief screening tool for mild cognitive impairment," *Journal of the American Geriatrics Society,* vol. 53, no. 4, pp. 695-699, 2005.

[706] C. Spielberger, S. Sydeman, A. Owen and B. Marsh, "Measuring anxiety and anger with the State-Trait Anxiety Inventory (STAI) and the State-Trait Anger Expression Inventory (STAXI)," in *The Use of Psychological Testing for Treatment Planning and Outcomes Assessment* , New York, Lawrence Erlbaum Associates Publishers, 1999, p. 993–1021.

[707] A. Smith, *Symbol digit modalities test,* Los Angeles: Western psychological services, 1973, pp. 1-22.

[708] M. McKeown and G. Peavy, "Biomarkers in Parkinson disease: It's time to combine," *Neurology,* vol. 84, no. 24, pp. 2392-2393, 2015.

[709] G. Patow, L. Stefanovski, P. Ritter, G. Deco, X. Kobeleva and A. D. N. Initiative, "Whole-brain modeling of the differential influences of Amyloid-Beta and Tau in Alzheimer's Disease," *Alzheimer's Research & Therapy,* vol. 15, no. 1, p. 210, 2023.

[710] L. Ross and D. Bassett, "Causation in neuroscience: keeping mechanism meaningful," *Nature Reviews Neuroscience,* vol. 25, pp. 81-90, 2024.

[711] Y. Xu, J. Yan, P. Zhou, J. Li, H. Gao, Y. Xia and Q. Wang, "Neurotransmitter receptors and cognitive dysfunction in alzheimer's disease and parkinson's disease," *Progress in neurobiology,* vol. 97, no. 1, p. 1–13, 2012.

[712] S. Snowden, A. Ebshiana, A. Hye, O. Pletnikova, R. O'Brien, A. Yang, J. Troncoso, C. Legido-Quigley and M. Thambisetty, "Neurotransmitter imbalance in the brain and Alzheimer's disease pathology," *Journal of Alzheimer's Disease,* vol. 72, no. 1, pp. 35-43, 2019.

[713] A. Rulseh, J. Keller, J. Tintěra, M. Kožíšek and J. Vymazal, "Chasing shadows: what determines DTI metrics in gray matter regions? An in vitro and in vivo study," *Journal of Magnetic Resonance Imaging,* vol. 38, no. 5, pp. 1103-1110, 2013.

[714] R. Ward, F. Zucca, J. Duyn, R. Crichton and L. Zecca, "The role of iron in brain ageing and neurodegenerative disorders," *The Lancet Neurology,* vol. 13, no. 10, pp. 1045-1060, 2014.

[715] R. Ward, D. Dexter and R. Crichton, "Iron, neuroinflammation and neurodegeneration," *International Journal of Molecular Sciences,* vol. 23, no. 13, p. 7267, 2022.

[716] B. Jeurissen, A. Leemans, J. Tournier, D. Jones and J. Sijbers, "Investigating the prevalence of complex fiber configurations in white matter tissue with diffusion magnetic resonance imaging," *Human brain mapping,* vol. 34, no. 11, pp. 2747-2766, 2013.

[717] K. Schilling, Y. Gao, V. Janve, I. Stepniewska, B. Landman and A. Anderson, "Can increased spatial resolution solve the crossing fiber problem for diffusion MRI?," *NMR in Biomedicine,* vol. 30, no. 12, p. e3787, 2017.

[718] T. Dhollander, A. Clemente, M. Singh, F. Boonstra, O. Civier, J. Duque, N. Egorova, P. Enticott, I. Fuelscher, S. Gajamange and S. Genc, "Fixel-based analysis of diffusion MRI: methods, applications, challenges and opportunities," *Neuroimage,* vol. 241, p. 118417, 2021.

[719] S. Vos, D. Jones, M. Viergever and A. Leemans, "Partial volume effect as a hidden covariate in DTI analyses," *Neuroimage,* vol. 55, no. 4, pp. 1566-1576, 2011.

[720] M. Chappell, F. McConnell, X. Golay, M. Günther, J. Hernandez-Tamames, M. van Osch and I. Asllani, "Partial volume correction in arterial spin

labeling perfusion MRI: A method to disentangle anatomy from physiology or an analysis step too far?," *Neuroimage,* vol. 238, p. 118236, 2021.

[721] J. Henf, M. Grothe, K. Brueggen, S. Teipel and M. Dyrba, "Mean diffusivity in cortical gray matter in Alzheimer's disease: The importance of partial volume correction," *NeuroImage: Clinical,* vol. 17, pp. 579-586, 2018.

[722] C. Caballero-Gaudes and R. Reynolds, "Methods for cleaning the BOLD fMRI signal," *Neuroimage,* vol. 154, pp. 128-149, 2017.

[723] P. Drew, "Vascular and neural basis of the BOLD signal," *Current opinion in neurobiology,* vol. 58, pp. 61-69, 2019.

[724] G. Krishnan, O. González and M. Bazhenov, "Origin of slow spontaneous resting-state neuronal fluctuations in brain networks," *Proceedings of the National Academy of Sciences,* vol. 115, no. 26, pp. 6858-6863, 2018.

[725] J. Cabral, E. Hugues, O. Sporns and G. Deco, "Role of local network oscillations in resting-state functional connectivity," *Neuroimage,* vol. 57, no. 1, pp. 130-139, 2011.

[726] G. Deco, V. Jirsa and A. McIntosh, "Emerging concepts for the dynamical organization of resting-state activity in the brain," *Nature reviews neuroscience,* vol. 12, no. 1, pp. 43-56, 2011.

[727] F. Su, T. Chu, Y. Wai, Y. Wan and H. Liu, "Temporal resolving power of perfusion-and BOLD-based event-related functional MRI," *Medical physics,* vol. 31, no. 1, pp. 154-160, 2004.

[728] L. Hernandez-Garcia, V. Aramendía-Vidaurreta, D. Bolar, W. Dai, M. Fernández-Seara, J. Guo, A. Madhuranthakam, H. Mutsaerts, J. Petr, Q. Qin and J. Schollenberger, "Recent technical developments in ASL: a review of the state of the art," *Magnetic resonance in medicine,* vol. 88, no. 5, pp. 2021-2042, 2022.

[729] A. Knight, C. Morrone, C. Varlow, W. Yu, P. McQuade and N. Vasdev, "Head-to-head comparison of tau-PET radioligands for imaging TDP-43 in post-mortem ALS brain," *Molecular Imaging and Biology,* vol. 25, no. 3, pp. 513-527, 2023.

[730] J. Xiang, Y. Tao, Y. Xia, S. Luo, Q. Zhao, B. Li, X. Zhang, Y. Sun, W. Xia, M. Zhang and S. Kang, "Development of an α-synuclein positron emission tomography tracer for imaging synucleinopathies," *Cell,* vol. 186, no. 16, pp. 3350-3367, 2023.

[731] G. Carli, G. Tondo, C. Boccalini and D. Perani, "Brain molecular connectivity in neurodegenerative conditions," *Brain sciences,* vol. 11, no. 4, p. 433, 2021.

[732] A. Whittington, D. Sharp and R. Gunn, "Spatiotemporal distribution of β-amyloid in Alzheimer disease is the result of heterogeneous regional carrying capacities," *Journal of Nuclear Medicine,* vol. 59, no. 5, pp. 822-827, 2018.

[733] A. Cain, M. Taga, C. McCabe, G. Green, I. Hekselman, C. White, D. Lee, P. Gaur, O. Rozenblatt-Rosen, F. Zhang and E. Yeger-Lotem, "Multicellular communities are perturbed in the aging human brain and Alzheimer's disease," *Nature Neuroscience,* vol. 26, no. 1267–1280, pp. 1-14, 2023.

[734] T. Wingo, Y. Liu, E. Gerasimov, S. Vattathil, M. Wynne, J. Liu, A. Lori, V. Faundez, D. Bennett, N. Seyfried and A. Levey, "Shared mechanisms across the major psychiatric and neurodegenerative diseases," *Nature communications,* vol. 13, no. 1, p. 4314, 2022.

[735] M. Diaz-Ortiz and A. Chen-Plotkin, "Omics in neurodegenerative disease: hope or hype?," *Trends in Genetics,* vol. 36, no. 3, pp. 152-159, 2020.

[736] P. Young, M. Estarellas, E. Coomans, M. Srikrishna, H. Beaumont, A. Maass, A. Venkataraman, R. Lissaman, D. Jiménez, M. Betts and E. McGlinchey, "Imaging biomarkers in neurodegeneration: current and future practices," *Alzheimer's research & therapy,* vol. 12, pp. 1-17, 2020.

[737] E. Hustad, A. Skogholt, K. Hveem and J. Aasly, "The accuracy of the clinical diagnosis of Parkinson disease. The HUNT study," *Journal of neurology,* vol. 265, pp. 2120-2124, 2018.

[738] R. Armstrong, P. Lantos and N. Cairns, "Overlap between neurodegenerative disorders," *Neuropathology,* vol. 25, no. 2, pp. 111-124, 2005.

[739] D. Berg, P. Borghammer, S. Fereshtehnejad, S. Heinzel, J. Horsager, E. Schaeffer and R. Postuma, "Prodromal Parkinson disease subtypes—key to understanding heterogeneity," *Nature Reviews Neurology,* vol. 17, no. 6, pp. 349-361, 2021.

[740] H. Hampel, J. Cummings, K. Blennow, P. Gao, C. Jack Jr and A. Vergallo, "Developing the ATX (N) classification for use across the Alzheimer disease continuum," *Nature Reviews Neurology,* vol. 17, no. 9, pp. 580-589, 2021.

[741] L. Ciranna, "Serotonin as a modulator of glutamate- and GABA-mediated neurotransmission: implications in physiological function and in pathology," *Current neuropharmacology,* vol. 4, no. 2, pp. 101-114, 2006.

[742] J. Shine, "Neuromodulatory influences on integration and segregation in the brain," *Trends in cognitive sciences,* vol. 23, no. 7, pp. 572-583, 2019.

[743] N. Titova and K. Chaudhuri, "Personalized medicine in Parkinson's disease: time to be precise," *Movement Disorders,* vol. 32, no. 8, p. 1147, 2017.

[744] J. Kim and D. Bassett, "Linear dynamics and control of brain networks," in *Neural Engineering*, Springer, 2020, pp. 497-518.

[745] L. Messeri and M. Crockett, "Artificial intelligence and illusions of understanding in scientific research," *Nature,* vol. 627, p. 49–58 , 2024.

[746] S. Gu, F. Pasqualetti, M. Cieslak, Q. Telesford, A. Yu, A. Kahn, J. Medaglia, J. Vettel, M. Miller, S. Grafton and D. Bassett, "Controllability of structural brain networks," *Nature communications,* vol. 6, no. 1, p. 8414, 2015.

[747] F. Pasqualetti, S. Gu and D. Bassett, "RE: Warnings and caveats in brain controllability," *NeuroImage,* vol. 197, pp. 586-588, 2019.

[748] H. Leonard, M. Nalls, A. Day-Williams, S. Esmaeeli, P. Jarreau, S. Bandres-Ciga, P. Heutink, P. Sardi and A. Singleton, "Open science in precision medicine for neurodegenerative diseases," *Nature Reviews Drug Discovery,* 2024.

[749] N. A. Bishop, T. Lu and B. A. Yankner, "Neural mechanisms of ageing and cognitive decline," *Nature,* vol. 464, no. 7288, p. 529–535, 2010.

[750] S. Guntupalli, J. Widagdo and V. Anggono, "Amyloid-β-induced dysregulation of AMPA receptor trafficking," *Neural plasticity,* vol. 2016, 2016.

[751] C. Maes, L. Hermans, L. Pauwels, S. Chalavi, I. Leunissen, O. Levin, K. Cuypers, R. Peeters, S. Sunaert, D. Mantini and N. Puts, "Age-related differences in GABA levels are driven by bulk tissue changes," *Human Brain Mapping,* vol. 39, no. 9, pp. 3652-3662, 2018.

[752] F. Nasrallah, J. Griffin, V. Balcar and C. Rae, "Understanding your inhibitions: modulation of brain cortical metabolism by GABAB receptors," *Journal of Cerebral Blood Flow & Metabolism,* vol. 27, no. 8, pp. 1510-1520, 2007.

[753] J. Pavia, M. De Ceballos and F. De La Cuesta, "Alzheimer's disease: relationship between muscarinic cholinergic receptors, β-amyloid and tau proteins," *Fundamental & clinical pharmacology,* vol. 12, no. 5, pp. 473-481, 1998.

[754] R. C. Petersen, P. S. Aisen, L. A. Beckett, M. C. Donohue, A. C. Gamst, D. J. Harvey, C. R. Jack, W. J. Jagust, L. M. Shaw, A. W. Toga, J. Q. Trojanowski

and M. W. Weiner, "Alzheimer’s disease neuroimaging initiative (ADNI): Clinical characterization," *Neurology,* vol. 74, no. 3, p. 201–209, 2010.

[755] F. Yeh, T. D. Verstynen, Y. Wang, J. C. Fernández-Miranda and W.-Y. I. Tseng, "Deterministic diffusion fiber tracking improved by quantitative anisotropy," *PloS One,* vol. 8, no. 11, p. e80713, 2013.

[756] O. Almkvist, E. Rodriguez-Vieitez, S. Thordardottir, K. Amberla, K. Axelman, H. Basun, A. Kinhult-Ståhlbom, L. Lilius, A. Remes, L. Wahlund and M. Viitanen, "Predicting cognitive decline across four decades in mutation carriers and non-carriers in autosomal-dominant Alzheimer’s disease," *Journal of the International Neuropsychological Society,* vol. 23, no. 3, pp. 195-203.

[757] M. Bilgel, B. Jedynak and A. D. N. Initiative, "Predicting time to dementia using a quantitative template of disease progression," *Alzheimer's & Dementia: Diagnosis, Assessment & Disease Monitoring,* vol. 11, no. 1, pp. 205-215, 2019.

[758] B. Tijms, E. Vromen, O. Mjaavatten, H. Holstege, L. Reus, S. van der Lee, K. Wesenhagen, L. Lorenzini, L. Vermunt, V. Venkatraghavan and N. Tesi, "Cerebrospinal fluid proteomics in patients with Alzheimer’s disease reveals five molecular subtypes with distinct genetic risk profiles," *Nature Aging,* pp. 1-15, 2024.

[759] D. Schoonhoven, E. Coomans, A. Millán, A. van Nifterick, D. Visser, R. Ossenkoppele, H. Tuncel, W. van der Flier, S. Golla, P. Scheltens and A. Hillebrand, "Tau protein spreads through functionally connected neurons in Alzheimer’s disease: a combined MEG/PET study," *Brain,* p. awad189, 2023.

[760] N. C. Berchtold and C. W. Cotman, "Evolution in the conceptualization of dementia and Alzheimer’s disease: Greco-Roman period to the 1960s," *Neurobiology of aging,* vol. 19, no. 3, pp. 173-189, 1998.

[761] D. Veitch, M. Weiner, M. Miller, P. Aisen, M. Ashford, L. Beckett, R. Green, D. Harvey, C. Jack Jr, W. Jagust and S. Landau, "The Alzheimer's Disease Neuroimaging Initiative in the era of Alzheimer's disease treatment: A review of ADNI studies from 2021 to 2022," *Alzheimer's & Dementia,* 2023.

[762] P. Calabresi, A. Mechelli, G. Natale, L. Volpicelli-Daley, G. Di Lazzaro and V. Ghiglieri, "Alpha-synuclein in Parkinson’s disease and other synucleinopathies: from overt neurodegeneration back to early synaptic dysfunction," *Cell death & disease,* vol. 14, no. 3, p. 176, 2023.

[763] J. Vohryzek, J. Cabral, F. Castaldo, Y. Sanz-Perl, L. Lord, H. Fernandes, V. Litvak, M. Kringelbach and G. Deco, "Dynamic sensitivity analysis: Defining personalised strategies to drive brain state transitions via whole brain modelling," *Computational and Structural Biotechnology Journal,* vol. 21, pp. 335-345, 2023.

[764] J. Vohryzek, J. Cabral, Y. Perl, M. Demirtas, C. Falcon, D. Gispert, B. Bosch, M. Balasa, M. Kringelbach, R. Sanchez and G. Ruffini, "Design of effective personalised perturbation strategies for enhancing cognitive intervention in Alzheimer's disease," *bioRxiv,* pp. 2023-04, 2023.

[765] H. Mathys, Z. Peng, C. Boix, M. Victor, N. Leary, S. Babu, G. Abdelhady, X. Jiang, A. Ng, K. Ghafari and A. Kunisky, "Single-cell atlas reveals correlates of high cognitive function, dementia, and resilience to Alzheimer's disease pathology," *Cell,* vol. 186, no. 20, pp. 4365-4385, 2023.

[766] W. Luo, W. Qu and L. Gan, "The AD odyssey 2023: Tales of single cell," *Cell,* vol. 186, no. 20, pp. 4257-4259, 2023.

[767] B. Okaty, K. Sugino and S. Nelson, "Cell type-specific transcriptomics in the brain," *Journal of Neuroscience,* vol. 31, no. 19, pp. 6939-6943, 2011.

[768] A. Young, N. Oxtoby, S. Garbarino, N. Fox, F. Barkhof, J. Schott and D. Alexander, "Data-driven modelling of neurodegenerative disease progression: thinking outside the black box," *Nature Reviews Neuroscience,* pp. 1-20, 2024.

[769] J. Whitwell, "Neuroimaging across the FTD spectrum," *Progress in molecular biology and translational science,* vol. 165, pp. 187-223, 2019.

[770] K. Lopes, R. Vialle, G. Green, M. Fujita, Y. Wang, C. Gaiteri, V. Menon, P. De Jager, N. Habib, S. Tasaki and D. Bennett, "Chasing the cell type-specific molecular networks involved in Alzheimer's Disease," *Alzheimer's & Dementia,* vol. 19, p. e073444, 2023.

[771] L. Parkkinen, T. Kauppinen, T. Pirttilä, J. Autere and I. Alafuzoff, "α-Synuclein pathology does not predict extrapyramidal symptoms or dementia," *Annals of Neurology: Official Journal of the American Neurological Association and the Child Neurology Society,* vol. 57, no. 1, pp. 82-91, 2005.

[772] K. Fiest, J. Roberts, C. Maxwell, D. Hogan, E. Smith, A. Frolkis, A. Cohen, A. Kirk, D. Pearson, T. Pringsheim and A. Venegas-Torres, "The prevalence and incidence of dementia due to Alzheimer's disease: a systematic review and meta-analysis," *Canadian Journal of Neurological Sciences,* vol. 43, no. S1, pp. S51-S82, 2016.

[773] J. Kim, D. Vitale, D. Otani, M. Lian, K. Heilbron, H. Iwaki, J. Lake, C. Solsberg, H. Leonard and M. Makarious, "Multi-ancestry genome-wide association meta-analysis of Parkinson's disease," *Nature genetics,* vol. 56, p. 27–36, 2023.

[774] A. Hogan-Cann and C. Anderson, "Physiological roles of non-neuronal NMDA receptors," *Trends in pharmacological sciences,* vol. 37, no. 9, pp. 750-767, 2016.

[775] A. M Tata, L. Velluto, C. D'Angelo and M. Reale, "Cholinergic system dysfunction and neurodegenerative diseases: cause or effect?," *CNS & Neurological Disorders-Drug Targets (Formerly Current Drug Targets-CNS & Neurological Disorders),* vol. 13, no. 7, pp. 1294-1303, 2014.

[776] A. Cain, M. Taga, C. McCabe, G. Green, I. Hekselman, C. White, D. Lee, P. Gaur, O. Rozenblatt-Rosen, F. Zhang and E. Yeger-Lotem, "Multicellular communities are perturbed in the aging human brain and Alzheimer's disease," *Nature Neuroscience,* vol. 26, p. 1267–1280, 2023.